

# **Interactions between Paramyxoviruses and Bacteria:**

Implications for Pathogenesis and Intervention

Duy Tien Nguyen

Cover design: Hung Tran & Duy Tien Nguyen  
Cover photographer: Hung Tran  
Cover models: Kyan & Lya

Cover:

Front:

View through microscope: The green circle with greenish spiked and T-shaped protusions represents a virus particle. Virus contains Kyan dressed as Popeye. The two blue circles represent bacteria, protected by a pink wall. Both bacteria contain Lya dressed as a Princess. The bacterium interacts with the virus. This interaction is shown by Lya giving Kyan some spinach. The clouds are a metaphor for air as in this thesis respiratory viruses and bacteria have been used.

Back:

Kyan's muscles and the virus particle have been enlarged by the bacterial substance (shown as spinach).

Lay-out: Duy Tien Nguyen  
Printed by: Proefschriftmaken.nl || Uitgeverij BOXpress

ISBN: 978-90-8891-891-9

Financial support for printing of this thesis by the following companies is gratefully acknowledged:

Viroclinics Biosciences B.V.  
Greiner Bio-One B.V.  
ABN AMRO Bank N.V.

Proefschriftenfonds NVMM/KNVM  
Erasmus University Rotterdam

The research described in this thesis was conducted at the department of Viroscience, Erasmus Medical Center, Rotterdam, the Netherlands, and supported by VIRGO consortium (grant number: BSIK 03012) from the Dutch government. Furthermore, the research for this thesis was performed within the framework of the Erasmus Postgraduate School Molecular Medicine.



Copyright © 2014, Duy Tien Nguyen

All rights reserved. No part of this publication may be reproduced, stored in a retrieval database or published in any form or by any means, electronic, mechanical or photocopying, recording or otherwise, without the prior written permission of the author.

# **Interactions between Paramyxoviruses and Bacteria:**

Implications for Pathogenesis and Intervention

# **Interacties tussen Paramyxovirussen en Bacteriën:**

Implicaties voor Pathogenese en Interventie

## **Proefschrift**

ter verkrijging van de graad van doctor aan de

Erasmus Universiteit Rotterdam

op gezag van de rector magnificus

Prof.dr. H.A.P. Pols

en volgens besluit van het College voor Promoties.

De openbare verdediging zal plaatsvinden op

donderdag 26 juni 2014 om 15:30 uur

door

**Duy Tien Nguyen**

geboren te Enschede



## **Promotiecommissie**

Promotor: Prof.dr. A.D.M.E. Osterhaus

Overige leden: Prof.dr. M. Koopmans

Prof.dr. A. van Belkum

Prof.dr. R. de Groot

Copromotor: Dr. R. L. de Swart

## Table of Contents

	<b>Page</b>
<b>Chapter 1</b> General introduction Partially based on: <i>Eurosurveillance, 2012</i> and <i>Journal of Virology, 2012</i>	9
<b>Chapter 2</b> The synthetic bacterial lipopeptide Pam3CSK4 modulates respiratory syncytial virus infection independent of TLR activation <i>PLoS Pathogens, 2010</i>	27
<b>Chapter 3</b> Evaluation of synthetic infection-enhancing lipopeptides as adjuvants for a live-attenuated canine distemper virus vaccine administered intra-nasally to ferrets <i>Vaccine, 2012</i>	49
<b>Chapter 4</b> Infection-enhancing lipopeptides do not improve intranasal immunization of cotton rats with a delta-G candidate live-attenuated human respiratory syncytial virus vaccine <i>Human Vaccines and Immunotherapeutics, 2013</i>	63
<b>Chapter 5</b> A recombinant human respiratory syncytial virus subgroup B virus expressing enhanced green fluorescent protein illuminates viral pathogenesis <i>Submitted, 2014</i>	73
<b>Chapter 6</b> Paramyxovirus infections in ex vivo lung slice cultures of different host species. <i>Journal of Virological Methods, 2013</i>	89
<b>Chapter 7</b> <i>Streptococcus pneumoniae</i> exposure is associated with human metapneumovirus seroconversion and increased susceptibility to <i>in vitro</i> HMPV infection. <i>Clinical Microbiology and Infection, 2011</i>	101
<b>Chapter 8</b> <i>Streptococcus pneumoniae</i> modulates human respiratory syncytial virus infection <i>in vitro</i> and <i>in vivo</i> <i>Submitted, 2014</i>	111
<b>Chapter 9</b> Summarizing Discussion	125
<b>Chapter 10</b> References	135

## **Table of Contents (cont'd)**

	<b>Page</b>
<b>Chapter 11</b> Nederlandse Samenvatting	161
<b>Chapter 12</b> Tóm tắt tiếng Việt	167
<b>Addenda</b> Addendum I: About the Author	174
Addendum II: PhD Portfolio	175
Addendum III: List of Publications	177
Addendum IV: Dankwoord	179

## **The whole world is your home**

(adapted from “The whole world is my homeland”

by Desiderius Erasmus, 1469? - 1536)

**To all, who are deprived of education**





# Chapter I

## General Introduction

### Partially based on:

Magreet J. Te Wierik, D. Tien Nguyen, Thijs F. Beersma, Steven Thijsen, Karen A. Heemstra

An outbreak of severe respiratory tract infection caused by human metapneumovirus in a residential care facility for elderly in Utrecht, the Netherlands, January to March 2010.

*Euro Surveill* 17(13). pii: 20132, 2012

Martin Ludlow, D. Tien Nguyen, Dimitry Silin, Oksana Lyubomska, Rory D. de Vries, Veronika von Messling, Stephen McQuaid, Rik L. de Swart, W. Paul Duprex

Recombinant canine distemper virus strain Snyder Hill expressing green or red fluorescent proteins causes meningoencephalitis in the ferret.

*Journal of Virology* 86(14): 7508-7519, 2012

## Introduction

Infectious diseases are of all times and affect all age groups, and can be associated with high morbidity and mortality. Notable infectious diseases historically associated with high mortality were the plague or Black Death of the 14th century and childhood infections such as measles and the now eradicated smallpox. More recently infections with (re-)emerging bacterial infections such as multidrug resistant *Mycobacterium tuberculosis*, methicillin-resistant *Staphylococcus aureus* (MRSA) *Escherichia coli* O157:H7, extended-spectrum beta-lactamase (ESBL) gram-

negative pan-resistant organisms, or viruses like avian influenza viruses (H1N1, H5N1 and H7N9) [1] or coronaviruses (SARS-coronavirus [Severe Acute Respiratory Syndrome] and MERS-coronavirus [Middle-East Respiratory Syndrome]) [2] caused smaller and larger disease outbreaks.

In 2011, the World Health Organisation (WHO) estimated 54.5 million deaths based on annual reports of each member state. Lower respiratory tract infections (LRTI) were responsible for 6.7% of total number of estimated deaths in 2011 (3.2 million deaths; Figure 1A). An estimated 6.9

million children under five years died in 2011 and 17.5% died due to LRTI (1.2 million deaths; Figure 1B). LRTI are generally caused by bacteria and/or viruses and especially children under five years in developing countries die [3].

Frequently, these infections start in the

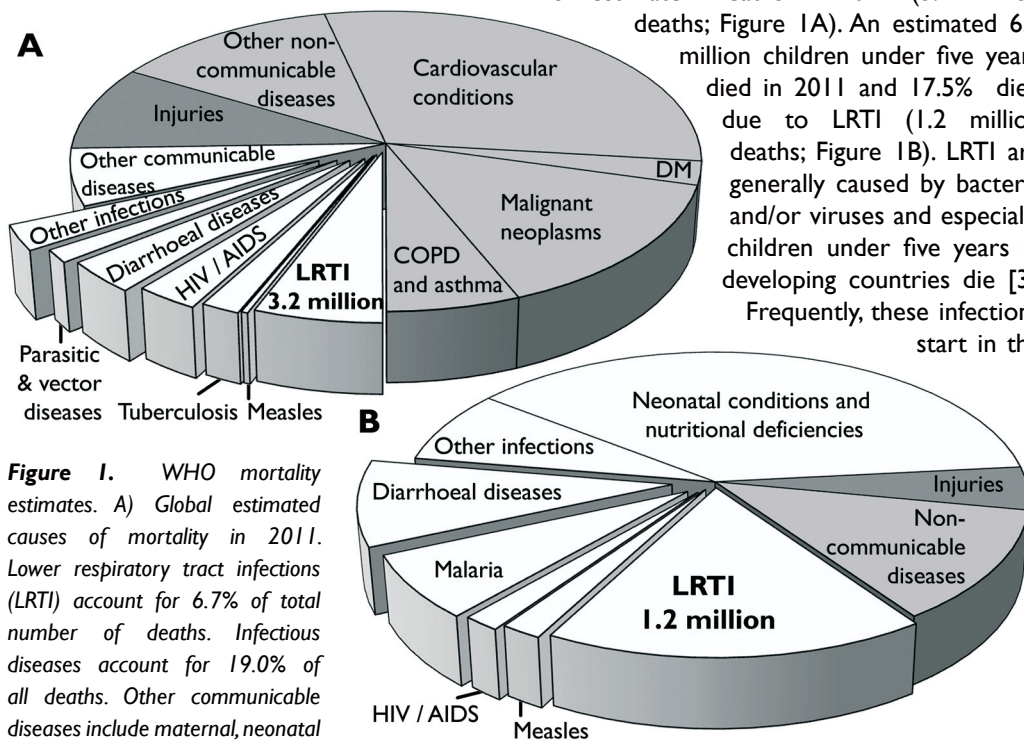


**Figure 1.** WHO mortality estimates. A) Global estimated causes of mortality in 2011. Lower respiratory tract infections (LRTI) account for 6.7% of total number of deaths. Infectious diseases account for 19.0% of all deaths. Other communicable diseases include maternal, neonatal and nutritional conditions. Non-communicable diseases (light grey) account for 66.4% of all deaths. DM: diabetes mellitus. Injuries (dark grey) account the remainder of the 54 million deaths in 2011. B) Global estimated causes of mortality of children under five years in 2011. LRTI account for 17.5% of all of deaths in children under five years. Forty-five percent of children under five years are caused by infectious diseases. Neonatal conditions and nutritional deficiencies account for 38%. Non-communicable diseases (light grey) and injuries (dark grey) result in 17% of all deaths in children under five years. Based on data from the WHO ([www.who.int](http://www.who.int)).

upper respiratory tract. The microbiome of the upper respiratory tract (URT) is extremely complex, and forms a reservoir for numerous bacterial commensals and pathobionts. These bacteria colonize the URT, but have the potential to cause invasive infectious disease. In children under five years the most prevalent pathobionts in the URT are *Streptococcus pneumoniae* (pneumococcus), *Haemophilus influenzae*, *Moraxella catarrhalis* and *Staphylococcus aureus*. As these four bacteria share their niche with respiratory viruses like human respiratory syncytial virus (HRSV) and human metapneumovirus (HMPV) [4] interactions between these pathogens can exist, and may have an effect on disease outcome. Pathogenesis studies can elucidate interactions between bacteria and viruses, thereby facilitating development of intervention strategies. The introduction of vaccines, antibiotics and antivirals, but also sanitation and access to clean water, has contributed to the reduction in global burden of disease due to infectious agents [5]. Vaccination (active immunization) is considered as the next most efficacious and cost-effective strategy to prevent infectious disease both at the individual and the population level [6].

This thesis focuses on interactions between paramyxoviruses and bacteria. The virus family *Paramyxoviridae* contains a number of important respiratory pathogens, including HRSV and HMPV. Other viruses of this family, measles virus (MV) and canine distemper virus (CDV), will be used to explore methodologies and intervention strategies.

### HRSV & HMPV

#### HRSV History

In 1956 Blount, Morris and Savage studied an outbreak of coryza in a colony of chimpanzees held under observation. They described the recovery of a cytopathogenic agent from

one of the fourteen chimpanzees and named it Chimpanzee Coryza Agent [7]. Soon after this discovery the agent was characterized as a (myxo)virus [8] and proved to be associated with acute respiratory disease in children. Two virus isolates (Long and Snyder) were obtained from children [9,10]. Epidemiological studies during the 1960s showed that this agent was a major cause of morbidity during early life, and suggested a wide prevalence of infection in the adult population [11-15]. The virus was renamed respiratory syncytial virus or RSV, as it gave a characteristic syncytial cytopathic effect in HEp-2 cultures (human epithelial cells derived from an epidermoid carcinoma of the larynx) [12]. The International Committee on Taxonomy of Viruses recently added the human feature to the name of the virus, and the virus is now formally called human respiratory syncytial virus (HRSV). To date HRSV is recognized as the most important viral agent of paediatric respiratory disease worldwide [16].

#### HRSV Molecular Biology

HRSV is a member of the family *Paramyxoviridae* of the order *Mononegavirales* [17]. This family consists of enveloped viruses with a negative stranded non-segmented RNA genome. The family *Paramyxoviridae* has two subfamilies: *Paramyxovirinae*, which includes the genus *Morbillivirus*, comprising MV and CDV, and *Pneumovirinae* which includes two genera: *Pneumovirus* to which HRSV belongs and *Metapneumovirus* to which HMPV belongs (Figure 2). The HRSV virion consists of a nucleocapsid surrounded by a lipid bilayer and appears as pleiomorphic spherical (100 - 350 nm in diameter) or long filamentous (60 - 200 nm in diameter) particles. The viral genome contains 15,222 base pairs and contains 10 transcription units encoding 11 proteins. There are 9 structural and 2 non-structural proteins.

## Family: Paramyxoviridae

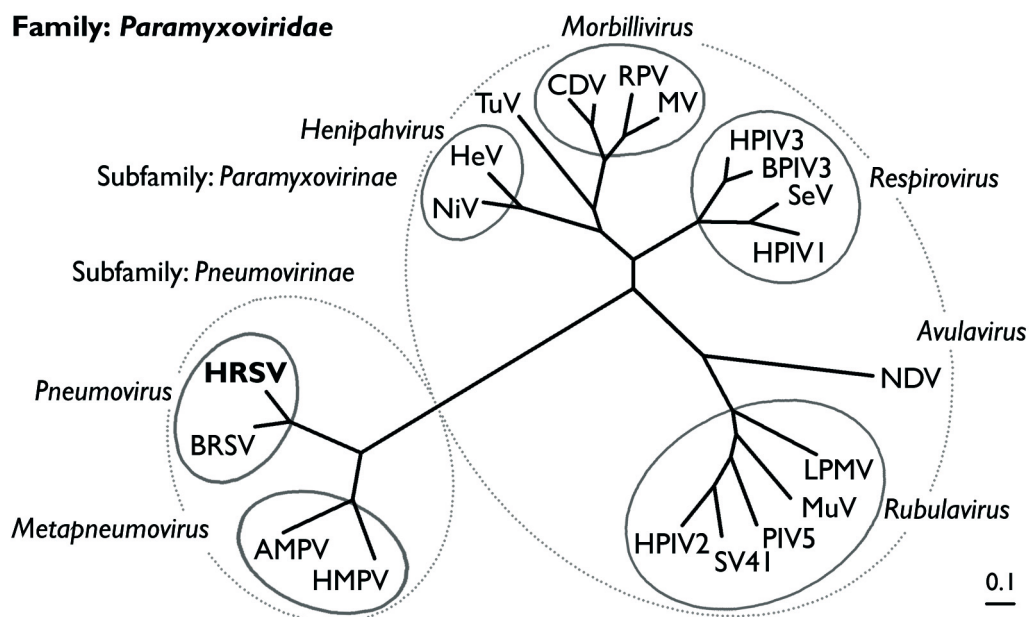


**Figure 2.** Phylogenetic tree of the family Paramyxoviridae based on analysis of the nucleotide sequences for the polymerase gene of these viruses. The family consists of two subfamilies each containing different genera. Abbreviations: HRSV: Human respiratory syncytial virus (marked in bold). BRSV: Bovine respiratory syncytial virus, AMPV: Avian metapneumovirus, HMPV: Human metapneumovirus, NiV: Nipahvirus, HeV: Hendravirus, TuV: Tupaia paramyxovirus, CDV: Canine distemper virus, RPV: Rinderpest virus, MV: Measles virus, HPIV3: Human parainfluenza virus 3, BPIV3: Bovine parainfluenza virus 3, SeV: Sendai virus, HPIV1: Human parainfluenza virus 1, NDV: Newcastle disease virus, LPMV: La Piedad Michoacán virus (porcine rubulavirus), MuV: Mumps virus, PIV5: Parainfluenza virus 5, SV41: Simian virus 41, HPIV2: Human parainfluenza virus 2. Phylogenetic tree courtesy of prof.dr. R.A.M. Fouchier

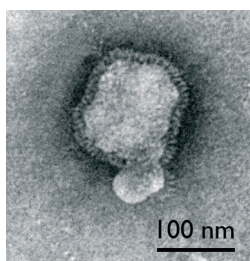


**Figure 3.** Negative contrast electron micrograph of HRSV virion. Bar represents 100 nm. Micrograph made by Georgina Aron.

The viral envelope is derived from the host cell, and contains three viral transmembrane glycoproteins: the fusion (F) protein, the attachment (G) protein, and the small hydrophobic (SH) protein. These proteins appear as brush-like spikes on the particle (Figure 3). The F protein mediates fusion of the virus membrane and the target

cell membrane, resulting in release of the viral ribonucleoprotein (RNP) into the cytoplasm [18]. The trimeric F protein rearranges from a metastable pre-fusion conformation to a highly stable post-fusion conformation [19]. Both the pre- and post-fusion conformation of the F protein can be present on the viral membrane simultaneously [19]. Furthermore, the F protein can also cause cell-cell fusion, resulting in the formation of multinucleated giant cells (syncytia) [20].

The glycoprotein G was first identified as the major attachment protein for HRSV [21]. Recombinant HRSV engineered without a G protein was still infectious *in vitro*, but highly attenuated *in vivo* [22]. The G protein is heavily glycosylated with a content of

about 60% carbohydrate by weight, of which approximately 20% is N-linked carbohydrate and 80% O-linked carbohydrate [23,24]. These carbohydrates are attached to an unusually high number of hydroxyl-aminoacids (serine and threonine), suggesting the G protein has a mucin-like structure [25,26]. The amino acid sequence of the G protein displays a high level of variability between HRSV strains, with the exception of the central conserved core domain [26].

The third membrane glycoprotein is the small hydrophobic protein SH, previously known as IA [27]. SH may have a role in immune evasion [28]. However, HRSV lacking SH can still replicate *in vitro* [22,29]. The non-structural proteins NS1 and NS2 have a role in immune evasion by antagonizing pivotal innate immune pathways [30,31] and suppress premature apoptosis [32]. The viral RNA is coated with the nucleoprotein (N) and forms a nucleocapsid complex with the phosphoprotein (P) and the large RNA polymerase protein (L).

The last two structural proteins M2-1 and M2-2 have a function in transcription [33]. Interestingly, M2-2 has an overlap with the L gene of 68 nucleotides. M2-1 and M2-2 are novel RNA synthesis factors. M2-1 is a transcription processivity factor: in its absence, transcription terminates prematurely and non-specifically within several hundred nucleotides [34,35]. M2-1 also enhances read-through transcription at gene junctions to generate polycistronic RNAs [36]. M2-1 is a homo-tetramer that binds to the P protein and RNA in a competitive manner [37].

### HRSV Epidemiology

HRSV circulates globally, and is considered as one of the most important causes of respiratory tract disease in infants (Figure 4A), immunocompromised and the elderly. Annually, HRSV causes epidemics in the rainy season in tropical climates and during the winter season in moderate climates (Figure

4B). Two subgroups of HRSV (A and B) have been described, mainly based on genetic differences in the G protein gene [17]. During epidemics HRSV subtypes A and B can co-circulate, but usually one subtype dominates. HRSV is highly contagious and is spread via droplets originating from coryza, sneezing or coughing. Major transmission routes are direct contact with an infected individual or with contaminated surfaces, like hands, doorknobs, toys, stethoscopes or clothes. HRSV can survive for several hours on these surfaces [38]. Infection is established by subsequent 'self-infection' to nasal and conjunctival mucosae. These features result in efficient transmission, particularly in day care centers, elementary school, hospitals or households.

HRSV causes respiratory tract infections in all age groups. By the age of two years nearly all children have been infected by HRSV at least once and 50% have experienced two or more HRSV infections [17]. The majority of HRSV infections remain limited to the upper respiratory tract. However, HRSV can also spread to the lower respiratory tract. An estimated 0.5-2% of all infected children under one year are hospitalized with a severe HRSV infection. Of these children 7-21% require ventilator support. These numbers are higher in developing countries [16].

HRSV also causes a significant burden in terms of morbidity and mortality in the elderly [39]. The same is true for immunocompromised adults [40,41]. The disease burden in healthy children and adults is significantly less, although multiple re-infections occur throughout life [42].

### HRSV Clinical Manifestations

The incubation time of HRSV is 4-5 days. Clinical signs of HRSV infection are rhinorrhea, sneezing, coughing and a low-grade fever. Two to five days later infection can spread to the lower respiratory tract [41,43] and clinical outcome can be more severe, like bronchiolitis and pneumonia or

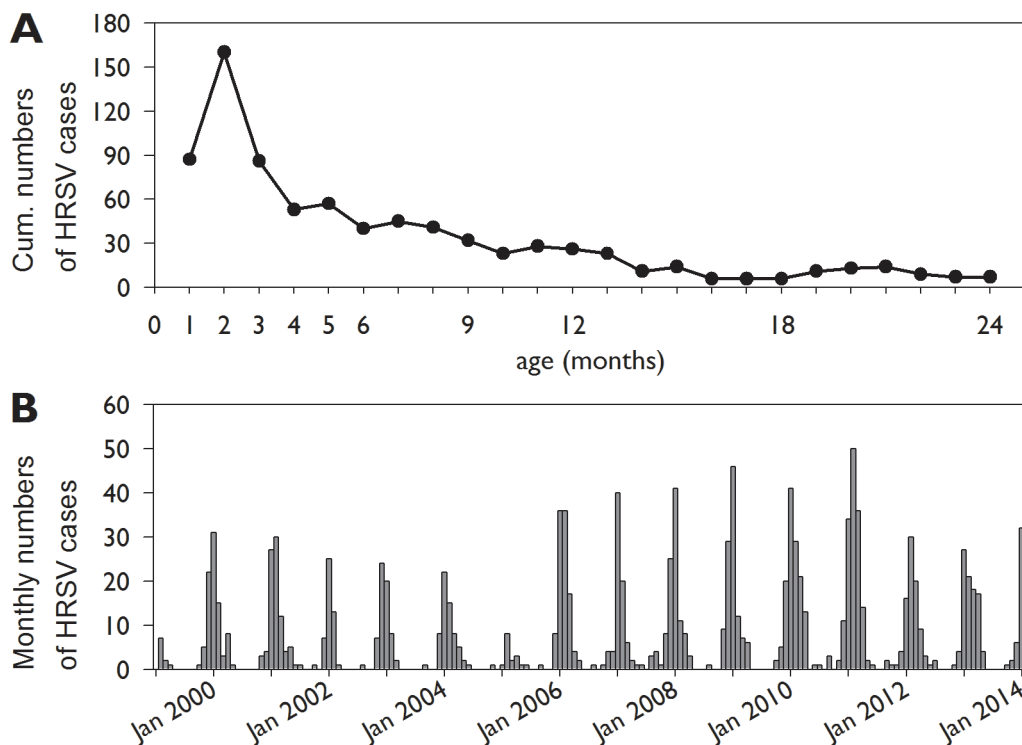


**Figure 4.** Epidemiology of HRSV. A) Cumulative number of HRSV patients by age (until 2 years) of the Erasmus MC Rotterdam from 1999 until 2013. Highest incidence is between birth and 6 months of age with peak at 2 months. B) Number of HRSV patients diagnosed monthly at the department of Viroscience of the Erasmus MC Rotterdam from 1999 until 2013. Annual winter outbreaks can clearly be recognized (data kindly provided by Hans Kruining).

death. The risk for severe HRSV disease is higher in individuals in whom the immune system is under development (infants younger than six months), suppressed (by disease, auto-immune disease, transplant patients) or immunosenescent (the elderly). Especially, children with underlying comorbidity such as prematurity, bronchopulmonary dysplasia, congenital heart disease with pulmonary hypertension or immune deficiency are at risk [37]. As a result of HRSV LRTI, the lumina of the lower airways can become obstructed, resulting in increased airway resistance, air trapping (hyperinflation), wheezing, apnea, and hypoxia. Apnea usually is an initial presenting symptom in short episodes. It occurs in approximately 20-25% of young infants. In

severely affected infants also nasal flaring, intercostal, subcostal, or sternal retractions, and circumoral and nailbed cyanosis can be present. Patients, especially children, with severe LRTI may require ventilatory support and in the worst case even extracorporeal membrane oxygenation.

### HRSV Pathogenesis

Inoculation of the nose or eyes occurs by large particle aerosols or direct contact, and results in viral replication in ciliated epithelial cells of the nasopharynx [44,45]. HRSV does not invade underlying cell layers of the respiratory tract [46], sparing the basal epithelium [47]. It is unknown how HRSV infection spreads from the upper respiratory tract to the lower

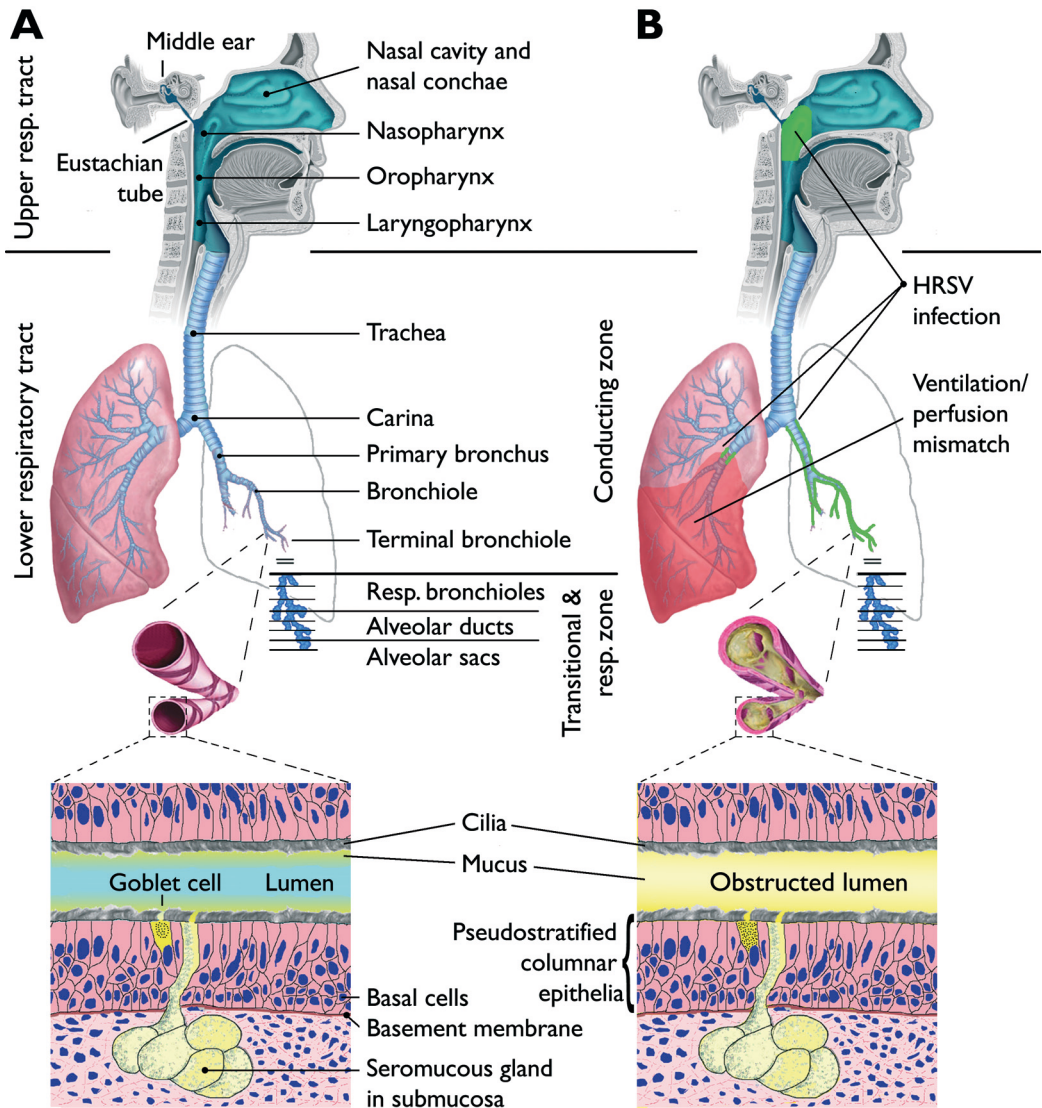


**Figure 5.** HRSV pathogenesis. A) Physiological situation. The upper respiratory tract includes the pharynx and the middle ear, which can be reached by the Eustachian tube (sinuses are not shown). The lower respiratory tract consists of the conducting zone, including trachea, primary bronchi, bronchioles, terminal bronchioles, and the transitional and respiratory zone, which includes respiratory bronchioles, alveolar ducts and alveolar sacs. The first magnification shows a terminal bronchiole. The second magnification shows a schematic representation of the histology of the ciliated epithelium in the airways. Mucus containing dust, debris, and pathogens is transported upwards by ciliated epithelial cells, which can be renewed by proliferation of cuboidal-shaped basal cells. Note the goblet cell, which produces mucins. Mucins mixed with the secretions of seromucous glands forms mucus. The respiratory epithelium also contains dendritic and lymphoid cells, which are not included in this schematic representation. B) HRSV infection. Ciliated epithelial cells of the nasopharynx are infected with HRSV (green), which has spread to the lower respiratory tract. In the magnification a terminal bronchiole with thickened alveolar walls and mucus plugging is shown. In the

## Chapter I

schematic representation the lumen of the airway is obstructed with a mucus plug containing virus, exfoliated cells, induced by HRSV infection. Alveolar sacs linked to obstructed (terminal) bronchioles are not ventilated. A ventilation/perfusion mismatch follows (see red area of left lung) with possible detrimental results.

respiratory tract, presumably this occurs by aspiration of contaminated secretions. Cell-to-cell spread is an unlikely mechanism, as in animal studies the tracheal epithelium rarely becomes infected [48]. Moreover, transmission to the LRT occurs against the direction of the mucociliary escalator. HRSV infection in the nose can lead to excess mucus secretion by glands in the nasal mucosa. Ciliated epithelial cells line the mucosa and project mucus with entrapped pathogens to the throat where it can be swallowed and digested by stomach juices, preventing spread to the lungs and worsening tissue damage. Under low temperature conditions cilia movement of nasal epithelial cells can be reduced, leading to accumulation of mucus and dripping from the nostrils (rhinorrhea). Furthermore, HRSV infection itself can lead to impaired cilia beating [49-51].

In the lower respiratory tract HRSV infection is mainly restricted to ciliated epithelial cells and is shed apically into the lumen of the airways. In addition, type 1 and 2 alveolar pneumocytes can become infected [47]. In very rare cases HRSV may be recovered from extrapulmonary tissues, such as liver [52], cerebrospinal fluid (CSF) [53], or pericardial fluid [54]. In two reports, HRSV genome could be detected in blood, but no infectious virus could be isolated [55,56]. This finding may represent phagocytized virus present in circulating monocytes. HRSV infection in the LRT may also lead to enhanced mucus secretion and impaired cilia movement. In affected lower airways apoptosis and necrosis of epithelial cells can be seen, resulting in mucus plugs which also contain inflammatory cell debris mixed with fibrin, mucus, and edema [47]. Infiltrates of monocytes and T cells can be observed around bronchial and pulmonary arterioles,

and neutrophils between the vascular structures and small airways. The combination of excessive mucus secretion, impairment of cilia beating and airway plugging leads to the classical signs of HRSV bronchiolitis [57].

### HMPV Background and History

HMPV is a respiratory virus closely related to HRSV (Figure 2). The virus was first described in 2001 in children with RTI and was soon after recognized as a ubiquitous human pathogen [58,59]. HMPV also belongs to the subfamily *Pneumovirinae* and the viral genome of HMPV resembles that of HRSV, but HMPV lacks the NS1 and NS2 genes [60]. HRSV and HMPV share many other properties, including clinical signs, transmission routes and the existence of two subgroups [61,62]. HMPV also causes seasonal outbreaks but these usually occur slightly later than those caused by HRSV, starting late winter until early spring [63]. Studies show that almost all children have been infected by HMPV at the age of five and re-infections occur throughout life [59,63,64]. Risk factors for severe HMPV disease are the same as those for severe HRSV disease [58,64,65]. Also in patients with HMPV-associated severe disease bacterial pathogens such as *Streptococcus pneumoniae* can often be detected [66]. Since the discovery of HMPV outbreaks in institutionalized adults and elderly has been reported [67-70].

We have studied a HMPV outbreak in a residential care facility for elderly in the Netherlands [71], including active surveillance for new cases. With the combination of real-time reverse transcriptase polymerase chain reaction (qPCR) and serology 9 confirmed, 6 probable and 6 possible cases could be identified. Four people died during the outbreak. We concluded that the combined approach of qPCR and serology had an added



diagnostic value and that HMPV is a serious pathogen for institutionalized elderly.

### **HRSV, HMPV and *Streptococcus pneumoniae***

Within hours after birth the human upper respiratory tract is colonized by diverse bacteria. This microbiome can be (transiently) changed by invasion by other bacteria and pathobionts. During both infancy and adulthood a substantial percentage of healthy people are colonized by *Streptococcus pneumoniae* (pneumococcus), *Haemophilus influenzae*, *Moraxella catarrhalis*, or *Staphylococcus aureus* [72]. *S. pneumoniae* causes a high disease burden in children, the elderly and immunocompromised. Up to 60% of children under five years and up to 20% of adults are colonized in the nasopharynx with *S. pneumoniae*. Once colonized by *S. pneumoniae*, the bacterium can cause respiratory tract infections, but also invasive diseases, such as meningitis and sepsis [73]. Polyvalent conjugated vaccines have been introduced that protect against several of the 92 serotypes of *S. pneumoniae* [74].

Respiratory bacteria and respiratory viruses such as HRSV and HMPV all target the respiratory epithelium of the URT. In addition to sharing the same niche, peak prevalence of disease burden coincides for *S. pneumoniae* and respiratory viruses during the winter season [75]. Immediately after the discovery of HRSV Beem *et al.* could culture pneumococcus from an HRSV infected infant [11]. These observations suggested that pneumococcus and HRSV / HMPV have the potential of bi-directional interactions.

Respiratory virus infection could lead to bacterial superinfection, and pneumococcus colonization could predispose for respiratory virus infection. Indeed, *in vitro* experiments show that HRSV-infected human epithelial cells enhanced adherence of *S. pneumoniae* [76]. Also, HRSV is able to bind directly to pneumococci [77,78]. Mice infected with HRSV

4 days before pneumococcal challenge or mice treated simultaneously with both virus and bacterium showed significantly higher levels of bacteraemia than controls [78]. Retrospective analysis of children who received high doses of HRSV-Ig developed fewer episodes of acute otitis media than controls that did not receive HRSV-Ig [79]. These results show that respiratory virus infection can predispose for bacterial superinfection. However, it has also been suggested that bacteria may predispose for or enhance respiratory virus infections. Mahdi *et al.* showed in a clinical trial that pneumococcal vaccination were able to reduce the incidence of hospitalization for pneumonia associated with HRSV by 32% [80]. The same authors showed that pneumococcal vaccination reduced the incidence of HMPV-associated LRTI by 45% and the incidence of clinical pneumonia was reduced by 55% [81]. Further research is needed to evaluate if pneumococcus colonization can enhance HRSV or HMPV infection and may elucidate possible mechanisms between bacterial and viral interactions.

### **Morbilliviruses**

As shown in Figure 2, the subfamily *Paramyxovirinae* includes the genus *Morbillivirus*, of which measles virus (MV), the causative agent of measles in humans, and canine distemper virus (CDV), the causative agent of distemper in many carnivores, are well-known members [82]. Morbilliviruses are transmitted via the respiratory route and cause systemic disease in humans and animals.

### **Measles virus**

Despite the availability of a safe and effective live-attenuated vaccine, measles remains a significant childhood disease. In 2011, there were 166,800 measles deaths globally, especially in the developing world [83]. The virus is highly infectious and is spread via the respiratory route [84]. Unlike HRSV, MV and CDV infections lead to systemic disease.

After initial infection of dendritic cells in the respiratory tract, these cells migrate to lymphoid tissues [85]. Here the virus is transmitted to T- and B-cells expressing the cellular receptor CD150, predominantly memory T-cells and follicular B-cells. Infection and subsequent immune-mediated depletion of these cells causes immune suppression mediated by temporary immunological amnesia [86], resulting in increased susceptibility to opportunistic infections. Thus bacterial pneumonias and other co-infections are the most important mediators of measles-associated mortality [82].

Recently, poliovirus receptor-related 4 (PVRL4 or nectin 4) was identified as a cellular receptor for morbilliviruses expressed by epithelial cells [87,88]. Interestingly, PVRL4 is an adherens junction protein which is expressed on the basolateral surface of differentiated epithelial cells. As a consequence, epithelial cells do not become infected until the late stage of disease, when MV-infected immune cells infiltrate the respiratory submucosa. Current models for the pathogenesis of measles fully explain the clinical signs: initial high fever, rhinorrhea, coughing, Koplik spots (small white spots on the gum), immune suppression, systemic rash and finally transmission facilitated by MV infected respiratory epithelial cells [84,89,90].

New insights into MV pathogenesis were facilitated by the availability of recombinant (r) viruses expressing enhanced green fluorescent protein (EGFP), which proved to be invaluable tools for tracing pathways of virus infection [91-93] and have enabled the rapid and sensitive identification of infected cells. In order to mimic the natural disease, it is of crucial importance that the molecular clone reflects the virulence and biological properties of a wild-type virus.

### Canine distemper virus

CDV has been well known as an important pathogen of domestic dogs (*Canis lupus familiaris*). However, other carnivores can also be infected [94]. Furthermore, three outbreaks of CDV were reported in captive non-human primate species (including *Macaca fuscata*, *Macaca mulatta* and *Macaca fascicularis*) [95-97]. Like the closely related MV, CDV initially targets lymphoid tissues and induces a profound lymphopenia, resulting in immune suppression [98,99]. Unlike MV, infection of the central nervous system (CNS) is common [94]. The combination of severe immune suppression, which causes increased susceptibility to opportunistic infections, and infection of the CNS may explain the high mortality rate associated with distemper.

Recombinant CDV strains expressing EGFP have been developed and facilitated our understanding of CDV pathogenesis [98,100]. These recombinant viruses retained virulence upon infection of ferrets and caused fatal disease. Silin *et al.* reported that insertion of the open reading frame of EGFP into the coding sequence of the viral polymerase attenuated a wild-type canine distemper virus [101]. Such rational attenuation of viruses could be a strategy in development of next generation vaccines. In addition to recombinant viruses expressing EGFP, we have also evaluated viruses expressing other fluorescent proteins.

Red fluorescence could have the additional benefit of increased tissue penetration [102]. A recombinant CDV strain containing an additional transcription unit encoding the red fluorescent protein dTomato (dTom) [103] was generated [100]. Interestingly, the red fluorescence observed in CDV-infected tissues at necropsy was indeed more intense than the green fluorescence mediated by EGFP. However, in brain parenchyma EGFP proved to be a more sensitive indicator of virus infection due to high levels of red autofluorescence emitted by neural tissue,

which hindered the sensitivity of dTom upon examination of vibratome-cut brain sections. Therefore, we concluded that the choice of fluorescent protein to be used for macroscopic and microscopic imaging in tissues is dependent on the specific tissue(s) targeted by the virus *in vivo*.

### Immunity to HRSV

#### Innate Immunity to HRSV

The innate defenses of the airways are complex, consisting of several physical, cellular and antimicrobial components. Mechanical defenses prevent antigens and microorganisms from entering the lungs. These mechanisms start in the nasopharyngeal cavity, which functions as a filter by capturing or trapping large particles in the nasal hair or fimbriae. The unfiltered smaller particles are inhaled and deposited in the upper and lower airways, where mucociliary blanket lining the airways surface act in two ways. A network of mucin polymers traps small particles [104] and these entrapped particles are then removed through ciliary movements [105]. In addition, a range of soluble mediators excreted into the mucus, such as lysozyme, lactoferrin, collectin and defensins also have a barrier function through direct lysis of pathogens, opsonization for phagocytic cells or the recruitment of inflammatory cells [106].

A second antiviral defense mechanism involves pattern recognition receptors (PRRs), which detect pathogen associated molecular patterns (PAMPs) of invading viruses, bacteria and other pathogens. Evolutionarily conserved PRRs on host cells can be present either extra- or intra-cellularly, and can be subdivided into different families. These include toll-like receptors (TLRs), retinoic acid-inducible gene (RIG)-I-like receptors (RLRs), and nucleotide-binding oligomerization domain (NOD)-like receptors (NLRs) [105,107-110]. Binding of PAMPs to PRRs ultimately leads to transcription and production of interferon

(IFN) via multiple signaling pathways and transcription factors such as Nuclear Factor Kappa B (NF- $\kappa$ B) and interferon regulatory factor (IRF) family [111,112]. IFN production is a key event in the initiation of the innate antiviral immune response against virus infections. It has been demonstrated that type-III rather than type-I interferons are the predominant innate immune response induced by HRSV in nasal epithelial cells [113].

HRSV predominantly targets ciliated epithelial cells, superficially located within the respiratory tract, but the hallmark of HRSV bronchiolitis is an exaggerated inflammatory response. Therefore, it is assumed that severe HRSV disease is to a large extent immune-mediated [114-116]. Dendritic cell (DC) activation, migration to and positioning within lymphatic tissue are critical for induction of an effective adaptive immune response [111,112,117]. For HRSV it has been shown that infection induces different patterns of maturation in different DC subsets [118]. Also HRSV-stimulated DC inefficiently migrate to lymphatic tissue thereby reducing adaptive responses to HRSV [119]. HRSV-infected epithelial cells in the URT and adjacent non-infected cells produce numbers of immunomodulatory and inflammatory mediators (such as IL-1, TNF- $\alpha$ , IL-6, and IL-11), chemokines (IL-8, GRO, MCP-1, MIP-1 $\alpha$ , RANTES), type 3 interferons and growth factors (GM-CSF, G-CSF) [49,120,121]. These HRSV-induced cytokines and chemokines can mobilize eosinophils, neutrophils, basophils, monocytes and T-cells from the bloodstream into the infected tissue. Under ideal circumstances these effector cells can mediate clearance of HRSV-infected cells, but the influx of inflammatory cells can sometimes be overwhelming, resulting in HRSV-induced lung disease mediated by host inflammatory immune responses [114,115]. HRSV-induced inflammatory infiltrates are usually co-localized with

bronchial and pulmonary arterioles and consist of monocytes, neutrophils and T-cells. Neutrophils are mainly located between arterioles and airways, while mononuclear cells can be found in both airways and lung parenchyma [122]. In a study of 14 intubated infants, 93% and 76% of the recovered inflammatory cells were neutrophils from the upper and lower respiratory airways, respectively [123]. Eosinophils are occasionally observed in peribronchiolar infiltrates, but are not a dominant component of the inflammatory process. Most inflammatory cells are concentrated submuscular to the airway, but many cells traversed the smooth muscle into the airway epithelium and lumen [122].

HRSV is able to counteract innate immune responses by various mechanisms. The non-structural HRSV proteins NS1 and NS2 have a role in immune evasion by antagonizing pivotal innate immune pathways, like NF- $\kappa$ B, IRF, STAT2, RIG-I [30,31,124,125]. In addition NS1 and NS2 suppress premature apoptosis and maturation of human DCs [32,126].

### **Associations between TLR Responses and HRSV Disease**

TLR-mediated innate immune responses have often been associated with the development of severe HRSV disease. These interactions can either result from co-infections or from direct interactions between HRSV and TLRs. Several *in vitro* and *in vivo* studies have suggested a role for TLR4 in HRSV-induced lung disease as HRSV-F protein can bind to TLR4 [127-132]. Also genome-wide association studies show a relation between TLR4 and increased risk of severe HRSV disease. Two mutations in TLR4 alleles (Asp229Gly and Thr399Ile) were associated with increased risk of severe HRSV bronchiolitis in infants [133-135]. However, this finding could not be confirmed by other groups [136-138]. TLR3, 7, 8 and 9 are involved in the innate response to viral infections and can directly bind to components of HRSV

genome [109].

### **Adaptive Immunity to HRSV**

Both the cellular and humoral compartment of the adaptive immune response may play a role in the immune response to HRSV. Virus neutralizing (VN) antibodies are predominantly directed to the transmembrane glycoproteins F or G. Antibodies to both HRSV-F and G have been associated with protection against HRSV [139]. Protection against HRSV is rarely sterile, as even in the presence of high VN titers the upper respiratory tract can be infected. However, VN antibodies can prevent development of severe LRTI [140-142]. The cellular immune response to HRSV includes virus-specific CD8<sup>+</sup> cytotoxic T-cells and CD4<sup>+</sup> T-helper (Th) cells [143]. T-cells play an important role in clearing HRSV infection. Children with a compromised cellular immune system can shed virus for many months, in contrast to 1-3 weeks in healthy children [41,144]. Also, T-cell depleted mice showed prolonged HRSV shedding, while transferring CD4<sup>+</sup> and CD8<sup>+</sup> T-cells cleared HRSV quicker [145,146].

HRSV-specific adaptive immune responses have not only been associated with (partial) protection from disease, but also with disease enhancement. Sub-neutralizing HRSV-specific antibody titers may result in virus opsonization or co-stimulation of infected dendritic cells [147-149]. Furthermore, cellular immune responses, in particular a misbalance between Th1, Th2 and Th17 responses, have been associated with development of severe HRSV disease [150]. Many of these events occur at the interphase between innate and adaptive immune responses, with a central role for professional antigen-presenting cells such as DCs [116,151].

### **HRSV prophylaxis**

Since HRSV infection is ubiquitous and causes a substantial disease burden, a globally

available safe and effective HRSV vaccine would be highly cost-effective. Unfortunately, at the moment there is no licensed vaccine available. In this section infection control and prophylaxis strategies will be discussed.

### **HRSV Infection Control**

Major transmission routes of HRSV can effectively be blocked by basic hygienic measures such as hand washing, avoiding self-inoculation to nasal and conjunctival mucosae, and disinfecting potentially contaminated surfaces, such as doorknobs, toys and clothes. Prevention of nosocomial HRSV transmission is achieved by strict hand washing between patients, disinfecting stethoscopes, use of gloves by caregivers and limiting exposure to infected patients. Nosocomial outbreaks in neonatal intensive care units have been described [152], and may be controlled by active surveillance, immunoprophylaxis and hygienic measures [153-155].

### **HRSV Vaccine Development**

Early after the discovery of HRSV, a candidate vaccine was constructed in the spirit of that time. Virus was inactivated with formalin, and formulated with aluminum hydroxide as an adjuvant. In clinical trials performed in the 1960s this formalin-inactivated HRSV (FI-HRSV) vaccine was shown to induce specific but transient antibody responses. However, following natural HRSV infection vaccinated children developed enhanced disease. Up to 80% of the vaccinated children were hospitalized due to bronchiolitis and pneumonia, and two children died [156-158]. Histopathological evaluation of the lungs of the two children who died showed inflammation around the small airways with cellular infiltrates [52,157]. Experimental infections in animal models demonstrated that FI-RSV primed for strong Th2 responses in the absence of protective CD8<sup>+</sup> responses [159,160]. This pulmonary hypersensitivity response was confirmed in mice in which Th2

skewed mice showed enhanced diseases, but not in Th1 skewed mice [161-165]. Additional studies suggested that the vaccine induced low avidity non-neutralizing antibodies, promoting immune complex deposition in the lungs [166,167].

The dramatic outcome of the clinical trials with the FI-HRSV vaccine has strongly influenced subsequent development of new generation vaccines against HRSV. Since HRSV causes severe disease in very young infants, a candidate vaccine must be effective at an early age, in the presence of maternal antibodies and an incompletely developed immune system. Furthermore, the vaccine must induce a better and more durable protective immune response than the natural HRSV infection, and should avoid priming for unbalanced immune responses that may be associated with disease enhancement. Finally, the lack of good animal models that reflect all aspects of HRSV pathogenesis restricts the evaluation of new vaccination strategies [168].

The use of a live-attenuated virus is an attractive approach and has already yielded major success in other vaccine fields. However, the difficulty for such a vaccine against HRSV experienced over the last several decades is to find a delicate balance between attenuation and immunogenicity [169,170]. Such a live-attenuated HRSV vaccine must be sufficiently attenuated to avoid vaccine-induced disease and must robustly elicit an immune response in order to protect human for (severe) HRSV disease. Several research groups and pharmaceutical companies are trying to develop alternative strategies towards developing an HRSV vaccine, and several candidate vaccines have undergone pre-clinical or clinical evaluation.

Candidate vaccines include live, inactivated, subunit, vectored or nucleic acid vaccines [171,172]. In addition to vaccination of infants, maternal vaccination is being considered as a strategy to prevent severe disease in young

infants [173]. During pregnancy maternal IgG antibodies are being transferred to the fetus, which protect the newborn during the first period of life against all kinds of pathogens. Indeed, HRSV-specific virus neutralizing antibodies are present in the sera of all full-term neonates [174]. High maternal antibody levels can result in LRT protection, which is confirmed by the observation that infants younger than 6 weeks are often spared from severe HRSV disease [175]. HRSV-specific maternal antibodies decline with a half-life of approximately 26 days, and become undetectable between 6 and 12 months of age [176,177]. As the greatest HRSV hospitalization burden lies in infants younger than 6 months of age, maternal immunization could potentially prevent a significant proportion of serious LRTI in early infancy.

### **HRSV Passive Immunization**

Passive administration of HRSV-specific VN antibodies provides substantial protection against severe HRSV disease [178,179]. Antibody prophylaxis does not prevent infection in the rather immune-privileged nasal cavity, but can restrict replication in and spread to the lower respiratory tract. In 1996 HRSV Intravenous Immune Globulin (RS-IVIG, Respigam™, MedImmune) was licensed. The product consisted of purified serum antibodies from donors screened for high HRSV-neutralizing activity. Monthly administration of RS-IVIG resulted in 55% reduction of hospitalization rates and 97% reduction of days spent on the neonatal intensive care unit [180]. However, HRSV-IVIG had some major disadvantages, including a relatively high infusion volume [181]. Therefore, new generation HRSV-specific VN antibody preparations were developed.

In 1998 Palivizumab (Synagis™; MedImmune) was licensed. Palivizumab is a humanized HRSV-neutralizing, F-specific monoclonal antibody derived from a murine monoclonal antibody 1129. The composition

is 95% human antibody sequences and 5% murine antibody sequences, and it is directed to an epitope in the A antigenic site of the F protein of HRSV [37,181-183]. Inhibition of HRSV replication occurs by its neutralizing and fusion-inhibitory activities of both A and B subtypes. At the moment Palivizumab is the only licensed product available. A large disadvantage is that Palivizumab is expensive. Fifteen mg/ kg intramuscularly injected per month is needed to prevent severe HRSV disease, resulting in debates about its cost-effectiveness [184,185]. Also, Palivizumab-resistant circulating viruses can cause a problem. Around 5% of individuals with prophylactic treatment still develop HRSV LRTI [186].

In recent years new monoclonal antibodies have been developed and tested in clinical trials. A derivative of Palivizumab, motavizumab (MEDI-524), showed superior results in binding, neutralization and in an animal model [178,181]. Also, in preterm infants motavizumab showed better protection than palivizumab [187,188]. However, motavizumab was associated with a slight increase in the incidence of hypersensitivity reactions and anti-drug antibodies. Therefore, further trials with motavizumab were discontinued. Another potent, neutralizing anti-HRSV monoclonal was compound 101F, which is a murine antibody [189]. Although this compound was not extended to clinical trials, it revealed the structure of a major antigenic site on HRSV-F protein [190]. A promising *Pneumovirinae* cross-neutralization human monoclonal antibody, MPE8, was recently developed [191]. This antibody can neutralize both HRSV and HMPV *in vitro* and *in vivo*.

### **HRSV Treatment**

The majority of HRSV infections do not require treatment. Re-infections are usually either asymptomatic or limited to the URT. In patients admitted to the hospital with severe HRSV disease treatment is primarily

supportive, which includes respiratory support and adequate fluid and nutrition management [192]. Nasal obstruction is a common problem, given that young infants are obligate nose breathers. Nasal toilet with saline drops and suction may improve breathing. Infants with hypoxemia refractory to supplemental oxygen, persistent respiratory distress require ventilatory support or even extra-corporeal membrane oxygenation (ECMO). Treatment with bronchodilators, corticosteroids, immunoglobulins or antivirals (palivizumab, ribavirin) is usually not effective [192,193]. Ribavirin, a nucleoside analogue that interferes with the replication of a number of RNA and DNA viruses, may be effective in immunocompromised patients who shed prolonged HRSV [40,194]. Antibiotics should be used in patients when specific evidence of coexistent bacterial infection is present as secondary bacterial infections are common in severe HRSV infections [195,196].

### **HRSV Chronic Sequelae**

Studies show that there is an increased risk of subsequent wheezing in HRSV infected children [197-202]. It is debated whether HRSV infection induces changes that lead to development or exacerbation of asthma. Several studies suggest a causal inference for HRSV for developing asthma. Two prospective epidemiologic studies suggest a 30-40% likelihood of recurrent asthma-like episodes after HRSV LRTI in early life [203,204]. In mice repeatedly infected HRSV impaired regulatory T-cell function and attenuated tolerance to inhaled allergens [205]. A recent industry-sponsored, prospective, multicenter trial concluded that palivizumab treatment resulted in a relative reduction of 61% in the total number of wheezing days during the first year of life and the proportion of infants with recurrent wheeze was 10 percentage points lower in patients treated with palivizumab [206]. These studies implicate HRSV infection as an important mechanism of recurrent

wheeze during early childhood.

### ***In vitro* and *in vivo* Models for HRSV Infection**

Understanding the pathogenesis of a disease is essential for prevention, diagnosis, treatment, and follow-up. However, pathogenesis studies of virus infections are rather inefficient if virus-infected cells and virus spread cannot be visualized. Recently recombinant paramyxoviruses encoding fluorescent proteins have been developed as described above. Infection with these viruses results in production of fluorescent proteins by the host, which can be detected macroscopically and microscopically with unprecedented high sensitivity.

Recombinant HRSV strains have also been developed, but these were based on laboratory-adapted strains. The recombinant HRSV strain A2 encoding green fluorescent protein, rgRSV, turned out to be more glycosaminoglycan-dependent than wild-type HRSV viruses [207]. Therefore, there is an urgent need for new molecular clones encoding fluorescent proteins based on non-cell culture-adapted virus sequences, which are expected to be less laboratory-adapted and more reminiscent of a true wild-type HRSV infection.

To study HRSV infection and replication *in vitro* a culture system is needed that resembles the respiratory epithelium *in vivo* in morphology and functionality, including mucin secretion and cilia movement [51]. This can be achieved by using well-differentiated normal human bronchial epithelium (wd-NHBE) cells or well-differentiated human airway epithelium (wd-HAE) [51,208]. These cells are cultured on air-liquid-interface and grow multi-layered. In order to study HRSV in the most affected population primary paediatric bronchial epithelial cells have been developed by collecting cells from healthy children undergoing elective surgery [49]. However, working with primary human airway cell

cultures brings inherent limitations: the amount of material available from a donor is limited and donor-to-donor variability can be substantial. Therefore, commercial availability of primary human NHBE now better allows implementation of this tissue culture technique in studies of HRSV pathogenesis.

Animal models for HRSV are indispensable for our understanding of pathogenesis, vaccination and treatment options. Animal models form a crucial step between (sophisticated) tissue culture experiments and clinical trials. There are different animal models for HRSV infection available, although none of these recapitulate all aspects of the disease in humans. HRSV was originally discovered in chimpanzees. Similar to humans, chimpanzees are highly susceptible to infection with HRSV, and develop clinical signs like rhinorrhea, sneezing and coughing [209]. Due to ethical constraints, high cost and availability of other animals models, use of chimpanzees as experimental animals has now been discontinued [210-212].

Well-established animal models for HRSV are inbred laboratory mouse strains, especially BALB/c, and cotton rats (*Sigmodon hispidus*). Mice are semi-permissive hosts for HRSV, and the infection in these animals does not resemble human HRSV infection. Infection requires a very high intranasal inoculum of  $10^5$ - $10^7$  plaque-forming units (PFU) per animal [213-218]. Advantages of the HRSV mouse model are the plethora of immunological reagents and the availability of transgenic mice. The most widely used animal model for HRSV vaccination, antivirals, and prophylaxis is the cotton rat (*Sigmodon hispidus*) [219-221]. In 1971 Dreizin *et al.* showed that cotton rats are ~100 fold more sensitive to HRSV than mice, as only  $10^4$  PFU is needed for productive infection [222]. The HRSV cotton rat model has played an important role in developing neutralizing antibody preparations, HRSV IVIG and palivizumab [223-225]. Disadvantages of

the HRSV cotton rat model include the lack of immunological reagents and transgenic animals. In addition, housing and handling of cotton rats is more difficult than those of mice [226].

Several additional animal species can be infected with HRSV, including ferrets, guinea pigs, hamsters, and chinchillas. For specific purposes experiments are performed in non-human primates, including African green monkeys, rhesus and cynomolgus macaques, baboons and marmosets [226]. Furthermore, alternative approaches focus on veterinary correlates of HRSV in their natural host species, such as the use of pneumonia virus of mice (PVM) in mice or bovine respiratory syncytial virus (BRSV) in calves or lambs [227-231].

### Aim and scope of this thesis

HRSV and HMPV are ubiquitous causes of respiratory tract infections. Early after its discovery HRSV has been recognized as the most prevalent, and HMPV as a major viral cause of severe LRTI in children. However, respiratory bacteria are also highly prevalent in the upper respiratory tract in children and thus interactions between bacteria (or bacterial components) and respiratory viruses may exist. For some respiratory bacteria vaccines exist that protect against lethal bacterial disease in children. The ultimate goal is to also have a vaccine against HRSV and/or HMPV globally available. To this end, major hurdles will have to be overcome.

The aim of the studies presented in thesis was to provide novel insights into interactions between paramyxoviruses and bacteria, with a focus on the pneumoviruses HRSV and HMPV and the respiratory bacterial pathogen *S. pneumoniae*.

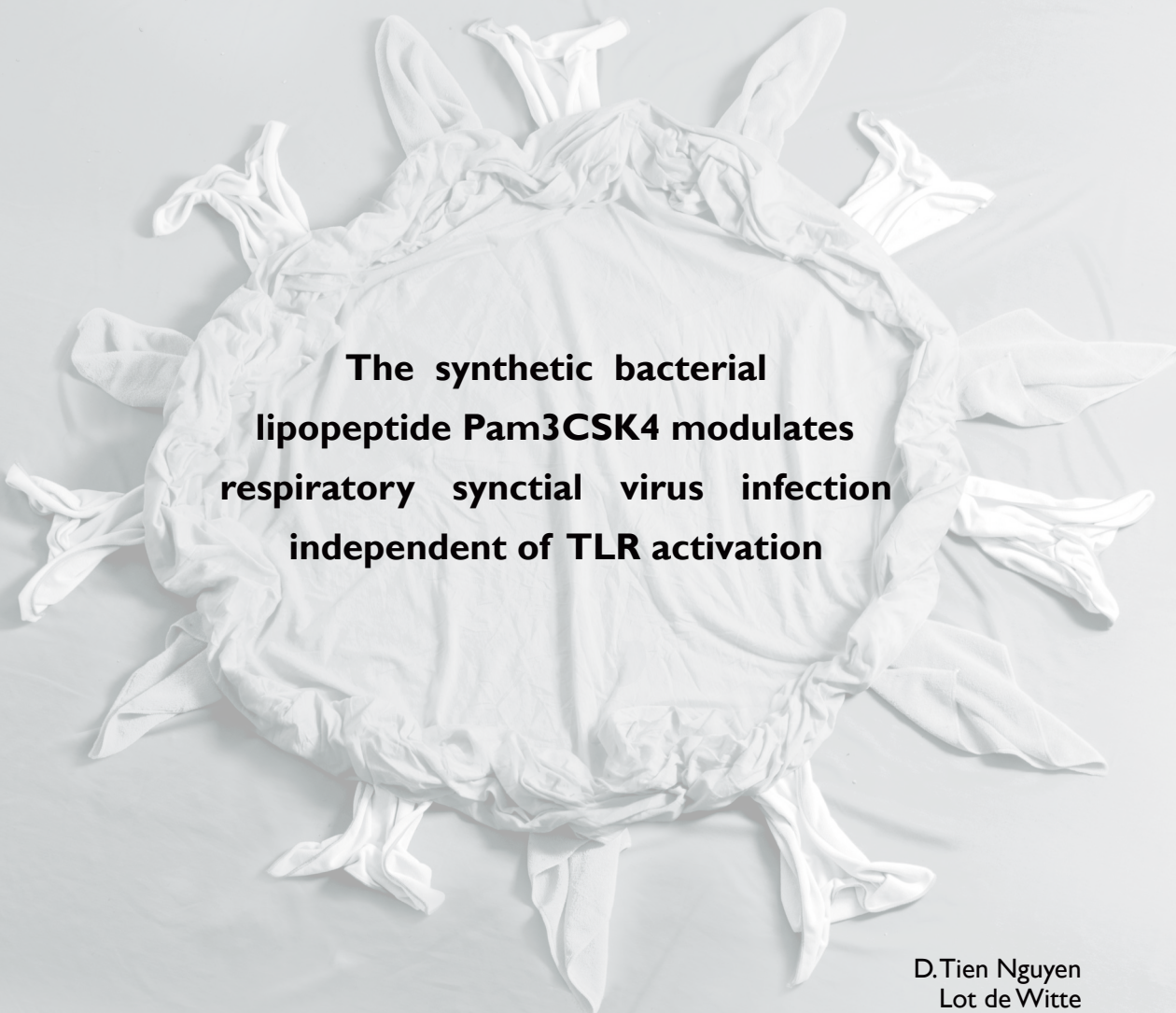
In **Chapter 2**, interactions between synthetic bacterial lipopeptides and paramyxovirus infections are discussed.



In **Chapter 3** and **4** the potential of the synthetic bacterial lipopeptides as adjuvants for live-attenuated virus candidate vaccines was explored. **Chapter 5** describes the generation and characterization of a next generation recombinant HRSV strain. **Chapter 6** elaborates on a new *ex vivo* model for the study of respiratory viruses. In **Chapters 7** and **8** the interactions between *S. pneumoniae* and HMPV or HRSV are explored. **Chapter 9** is a summarizing discussion of the findings described in this thesis.



## Chapter 2



**The synthetic bacterial  
lipopeptide Pam3CSK4 modulates  
respiratory syncytial virus infection  
independent of TLR activation**

D.Tien Nguyen  
Lot de Witte  
Martin Ludlow  
Selma Yüksel  
Karl-Heinz Wiesmüller  
Teunis B.H. Geijtenbeek  
Albert D. M. E. Osterhaus  
Rik L. de Swart

*PLoS Pathogens* 6(8): e1001049 (2010)

### Abstract

Human respiratory syncytial virus (HRSV) is an important cause of acute respiratory disease in infants, immunocompromised subjects and the elderly. However, it is unclear why most primary HRSV infections are associated with relatively mild symptoms, whereas some result in severe lower respiratory tract infections and bronchiolitis. Since HRSV hospitalization has been associated with respiratory bacterial co-infections, we have tested if bacterial Toll-like receptor (TLR) agonists influence HRSV-A2-GFP infection in human primary cells or cell lines. The synthetic bacterial lipopeptide Pam3-Cys-Ser-Lys4 (Pam3CSK4), the prototype ligand for the heterodimeric TLR1/TLR2 complex, enhanced HRSV infection in primary epithelial, myeloid and lymphoid cells. Surprisingly, enhancement was optimal when lipopeptides and virus were added simultaneously, whereas addition of Pam3CSK4 immediately after infection had no effect. We have identified two structurally related lipopeptides without TLR-signaling capacity that also modulate HRSV infection, whereas Pam3CSK4-reminiscent TLR1/2 agonists did not, and conclude that modulation

of infection is independent of TLR activation. A similar TLR-independent enhancement of infection could also be demonstrated for wild-type HRSV strains, and for HIV-1, measles virus and human metapneumovirus. We show that the effect of Pam3CSK4 is primarily mediated by enhanced binding of HRSV to its target cells. The N-palmitoylated cysteine in combination with the cationic lysines were identified as pivotal for enhanced virus binding. Surprisingly, we observed inhibition of HRSV infection in immortalized epithelial cell lines, which was shown to be related to interactions between Pam3CSK4 and negatively charged glycosaminoglycans on these cells, which are known targets for binding of laboratory-adapted but not wild-type HRSV. These data suggest a potential role for bacterial lipopeptides in enhanced binding of HRSV and other viruses to their target cells, thus affecting viral entry or spread independent of TLR signaling. Moreover, our results also suggest a potential application for these synthetic lipopeptides as adjuvants for live-attenuated viral vaccines.

## Introduction

Human respiratory syncytial virus (HRSV) is a major cause of respiratory tract disease in infants, immunocompromised subjects and the elderly [232]. The virus is a member of the family *Paramyxoviridae*, which also includes human metapneumovirus (HMPV) and measles virus (MV). HRSV owes its name to the formation of multinucleated syncytia within infected epithelial cells of the respiratory tract [9,10,233]. HRSV shows a seasonal epidemiology associated with worldwide peaks in virus transmission during the winter or rainy season [57]. In most cases the virus causes a mild and self-limiting upper respiratory tract infection. However, in some cases (usually estimated as 1-2%) the virus spreads to the lower respiratory tract, and may cause severe bronchiolitis or pneumonia [57,232]. A substantial proportion of these patients require hospitalization, and occasionally mechanical ventilation.

Risk factors for developing severe HRSV disease include premature birth, immune deficiency, underlying chronic lung disease or congenital heart disease [57,232]. However, in the majority of hospitalized cases no risk factor can be identified. The pathogenesis of these severe HRSV cases remains poorly understood. Different explanations have been proposed, such as anatomical predispositions, mucus overproduction, skewed T-helper 2 immune responses or co-infections. Some studies have suggested that co-infections by HRSV and the closely related HMPV may result in severe disease [234,235], but co-infections with bacteria or other respiratory viruses have also been described, especially for *Streptococcus pneumoniae* [236-239]. Invasive pneumococcal disease has been shown to be more prevalent during the HRSV season [240]. In addition, the frequency of hospitalization for severe HRSV disease is reduced in children who have been vaccinated

against *S. pneumoniae* [80].

In addition to *S. pneumoniae*, different bacteria have been detected in nasal swabs, nasopharyngeal aspirates or bronchoalveolar lavages of children with severe HRSV infections, including *Staphylococcus aureus*, *Haemophilus influenzae* and *Moraxella catarrhalis*. HRSV-infected children are often co-diagnosed with otitis media caused by *S. pneumoniae*, *H. influenzae* or *M. catarrhalis*. [241]. It is often assumed that viral infections precede superinfection with bacteria [242-244], by causing epithelial damage that allows bacterial colonization or by facilitating bacterial binding to epithelial cells [76,78,245]. However, an inverse order of events cannot be excluded: respiratory bacteria may facilitate virus infections by activating target cells or modulating virus-specific immune responses [246].

The mammalian immune system has developed pattern recognition molecules such as Toll-like receptors (TLRs) [247], which are not only expressed by professional antigen-presenting cells but also by epithelial cells of the respiratory tract [248-250]. TLR triggering by pathogens, including bacterial structures, leads to an innate and adaptive immune response to specifically combat the invading pathogen. However, by changing the phenotype of the cell, TLR signaling might also increase the susceptibility of cells to virus infection. For HIV-1 it has been described that bacterial TLR ligands enhance infection of and transmission to target cells [251-255]. Here, we have examined the effect of bacterial TLR ligands and structurally related molecules on HRSV infection in different cell types.

## Results

### The lipopeptide and prototype TLR1/2 agonist Pam3CSK4 modulates HRSV infection of epithelial and antigen presenting cells.

The TLR family consists of more than ten members, each interacting with specific pathogenic structures [109]. TLR1, 2, 4, 5 and 6 have been shown to interact with bacterial structures. A panel of prototype bacterial TLR ligands was tested for their ability to modulate HRSV infection of different target cells. Both primary cells and immortalized cell lines were used, since TLR expression is influenced by the activation status of cells. The epithelial cells, the main target cells for HRSV infection, were the initial focus of our investigation. Following a previously described protocol [253], cells were pre-incubated with the respective TLR ligands and subsequently infected with a recombinant HRSV (strain A2) that encodes enhanced GFP (rgRSV) [256]. In primary undifferentiated normal human bronchial epithelial (NHBE) cells, pre-incubation with the synthetic bacterial lipopeptide Pam3-Cys-Ser-Lys4 (Pam3CSK4) enhanced rgRSV infection ( $p < 0.05$ ), whereas the other TLR ligands did not modulate infection (Figure 1A). Pam3CSK4 was also found to enhance rgRSV infection in well-differentiated NHBE cells grown on air-liquid interface (results not shown). The epithelial cell lines A549 and HEp-2 are frequently used to study HRSV infection and the percentage of infected cells is higher compared to the primary NHBE cells (Figure 1A). Surprisingly, and in contrast to NHBE cells, Pam3CSK4 and to a lesser extent Pam2CSK4 did not enhance but rather decreased rgRSV infection in A549 and HEp-2 ( $p < 0.05$ ) (Figure 1B,C).

Antigen presenting cells (APC) in the respiratory tract, such as alveolar macrophages and dendritic cells, are exposed to HRSV during infection. The level of infection

of these cells *in vivo* and the contribution of these cells to HRSV pathogenesis is currently unknown. Since APC are highly responsive to TLR agonists, we studied infection of primary antigen presenting cells, including monocyte-derived dendritic cells and BAL cells, in the presence and absence of TLR agonists. In addition, we also used an Epstein-Barr virus-transformed B-lymphoblastic cell line (B-LCL) representing HRSV infection of lymphoid APC. APC can be infected with HRSV but are relatively resistant compared to epithelial cells. Using a 5-fold higher dose in immature monocyte-derived dendritic cells (DCs, Figure 1D) and a 10-fold higher dose in BAL cells and B-LCL (Figure 1E,F), infection with rgRSV resulted in 2%, 1%, and 5% GFP-expressing cells, respectively. Similar to NHBE cells, pre-incubation of APC with Pam3CSK4 strongly increased rgRSV infection levels in these cells ( $p < 0.05$ , Figure 1D-F). These results demonstrate that the TLR1/TLR2 ligand Pam3CSK4 modulates rgRSV infection of different target cells.

### Pam3CSK4-mediated enhancement of HRSV infection in APC is a rapid and dose-dependent process.

To further investigate the mechanism by which Pam3CSK4 enhances HRSV infection, the optimal time for addition of the lipopeptide before or after infection was determined. For these studies B-LCL were used, as these are easier to work with than the primary epithelial cells or myeloid APC and thus facilitated further experiments. At different time points before or after infection with rgRSV B-LCL were incubated with Pam3CSK4. Interestingly, addition of the lipopeptides at the same time as the virus resulted in the highest percentages of infected cells ( $p < 0.005$ , Figure 2A). This result suggests that the effect for enhancement occurs directly and influences binding or entry of the virus. A similar enhancement of rgRSV infection could also be demonstrated using alternative readout

## Lipopeptide-Mediated Enhancement of Virus Binding

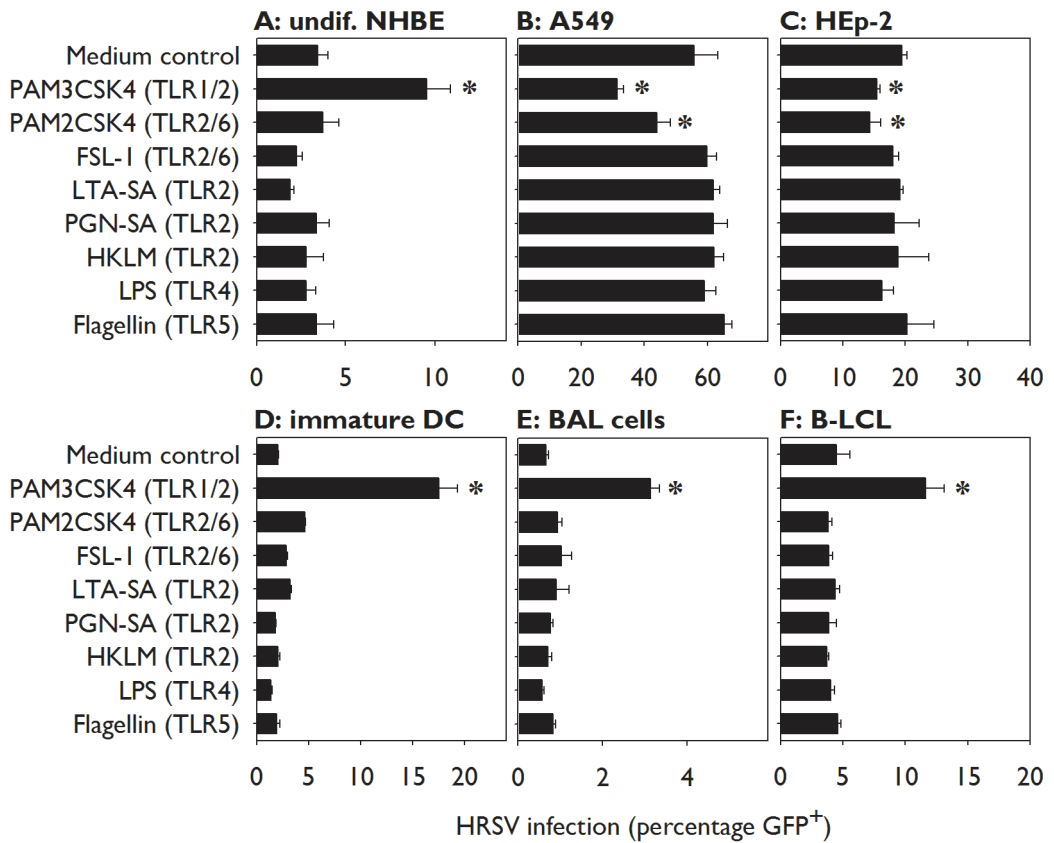


**Figure 1.** Pam3CSK4 modulates rgRSV infection in different cell types. A-F) Primary cells or immortalized cell-lines were incubated with bacterial TLR ligands using conditions as described previously [253]. In undifferentiated primary normal human bronchial epithelial (NHBE) cells, antigen presenting cells (immature DC, BAL cells and EBV-transformed B-LCL), Pam3CSK4 mediated significant enhancement of rgRSV infection (\* $p < 0.05$  in 1-way ANOVA and posthoc Dunnett's correction for multiple comparisons with medium control). In contrast, treatment of A549 or HEp-2 cells with Pam3CSK4 and Pam2CSK4 resulted in reduced rgRSV infection levels (\* $p < 0.05$  using Dunnett's correction). Data are presented as percentages GFP<sup>+</sup> cells (means  $\pm$  SD of triplicates). A representative experiment out of three is shown.

parameters, including measurement of virus titers in supernatant by endpoint titration or assessment of numbers of infected cells by infectious centre assay (data not shown).

Subsequently, HRSV or B-LCL were pre-incubated with different concentrations of Pam3CSK4 for 30 min at 37°C before infection and overnight culture. A convincing and dose-dependent enhancement of infectivity was observed in both conditions ( $p < 0.05$ , Figure

2B). At 30  $\mu$ g/ml Pam3CSK4 became toxic for the cells, resulting in a declining percentage of infected cells especially in the condition where cells had been exposed directly. To discriminate between pre- and post-entry mechanisms, B-LCL were incubated with different concentrations of Pam3CSK4 directly before or after rgRSV infection. In B-LCL incubated with Pam3CSK4 and washed before rgRSV infection, enhancement of

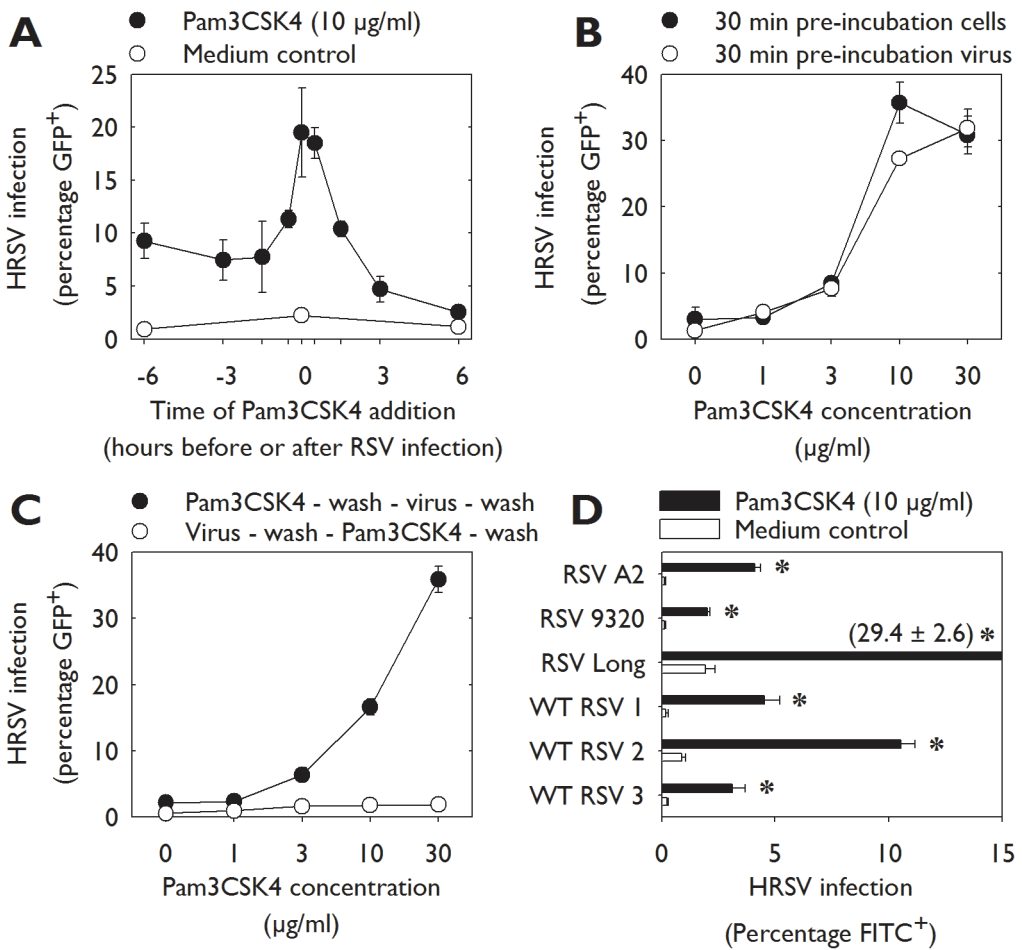


**Figure 2.** Pam3CSK4 mediates rapid and dose-dependent enhancement of HRSV infection in B-LCL. A) B-LCL were incubated at 37°C with Pam3CSK4 (10 µg/ml) at 6h, 3h, 1.5h, 0.5h or 0h before or 0.5h, 1.5h, 3h, and 6h after rgRSV infection. Pam3CSK4 treatment resulted in significantly increased rgRSV infection percentages in B-LCL at all time points (\* $p < 0.005$  with Student's *t*-tests with Bonferroni correction for multiple comparisons). B) B-LCL or virus were pre-incubated with different concentrations of Pam3CSK4 for 30 minutes at 37°C before infection with rgRSV. Pam3CSK4 treatment resulted in significantly increased rgRSV infection percentages ( $p < 0.05$  for Pam3CSK4 concentrations  $\geq 3$  µg/ml), but no biologically relevant differences were detected between pre-incubation of cells or virus. C) Cells were treated with different concentrations of Pam3CSK4 either directly before or after rgRSV infection. In all conditions free lipopeptide or free virus was washed away before proceeding to the next step. Pam3CSK4 treatment resulted in significantly higher percentages of infected cells ( $p < 0.01$ , significant under Bonferroni correction for Pam3CSK4 concentrations  $\geq 3$  µg/ml). However, addition of Pam3CSK4 after rgRSV infection and subsequent removal of free virus had no effect. D) B-LCL were incubated for 30 minutes at 37°C with or without Pam3CSK4 (10 µg/ml) before infection with different HRSV strains. Pam3CSK4 treatment resulted in increased HRSV infection percentages ( $p < 0.05$ ) for all strains tested. In all panels data are presented as percentages HRSV-infected cells (means  $\pm$  SD) 20-24 hrs after infection as determined by flow cytometry, using GFP expression in panels A-C and staining with FITC-labeled HRSV-specific antibodies in panel D. A representative experiment out of three is shown.



infection was still detectable ( $p < 0.01$ , Figure 2C), suggesting that cell-bound Pam3CSK4 directly or indirectly increased rgRSV infection. In contrast, Pam3CSK4 did not influence the percentage of GFP-expressing cells when the lipopeptide was added immediately after rgRSV infection and subsequent washing to remove unbound virus, suggesting that Pam3CSK4 does not affect post-binding or -entry steps of HRSV infection, such as transcription, replication, release and second round infection. In addition, as Pam3CSK4 was washed away the toxic effect was not present anymore, resulting in enhancement for all tested concentrations. Moreover, the level of GFP expression in Pam3CSK4-stimulated cells was similar to GFP expression in untreated cells, suggesting that HRSV transcription was not influenced (data not shown). In order to exclude that the observed effect was related to a specific property of the recombinant HRSV strain used in these experiments, we also tested the effect of Pam3CSK4 on infection of B-LCL with different laboratory or wild-type strains of HRSV, which resulted in a similar enhancement of infection ( $p < 0.05$ , Figure 2D). Thus, we conclude that Pam3CSK4 enhances HRSV binding or entry in B-LCL. These findings were corroborated in primary epithelial cells and DCs (data not shown).

### **Pam3CSK4 enhances HRSV binding to target cells independent of TLR signaling.**

Since the addition of Pam3CSK4 together with HRSV had the largest influence on rgRSV infection, we hypothesized that TLR triggering and subsequent phenotypical changes might not be involved in this effect. Indeed, neither blocking of Pam3CSK4 binding to TLR by neutralizing antibodies nor blocking of TLR signaling by blocking peptides abrogated enhancement of rgRSV infection by Pam3CSK4 ( $p < 0.05$ , Figure 3A). To further support these results, different lipopeptides were used that were structurally

similar to Pam3CSK4 but do not contain TLR signaling capacities (Figure S1 for molecular structures). Pam-Cys-SK4 and PHCSK4 do not induce TLR signaling [257,258], but enhanced rgRSV infection in B-LCL ( $p < 0.05$ , Figure 3B). Furthermore, Pam3CSP4, which is equally effective in inducing TLR responses as Pam3CSK4 [259], did not enhance rgRSV infection under these conditions (Figure 3B). Thus, Pam3CSK4 enhances HRSV infection independently of TLR signaling.

To investigate whether Pam3CSK4, Pam-Cys-SK4 and PHCSK4 enhance attachment of rgRSV to target cells, an HRSV binding assay was performed. In contrast to Pam3CSP4, pre-incubation of rgRSV with Pam3CSK4, Pam-Cys-SK4 or PHCSK4 increased binding to B-LCL ( $p < 0.05$ , Figure 3C). Subsequently, the direct interaction of lipopeptides and viruses was investigated in an HRSV binding ELISA. The different lipopeptides were coated onto ELISA plates and subsequently incubated with rgRSV. Pam3CSK4, Pam-Cys-SK4 and PHCSK4, but not Pam3CSP4, were found to bind rgRSV ( $p < 0.05$ , Figure 3D). Finally, B-LCL were incubated with the fluorescent (lipo) peptides Pam3CSK4-CF or CSK4-CF at 4°C or 37°C, demonstrating effective membrane binding of Pam3CSK4-CF at concentrations that were also found to enhance rgRSV infection ( $p < 0.01$ , Figure 3E). Together these results demonstrate that Pam3CSK4 interacts directly with rgRSV or its target cells, enhances binding of rgRSV to target cells and thereby increases infection efficiency, all independent of TLR signaling.

### **Charge and structure of lipopeptides play an essential role for enhancement.**

Charge and structure can play important roles in molecular interactions. Several cationic molecules have been described to enhance viral infections [260-262]. To determine the role of the four lysines in Pam3CSK4, which are strongly cationic, these were replaced

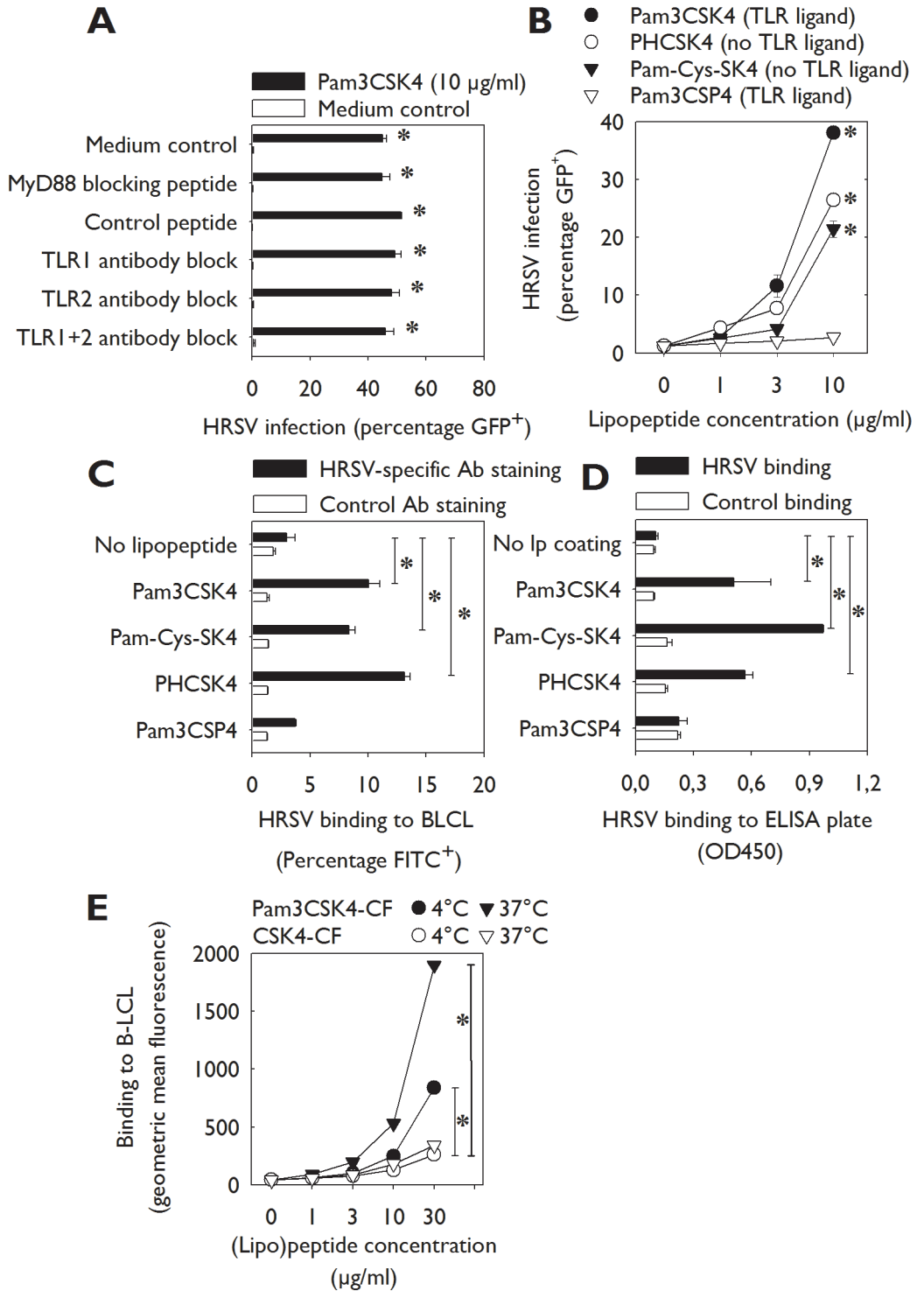
by either the neutral amino acid proline (Pam3CSP4), the weakly cationic histidine (Pam3CSH4) or the strongly cationic arginine (Pam3CSR4), or the negatively charged glutamic acid (Pam3CSE4, Figure S1 for molecular structures). Of these lipopeptides, only Pam3CSK4 was able to enhance rgRSV infection (Figure 4A). Despite their positive charge, neither Pam3CSH4 nor Pam3CSR4 were capable of enhancing HRSV infection. In contrast to the other three lipopeptides, Pam3CSE4 reproducibly inhibited HRSV infection ( $p < 0.05$ ).

To explore the importance of electrostatic interactions between Pam3CSK4 and cells or virus, various polyanionic compounds were tested to shield the positive charge of Pam3CSK4, using previously described conditions [262]. Two naturally occurring polyanionic compounds, heparin and chondroitin sulphate, and four chemically

desulfated or oversulfated anionic polymers, dextran sulfate, over-sulfated heparin, desulfated heparin and oversulfated chondroitin sulfate, were tested for their effect on the interaction between Pam3CSK4 and HRSV. Desulfated or oversulfated anionic polymers were used to normalize for differences in relative anionic strengths between the naturally existing compounds. After incubation of B-LCL with Pam3CSK4, heparin, dextran sulfate, or chondroitin sulfate were added, resulting in a decreased levels of rgRSV infection after treatment with heparin and dextran sulfate ( $p < 0.05$ ), whereas chondroitin sulfate did not effectively block rgRSV infection (Figure 4B). Oversulfated heparin and oversulfated chondroitin sulfate inhibited Pam3CSK4-mediated enhancement of HRSV infection ( $p < 0.05$ ), but desulfated heparin did not. In addition, HRSV binding experiments using B-LCL incubated with Pam3CSK4 showed decreased virus binding after treatment with

**Figure 3.** The effect of Pam3CSK4 on B-LCL is independent of TLR signaling, but mediated by enhanced virus binding. A) B-LCL were pre-incubated with the myeloid differentiating factor 88 (MyD88) homodimerization inhibitory peptide, a control peptide, or polyclonal blocking antibodies to TLR1, TLR2 and/or TLR4, followed by Pam3CSK4 incubation (10  $\mu\text{g/ml}$ , 30 minutes, 37°C) and subsequent infection with rgRSV. In all conditions Pam3CSK4 treatment resulted in enhancement of rgRSV infection ( $p < 0.05$ ). B) B-LCL were incubated with different lipopeptides (for molecular structures see Figure S1) with or without TLR signaling capacities. In addition to TLR agonist Pam3CSK4 two non-TLR2 activating lipopeptides Pam-Cys-SK4 and PHCSK4 enhanced rgRSV infection, whereas the TLR agonist Pam3CSP4 did not ( $p < 0.05$  with Dunnett's correction for multiple comparisons for Pam3CSK4, Pam-Cys-SK4, and PHCSK4 concentrations 3 and 10  $\mu\text{g/ml}$ ). C) HRSV binding to B-LCL was determined by pre-incubating rgRSV with the different lipopeptides, followed by assessment of binding to cells. HRSV binding was quantified by staining with FITC-labeled antibodies to HRSV or to influenza-B as a control. Addition of the lipopeptides Pam3CSK4, Pam-Cys-SK4 and PHCSK4 but not Pam3CSP4 significantly increased binding of HRSV to the cells ( $p < 0.05$  using Dunnett's correction for multiple testing). D) Direct HRSV binding to lipopeptides was examined in an ELISA format. Lipopeptides were coated on high-binding ELISA plates and incubated with HRSV, or with MV strain Edmonston as a control. HRSV binding was measured using an HRSV-specific monoclonal antibody, followed by detection using a goat-anti-mouse peroxidase and TMB as a substrate. Coating with Pam3CSK4, Pam-Cys-SK4 and PHCSK4 but not with Pam3CSP4 resulted in increased HRSV binding ( $p < 0.05$  compared with Dunnett's correction). Data are shown as extinctions at 450nm (means  $\pm$  SD of duplicates). E) B-LCL were incubated with Pam3CSK4-CF or CSK4-CF at 4°C or 37°C to measure direct (lipo)peptide binding to the cells. At both temperatures Pam3CSK4-CF showed significantly stronger binding than CSK4-CF ( $p < 0.01$  with Bonferroni correction at concentrations 10 and 30  $\mu\text{g/ml}$ ). In panels A-C results are shown as percentages GFP<sup>+</sup>- or FITC<sup>+</sup> cells (means  $\pm$  SD of duplicates) and in Panel E data are shown as geometric mean fluorescence (means  $\pm$  SD of triplicates). Representative examples of at least three experiments are shown.

# Lipopeptide-Mediated Enhancement of Virus Binding



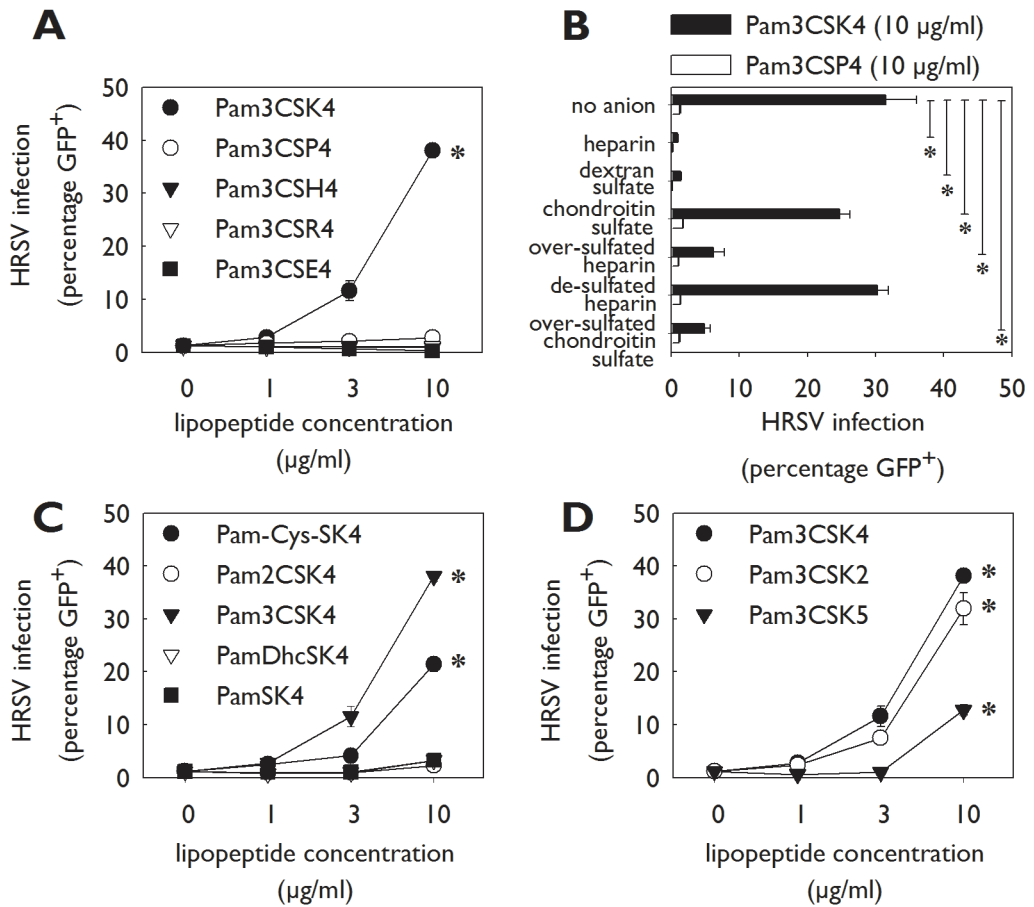


**Figure 4.** Importance of lipopeptide charge and structure. A, C, D) B-LCL were incubated with different lipopeptides for 30 minutes at 37°C before infection with rgRSV. Only Pam3CSK4, Pam-Cys-SK4, Pam3CSK2 and Pam3CSK5 resulted in enhancement of rgRSV infection, whereas Pam3CSE4 resulted in inhibition of rgRSV infection compared to medium control ( $p < 0.05$  in 1-way ANOVA and posthoc Dunnett’s correction). B) Natural and chemically-derived polyanionic compounds were assessed to block the Pam3CSK4-mediated enhancement of HRSV infection. The compounds were added to cells that had been pre-incubated with Pam3CSK4 or Pam3CSP4 as a control, followed by infection with HRSV. The next day percentages GFP-expressing cells were determined by flow cytometry. The strongly polyanionic compounds heparin, dextran sulfate, over-sulfated heparin and over-sulfated chondroitin sulfate were able to abrogate the Pam3CSK4-mediated enhancement of rgRSV infection ( $p < 0.05$  using posthoc Dunnett’s correction), whereas the control compounds chondroitin sulfate and de-sulfated heparin had only a minimal effect or no effect, respectively. Error bars represent the standard deviation of triplicates. A representative experiment out of three is shown.

heparin, dextran sulfate, oversulfated heparin or over-sulfated chondroitin sulfate, but not after treatment with chondroitin sulfate or de-sulfated heparin (data not shown). These

results suggest that highly sulfated polyanions neutralize the cationic property of the cell-bound Pam3CSK4, resulting in abrogation of the Pam3CSK4-mediated enhancement of

HRSV binding and infection, and confirm that cationic properties of Pam3CSK4 are crucial for their capacity to enhance HRSV infections.

Subsequently, other properties of the lipopeptide structure were studied. Two lipopeptides with either one (Pam-Cys-SK4), two (Pam2CSK4) or three (Pam3CSK4) palmitoyl residues were tested for their capacity to enhance rgRSV infection in B-LCL (Figure S1 for molecular structures). Pam-Cys-SK4 strongly enhanced rgRSV infection ( $p < 0.05$ ), whereas Pam2CSK4 had limited to no enhancing properties, demonstrating that the amino-linked palmitoyl group is crucial for the enhancing properties (Figure 4C). In addition, a Pam-Cys-SK4-reminiscent lipopeptide, containing the prokaryotic amino acid S-(2,3-dihydroxypropyl)cysteine (Dhc) characterized by two free hydroxyl groups (PamDhcSK4), and a lipopeptide completely lacking the cysteinyl partial structure (PamSK4) were tested, which both were unable to enhance infection. These results demonstrated that the amphiphilic feature and cationic lysins per se are insufficient for enhancement, and strongly suggest that the N-palmitoylated cysteine is necessary as membrane anchor. Evaluation of Pam3CSK4-reminiscent lipopeptides with two or five instead of four lysins (Pam3CSK2 and Pam3CSK5, respectively) showed that all could enhance rgRSV infection in B-LCL ( $p < 0.05$ , Figure S1 for molecular structures). However, the level of enhancement was not simply related to the number of cationic lysins in the lipopeptide, as Pam3CSK2 showed a stronger enhancement than Pam3CSK5 (Figure 4D).

### **Pam3CSK4, Pam-Cys-SK4 and PHCSK4 also enhance infection with other enveloped viruses.**

Previously, it has been described that Pam3CSK4 enhances infection with or transmission of HIV-1 [253-255]. Here we show that the non-TLR agonists Pam-Cys-SK4

and PHCSK4 are equally capable of enhancing HIV-1 infection of a Jurkat-CCR5 cells as Pam3CSK4 ( $p < 0.05$ , Figure 5A), indicating that also for HIV-1 TLR signaling-independent enhancement of infection can be observed. The same could be shown for two viruses from the same family as HRSV: HMPV and two different MV strains ( $p < 0.05$ , Figure 5B-D). For MV we also performed a virus binding assay and were able to show that, similar as described above for HRSV, the enhancement was indeed mediated by enhancement of MV binding to their target cells (Figure S2). These viruses share membrane fusion as a common entry mechanism [263], but contain different attachment proteins and target different cellular receptors, suggesting that enhancement of virus binding is based on interactions between lipopeptides and biomembranes or common membrane-associated structures rather than with specific cellular or viral proteins.

### **Interactions between cationic lipopeptides and GAGs explain inhibition of HRSV infection in A549 and HEp-2 cells**

As described above and shown in Figure 1, and in sharp contrast to the reproducible enhancement of HRSV infection in undifferentiated NHBE cells, BAL cells, dendritic cells and B-LCL, Pam3CSK4 inhibited HRSV infection in the epithelial cell lines A549 and HEp-2. An important difference between these cell lines and the other cell types used in this study is the high expression level of GAGs in the immortalized epithelial cell lines A549 and HEp-2. GAGs are negatively charged long unbranched polysaccharides associated with proteoglycans (chondroitin-, dermatan-, heparan- and keratan-sulfate) expressed on cell membranes. It has been described that rgRSV and other laboratory-adapted HRSV strains can use GAGs as cellular receptor, although this is considered an *in vitro* artifact and these molecules are not used as cellular

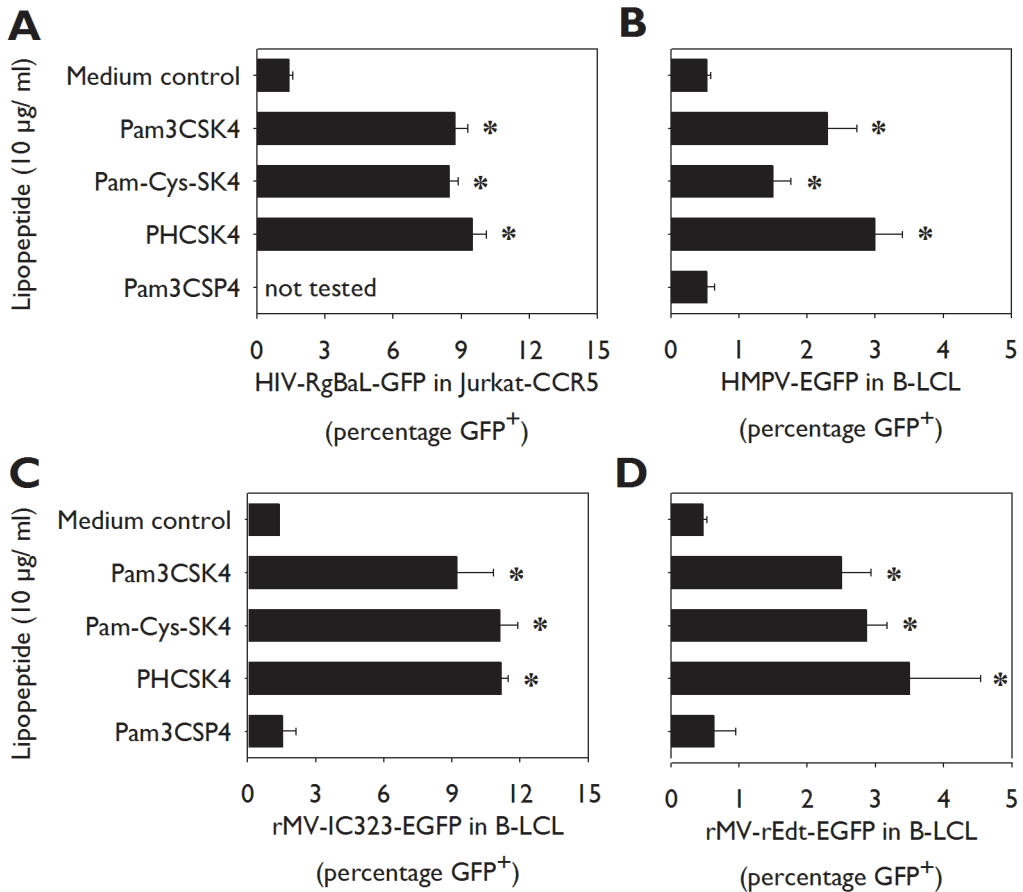


**Figure 5.** Enhancement of infection with other enveloped viruses. A-D) Jurkat-CCR5 cells (A) or B-LCL (B-D) were incubated with different lipopeptides (10 µg/ml, Pam3CSK4, Pam-Cys-SK4, PHCSK4, or Pam3CSP4) before infection with HIV-RgBaL-GFP (A), HMPV-EGFP (B), rMV-Edmonston-EGFP (C) or rMV-IC323-EGFP (D), respectively. Two (HIV-1) or one (HMPV, MV) day later the percentage of GFP-expressing cells was determined by flow cytometry. In all experiments Pam3CSK4, Pam-Cys-SK4 and PHCSK4 treatment resulted in significantly higher infection percentages ( $p < 0.05$  using posthoc Dunnett's correction for multiple comparisons). Error bars represent the standard deviation of triplicates. A representative experiment out of three is shown.

receptors *in vivo* [207]. To address the role of GAGs in the observed Pam3CSK4-mediated inhibition of rRSV infection in epithelial cell lines, we used Chinese hamster ovary cell (CHO) mutants deficient in GAG synthesis [207]. Wild-type and two GAG-deficient CHO cell lines (CHO-pgsA745 completely deficient in GAGs and CHO-pgsD677 deficient for heparan sulfate) were tested at the same multiplicity of infection (MOI) in two

conditions. As expected, the percentage of rRSV infection in A549 and wild-type CHO in the absence of lipopeptide was significantly higher than in the mutant CHO cells ( $p < 0.01$ ). Pre-incubation of cells with Pam3CSK4 decreased HRSV infection levels in A549 and wild-type CHO cells, but enhanced infection in the GAG-deficient CHO cells (Figure 6). If the virus was pre-treated with the lipopeptide instead of the cells, enhancement

## Lipopeptide-Mediated Enhancement of Virus Binding

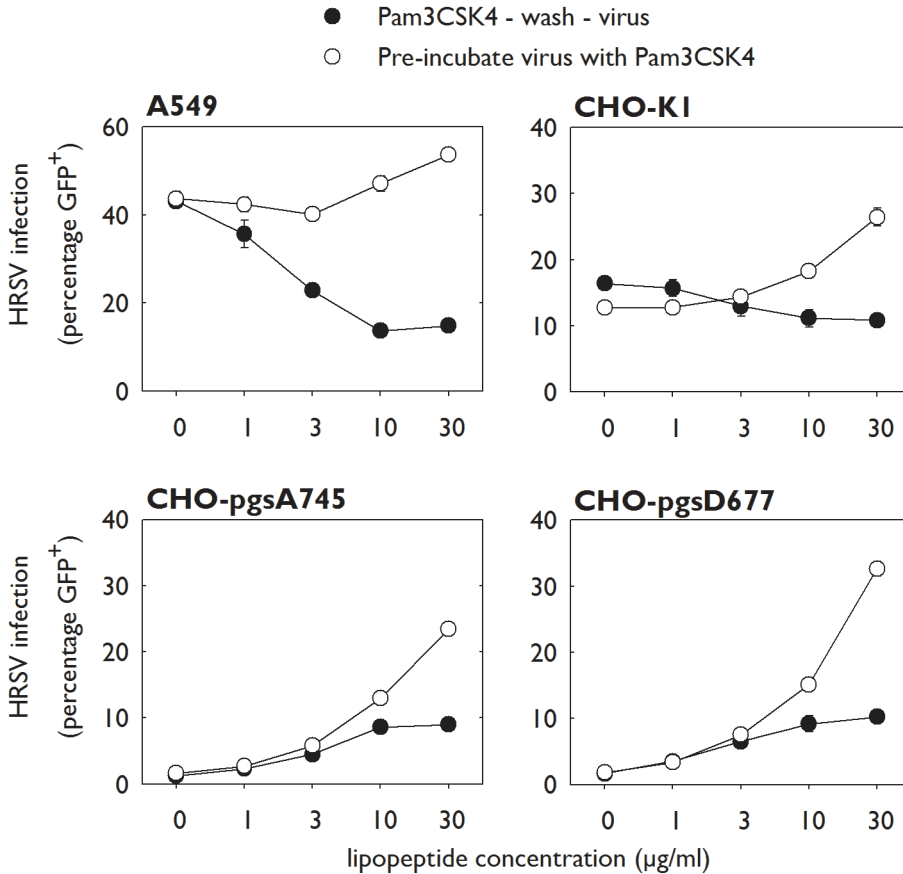


**Figure 6.** Mechanism of reduced rgRSV infection of A549 cells in relation to GAG expression. A549, CHO-K1, CHO pgsA-745 or CHO pgsD-677 cells were infected with rgRSV after pre-incubation of the cells (black symbols) or the virus (white symbols) with Pam3CSK4 (10 µg/ml) for 30 minutes at 37°C. In the GAG-expressing cell lines A549 and CHO-K1 pre-incubation of cells with Pam3CSK4 resulted in reduction of HRSV infection, but in the GAG-deficient cell lines CHO-pgsA745 and CHO-pgsD677 this same condition resulted in enhancement of infection ( $p < 0.01$  in multiple Student's *t*-test with Bonferroni correction). Data are presented as percentages GFP<sup>+</sup> cells (means ± SD of triplicates). A representative experiment out of three is shown.

was observed in all four cell lines (Figure 6). These findings demonstrate that Pam3CSK4-mediated inhibition of rgRSV infection in immortalized epithelial cell lines is related to interactions between the cationic lipopeptides and the negatively charged GAGs.

### Discussion

In the present study we have shown that Pam3CSK4 and at least two other structurally-related cationic lipopeptides can enhance infections with HRSV, HIV-1, HMPV or MV independent of TLR signaling. By using rgRSV infection of B-LCL as a model system, we have shown that these lipopeptides can bind directly to both cells and virus, and

strongly enhance virus binding to target cells. In contrast, Pam3CSK4 reduced rgRSV infection levels of A549 and HEp-2 cells under specific conditions, due to interactions with the negatively charged GAGs expressed on the surface of these cells.

Pam3CSK4 is a synthetic tripalmitoylated bacterial lipopeptide and is a potent activator of the NF- $\kappa$ B pathway, by forming an m-shaped heterodimer of TLR1 and TLR2 [264]. It has been described that Pam3CSK4 enhances infection or transmission of HIV-1 in different systems [253-255]. Our data show that Pam3CSK4-mediated enhancement of infection is not specific for HIV-1, but can also be shown for a number of other enveloped viruses including HRSV, HMPV and MV. By blocking either binding to TLR1/2 or TLR1/2 signaling, and by using enhancing lipopeptides that do not activate TLR1/2, we demonstrate that this enhancement of HRSV infection is independent of TLR signaling. Although we cannot exclude a role for TLR stimulation in HIV-1 transmission by Langerhans cells, our observations in Jurkat cells that Pam-Cys-SK4 and PHCSK4 showed a similar enhancement of HIV-1 infection as Pam3CSK4 demonstrate that also for HIV-1 TLR-signaling-independent enhancement of infection can be observed, and is likely related to a similar mechanism as shown for HRSV and MV.

Using different lipopeptides we identified the cationic properties and the N-palmitoylated cysteine in Pam3CSK4 as crucial characteristics for enhancement of virus infection. We suggest that the N-palmitoylated cysteine may function as a structure interacting directly with the viral or target cell membrane. It has previously been described in the murine B-cell leukemia line BCL1 that already 20 minutes after incubation with Pam3-Cys-Ser a major amount of the lipopeptide can be found in the plasma membrane [265]. After membrane binding by

Pam3CSK4 the exposed cationic SK4 sequence could subsequently interact with negatively charged structures on the membrane of virus or cell, and result in infection enhancement similar to what has been described for other cationic agents such as DEAE-dextran, polybrene or semen-derived enhancer of viral infection (SEVI) [261,262,266]. Interestingly, we found that highly sulfated polyanions could abrogate Pam3CSK4-mediated enhancement of rgRSV infection or binding, in a pattern almost completely identical to that described for the interaction between these compounds and SEVI [262]. However, additional non-electrostatic forces may be of importance, as two other lipopeptides containing positively charged amino acids, Pam3CSH4 and Pam3CSR4, could not mediate enhancement of HRSV infection.

Pam3CSK4 was found to decrease HRSV infection in epithelial cell lines A549 and HEp-2. However, this effect was only observed when the cells were pre-incubated with the lipopeptide, and not when the virus was pre-incubated with the lipopeptide. It has been described that rgRSV can efficiently bind to GAGs expressed on immortalized epithelial cell lines [267]. This effect is generally considered an *in vitro* artifact, as wild-type HRSV strains cannot use GAGs as cellular receptors [207]. We reasoned that pre-incubation of A549 cells with the cationic Pam3CSK4 may reduce virus binding to the negatively charged GAGs, thus interfering with the normal attachment of HRSV to these cells. Using a GAG-independent virus (MV) we could not detect reduced infection levels in A549 cells pre-incubated with Pam3CSK4 (data not shown). In order to test our hypothesis we performed HRSV infections in normal or GAG-deficient CHO cells and indeed measured inhibition on pre-incubated CHO-cells expressing GAGs, but not in GAG-deficient CHO-cells. Since Pam3CSK4 not only enhanced infection of rgRSV but



also of wild-type HRSV isolates in B-LCL and primary epithelial cells, and this lipopeptide also enhanced infections with HMPV, MV and HIV-1, we believe that the inhibition of rgRSV infection in A549 and Hep-2 cells is solely related to the laboratory adaptation of rgRSV to efficiently bind GAGs, and does not reflect potential interactions between bacterial lipopeptides and wild-type HRSV infection *in vivo*.

Other cationic compounds, such as DEAE-dextran, polybrene, RANTES, and SEVI, have also been shown to enhance viral infection [262,266,268]. Polybrene, a synthetic cationic polymer neutralizing the charge repulsion between the virus and the cell surface, leads to enhancement of infection of a variety of retroviruses, including HIV [269]. SEVI enhances HIV infection by cross-linking HIV viruses to target cells, facilitating subsequent fusion [262,268]. RANTES, a cationic chemokine, has been reported to enhance HIV-1 infection by binding to proteoglycans on the surface of target cells [270]. Interestingly, RANTES has also been associated with inhibition of HRSV infection in HEp2-cells [271], which could be mediated through an analogous mechanism to Pam3CSK4-mediated reduction of rgRSV infection in A549 cells described here.

Pam3CSK4 is a synthetic mimic of the N-terminal parts of lipopeptides present in the cell walls of gram-positive and gram-negative bacteria, which have been identified as TLR agonists [272]. Therefore, the biological property of these lipopeptides as potential enhancers of HRSV binding could explain in part the observed interactions between HRSV and pneumococci [76,78]. We speculate that carriage of respiratory bacteria in the upper or lower respiratory tract could facilitate binding of HRSV to their target cells and thus play a role in the pathogenesis of severe HRSV bronchiolitis. This would be a possible explanation for the

fact that polyvalent pneumococcal vaccination has been associated with reduced HRSV hospitalization rates [80]. Our results indicate that APCs are normally relatively resistant to HRSV infection. However, lipopeptides such as Pam3CSK4 strongly enhanced rgRSV infection of these cells. Increased binding of HRSV to and infection of APCs may boost immune activation and might as such be involved in pulmonary disease during HRSV and bacterial co-infections.

Pam3CSK4 has been evaluated in several studies as a potential adjuvant for peptide vaccines [273-275]. Interestingly, our data suggest that the lipopeptide could also be considered as a potential adjuvant for live-attenuated virus vaccines. Development of a live-attenuated HRSV vaccine has been hampered by difficulties in finding a proper balance between attenuation and immunogenicity of candidate vaccine viruses [276]. Pam3CSK4 has the potential to enhance binding of a live-attenuated HRSV vaccine administered intra-nasally, while also stimulating innate immune responses through TLR1/2 interactions. However, as HRSV vaccines will need to be given to very young infants, this latter property may be undesired. Alternatively, the non-TLR agonists Pam-Cys-SK4 or PHCSK4 could be considered as adjuvants, resulting in enhanced binding of an over-attenuated live-attenuated HRSV vaccine without resulting in immune stimulation. Currently, we are performing studies in animal models to test this hypothesis.

In conclusion, we have shown that Pam3CSK4 and at least two structurally related cationic lipopeptides can enhance infections with HRSV, measles virus, human metapneumovirus and HIV-1. In contrast to our initial hypothesis, this effect proved to be independent of TLR1/2 signaling but was mediated by enhancing binding of the viruses to their target cells.

### Materials & Methods

#### Ethics statement

Human BAL cells were collected from patients suspected for pulmonary sarcoidosis in the framework of another study [277]. After written informed consent patients underwent fibre-optic bronchoscopy. The protocol was approved by the Medical Ethical Committee of the Erasmus University, Rotterdam.

#### Cells

A549 cells (human pneumocyte type II carcinoma cells, ATCC CCL-185) and Epstein-Barr virus-transformed human B-LCL [278] GR were cultured in RPMI-1640 medium (Lonza) supplemented with L-glutamine, penicillin, streptomycin (Lonza) and 10% fetal bovine serum (FBS, Sigma-Aldrich). HEp-2 cells (human nasopharyngeal carcinoma cells, ATCC CCL-23) were cultured in Dulbecco's Modified Eagle Medium (Lonza) supplemented with L-glutamine, penicillin, streptomycin and 10% FBS. Monocyte-derived immature DCs were cultured as described [279]. In short, human peripheral blood monocytes were isolated from buffy coats (provided by Sanquin Blood Bank South West Region, Rotterdam) by density centrifugation, followed by selection of CD14<sup>+</sup> cells using magnetic beads (MACS, Milteny Biotec GmbH). Purified monocytes were cultured in RPMI-1640 medium supplemented with L-glutamine, penicillin, streptomycin and 10% FBS and differentiated into immature DCs in the presence of IL-4 and GM-CSF (500 and 800 U/ml, respectively; Schering-Plough). Human broncho-alveolar (BAL) cells were cultured in RPMI-1640 supplemented with antibiotics and 10% FBS. NHBE cells (Clonetics) were used undifferentiated. Cells were cultured in 30 µg/ml type I collagen- (Nutacon) and 10 µg/ml fibronectin- (Sigma-Aldrich), coated culture flasks (Corning) or flat-bottom 96-well plates (Greiner Bio-One B.V.) in bronchial epithelial cell basal medium (Clonetics) supplemented

with penicillin and streptomycin. CHO K-1 cells (ATCC CCL-61), CHO pgsA-745 cells (ATCC CRL-2242) and CHO pgsD-677 cells (ATCC CRL-2244) were cultured in Ham's F12K medium supplemented with 10% FBS, penicillin and streptomycin. Jurkat T cells expressing CCR5 were previously described [253] and cultured in RPMI-1640 medium (Lonza) supplemented with 4500 mg/L glucose, 110 mg/l sodium pyruvate, 4 mM L-glutamine, 10% FBS, penicillin and streptomycin.

#### Viruses

To generate HIV-1-GFP, 293T cells were transfected with the NL4.3-eGFP-BaL proviral plasmid (4 µg; generously provided by C. Aiken (Vanderbilt University, Tennessee, USA). After 3 days the NL4.3-eGFP-BaL virus was harvested and titrated using the indicator cells TZM-blue (contributed by John C. Kappes, Xiaoyun Wu [both at University of Alabama, Birmingham, Alabama, USA], and Tranzyme Inc. through the NIH AIDS Research and Reference Reagent Program). HMPV-EGFP (strain 00-1) was grown as described previously [280] and had a titer of  $6.3 \times 10^6$  TCID<sub>50</sub>/ml. Recombinant pathogenic and attenuated MV expressing EGFP were grown as described previously [281,282]. The titers of recombinant pathogenic and attenuated MV were  $1 \times 10^6$  TCID<sub>50</sub>/ml and  $6.3 \times 10^4$  TCID<sub>50</sub>/ml, respectively. rgRSV is a recombinant virus based on HRSV strain A2, which was a kind gift of Dr. M.E. Peeples and Dr. P.L. Collins. The construction and rescue of rgRSV has been described in detail elsewhere [256]. Briefly, GFP was inserted as the first, promoter-proximal gene in a full-length cDNA of the HRSV A2 antigenomic RNA. As a consequence rgRSV-infected cells express GFP upon infection. rgRSV has been described to have the same growth kinetics and virological characteristics as the HRSV A2 strain [207,256]. rgRSV was grown and titrated on HEp-2 cells and aliquots were stored at -80°C until use. The titer of the virus used

in these studies was  $1 \times 10^7$  TCID<sub>50</sub>/ml. Other (non-recombinant) HRSV strains used were the HRSV subgroup A strains HRSV Long (ATCCVR-26) and HRSV A2 (ATCCVR1302), the HRSV subgroup B strain 9320 (ATCC VR955) and three wild-type HRSV isolates from our hospital archives, which were used at passage 2 in HEp-2 cells.

### Lipopeptides

Pam-Cys-SK4, PamDhcSK4, PamSK4, Pam2CSK4, Pam3CSE4, Pam3CSH4, Pam3CSK2, Pam3CSK4, Pam3CSK5, Pam3CSP4, Pam3CSR4, PHCSK4, Pam3CSK4-CF and CSK4-CF were synthesized by EMC microcollections, Germany (Figure S1 for molecular structures). Stocks were prepared in distilled water at 1 mg/ml.

### TLR agonist experiment

A549, HEp-2, NHBE cells ( $2 \times 10^4$  cells per well), monocyte-derived immature DCs, BAL cells or B-LCL ( $5 \times 10^4$  cells per well in 96-well flat-bottom plates) were incubated with different TLR agonists (Invivogen) for 6 hrs as described previously [253]. Pam3CSK4, Pam2CSK4, purified LTA-SA, peptidoglycan from *S. aureus* (PGN-SA), lipopolysaccharide from *E. coli* (LPS) were incubated at final concentrations of 10 µg/ml and a synthetic diacylated lipoprotein (FSL-1) and flagillin from *B. subtilis* at final concentrations of 1 µg/ml. Heat killed *L. monocytogenes* (HKLM) was used at a concentration of  $1 \times 10^9$ /ml. After the 6 hour incubation, all cells were infected with rgRSV ( $1 \times 10^4$  TCID<sub>50</sub> per well for A549, HEp-2 and NHBE cells,  $5 \times 10^4$  TCID<sub>50</sub> per well for immature DCs and  $1 \times 10^5$  TCID<sub>50</sub> per well for BAL cells and B-LCL). Twenty-four hrs post infection the cells were trypsinized (only for adherent cells) and percentages of GFP<sup>+</sup> cells were determined by flow cytometry (FACS Canto II, Becton-Dickinson).

### Experiments with lipopeptides only

$5 \times 10^4$  B-LCL were seeded in 96-well flat-bottom plates (V-bottom plates, if the cells were washed during the experiment). Unless stated otherwise, cells were pre-incubated with lipopeptides for 30 min before rgRSV was added ( $1 \times 10^5$  TCID<sub>50</sub>), hereafter referred to as pre-incubation on cells. In some experiments, virus was pre-incubated with Pam3CSK4 for 30 min before addition to the cells, hereafter referred to as pre-incubation of virus. In these experiments, the virus was pre-incubated in a small volume and subsequently diluted at least 1:10 before addition to the cells. Twenty - twenty-four hrs post infection the percentages of GFP<sup>+</sup> cells were determined by flow cytometry (FACS Canto II, Becton-Dickinson).

### MyD88 experiment / TLR1/2 blocking

$5 \times 10^4$  B-LCL cells were plated in 96-well v-bottom plates. The cells were either pre-incubated with the myeloid differentiating factor 88 (MyD88) homodimerization inhibitory peptide (100 µM, Imgenex, USA) for 24 hrs or with polyclonal blocking antibodies to TLR1, TLR2, TLR4 or the combination of TLR1 and TLR2 (20 µg/ml, Invivogen, USA) for 30 minutes. The cells were then incubated with Pam3CSK4 and subsequently infected with rgRSV ( $1 \times 10^5$  TCID<sub>50</sub>). Twenty - twenty-four hrs post infection the percentages of GFP<sup>+</sup> cells were determined by flow cytometry.

### HRSV binding assays

To assess lipopeptide-mediated enhancement of HRSV binding to cells, B-LCL ( $3 \times 10^4$ ) were incubated with rgRSV ( $2.2 \times 10^5$  TCID<sub>50</sub>) that had been pre-incubated (30 minutes, 37°C) with lipopeptide (10 µg/ml). After 15 minutes at 37°C, cells were washed and incubated with FITC-labeled anti-HRSV or anti-influenza-B as a control (Imagen immunofluorescence tests, OXOID, diluted 1:10 in complete RPMI).

To assess binding of lipopeptides to HRSV, lipopeptides were coated on high-

binding 96-wells flat-bottom ELISA plates at a concentration of 300 ng/well in acetate buffer (pH 4.6) for 2 hrs (37°C), after which free binding sites were blocked for 1 hr (37°C) with DMEM supplemented with 10% FBS. After washing, wells were incubated with HRSV-A2 or with measles virus strain Edmonston as a control (both  $10^6$  TCID<sub>50</sub> per well) as control (1 hr, 37°C), followed by washing and addition of anti-HRSV antibody (NIH clone 1107). ELISA plates were subsequently stained with goat-anti-mouse peroxidase and TMB as a substrate, and extinctions were determined at 450 nm.

To assess binding of lipopeptides to cells, B-LCL were incubated with different concentrations of carboxyfluorescein-labeled Pam3CSK4 (Pam3CSK4-CF, Mw 2094) or CSK4 (CSK4-CF, Mw 1079) for 30 minutes at 4°C or 37°C. Subsequently, cells were washed twice and fluorescence was measured by flow cytometry. Results are shown as the geometric mean fluorescence (mean  $\pm$  SD of triplicates).

### **Polyanion experiments**

Polyanion reagents (heparin, dextran sulfate, and chondroitin sulfate) were obtained from Sigma-Aldrich. Oversulfated heparin, de-O-sulfated heparin and oversulfated chondroitin sulfate were obtained from Neoparin. The polyanions were stored in PBS at a concentration of 30 mg/ml at -20°C.  $5 \times 10^4$  B-LCL were plated in 96-well v-bottom plates. The cells were pre-incubated with different lipopeptides for 15 minutes at 37°C and subsequently incubated for 15 minutes with the indicated polyanions (30  $\mu$ g/ml). The cells were washed three times and infected with rgRSV ( $1 \times 10^5$  TCID<sub>50</sub>).

### **Enhancement studies with HIV, HMPV and MV**

$5 \times 10^4$  Jurkat-CCR5 cells were plated in 96-well u-bottom plates and pre-incubated with different lipopeptides and subsequently

inoculated with NL4.3-eGFP-BaL at different concentrations in the presence or absence of the indicated lipopeptides (all at 10  $\mu$ g/ml). Two days post infection the cells were fixed and percentages of EGFP<sup>+</sup> cells were determined by flow cytometry. The other viruses were tested in B-LCL, using a single MOI and a concentration range of lipopeptide as described above, and determining percentages GFP<sup>+</sup> cells 20-24 hrs post infection.

### **Statistical Analysis**

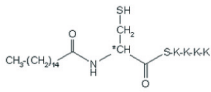
All experiments were performed at least three times using triplicate measurements, except for the ELISA experiment with lipopeptides, which had duplicate measurements. Data are expressed as means  $\pm$  standard deviations. Differences between two groups (treatment and control) were analyzed with Student's t-test, using Bonferroni's correction to correct for multiple comparisons. When comparing multiple treatment groups to the same control, differences were compared using 1-Way ANOVA with Dunnett's Correction for multiple comparisons. A two-sided (uncorrected) *p*-value <0.05 was considered statistically significant. Methods for specific statistical comparisons are given in the figure legends.

### **Acknowledgements**

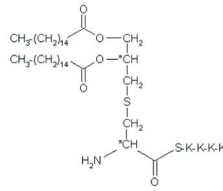
We thank M.E. Peeples and P.L. Collins for providing rgRSV, and G.I. Aron, W.P. Duprex, B.G. van den Hoogen, M.A.W.P. de Jong, A. Kleinjan, D. van Riel, R.D. de Vries and L. de Waal for their contributions to these studies.

# Lipopeptide-Mediated Enhancement of Virus Binding

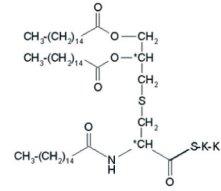
Pam-Cys-SK4



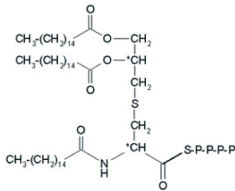
Pam2CSK4



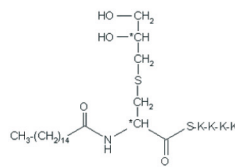
Pam3CSK2



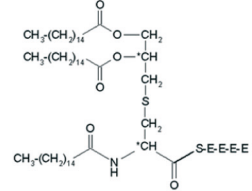
Pam3CSP4



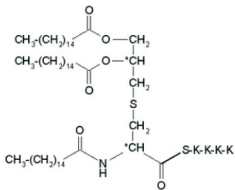
PamDhcSK4



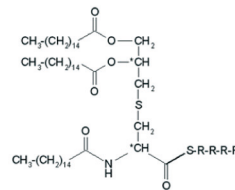
Pam3CSE4



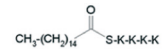
Pam3CSK4



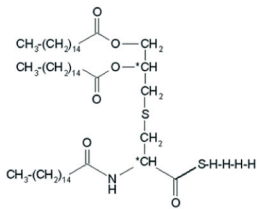
Pam3CSR4



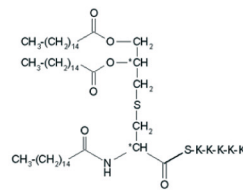
PamSK4



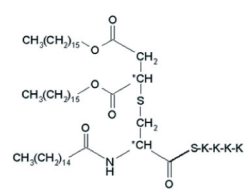
Pam3CSH4



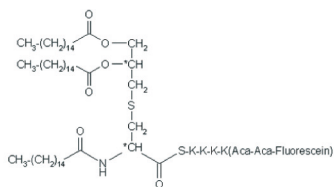
Pam3CSK5



PHCSK4



Pam3CSK4-CF



CSK4-CF

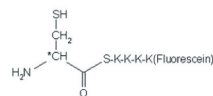
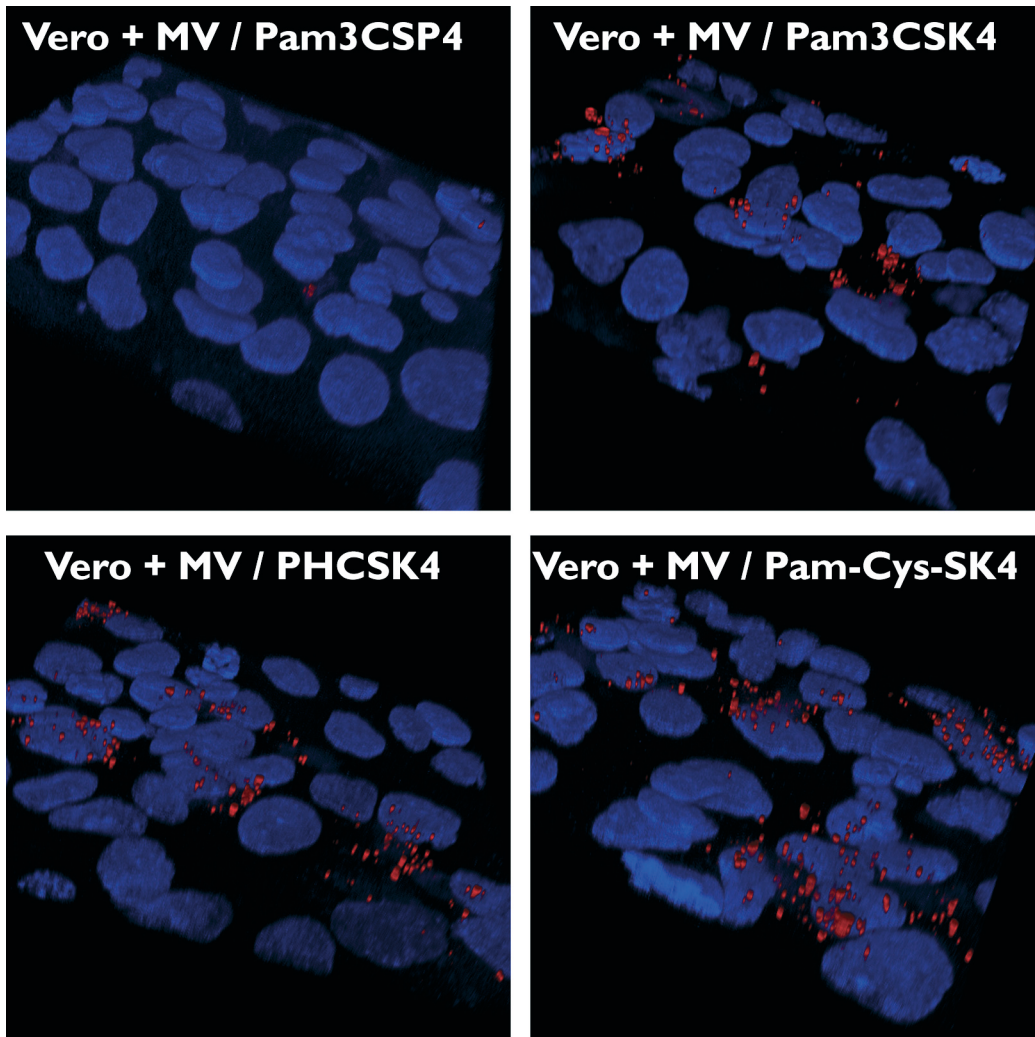


Figure S1. Molecular structures of (lipo)peptides used in this study.



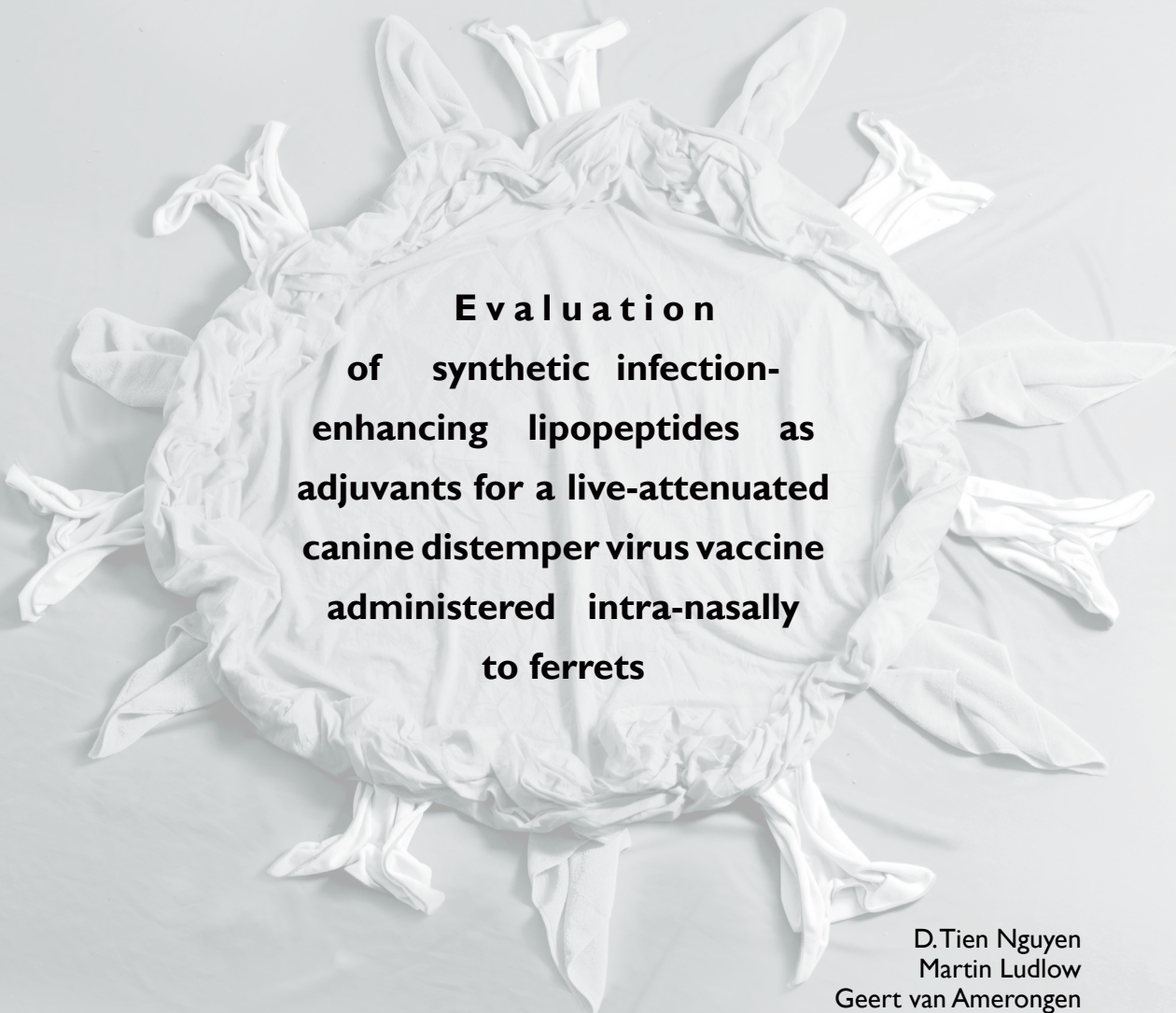
**Figure S2.** Binding of measles virus (MV) pre-incubated with different lipopeptides to Vero cells with different lipopeptides to Vero cells. MV strain Edmonston was pre-incubated with lipopeptide (10  $\mu$ g/ml) at 37°C (30 min), and subsequently added to Vero cells (40 min, 4°C). After washing, cells were stained with MV hemagglutinin-specific monoclonal antibody C28-10, washed and fixed with 4% PFA and stained with an anti-mouse Alexa-568 conjugate. Cells were washed again, counterstained with DAPI and imaged on a Zeiss LSM700 confocal microscope. Incubation with MV only or no virus controls resulted in similar staining as Vero + MV / Pam3CSP4 (not shown)







## Chapter 3



**Evaluation  
of synthetic infection-  
enhancing lipopeptides as  
adjuvants for a live-attenuated  
canine distemper virus vaccine  
administered intra-nasally  
to ferrets**

D.Tien Nguyen  
Martin Ludlow  
Geert van Amerongen  
Rory D. de Vries  
Selma Yüksel  
R. Joyce Verburgh  
Albert D. M. E. Osterhaus  
W. Paul Duprex  
Rik L. de Swart

*Vaccine*. 30(34):5073-80 (2012)

## Chapter 3

### Abstract

Background: Inactivated paramyxovirus vaccines have been associated with hypersensitivity responses upon challenge infection. For measles and canine distemper virus (CDV) safe and effective live-attenuated virus vaccines are available, but for human respiratory syncytial virus and human metapneumovirus development of such vaccines has proven difficult. We recently identified three synthetic bacterial lipopeptides that enhance paramyxovirus infections *in vitro*, and hypothesized these could be used as adjuvants to promote immune responses induced by live-attenuated vaccines.

Methods: Here, we tested this hypothesis using a CDV vaccination and challenge model in ferrets. Three groups of six animals were intra-nasally vaccinated with recombinant (r) CDV<sup>5804P</sup>L(CC<sub>EGFP</sub>C) in the presence or absence of the infection-enhancing lipopeptides Pam3CSK4 or PHCSK4. The recombinant CDV vaccine virus had previously been described to be over-attenuated in ferrets. One group of six animals was mock-vaccinated as control. Six weeks after vaccination all animals were challenged with a lethal dose of rCDV strain Snyder-Hill expressing the red fluorescent protein dTomato.

Results: Unexpectedly, intra-nasal vaccination of ferrets with rCDV<sup>5804P</sup>L(CC<sub>EGFP</sub>C) in the absence of lipopeptides resulted in good immune responses and protection against lethal challenge infection. However, in animals vaccinated with lipopeptide-adjuvanted virus significantly higher vaccine virus loads were detected in nasopharyngeal lavages and peripheral blood mononuclear cells. In addition, these animals developed significantly higher CDV neutralizing antibody titers compared to animals vaccinated with non-adjuvanted vaccine.

Conclusions: This study demonstrates that the synthetic cationic lipopeptides Pam3CSK4 and PHCSK4 not only enhance paramyxovirus infection *in vitro*, but also *in vivo*. Given the observed enhancement of immunogenicity their potential as adjuvants for other live-attenuated paramyxovirus vaccines should be considered.

## Introduction

Canine distemper virus (CDV) is a member of the family *Paramyxoviridae*, which also includes measles virus (MV), human respiratory syncytial virus (HRSV) and human metapneumovirus (HMPV). CDV is best known as a pathogen of dogs, but has a broad host range and causes disease in different carnivore species and in non-human primates [96,283]. CDV infection induces a systemic disease, which is associated with immunosuppression and often involves infection of the central nervous system [98,99].

We recently demonstrated that the synthetic bacterial lipopeptide Pam3-Cys-Ser-Lys4 (Pam3CSK4) enhanced *in vitro* infections with HRSV, HMPV and MV [284]. Pam3CSK4 is a synthetic tripalmitoylated lipopeptide and is the prototype agonist for the heterodimeric TLR1/2 complex [264,285], and had previously been associated with enhancement of infections with human immunodeficiency virus (HIV) type-1 [253-255]. Although in these studies it was assumed that enhancement of infection was related to TLR activation, we identified two structurally-related synthetic lipopeptides, PHCSK4 and Pam-Cys-SK4, which did not function as TLR ligands, but showed a similar enhancement of paramyxovirus or HIV-1 infections as Pam3CSK4. In contrast, other lipopeptides that did stimulate TLR1/2 responses did not enhance paramyxovirus or HIV-1 infections [284]. Enhancement of infection seemed dependent on the cationic properties and the N-palmitoylated cysteine of the lipopeptides, and was mediated by increased virus binding. We hypothesized that these synthetic infection-enhancing lipopeptides could be used as adjuvants for live-attenuated virus vaccines. Formulation of an over-attenuated paramyxovirus vaccine with an infection-enhancing lipopeptide may enhance the capacity of the virus to infect cells during the

first round of infection. Thus the formulated vaccine could induce adequate immune responses, whereas the risk of (serious) adverse effects for the vaccinee remains low.

We selected a CDV vaccination and challenge model in ferrets for a proof-of-concept study to address this question. In this model ferrets were intra-nasally (i.n.) vaccinated with a live-attenuated CDV vaccine virus [101], followed by a lethal challenge infection with a wild-type CDV strain [100]. The rCDV vaccine used in this model was previously described to induce sub-optimal protective immune responses in ferrets [101]. The virus, rCDV<sup>5804P</sup>L(CC<sub>EGFP</sub>C) was generated by inserting the open reading frame encoding enhanced green fluorescent protein (EGFP) into the sequence coding for the second hinge of the CDV large (L) protein, which is the major component of the viral RNA-dependent RNA polymerase. Such manipulations of morbillivirus L proteins attenuate pathogenic viruses in a single step, whilst keeping all of the structural proteins authentic wild-type. It was reported that the level of attenuation was greater than desired, resulting in sub-optimal vaccine virus replication in ferrets and incomplete protection following challenge with a wild-type virus. However, in that study only six animals were challenged and two succumbed to the infection. We hypothesized that in the ferret model, formulation of the vaccine virus in infection-enhancing lipopeptides would result in improved vaccination efficacy after a single i.n. administration of the rCDV which, in turn, would result in enhanced CDV-specific immune responses and thus better protection.

### Materials & Methods

#### Ethical statement

The animal protocol was approved by an independent animal experimentation ethics committee prior to the start of the experiments. All experiments were performed in compliance with European guidelines for animal experimentation (EU Directive 2010/63/EU). Animals were monitored daily, and animal care was in compliance with institutional guidelines.

#### Animals

Twenty-four 12-month-old unvaccinated female European ferrets (*Mustela putorius furo*) were purchased from a breeding farm in the Netherlands. Animals were tested for the presence of serum antibodies against CDV using virus neutralization assays (for method see below). A temperature probe was inserted intraperitoneally two weeks before the beginning of the experiments to monitor body temperatures non-invasively. Following infection animals were housed in groups of six in negatively pressurized, HEPA-filtered biosafety level 3 (BSL-3) isolator cages and received food and water *ad libitum*.

#### Cells

Lymph nodes were collected from control ferrets in unrelated approved animal experiments prior to vaccination. These were stored in phosphate-buffered saline (PBS) for a maximum time of 4 hrs, after which single cell suspensions were prepared using cell strainers with a 100  $\mu\text{m}$  pore size (BD Biosciences). Cells were resuspended in RPMI-1640 medium (Lonza) supplemented with L-glutamine (2 mM), penicillin (100 U/ml), streptomycin (100  $\mu\text{g}/\text{ml}$ ) and 10% (v/v) heat-inactivated fetal bovine serum (FBS, Sigma-Aldrich) and used directly for virus infections. African green monkeys kidney cells transfected with signaling lymphocyte activation molecule (VeroDogSLAM cells) [286] were a kind gift of

Dr.Y. Yanagi, Kyushu University, Fukuoka, Japan, and were cultured in Dulbecco's Modified Eagle Medium (DMEM; Lonza) supplemented with L-glutamine, penicillin, streptomycin and 10% (v/v) FBS.

#### Viruses

The live-attenuated rCDV strain, rCDV<sup>5804P</sup>L(CC<sub>EGFP</sub>C), and the challenge rCDV Snyder-Hill (SH) strain expressing the red fluorescent protein dTomato, rCDV<sup>SH</sup>dTom(6), had been generated previously [100,101]. A challenge virus expressing a fluorescent protein different from EGFP was used to avoid interfering specific T-cell responses directed against the fluorescent protein following challenge. Virus titers were calculated by the Reed and Muench method at  $3.5 \times 10^5$  and  $3.5 \times 10^6$  50% tissue culture infective dose (TCID<sub>50</sub>)/ml for rCDV<sup>5804P</sup>L(CC<sub>EGFP</sub>C) and rCDV<sup>SH</sup>dTom(6), respectively.

#### Lipopeptides

Pam3CSK4, PHCSK4, Pam-Cys-SK4, and Pam3CSP4 were a kind gift of Dr. K.H. Wiesmüller (EMC microcollections, Germany) and their molecular structures have been previously reported [284]. Stocks were prepared in distilled water at 1 mg/ml.

#### Ex vivo CDV infection of lymphocytes

The lipopeptides Pam3CSK4, PHCSK4, Pam-Cys-SK4 or Pam3CSP4 were added to the viruses to a final concentration of 10  $\mu\text{g}/\text{ml}$ , and the mixtures were incubated for 5 minutes at 37°C to allow binding of the lipopeptides to the viruses. Ferret lymph node cells were infected with rCDV<sup>5804P</sup>L(CC<sub>EGFP</sub>C) or rCDV<sup>SH</sup>dTom(6), at a multiplicity of infection (MOI) of 0.1. One day post infection (d.p.i.) cells were analyzed for fluorescence by flow cytometry [284].

#### In vivo CDV infection experiment

The study included four groups of six ferrets. Groups 1-3 were vaccinated i.n. with 200  $\mu\text{l}$

# Lipopeptides as Adjuvants for a CDV Vaccine

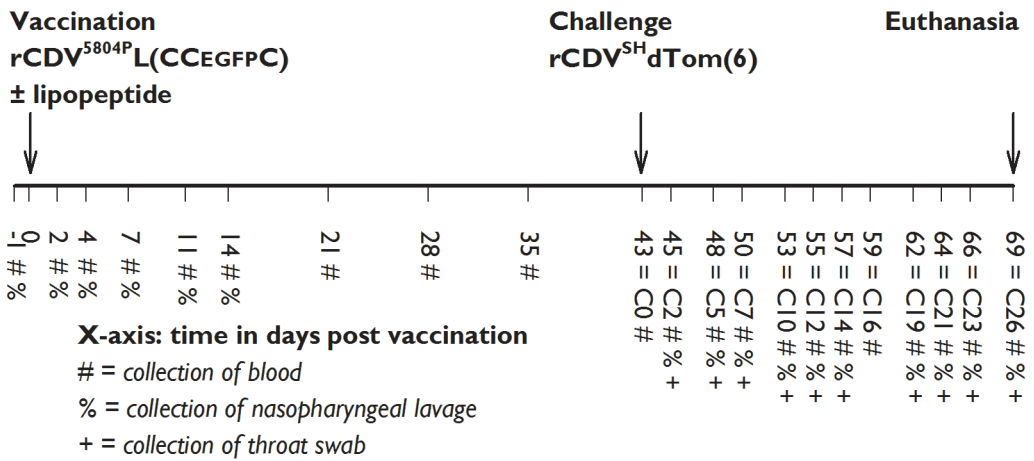


**Figure 1.** Study design of *in vivo* experiment. Time schedule for the vaccination and challenge period. Numbers represent sampling time points in days post vaccination, C-numbers in days post challenge infection. Sampling time points of blood, nasopharyngeal lavages and throat swabs are depicted by #, % and +, respectively.

(100 µl in each nostril) PBS containing  $3 \times 10^4$  TCID<sub>50</sub> rCDV<sup>5804P</sup>L(CC<sub>EGFP</sub>C). In two of these groups, the virus was mixed with lipopeptide (group 2: Pam3CSK4 or group 3: PHCSK4, 30 µg/ml). The mixture was incubated for 5 minutes at 37°C. The fourth group was mock-vaccinated and served as controls in the challenge experiment, which followed six weeks after vaccination. For challenge infection, animals received rCDV<sup>SH</sup>dTom(6) *i.n.* ( $3.5 \times 10^5$  in 200 µl) and intra-tracheally (*i.t.*,  $3.5 \times 10^4$  TCID<sub>50</sub> in 3 ml).

The total study lasted 69 days (Figure 1). Nasopharyngeal lavages were collected on days -1, 2, 4, 7, 11, and 14 after vaccination. Nasopharyngeal lavages and throat swabs were collected on days 2, 5, 7, 10, 12, 14, 16, 19, 21 and 23 after challenge. Blood samples were collected at the same time points and additionally on days 21, 28, 35 and 43 after vaccination. The endpoints of the study were body weight loss (>15% in two days or >20% of total body weight [bw]), severe respiratory or cardiac complications, or abnormal behavioral changes. All remaining animals were euthanized 26 days after challenge.

All procedures were performed under anesthesia with ketamine and medetomidine (0.2 and 0.01 ml/kg bw, respectively) and antagonized with atipamezole (0.005 ml/kg bw).

## Clinical samples

Nasopharyngeal lavages were obtained by flushing one nostril with 1 ml PBS, collecting the wash from the opposing nostril and adjusting the total volume to 650 µl. Throat swabs were collected by brushing the back of the oro-pharyngeal cavity, after which the brush (Medscand Medical, Cytobrush Plus cell collector) was placed in 1.5 ml virus transport medium (EMEM with Hanks' salts, supplemented with lactalbumin enzymatic hydrolysate [0.5 g/ml], penicillin, streptomycin, polymyxin B sulphate [100 U/ml], nystatin [50 U/ml], gentamicin [2.5 mg/ml] and glycerol [10% (v/v)]). Samples were vortexed, after which 200 µl was combined with 200 µl high pure RNA lysis buffer (Roche Diagnostics), the remainder was used directly for virus isolations. Blood samples (approximately 700 µl per animal per time point) were collected in tubes containing K3EDTA as an anticoagulant.

Plasma was separated from the blood by centrifugation, heat inactivated at 56°C for 30 minutes and stored at -20°C. Peripheral blood mononuclear cells (PBMC) were isolated from blood by density gradient centrifugation. Cells were resuspended in 700 µl complete RPMI 1640 medium, supplemented with L-glutamine, penicillin, streptomycin, and FBS. Cell suspensions were used for RT-PCR (200 µl), virus isolation (400 µl) or flow cytometry for direct detection of EGFP<sup>+</sup>- or dTom<sup>+</sup>-cells.

### Virus isolations

VeroDogSLAM ( $2 \times 10^4$  cells/well) were seeded in flat-bottom 96-wells plates one day before sampling. Clinical samples were divided over the wells of the first column, followed by three-fold serial dilution over the complete plate. Plates with throat and nasopharyngeal samples were spinoculated at 1,000xg for 15 minutes. After 1 hr incubation at 37°C, supernatant was removed and DMEM (100 µl) supplemented with L-glutamine, penicillin, streptomycin, amphotericin B (250 ng/ml) and 2% (v/v) FBS was added. Virus isolations were monitored by fluorescence microscopy for EGFP or dTom fluorescence 5-7 d.p.i., and titers expressed in TCID<sub>50</sub>/ml, which were calculated by the Reed and Muench method.

### TaqMan RT-PCR

The presence of CDV genomic RNA in nasopharyngeal lavages was determined by RT-PCR, using primers in the nucleocapsid (N) gene as previously described with slight modifications [287]. Primers used for amplification were as follows: forward 5'-GTC AGT AAT CGA GGA TTC GAG AG-3' (rCDV<sup>5804P</sup>L(CC<sub>EGFP</sub>C)-N nucleotides 2216-2229), forward 5'-GTC GGT AAT CGA GGA TTC GAG AG-3' (rCDV<sup>SH</sup>dTom(6)-N, nucleotides 2216-2229) and reverse, 5'-CTA ACT GGG GAT ATT CTT TCG GC -3' (rCDV<sup>5804P</sup>L(CC<sub>EGFP</sub>C) and rCDV<sup>SH</sup>dTom(6)-N, nucleotides 2297-2319). Sequence for the TaqMan probe was 5'-FAM-

AGC ACT GAG GAT TCT GGC GAA GAT-TAMRA-3' (rCDV<sup>5804P</sup>L(CC<sub>EGFP</sub>C) and rCDV<sup>SH</sup>dTom(6)-N, nucleotides 2251-2274). The cycle threshold (Ct) value was calculated automatically when the FAM-specific CDV signal was above the background and was used to give a semi-quantitative indication of viral loads.

### Necropsy

Animals were euthanized by exsanguination under anesthesia. Macroscopic detection of EGFP and dTom was performed at necropsy as previously described [92,100]. Briefly, tissues were illuminated with custom-made blue or green lamps containing six LEDs mounted with the appropriate excitation filters for EGFP and dTom, respectively. Orange or red goggles or camera filters (Sirchie) were used as emission filters. Photographs were made using a Nikon D80 SLR camera.

### Virus neutralization assay

Two-fold serial dilutions of heat inactivated plasma (50 µl) in flat-bottom 96 wells plates were mixed with 150 TCID<sub>50</sub> of rCDV<sup>SH</sup>dTom(6) (50 µl/well) and incubated for 1 hr at 37°C. Next,  $2 \times 10^6$  VeroDogSLAM cells / plate (100 µl/well) were added at a final FBS concentration of 2% (v/v). Infection was screened by fluorescence microscopy for 5-7 days. Neutralizing antibody titers were calculated by the Reed and Muench method. Results are shown as the reciprocal <sup>2</sup>log virus neutralizing (VN) antibody titer.

### Statistical Analysis

*Ex vivo* infections were performed three times, using triplicate measurements in each experiment. Multiple treatment groups to the same control, differences were compared using 1-Way ANOVA with Dunnett's Correction for multiple comparisons. For *in vivo* data, differences between the groups in body temperatures, body weights, virus loads, or VN antibody titers were compared

with area under the curve (AUC) integrated using the trapezoidal rule and statistically tested with Mann-Whitney *U* tests. Data are expressed as mean  $\pm$  standard error of the mean (SEM) or geometric mean  $\pm$  geometric standard deviation (GSD), where appropriate. A two-sided (uncorrected) *p*-value  $< 0.05$  was considered statistically significant. All statistical analyses were performed with SPSS version 17 software (SPSS, Inc., Chicago, USA).

## Results

### Lipopeptide-mediated enhancement of *in vitro* CDV infection of ferret lymph node cells

Three synthetic cationic bacterial lipopeptides were previously described to enhance HRSV, HMPV, MV and HIV-1 infection *in vitro* in different primary cells and cell lines [284]. To determine if these lipopeptides also enhanced *in vitro* CDV infection, ferret lymph node cells were infected with the rationally-attenuated wild-type stain, rCDV<sup>5804P</sup>L(CC<sub>EGFP</sub>C)[101], or the pathogenic CDV strain rCDV<sup>SH</sup>dTom(6) [100], in the presence or absence of lipopeptide (10  $\mu$ g/ml). Pam3CSK4 and PHCSK4 significantly enhanced infection with both CDV strains as compared to the medium and lipopeptide control (Figure 2, *p*  $< 0.05$ ) and were selected as potential adjuvants for the rationally attenuated rCDV.

### Vaccination - clinical signs

Four groups of six ferrets were i.n. vaccinated with rCDV with or without lipopeptides as adjuvants (or mock-vaccinated with PBS). Limited changes in body temperature were recorded during the vaccination period for groups 2, 3, and 4 (Figure 3A-D). Three animals in group 1 experienced fever ( $> 1.5^{\circ}\text{C}$  temperature rise) for three days, and two had a subfebrile period lasting five days (Figure 3A). Two animals of group 2 and one of group 3 also experienced subfebrile periods of a week (Figure 3B, C). However, this temperature

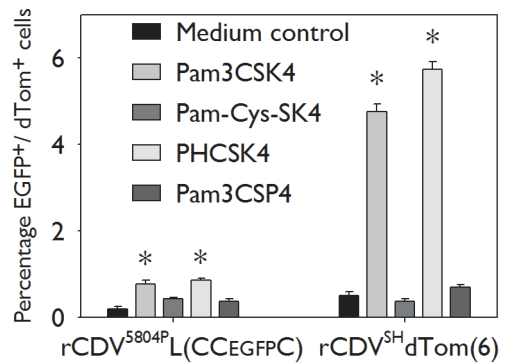


**Figure 2.** Lipopeptide-mediated enhancement of CDV infection in ferret lymph node cells. Two CDV strains (rCDV<sup>5804P</sup>L(CC<sub>EGFP</sub>C) or rCDV<sup>SH</sup>dTom(6)) were incubated with four different lipopeptides (10  $\mu$ g/ml) for 5 minutes at 37°C before the virus suspension was added to ferret lymph node cells. Formulation with Pam3CSK4 or PHCSK4 resulted in significantly increased rCDV infection percentages (bars represent mean  $\pm$  SEM, \* *p*  $< 0.05$  in 1-way ANOVA and posthoc Dunnett's correction for multiple comparisons with medium control).

increase was one week later and the duration was shorter in comparison to group 1.

All ferrets lost some weight in the first few days after vaccination (Figure 3, dashed lines). Over the next month the body weights of the majority of the animals stabilized or increased, and no statistically significant differences were observed between the treatment groups.

One animal, vaccinated with rCDV<sup>5804P</sup>L(CC<sub>EGFP</sub>C) formulated in PHCSK4, died 17 days after vaccination. Necropsy revealed a large bacterial jaw abscess as the cause of death. A similar, more superficially located abscess was observed an animal from group 4 and in several other ferrets not included in the present study but from the same source. Therefore, it was considered unlikely that either the abscess or the death were related to the virus or lipopeptide.

### Vaccination – virus loads and VN titers

Vaccine virus loads in nasopharyngeal lavages

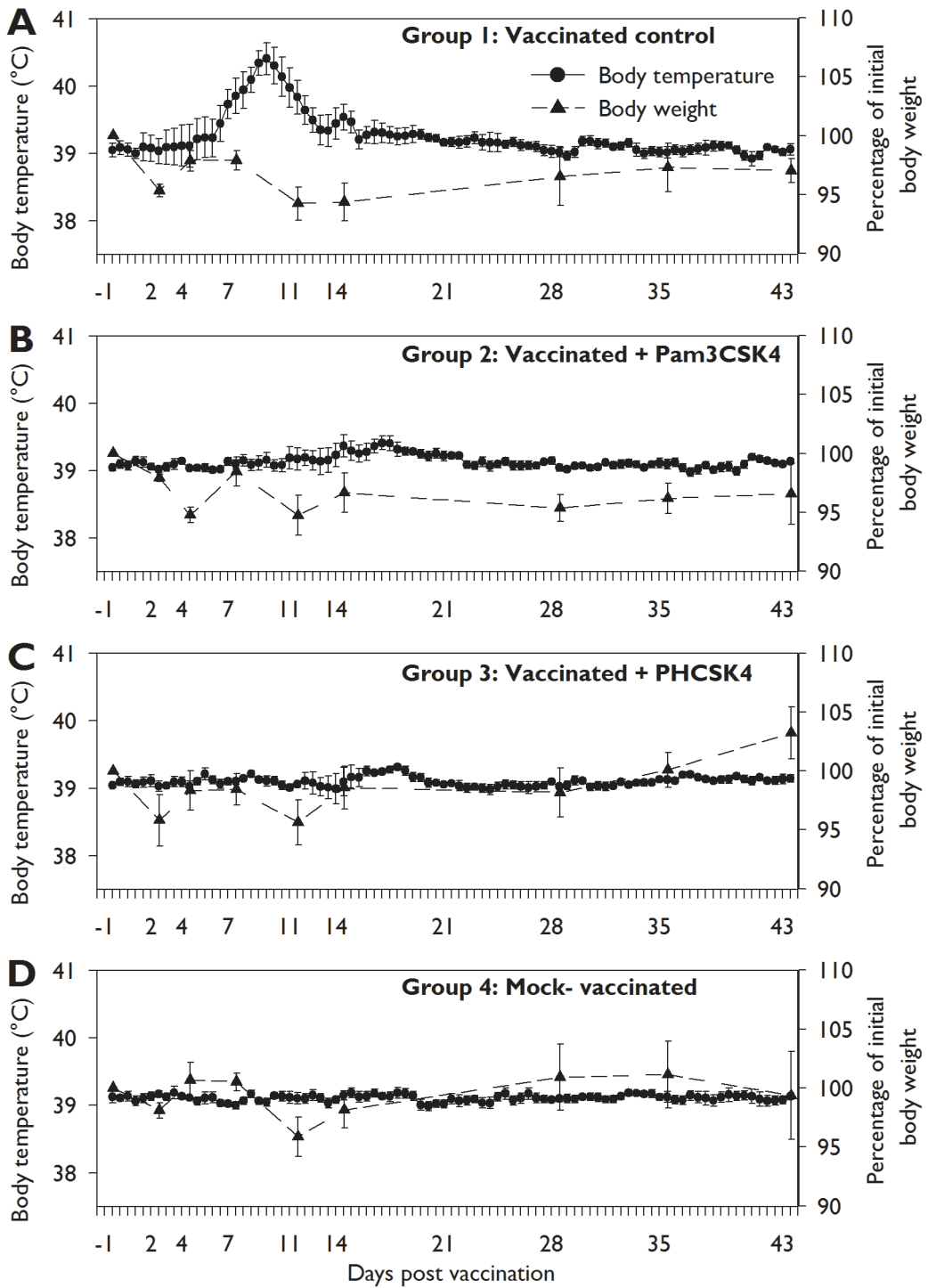




**Figure 3.** Vaccination - Body temperatures and body weights. Solid lines with round symbols represent the body temperatures (mean±SEM of six ferrets, left y-axis; group 3: five ferrets). In contrast to the adjuvanted groups, the vaccinated control showed an average body temperature increase during the second week after vaccination. Dashed lines with triangle symbols correspond to percentages of initial body weight (mean±SEM, right y-axis). Body weight losses were comparable for all groups.

and PBMC were detected by virus isolation (Figure 4 A, C) or Taqman RT-PCR (Figure 4B). Virus could be isolated from 7 days post

vaccination (d.p.v.) onwards, peaked at 11 d.p.v., and decreased afterwards. At 14 d.p.v. one animal of the control group infectious

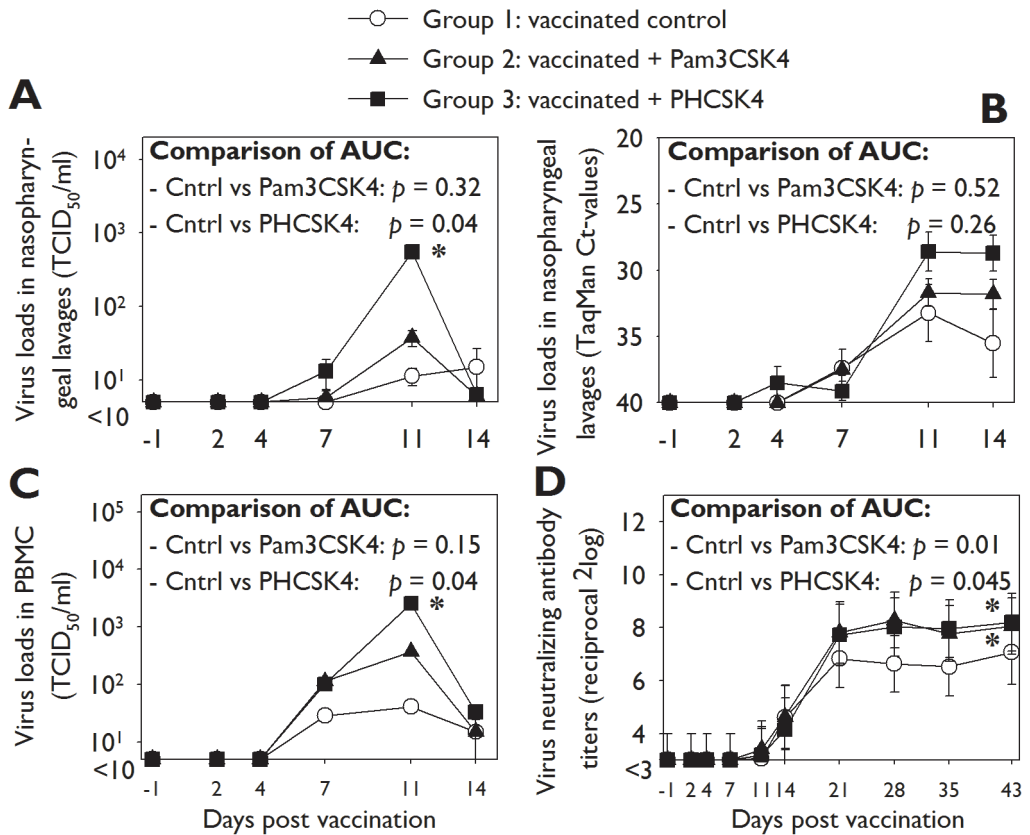


**Figure 4.** Vaccination - viral loads and neutralizing antibody titers. A) Vaccine virus loads in nasopharyngeal lavages as measured by virus isolation. Virus loads in the PHCSK4-adjuvanted group were statistically significantly higher compared to the non-adjuvanted group (lines represent geometric mean±GSD, \*  $p < 0.05$ ). B) Vaccine virus loads in nasopharyngeal lavages as measured by Taqman RT-PCR (lines represent mean±SEM). C) Vaccine virus loads in PBMC as measured by virus isolation. Virus loads in the PHCSK4-adjuvanted group were statistically significantly higher compared to the non-adjuvanted group (lines represent geometric mean±GSD, \*  $p < 0.05$ ). D) Virus neutralizing (VN) antibody titers were measured between 0 and 43 days post vaccination. At 11 d.p.v. the first ferrets seroconverted. Ferrets vaccinated with lipopeptide-adjuvanted CDV vaccine mounted significantly higher VN antibody titers (lines represent geometric mean±GSD, \*  $p < 0.05$ , AUC).

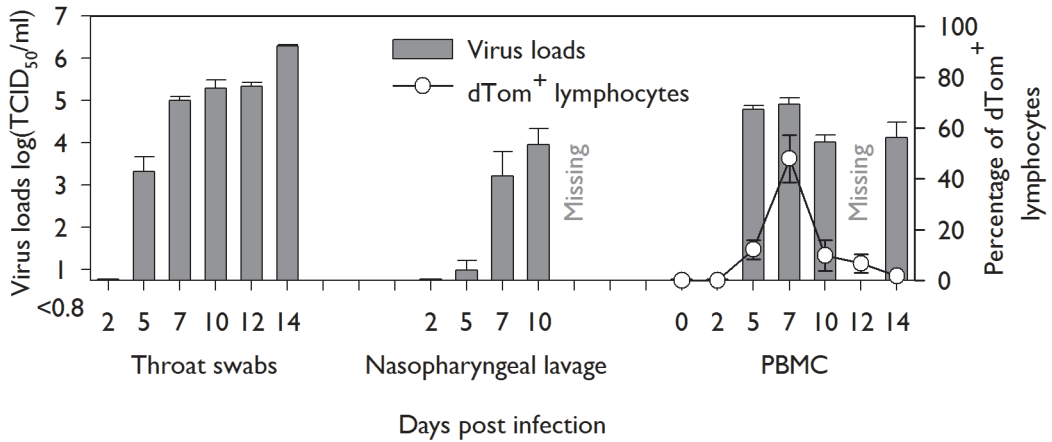


**Figure 5.** rCDV<sup>SH</sup>dTom(6) infection of control ferrets. Bars correspond to rCDV<sup>SH</sup>dTom(6) virus loads in throat swabs, nasopharyngeal lavages and PBMC collected from ferrets of group 4. The black line with round white symbols shows the percentages of dTom<sup>+</sup> lymphocytes as measured by flow cytometry in PBMC (bars and symbols represent mean±SEM).

virus was present. For the PHCSK4-adjuvanted group volume-adjusted virus titers were significantly higher compared to the mock controls for the whole sample period ( $p < 0.05$ ). For all groups viral genomes were detected in nasopharyngeal lavages at 7 d.p.v., increased between 7 and 11 d.p.v., and stabilized at the final nasopharyngeal lavage sample day.

Vaccine virus could also be isolated from PBMC from 7 d.p.v. onwards (Figure 4C). At 14 d.p.v. virus in PBMC was detected in one animal of groups 1 and 2, and 4 animals of group 3. Significantly higher virus loads were detected in group 3 compared to the control group ( $p < 0.05$ ).

VN antibodies were first detected 11 d.p.v. in  $n=3$ ,  $n=5$  and  $n=3$  animals of groups 1, 2, and 3, respectively, increased exponentially until 21 d.p.v. and stabilized afterwards (Figure 4D). All ferrets in groups 1, 2 and 3 had seroconverted by day 14. Neutralizing antibody titers of the lipopeptide-adjuvanted groups were on average 2.3 fold higher compared to animals vaccinated with non-adjuvanted virus (geometric mean VN

titers measured during the period 21 to 43 d.p.v.: group 1: 113, group 2: 260, and group 3: 263). For the complete vaccination period VN antibody titers in groups 2 and 3 were significantly higher than those of group 1 ( $p < 0.05$ ).

**Challenge – virus loads in mock-vaccinated animals**

Forty-three d.p.v., all vaccinated animals ( $n=17$ ) and six mock-vaccinated control animals were infected with rCDV<sup>SH</sup>dTom(6) by both i.n. ( $3.5 \times 10^5$  TCID<sub>50</sub>) and i.t. ( $3.5 \times 10^4$  TCID<sub>50</sub>) inoculation. During the challenge period virus isolations from throat swabs, nasal lavages and PBMC were performed in VeroDogSLAM cells (Figure 5). Up to  $6.3 \times 10^6$  TCID<sub>50</sub>/ml was isolated from the throat swabs. PBMC were analyzed in flow cytometry to determine the percentage of infected cells. A significant viremia was observed and up to 60% of lymphocytes were infected at the peak of infection (7 d.p.i.). Macroscopically, red fluorescence produced in rCDV<sup>SH</sup>dTom(6)-infected cells was first observed 5 d.p.i. on the throat/lower jaw and at later time-points on other body parts, like the conjunctivae of the

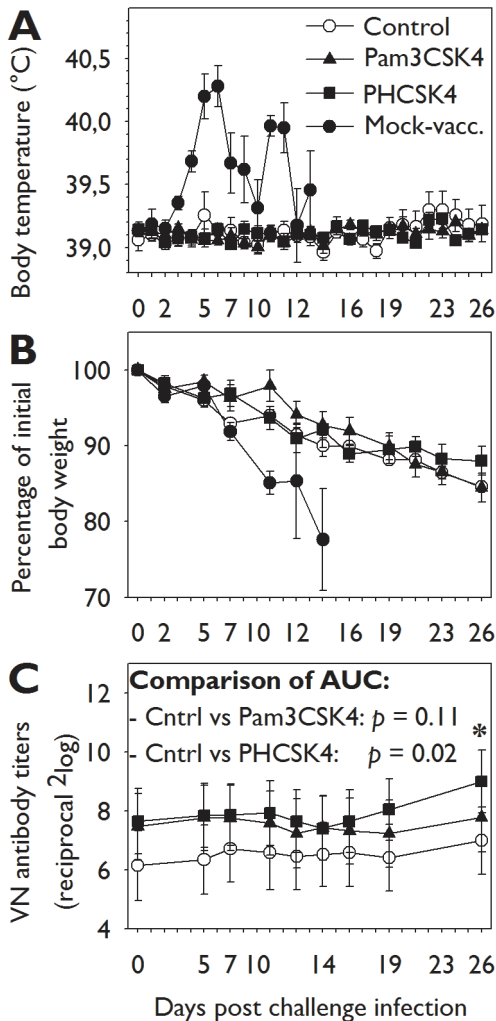


**Figure 6.** *rCDV<sup>SH</sup>dTom(6)* challenge infection: body temp., body weights and VN serum antibody responses. A) Symbols represent the body temperatures of the four groups (mean±SEM). The mock-vacc. group developed a typical biphasic (sub)febrile period. B) Symbols represent body weights relative to day C0, expressed in percentage (mean±SEM). All animals lost weight during the challenge period, but this was more dramatic in the mock-vacc. than in the vacc. animals. C) During the challenge period almost no secondary humoral immune response was observed. Overall, mean VN antibody titers of groups 2 and 3 remained higher compared to those of group 1 (GMT±GSD, \*  $p < 0.05$ , AUC).

eyes, rectum, skin (systemic) and footpads.

The rapid deterioration of the condition of all mock-vaccinated animals after infection was also evidenced by fever and weight loss (Figure 6A and 6B). Recorded body temperatures showed a typical biphasic (sub)febrile period in mock-vaccinated control animals. One animal was euthanized ten d.p.i., the remaining animals were euthanized at 14 d.p.i.

### Challenge – protective immunity in all vaccinated ferrets

I.n. vaccination with *rCDV<sup>5804P</sup>L(CC<sub>EGFP</sub>C)* protected all ferrets against lethal challenge infection with *rCDV<sup>SH</sup>dTom(6)*, irrespective of the formulation in lipopeptides. No significant differences were observed in behavioral changes, body temperatures (Figure 6A), body weights (Figure 6B), or virus detection. One animal of group 1 had a subfebrile period, which was not seen in groups 2 or 3. We did not observe a strong secondary humoral immune response during the challenge period (Figure 6C).

### Discussion

Two infection-enhancing lipopeptides [284] were evaluated as potential adjuvants for live-attenuated paramyxovirus vaccines using a CDV vaccination and challenge model in ferrets. The rationally attenuated CDV vaccine delivered by the i.n. route was very effective in inducing protective immunity, indeed more so than expected on basis of a previous study [101]. All vaccinated ferrets were fully protected against a high dose lethal i.n. and i.t. challenge with a highly virulent wild-type virus, irrespective of the presence or absence of lipopeptides. However, vaccination with lipopeptide formulated live-attenuated *rCDV* elicited statistically significantly higher vaccine virus loads and VN antibody titers. This is the first demonstration of the *in vivo* infection-enhancing properties of Pam3CSK4 and PHCSK4, and proves their potential as

adjuvants for needle-free paramyxovirus vaccination.

Currently there are no licensed adjuvants for live-attenuated virus vaccines. The synthetic lipid  $\alpha$ -galactosylceramide (alpha-GalCer) stimulates natural killer (NK) T-cells modulating cells of the adaptive immune response [288]. Alpha-GalCer can be used as an adjuvant for both live recombinant vaccines and inactivated vaccines [289,290]. Alpha-GalCer was successfully tested as an adjuvant for a live-attenuated influenza virus vaccine, but the mode of action is different than the proposed lipopeptide adjuvant [290].

The lipopeptide Pam3CSK4 has been tested as an adjuvant in peptide vaccination studies, based on its TLR-activating properties [291,292] being covalently conjugated to synthetic peptides containing the T- or B-lymphocyte epitopes [292,293]. It also functions as an adjuvant in DNA and virosomal immunization studies [294,295]. The mode of action uses the TLR activating properties of Pam3CSK4 to elicit powerful innate immune responses, thereby modulating the adaptive immune responses. However, we used the lipopeptides in a fundamentally different manner, namely to enhance infectivity of a live-attenuated virus. This could increase the number of host cells in which the virus can replicate, thereby leading to larger amounts of viral antigen produced. In addition, the lipopeptide could potentially decrease the percentage of non-responders when giving a live-attenuated paramyxovirus vaccine via the intra-nasal route, or could be used for dose-sparing of vaccines that are hard to produce. However, it should be noted that formulation in infection-enhancing lipopeptides could also result in an effect equivalent to partial vaccine virus de-attenuation. Therefore, clinical evaluation and assessment of tolerability will be crucial.

Initially, it was planned that vaccinated ferrets would only be challenged i.n. with rCDV<sup>SH</sup>dTom(6), as we anticipated that the vaccine virus was over-attenuated. However, as VN antibodies to CDV lead to protection [99,296], and we observed high VN antibody levels in all vaccinated ferrets, it was decided to administer a higher dose of the virus via both the i.n. and i.t. route and thus provide a stronger challenge for the protective immune response.

All vaccinated ferrets lost weight after challenge infection, which was consistent with a previous study [297] in which ferrets lost weight for 16 days for an unknown reason without any lipopeptides being used. Virus isolations from all groups 9 d.p.i. (data not shown) suggest that despite the presence of protective immunity the challenge virus may have caused a subclinical infection.

The ultimate objective is to achieve a similar effect of these lipopeptides on a live-attenuated HRSV vaccine. Despite the high global burden of HRSV disease, no licensed vaccines against HRSV are available [16,37]. Main challenges for the development of HRSV vaccines are these should be safe and effective at an early age in the presence of maternal antibodies and an immature immune system [168]. Over the last few decades several candidate live-attenuated RSV vaccines have been developed for i.n. vaccination, but is has proven difficult to find a proper balance between attenuation and immunogenicity.

There are significant differences in the pathogenesis of and immune response to morbilliviruses and pneumoviruses. Morbilliviruses initially infect lymphocytes, macrophages and dendritic cells in the airways [85,98]. Subsequently, the viruses cause viremia and systemic disease. Therefore, pre-existing VN antibodies in the bloodstream can effectively inhibit infections [99,296].

Dependent on the CDV strain, infections in dogs and ferrets are associated with mortality of 30 - 100% and in animals that survive, the resulting immunity is normally life-long. The same is true for measles in humans. In contrast, HRSV mainly infects respiratory epithelial cell and spreads locally. In addition, re-infections can occur after several HRSV infections, despite high VN antibody titers in blood. Unlike for morbilliviruses, VN antibodies to HRSV wane to pre-infection levels within one year [298,299].

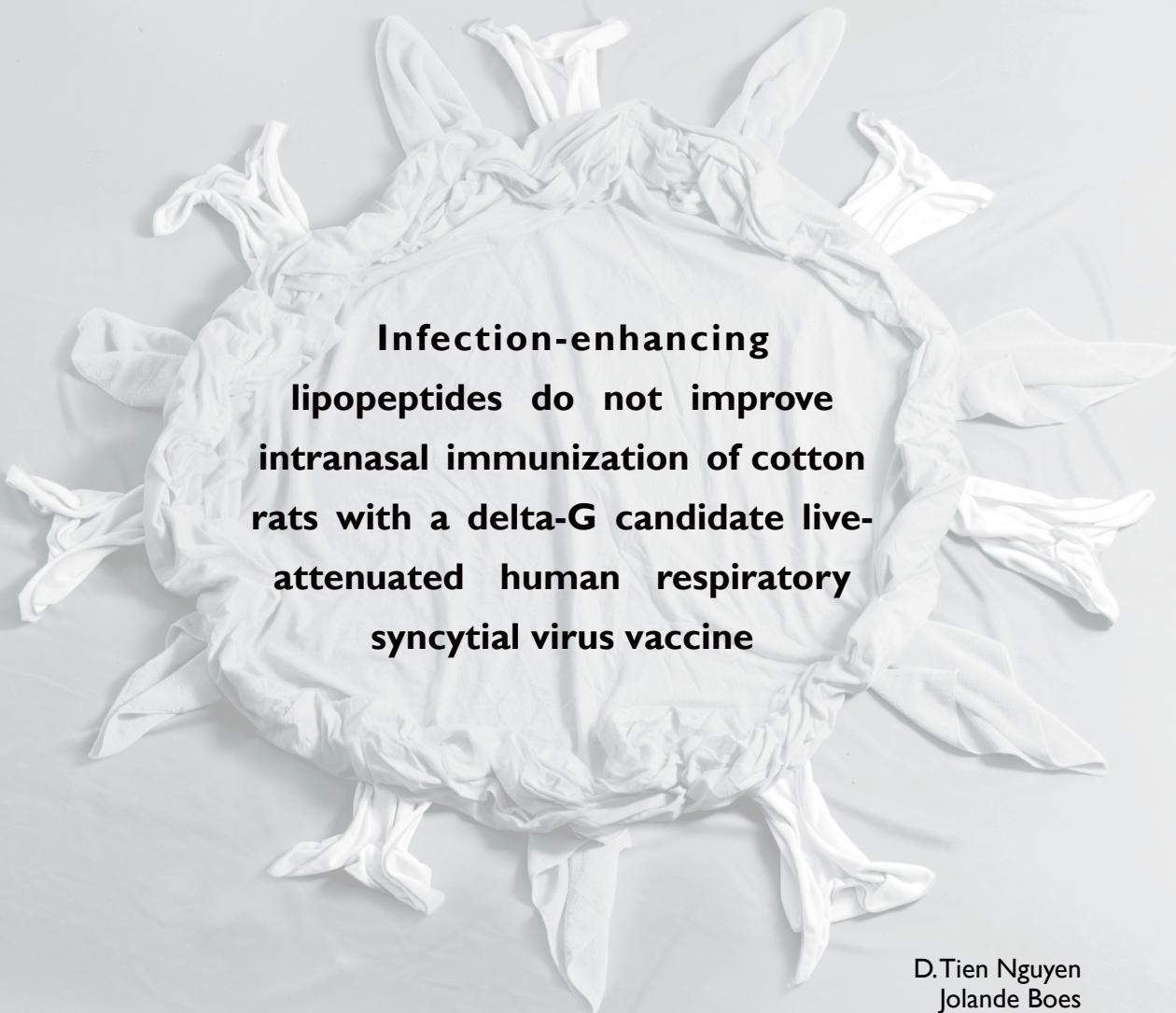
In conclusion, we have shown that the infection-enhancing lipopeptides Pam3CSK4 and PHCSK4 can enhance CDV infection *in vivo*. Further studies are required to evaluate if these lipopeptides can be used as adjuvants for vaccination with other live-attenuated paramyxovirus vaccines.

### Acknowledgements

We thank Steven McQuaid, Queen's University of Belfast, Belfast, United Kingdom, and all zootechnicians at the isolator facility of the Netherlands Vaccine Institute in Bilthoven, the Netherlands, for their contributions to this study. This study received financial support from the VIRGO project and from MRC (grant# G0801001). RDdV and SY were funded by ZonMw (grant# 91208012). The funding sources had no involvement in study design or data analysis.



## Chapter 4



**Infection-enhancing  
lipopeptides do not improve  
intranasal immunization of cotton  
rats with a delta-G candidate live-  
attenuated human respiratory  
syncytial virus vaccine**

D.Tien Nguyen  
Jolande Boes  
Geert van Amerongen  
Yvonne van Remmerden  
Selma Yüksel  
Teun Guichelaar  
Albert D. M. E. Osterhaus  
Rik L. de Swart

## Chapter 4

### Abstract

Development of live-attenuated human respiratory syncytial virus (HRSV) vaccines has proven difficult. Several vaccine candidates were found to be over-attenuated and displayed limited immunogenicity. We recently identified three synthetic cationic lipopeptides that enhanced paramyxovirus infections *in vitro*. The infection enhancement proved to be mediated by enhanced virus binding to target cells. We hypothesized these lipopeptides could be used as adjuvants to promote immune responses induced by live-attenuated paramyxovirus vaccines. Here this hypothesis was tested in a vaccination and challenge

model in cotton rats, using a previously described recombinant live-attenuated candidate HRSV vaccine lacking the gene encoding the G glycoprotein (rHRSV $\Delta$ G). Surprisingly, intranasal vaccination of cotton rats with rHRSV $\Delta$ G formulated in infection-enhancing lipopeptides resulted in reduced virus loads in nasopharyngeal lavages, reduced seroconversion levels and reduced protection from wild-type HRSV challenge. In conclusion, we were unable to demonstrate the feasibility of lipopeptides as adjuvants for a candidate live-attenuated HRSV vaccine.



## Introduction

Human respiratory syncytial virus (HRSV) is a major cause of respiratory tract disease in infants, immunocompromised subjects and the elderly [37,300]. In most cases the virus causes a mild and self-limiting upper respiratory tract infection, but in some cases (usually estimated as 1-2%) it may cause a severe lower respiratory tract infection requiring hospitalization [143]. Despite the huge global burden of HRSV disease, no licensed vaccines against HRSV are available. Main challenges for the development of HRSV vaccines are that these should be safe and effective at an early age in the presence of maternal antibodies and an immature immune system [168].

Several different HRSV vaccination approaches have been evaluated over the last few decades, including live-attenuated, inactivated, subunit and vector vaccines [301]. Studies with formalin-inactivated HRSV vaccines in the 1960s resulted in vaccine-mediated disease enhancement [158], an observation which hinders development of non-replicating HRSV vaccines for administration to immunologically naive infants [302]. Live-attenuated HRSV vaccines have not been associated with priming of enhanced disease, and therefore constitute a promising approach for intranasal (i.n.) vaccination of young infants. However, the vaccine virus needs to achieve sufficient levels of virus replication in the host to induce protective immune responses, but vaccine virus replication should not result in HRSV disease. Despite many attempts, it has proven difficult to find a proper balance between attenuation and immunogenicity [170].

Previously, we have identified three synthetic cationic lipopeptides that enhanced paramyxovirus infections *in vitro* [284]. The synthetic bacterial lipopeptide Pam3-Cys-Ser-Lys4 (Pam3CSK4), the prototype ligand for

the heterodimeric Toll-like receptor (TLR) 2/1 complex, enhanced HRSV infection in primary epithelial, myeloid and lymphoid cells. Moreover, two structurally related lipopeptides without TLR-signaling capacity, Pam-Cys-SK4 and PHCSK4 [257,258], were also found to enhance HRSV infection, suggesting that infection enhancement was independent of TLR activation. This was confirmed by the observation that Pam3-Cys-Ser-Pro4 (Pam3CSP4), a synthetic lipopeptide that does stimulate TLR1/2 responses, did not enhance infection with HRSV, demonstrating the pivotal role of the four cationic lysins in this process. A similar TLR-independent enhancement of *in vitro* virus infection could be demonstrated for several wild-type HRSV strains, but also for HIV-1, measles virus and human metapneumovirus [284]. The infection enhancement proved to be mediated by enhanced virus binding to target cells, in which the N-palmitoylated cysteine interacts with the membrane of the virus and/or the host cell and the cationic lysines change the membrane potential [284]. Previously, other cationic compounds, such as DEAE-dextran, polybrene, RANTES and SEVI, have also been shown to enhance viral infection [262,266,268]. We hypothesized that the synthetic cationic lipopeptides could be used as adjuvants to promote immune responses induced by live-attenuated paramyxovirus vaccines [284].

This hypothesis was recently tested using a canine distemper virus (CDV) vaccination and challenge model in ferrets [303]. Intranasal immunization with a live-attenuated CDV vaccine [101] formulated in synthetic infection-enhancing cationic lipopeptides indeed resulted in increased vaccine virus loads in nasopharyngeal lavages and peripheral blood mononuclear cells as compared to immunization with non-adjuvanted CDV. In

addition, adjuvantation of CDV vaccine with infection-enhancing lipopeptides induced significantly higher CDV neutralizing serum antibody titers as compared to animals vaccinated with non-adjuvanted live-attenuated CDV. Although this study provided proof of principle for *in vivo* enhancement of replication and immunogenicity of a live-attenuated paramyxovirus vaccine, we sought to reproduce our results in a vaccination and challenge model for HRSV, another member of the *Paramyxoviridae* family.

To this end, we selected a recently described candidate live-attenuated recombinant HRSV vaccine lacking the gene encoding the G glycoprotein [304]. Using reverse genetics, recombinant (r)HRSV-X and an rHRSV lacking the G gene ( $\Delta$ G) were constructed based on a clinical HRSV isolate (strain 98-25147-X). A single dose immunization with the highly attenuated rHRSV $\Delta$ G conferred long term protection in cotton rats, without priming for vaccine-enhanced disease [304]. Moreover, for both viruses molecular clones expressing enhanced green fluorescent protein (EGFP) were also available [305], facilitating *in vitro* lipopeptide-mediated infection enhancement studies.

## Results

### Lipopeptide-mediated enhancement of rHRSV infection *in vitro*

We have previously shown that the synthetic lipopeptides Pam3CSK4, Pam-Cys-SK4 and PHCSK4 can enhance paramyxovirus infections *in vitro*. Pam3CSP4, which does not enhance infection *in vitro*, was used as a negative control [284]. In order to test if these lipopeptides could also enhance infection of the HRSV strains used in the present study, human Epstein-Barr virus-transformed B-lymphoblastic cell lines (B-LCL) were infected with either rHRSV $\Delta$ G or HRSV-X in the presence or absence of lipopeptide (10

$\mu$ g/ml). Pam3CSK4 and PHCSK4 significantly enhanced infection with both viruses as compared to the medium and lipopeptide control (Figure 1A,  $p < 0.05$ ). To test if the lipopeptides also enhanced infection in natural target cells of HRSV, well-differentiated normal human bronchial epithelial (wd-NHBE) cells were infected and 2 d.p.i. the numbers of infected cells were counted. Again, Pam3CSK4 and PHCSK4 significantly enhanced HRSV infection (Figure 1B,  $p < 0.05$ ). In order to test whether infection enhancement could also be shown in cotton rat cells, cotton rat lymph node cells or lung slices [306] were infected with HRSV in the presence or absence of lipopeptide. In lymph node cells Pam3CSK4 and PHCSK4 significantly enhanced infection with both viruses as compared to the medium and lipopeptide control (Figure 1C,  $p < 0.05$ ). In lung slices the intra-assay variation was relatively high, but Pam3CSK4 and PHCSK4 still caused a significant enhancement of HRSV infection (Figure 1D,  $p < 0.05$ ). Based on these *in vitro* data, Pam3CSK4 and PHC4SK4 were selected for *in vivo* testing as potential adjuvants for the rationally attenuated rHRSV $\Delta$ G.

### Vaccination – virus loads and VN titers

Twenty three cotton rats were vaccinated i.n. with a dose of  $10^4$  TCID<sub>50</sub> rHRSV $\Delta$ G in a volume of 10  $\mu$ l. In previous animal experiments this dose was found to induce suboptimal immune responses. The first group (n=7) was rHRSV $\Delta$ G-vaccinated without lipopeptide and served as a control in the challenge experiment. In groups 2 and 3 (both n=8) the virus was mixed with Pam3CSK4 or PHCSK4 (final concentration 30  $\mu$ g/ml), respectively. To determine the effect of lipopeptides on rHRSV $\Delta$ G infection *in vivo*, vaccine virus loads in nasopharyngeal lavages and throat swabs were analyzed by virus isolation. No virus was detected in throat swabs in any of the groups. Low amounts of virus were detected in nasopharyngeal lavages of 1 and 3 animals of the control group at 2 and 4 days post-

## Lipopeptides as Adjuvants for an HRSV Vaccine

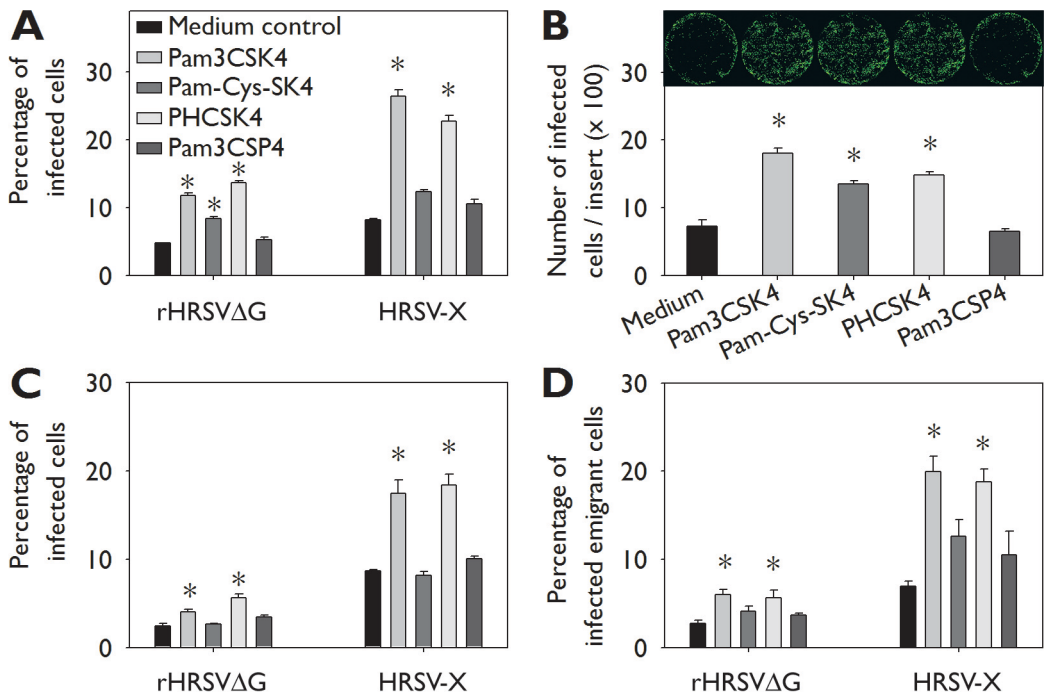


**Figure 1.** *In vitro* lipopeptide-mediated enhancement of rHRSV infection. *In vitro* infection experiments were performed in human EBV-transformed B-lymphoblastic cells (A), well-differentiated normal human bronchial epithelial cells (B), cotton rat lymph node cells (C) and cotton rat lung slices (D). HRSV was incubated with different lipopeptides (10 µg/ml) or medium as control for 5 minutes at 37°C before the virus suspension was added to the cells. In panels A, C and D data are shown as percentages HRSV-infected cells, as determined by flow cytometry. In panel B data are shown as the numbers of GFP<sup>+</sup> cells per insert. In panel B photographs of representative inserts are shown for each condition. Formulation with Pam3CSK4 or PHCSK4 resulted in significantly increased rHRSV infection percentages. Bars represent means ± SEM of triplicates (A, C), quadruplicates (B) or sextuplicates (D), \*  $p < 0.05$  in 1-way ANOVA and posthoc Dunnett's correction for multiple comparisons with medium control.

vaccination (d.p.v.), respectively. However, no virus was detected in the nose of the animals vaccinated with rHRSVΔG formulated in lipopeptide (Figure 2A).

VN antibody levels were measured 29 and 63 d.p.v. (Figure 2B). At 29 d.p.v. VN antibodies were detected in 5/7, 3/8 and 3/8 animals of groups 1 (non-adjuvanted control), 2 (Pam3CSK4) and 3 (PHCSK4), respectively.

### Challenge – virus loads

Animals were challenged i.n. with a high dose of HRSV-X 67 d.p.v. In all animals challenge virus was isolated from nasopharyngeal lavages,

throat swabs and lung homogenates 5 days post challenge (Figure 3). The virus loads in group 1 (non-adjuvanted) tended to be lower than, but were not statistically significant from those in groups 2 (Pam3CSK4-adjuvanted) and 3 (PHCSK4-adjuvanted).

### Discussion

In the current study, infection-enhancing lipopeptides [284] were evaluated in the cotton rat model as potential adjuvants for a live-attenuated recombinant HRSV vaccine lacking the G glycoprotein. This candidate

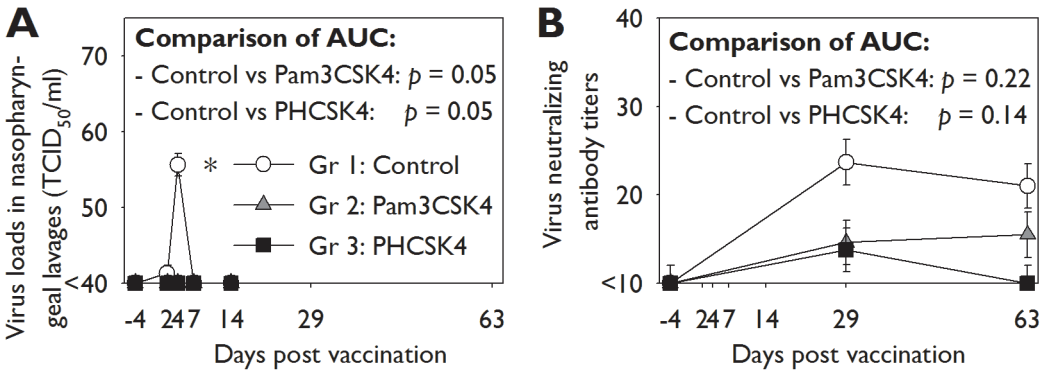


**Figure 2.** Vaccination period - virus loads and VN antibodies. A) Vaccine virus loads in nasopharyngeal lavages as measured by virus isolation. Virus loads in the non-adjuvanted control group ( $n=7$ ) were statistically significantly higher than those of the lipopeptide-adjuvanted groups ( $n=8$ ) (lines represent geometric mean  $\pm$  geometric standard deviation [GSD], \*  $p < 0.05$ ). B) Virus neutralizing (VN) antibody titers were measured at days -4, 29 and 63 days post vaccination. In the control group more animals seroconverted than in the adjuvanted groups (lines represent geometric mean  $\pm$  GSD, \*  $p < 0.05$ , area under the curve [AUC]).

vaccine was previously shown to induce protective immunity in cotton rats [304]. However, in the current study we selected a suboptimal vaccine virus dose, with the aim of demonstrating enhancement of infectivity and immunogenicity following intranasal infection in the presence of infection-enhancing lipopeptides. Unfortunately, vaccination in the

presence of infection-enhancing lipopeptides was inferior to vaccination in absence of lipopeptides, as evidenced by reduced virus loads in nasopharyngeal lavages, a tendency of reduced seroconversion rates and reduced protection upon HRSV-X challenge infection.

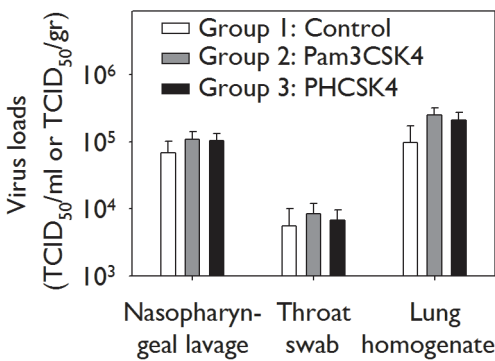


**Figure 3.** Challenge period - virus loads. Challenge virus was isolated from all animals in all specimens tested. The virus loads in group 1 ( $n=7$ ) were not statistically significantly different from those in groups 2 ( $n=8$ ) and 3 ( $n=8$ ). Bars represent means  $\pm$  SEM, virus loads in lung homogenates are shown per gram lung tissue.

These observations are in contrast with our previously reported data using a canine distemper virus vaccination and challenge model in ferrets [303]. A number of potential explanations for this observation were evaluated. Firstly, the lipopeptides could have induced a strong innate immune response, thereby accelerating clearance of the vaccine virus. However, there were no differences in intensities of RT-PCR products detecting mRNA encoding innate immunity genes (IFN- $\alpha$  and Mx1) in nasopharyngeal lavages between animals vaccinated with or without lipopeptides (data not shown). Secondly, in comparison to our ferret study the i.n. inoculation volume used in cotton rats was smaller, avoiding direct deposition of vaccine virus in the lungs. As a consequence, it may have been more difficult for the virus to cross the mucus barrier in the nose. However, in

*vitro* enhancement of rHRSV $\Delta$ G infections of human epithelial or lymphoid cells proved unaffected by the presence or absence of mucus-containing washings obtained from wd-NHBE or of the volume of the virus inoculum. Thirdly, formulation of the vaccine virus in cationic lipopeptides may have resulted in a positive membrane potential of the vaccine virus particles, resulting in electrostatic interactions with cotton rat mucin polymers on the respiratory mucosa [104]. As shown in Figure 1, *ex vivo* HRSV infection of well-differentiated normal human bronchial epithelial cells (wd-NHBE) with tight junctions, moving cilia and goblet cells was enhanced by these cationic lipopeptides. However, it is important to note that in these primary epithelial cells enhancement was not observed in every experiment: in some experiments the addition of lipopeptides to the virus appeared to have little or no effect on the efficiency of HRSV infection, and in one experiment we actually observed lipopeptide-mediated inhibition of HRSV infection. In this particular experiment the epithelial layer contained a relatively large number of mucus-producing cells. Thus, we hypothesize that under some conditions the cationic lipopeptides can promote HRSV binding to negatively charged mucin polymers, resulting in immobilization of the virus and inhibition of infection. This may also have occurred in our vaccination study.

In conclusion, we were unable to demonstrate the feasibility of infection-enhancing lipopeptides as adjuvants for a candidate live-attenuated HRSV vaccine.

### Materials & Methods

#### Ethical statement

The animal protocol was approved by an independent animal experimentation ethics committee. Experiments were performed in compliance with European guidelines

for animal experimentation. Animals were monitored daily, and animal care was in compliance with institutional guidelines.

#### Animals

Four- to eight week old cotton rats (*Sigmodon hispidus*) were obtained from an in-house specific pathogen-free breeding colony. All animals were housed individually in filter-top cages supplemented with paper as cage enrichment and received food and water *ad libitum*. One animal of the control group died three days before vaccination of unknown causes.

#### Cells, viruses and lipopeptides

Vero cells (ATCC CCL-81) were cultured in M199 medium (Invitrogen) with 5% FBS and supplements. HEp-2 cells (ATCC CCL-23) were grown in DMEM (Lonza) with 10% FBS and supplements. Epstein-Barr virus (EBV)-transformed human B-lymphoblastic cells (B-LCL) were grown in RPMI-1640 medium (Lonza) with 10% fetal bovine serum (FBS). Well-differentiated human normal bronchial epithelial cells (wd-NHBE) were grown on transwell filters with 0.4  $\mu$ m pore size (Corning) as described elsewhere [307]. Lymph nodes were collected from cotton rats of an unrelated approved study, and stored in phosphate-buffered saline. Single cell suspensions were prepared using cell strainers with a 100  $\mu$ m pore size (BD Biosciences), and resuspended in RPMI-1640 medium (Lonza) with 10% FBS and supplements as described before [303]. Cotton rat lung slices were prepared by inflation with low melting point agarose as described elsewhere [306].

Stocks of the live-attenuated recombinant HRSV lacking the G gene (rHRSV $\Delta$ G) and the challenge virus (HRSV-X) were prepared in Vero cells and purified as described previously [304]. Infection studies in wd-NHBE cells were also performed using rgRSV, a recombinant HRSV strain A2 virus expressing GFP [267] (kind gift of Dr. ME Peeples and Dr.

PL Collins). Stocks of rgRSV were prepared in HEp-2 cells. Pam3CSK4, PHCSK4, Pam-Cys-SK4 and Pam3CSP4 [284] were a kind gift of Dr. K.H. Wiesmüller (EMC microcollections, Germany).

#### ***In vitro* and *ex vivo* HRSV infections**

The lipopeptides were added to the viruses to a final concentration of 10 µg/ml, and the mixtures were incubated for 5 minutes at 37°C. Cells were infected at a multiplicity of infection (MOI) 2 (rHRSVΔG) or 20 (HRSV-X and rgRSV). One day (B-LCL, LN cells) or two days (wd-NHBE, lung slices) post infection cells were analyzed by automated counting (wd-NHBE) or flow cytometry.

#### ***In vivo* HRSV infection experiment**

Twenty three cotton rats were vaccinated i.n. at day 0 with a suboptimal dose of  $10^4$  TCID<sub>50</sub> rHRSVΔG in a volume of 10 µl. The first group (n=7) was rHRSVΔG- vaccinated without lipopeptide and served as a control in the challenge experiment. In groups 2 and 3 (both n=8) the virus was mixed with Pam3CSK4 or PHCSK4 (final concentration 30 µg/ml), respectively. The mixture was incubated for 5 minutes at 37°C.

Animals were challenged i.n. with 100 µl  $3 \times 10^5$  TCID<sub>50</sub> HRSV-X 67 days post vaccination (d.p.v.), and euthanized by exsanguination five days post challenge. All procedures were performed under 4% isoflurane anesthesia.

#### **Samples and assays**

Virus isolation from nasopharyngeal lavages and throat swabs was performed as previously described [303,304]. Right lungs were homogenized with a FastPrep-24® (MP Biomedicals) in 600 µl virus transport medium [303] and centrifuged at 640 × g for 15 minutes. The lower limit of detection of the assay was 40 TCID<sub>50</sub>/ml. For calculation of group averages, samples with undetectable virus loads were given a value of 40.

Virus neutralizing (VN) antibody levels

were determined using a plaque reduction neutralization assay as described [305]. The lower limit of detection of the assay was a serum dilution of 1:10. For calculation of group averages, samples with undetectable antibody levels were given a value of 10.

Statistical analyses were performed as described previously [303]. Statistical analyses were performed with ANOVA with Dunnet's correction of Mann-Whitney *U* test for AUC where appropriate [284,303]. A *p*-value <0.05 was considered statistically significant. All *in vitro* and *ex vivo* experiments were performed at least three times, with the exception of the cotton rat lung slice experiment which was performed once.

#### **Acknowledgements**

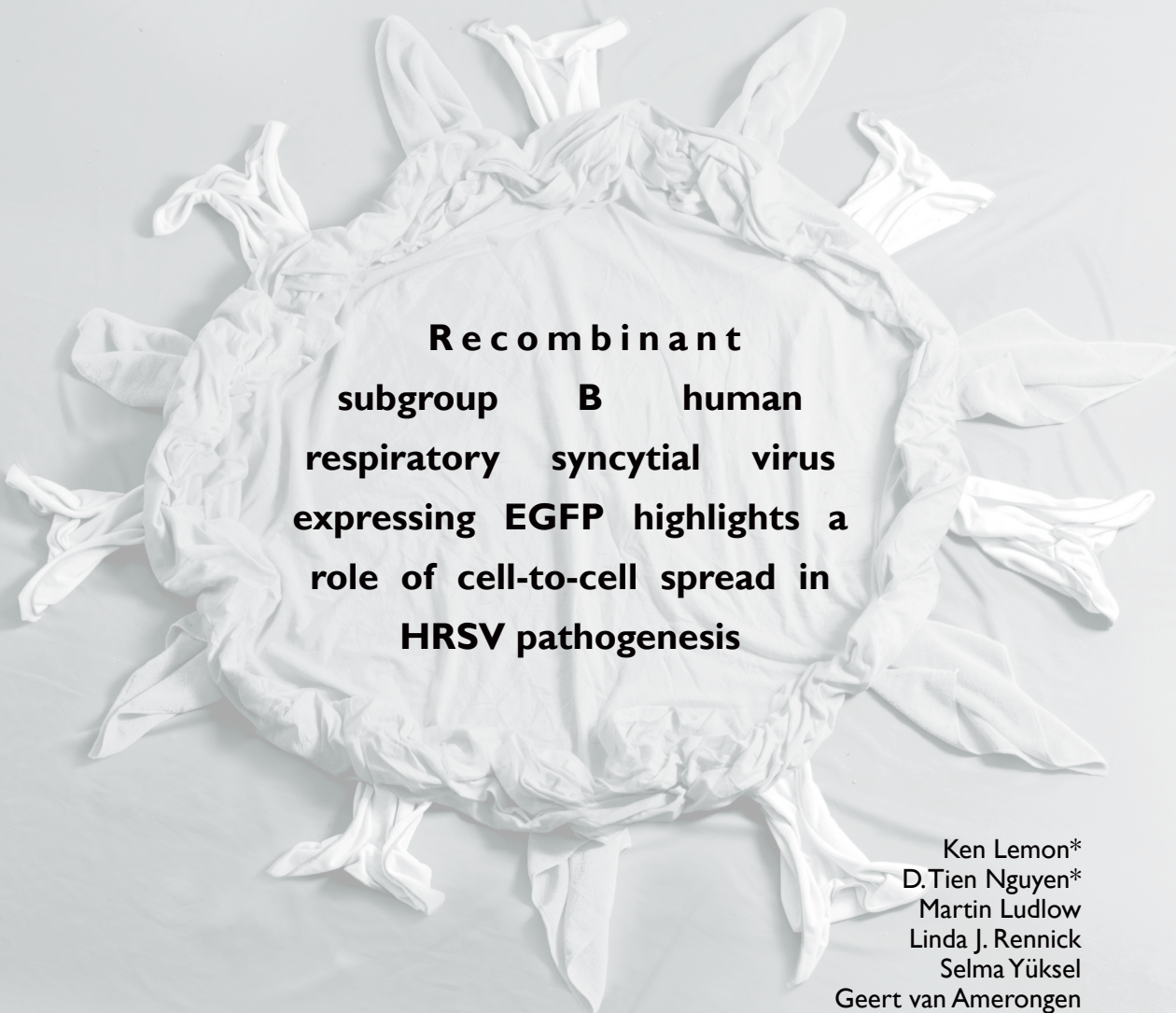
We thank all zootechnicians at the isolator facility of the Netherlands Vaccine Institute in Bilthoven, the Netherlands, for their contributions to this study. This study was supported by the Virgo consortium, funded by the Dutch government project number FES0908. SY was funded by ZonMw (grant# 91208012).







## Chapter 5



**Recombinant  
subgroup B human  
respiratory syncytial virus  
expressing EGFP highlights a  
role of cell-to-cell spread in  
HRSV pathogenesis**

Ken Lemon\*  
D.Tien Nguyen\*  
Martin Ludlow  
Linda J. Rennick  
Selma Yüksel  
Geert van Amerongen  
Stephen McQuaid  
Bert K Rima  
Rik L. de Swart  
W. Paul Duprex

\*these authors contributed equally to this study

*Submitted*

## Chapter 5

### Abstract

Human respiratory syncytial virus (HRSV) is the most important viral cause of severe respiratory tract disease in infants. Two subgroups (A and B) have been identified, which co-circulate during or alternate between yearly epidemics and cause indistinguishable disease. Existing *in vitro* and *in vivo* models of HRSV focus almost exclusively on subgroup A viruses, and the prototypic strain A2 is commonly used. Here, a recombinant (r) subgroup B virus (rHRSV<sup>B05</sup>) was generated based on a consensus genome sequence obtained directly from an unpassaged clinical specimen from a hospitalized infant. An additional transcription unit containing the gene encoding enhanced green fluorescent protein (EGFP) was introduced between the phosphoprotein and matrix genes (position 5) of the genome to generate rHRSV<sup>B05</sup>EGFP(5). This virus infected well-differentiated

normal human bronchial epithelial cells more efficiently than rgRSV, a recombinant A2 virus expressing GFP. Intranasal infection of cotton rats (*Sigmodon hispidus*) resulted in high numbers of EGFP<sup>+</sup> cells in epithelia of the nasal septum and conchae. The virus replicated efficiently in bronchiolar epithelial cells and spread extensively in both the upper and lower respiratory tract. Virus replication was not observed in ciliated epithelial cells of the trachea. Even though the clinical isolate infected more cells, less cell-free virus was produced. This is the first rHRSV strain with the phenotype and full genetic background of currently circulating wild-type viruses. *In vivo* tracking of infected cells in the absence of cytopathic effects illuminates HRSV pathogenesis and highlights the critical role of cell-to-cell spread in the disease process.

## Introduction

Human respiratory syncytial virus (HRSV) is the most important viral cause of respiratory tract disease in infants [17]. HRSV infections are observed during seasonal outbreaks in winter or during the rainy season in the tropics [308]. The virus usually causes a self-limiting upper respiratory tract (URT) infection, resulting in rhinorrhea and other common cold-like clinical signs [309]. However, in a minority of cases the infection can also spread to the lower respiratory tract (LRT), resulting in severe pneumonia or bronchiolitis. Risk factors for developing severe LRT infections include prematurity, pulmonary or cardiac disease, compromised immunity and old age [37]. Current treatment options are limited although specific monoclonal antibody preparations directed against the fusion (F) glycoprotein have been developed for prophylactic use [140]. Despite significant efforts in vaccine development over the past fifty years, no HRSV vaccines are currently licensed [168]. Limited availability of natural animal models of disease adds to the challenge of developing vaccines and antivirals.

HRSV is a member of the family *Paramyxoviridae*, subfamily *Pneumovirinae*, genus *Pneumovirus* [17]. It is an enveloped virus with a negative sense, single stranded RNA genome containing ten transcription units. Both F and glyco- (G) proteins facilitate virus attachment and entry [17,310] and the F glycoprotein is an important target of virus neutralizing antibodies [19]. Molecular epidemiological studies have identified two HRSV subgroups (A and B) which cause indistinguishable disease and co-circulate during, or alternate between, yearly outbreaks [25,311].

An improved understanding of HRSV pathogenesis would facilitate the development of novel intervention strategies. This requires virulent, well-characterized virus strains of

known provenance and disease-relevant *in vitro* and *in vivo* model systems. Well-differentiated (wd) normal human bronchial epithelial (wd-NHBE) cultures grown at air-liquid interphase (ALI) have been identified as a useful *in vitro* model for HRSV as they contain ciliated cells which are natural HRSV targets [49,51,208]. Such cells provide a valuable “bridge” from *in vitro* to *in vivo* studies. Cotton rats represent a highly susceptible small animal model for HRSV pathogenesis studies [221]. Recently adult human volunteers have been infected with wild-type A strains to assess the effectiveness of HRSV antivirals [44,312].

Irrespective of the approach used, it is critical to use naturally circulating viruses to ensure that study outcomes can be correlated with clinical outcomes. A longstanding challenge in virology is that clinical isolates often fail to cause overt cytopathic effect (CPE) in primary cells and *in vivo* thus infected cells must be stained to monitor the infection. This is already challenging *in vitro* and particularly magnified *in vivo* when low numbers of infected cells are present in tissues, which must be examined using ultrathin sections. Blind passage *in vitro* and selection of particularly fusogenic variants by plaque picking leads to genotypic and phenotypic changes. These challenges have been addressed by generating recombinant (r) viruses from clinical samples and engineering them to express fluorescent proteins, for example enhanced green fluorescent protein (EGFP) from an additional transcription unit (ATU), permitting novel insights into viral pathogenesis and targeted-pathological assessment in appropriate cell lines and animal models [313].

To extend these studies we obtained the genome sequence of HRSV<sup>B05</sup>, a wildtype subgroup B strain. Assembly of a full-length molecular clone allowed the recovery of rHRSV<sup>B05</sup> and insertion of an ATU containing the EGFP open-reading frame at

position 5 between the phospho- (P) and matrix (M) genes led to the generation of rHRSV<sup>B05</sup>EGFP(5). A recombinant subgroup A virus based on laboratory-adapted HRSV strain A2 expressing GFP (rgRSV) was available [267]. Therefore we characterized rHRSV<sup>B05</sup> *in vitro* and *in vivo* to determine the similarities with and differences from rgRSV and to dissect viral pathogenesis.

## Results

### Generation of a wild-type, subgroup B Buenos Aires genotype rHRSV

Total RNA was extracted directly from a tracheal rinse sample obtained from an infant infected with HRSV and high-fidelity RT-PCR and rapid amplification of cDNA ends was used to generate amplicons. The consensus genome sequence indicated that the virus belonged to the Buenos Aires (BA) genotype of HRSV subgroup B. This genotype was first detected in Argentina in 1999 and is characterized by a 60-nucleotide duplication in the G gene [314]. Viruses of the BA genotype have become the dominant circulating HRSV subtype B genotype globally [315,316]. Eukaryotic expression plasmids encoding HRSV<sup>B05</sup> nucleocapsid (N), phospho- (P), M2-1 and large (L) proteins and a negative sensed minigenome (HRSV<sup>B05</sup>DI-EGFP) were constructed (Figure 1A) and a replication/transcription assay established to optimize the conditions required to generate rHRSV<sup>B05</sup>. Most negative strand reverse genetics systems utilize T7 RNA polymerase to generate a full-length viral antigenomic RNA. Since T7 RNA polymerase initiates most efficiently on a stretch of guanine residues, efficient rHRSVA2 rescue has previously been achieved by inserting three guanine nucleotides between the T7 promoter and the HRSV leader (Le) sequence [317-319]. However, it is not clear whether this sequence is copied faithfully during viral replication. To negate this possibility, a hammerhead ribozyme was

inserted after the T7 promoter and three guanine nucleotides, which along with the hepatitis delta ribozyme at the other end of the minigenome, allowed post-transcriptional cleavage to generate precise, authentic trailer (Tr) and Le termini at the ends of the minigenome (Figure 1A). EGFP<sup>+</sup> cells were observed following transfection of the five plasmids into HEp-2 cells indicating that the genomic termini and helper plasmids were functional (Figure 1B). No EGFP<sup>+</sup> cells were observed when the L protein expression plasmid was omitted (-L), indicating that EGFP expression was driven exclusively by the viral RNA-dependent RNA polymerase (Figure 1B). Based on these findings a positive-sensed full-length genome plasmid (pHRSV<sup>B05</sup>) was constructed and rHRSV<sup>B05</sup> was recovered following transfection into HEp-2 cells (Figure 1C). Importantly it was not necessary to mutate nucleotide 4 of the Le sequence to achieve efficient rescue as has been described for rHRSV<sup>A2</sup> [319,320]. Indirect immunofluorescence (Figure 1D, E) and *in situ* plaque staining (Figure 1F, G) using an anti-HRSV F glycoprotein antibody permitted the detection of foci of infection. The full-length HRSV plasmid was modified by insertion of an ATU encoding EGFP at position 5 in the genome (Figure 1H) and rHRSV<sup>B05</sup>EGFP(5) was recovered (Figure 1I). High levels of EGFP expression were obtained and both single infected cells were detected by UV microscopy (Figure 1I). Thus an rHRSV<sup>B05</sup> genetically identical to a clinical isolate was successfully generated which can be tracked in living cells in the absence of any overt CPE.

### rHRSV<sup>B05</sup> exhibits the phenotype of a clinical isolate

HEp-2 cells were infected with rHRSV<sup>B05</sup>, rHRSV<sup>B05</sup>EGFP(5) and rgRSV at an equivalent multiplicity of infection (MOI). Both B05-based viruses displayed similar growth kinetics reaching equivalent peak titers of 10<sup>6</sup> TCID<sub>50</sub>/ml whereas rgRSV reached a titer

# Newly Generated Recombinant HRSV

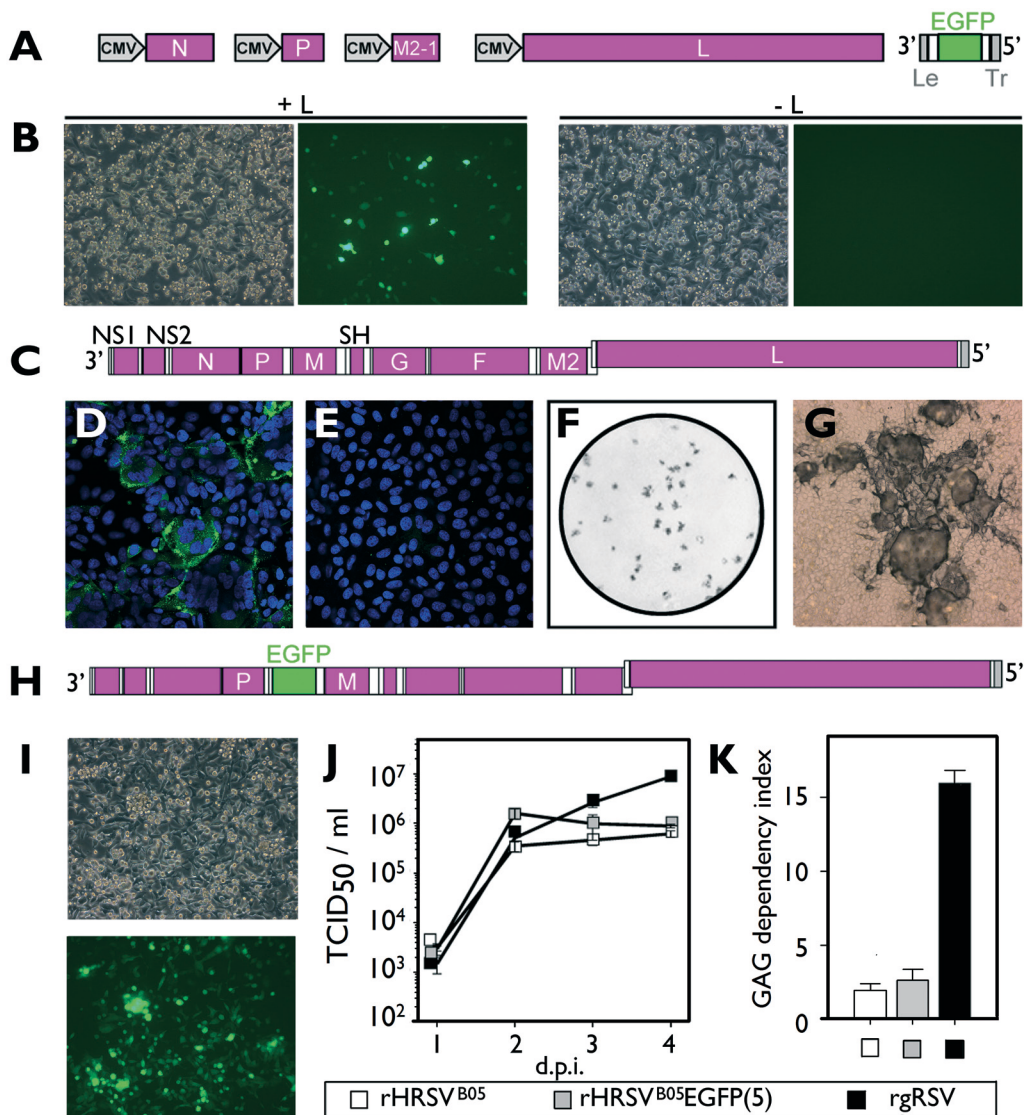


**Figure 1.** Development of a reverse genetics system for HRSV<sup>B05</sup>. A) Schematic representation of HRSV eukaryotic N, P, M2-1 and L protein expression constructs and minigenome HRSV<sup>B05</sup> DI-EGFP showing the Le, EGFP gene and Tr. B) Phase contrast and UV photomicrographs of HEp-2 cells 2 days posttransfection with p(-)HRSV<sup>B05</sup> DI-EGFP and helper plasmids with (+ L) and without (- L) the L protein expression clone. C) Schematic representation of the rHRSV<sup>B05</sup> genome. D) Detection of the F glycoprotein of rHRSV<sup>B05</sup> syncytia by indirect immunofluorescence, E) a negative control omitted the primary monoclonal antibody. F,G) Detection of HRSV<sup>B05</sup> by immuno-plaque assay. H) Schematic representation of the rHRSV<sup>B05</sup>EGFP(5) genome. I) Phase contrast and fluorescent photomicrographs of rHRSV<sup>B05</sup>EGFP(5) infected HEp-2 cells. J) Growth curves determined by ten-fold titrations at four consecutive days on HEp-2 cells. K) CHO cells expressing GAG and cells deficient in GAG were infected and ratios were calculated and expressed as a GAG index. Data are presented as geometric mean titers  $\pm$  standard error (se)

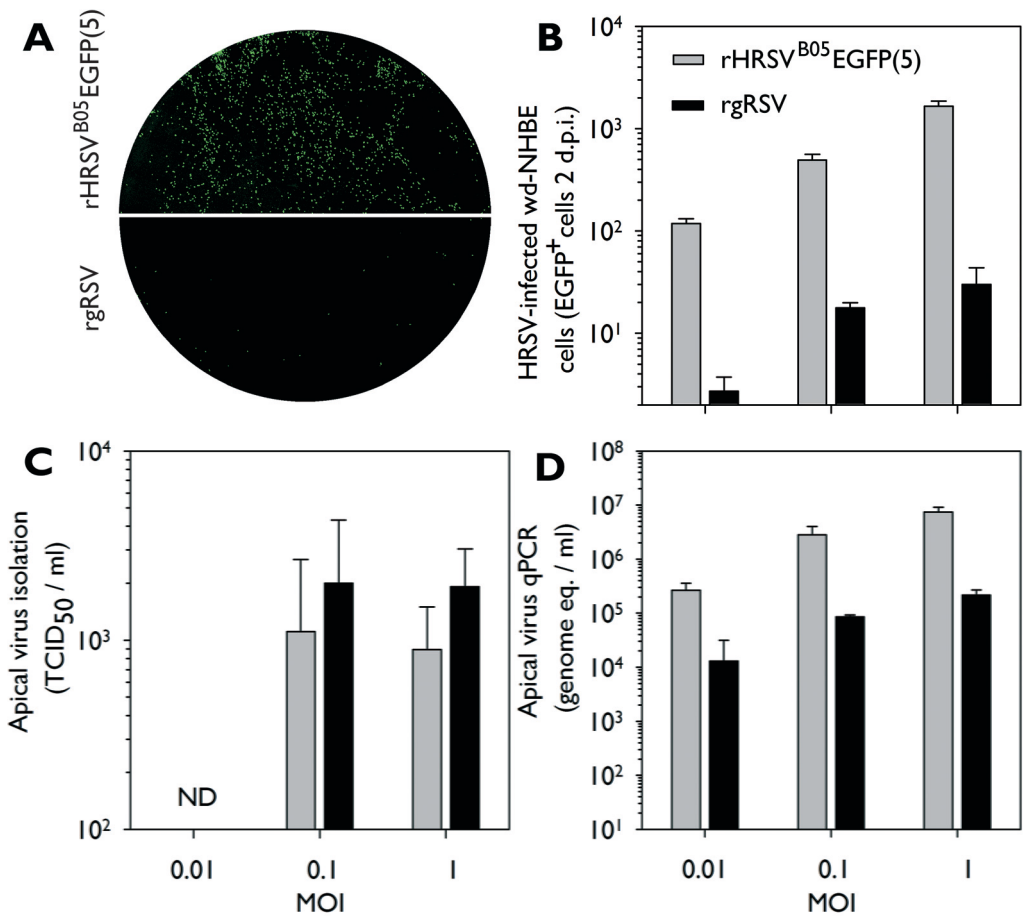


**Figure 2.** Infection of primary wd-NHBE grown in ALI with rHRSV<sup>B05</sup>EGFP(5) and rgRSV. A) Fluorescent photomicrographs. B) Absolute counts of EGFP<sup>+</sup> cells/well for MOI 0.01, 0.1 and 1. C) Virus isolations of corresponding apical rinses. D) Genome equivalents in apical rinses measured by qPCR. Data are presented as geometric mean titers ± se

of 10<sup>7</sup> TCID<sub>50</sub>/ml (Figure 1J). Non-specific binding of HRSV to glycosaminoglycan (GAG) moieties on the cell surface correlates with a laboratory-adapted phenotype [207,256]. Both rHRSV<sup>B05</sup> and rHRSV<sup>B05</sup>EGFP(5) displayed low GAG dependency indices (Figure 1K), indicating they share this key characteristic of a clinical isolate. In contrast, rgRSV had a high GAG dependency index correlating with a laboratory-adapted phenotype.

**rHRSV<sup>B05</sup> infects primary wd-NHBE cells very efficiently**

Primary NHBE cells were differentiated at air-liquid interface (ALI) to form polarized ciliated, non-ciliated, basal and goblet cells with functional tight junctions. These wd-NHBE cells were infected at an MOI of 0.01, 0.1 or 1 and the number of EGFP<sup>+</sup> infected cells was counted two days post-infection (d.p.i.). Unlike in HEp-2 cells (Figure 1D, I) CPE was not observed, further proving the utility of the EGFP-expressing wild-type virus. Significantly more cells were infected by rHRSV<sup>B05</sup>EGFP(5)

compared to rgRSV (Figure 2A). Virus loads in apical rinses were determined both by virus isolation and qPCR. Surprisingly, up to 100 fold higher numbers of infected cells gave rise to lower titers of released infectious virus for rHRSV<sup>B05</sup>EGFP(5) (Figure 2C). In contrast, virus loads determined by qPCR reflected the differences in numbers of infected cells (Figure 2D). As expected neither released virus nor virus genome was detected in the basolateral compartment. These data demonstrate that rHRSV<sup>B05</sup>EGFP(5) is either more cell-associated or less stable as cell-free virus than rgRSV.

### Infection of cotton rats shows efficient cell-to-cell spread

Cotton rats were infected intranasally with  $10^4$  TCID<sub>50</sub> of rHRSV<sup>B05</sup>EGFP(5) or rgRSV in a low volume (10  $\mu$ l) to target the URT. Animals were sacrificed 4 or 6 d.p.i. and unfixed respiratory tracts were screened by UV microscopy. Massive numbers of EGFP<sup>+</sup> cells were detected 4 d.p.i. in the nasal cavity of rHRSV<sup>B05</sup>EGFP(5) (Figure 3A) and rgRSV infected animals (Figure 3B). Discrete tracks of fluorescent cells were present in the epithelium of the nasal septum reminiscent of what was previously observed in wd-NHBE cells [51]. No EGFP<sup>+</sup> cells were detected microscopically in trachea or lungs.

Pathological assessment and immunohistochemistry (IHC) in 7  $\mu$ m formalin fixed lung sections indicated that both viruses predominantly infected ciliated respiratory epithelial cells (Figure 3C to F), but HRSV<sup>B05</sup> may lead to greater destruction of the epithelium (arrows).

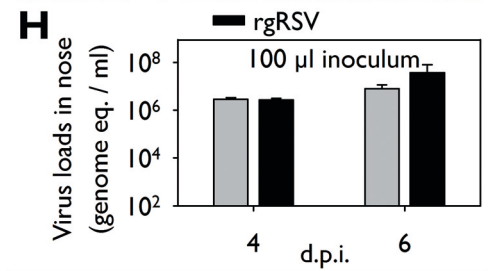
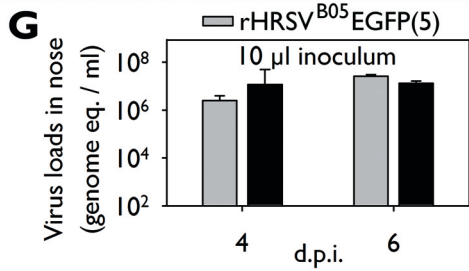
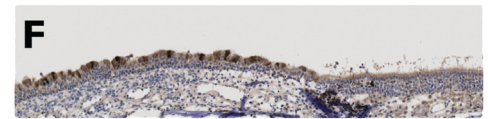
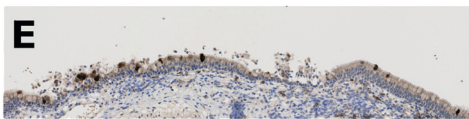
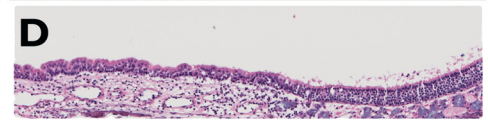
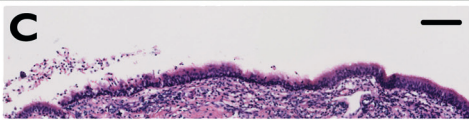
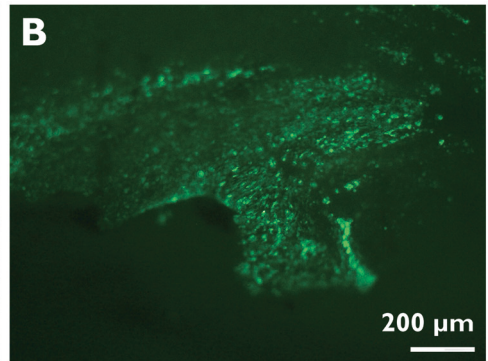
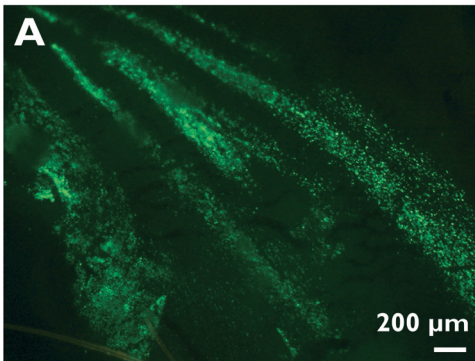
Nasopharyngeal samples were collected at necropsy and HRSV genome equivalents were determined by qPCR using internal RNA controls. These were similar for both viruses (Figure 3G).

### rHRSV<sup>B05</sup>EGFP(5) efficiently replicates in bronchial and bronchiolar epithelia

Cotton rats were intranasally infected with  $10^4$  TCID<sub>50</sub> in a larger volume (100  $\mu$ l) to target both the URT and LRT [219]. Similar to the low inoculum volume infections described above, there was no difference between the two viruses in the URT in terms of genome equivalents in nasopharyngeal samples (Figure 3H). Microscopically fluorescence levels in the nasal concha and nasal septum were indistinguishable between animals infected with the different viruses and between the animals infected using the low or high volume inocula, and no EGFP<sup>+</sup> cells were detected in the trachea. However, vastly different outcomes were seen between the clinical isolate and rgRSV when the lungs from infected animals were removed, inflated with agarose, sectioned and screened for fluorescence. Infection with rHRSV<sup>B05</sup>EGFP(5) resulted in high numbers of EGFP<sup>+</sup> cells at 4 d.p.i. in the epithelium of the bronchi and bronchioles in the lung slices (Figure 3I). Dramatically lower numbers of fluorescent cells were present in the bronchi and bronchioles of rgRSV-infected animals and only a few discrete, small fluorescent foci were present in the entire lung. Extensive screening was used to find them, the largest focus observed at 4 d.p.i. is shown (Figure 3J). The number of infected cells in the LRT was lower for both viruses at 6 d.p.i. Almost all rHRSV<sup>B05</sup>EGFP(5) fluorescent cells were cleared and a few isolated rgRSV-infected cells remained.

Virus loads detected in the lungs of the animals infected with an inoculum of 10  $\mu$ l are close to the background (Figure 3K). Irrespective of the time point analyzed, significantly higher qPCR genome equivalents were present in homogenized lung samples of the rHRSV<sup>B05</sup>EGFP(5)-infected than in rgRSV-infected animals (Figure 3L). The majority of animals infected with rHRSV<sup>B05</sup>EGFP(5) had enlarged tracheo-bronchial lymph nodes at necropsy 6 d.p.i., which was not observed in

Upper respiratory tract



Lower respiratory tract

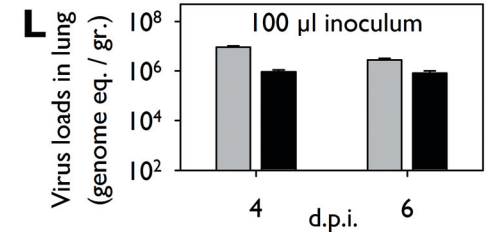
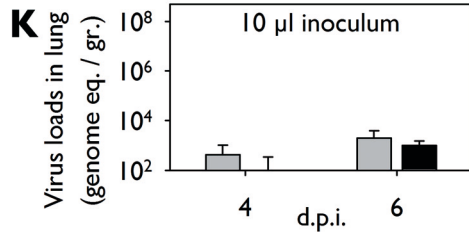
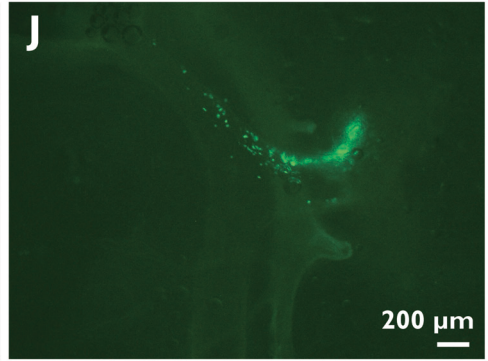
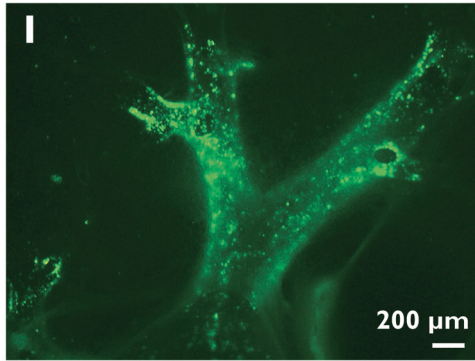




**Figure 3.** HRSV clinical isolate replicates very efficiently *in vivo*. A-F) Fluorescent microscopy, H&E staining and IHC photomicrographs of nasal septum of rHRSV<sup>B05</sup>EGFP(5) (A, C and D) and rgRSV (B, E and F) infected cotton rats at 4 d.p.i. showing equivalent levels of infection in the URT and “cometlike” spread. D, arrows) More destruction of epithelia was present in rHRSV<sup>B05</sup>EGFP(5)-infected animals. G, H) Virus loads in the nose were identical 4 and 6 d.p.i. regardless of the dose. I, J) Differences were magnified in the LRT where rHRSV<sup>B05</sup>EGFP(5) infection and spread was dramatic (I) compared to rgRSV (J). K, L) Virus loads in the lung showed marginal spillover from the URT (K) whereas rHRSV<sup>B05</sup>EGFP(5)-infected animals had significantly greater loads in the LRT (L). Bars represent 200  $\mu$ m.

animals infected with rgRSV.

### HRSV lung infection illuminated in 3D by optical sectioning

The power of targeted pathology in understanding the spatial dynamics of rHRSV<sup>B05</sup>EGFP(5) infection is evident when standard IHC in 7  $\mu$ m formalin fixed lung sections (Figure 4A,B) is compared with optical sectioning of living tissues immediately after necropsy (Figure 4C-G and supplementary movies S1 and S2). Dramatically more infected cells were detected in agarose-inflated lung slices reconstructed in 3D using confocal scanning laser microscopy (CSLM) than by IHC and sheets of infected, interconnected, luminal epithelial cells of bronchi and bronchioles were present (Figure 4C). Small numbers of individual cells in the parenchyma of the lung were also present (Figure 4C, insert and asterisk). These cells could not be phenotypically characterized by IHC due to the section size and lower level of sensitivity due to backgrounds. Optical sectioning also allows greater cellular resolution since EGFP floods the cytoplasm of the cell, meaning fine processes and cell-to-cell contacts were readily visible (Figure 4D, E, arrow). *In vivo* cell-to-cell spread recapitulates what is seen in primary human bronchial cells, again highlighting the importance of the mode of transmission for a virus which has evolved to replicate in the hostile environment of luminal bronchial and bronchiolar epithelial cells, where ciliated cells are the primary targets (Figure 4F, G).

### Discussion

We have developed a unique reverse genetics system based on an HRSV serogroup B clinical isolate, and generated the first rHRSVs that fully reflect the sequence of a clinical specimen obtained from an HRSV-infected patient. Use of rHRSV<sup>B05</sup>EGFP(5) allowed detection of infected cells both *in vitro* and *in vivo*, in the absence of CPE at unparalleled levels of sensitivity. HEp-2 cells were suitable for virus passage *in vitro* and the genomes were genetically stable. In addition, the growth kinetics of rHRSV<sup>B05</sup> and rHRSV<sup>B05</sup>EGFP(5) were comparable suggesting that insertion of an ATU into the HRSV genome at position 5 did not result in virus attenuation. Laboratory-adapted viruses generated by extensive passage through a variety of disease-relevant and non-relevant cells and tissues, have traditionally been used to develop molecular clones meaning there are short-comings using such viruses for pathogenesis studies [100,317,321,322]. Positional effects of an ATU on gene expression are important, an observation best illustrated by three recombinant canine distemper viruses based on a ferret-adapted strain which were attenuated (position 1), partially attenuated (position 3) and equivalently virulent to wild-type (position 6) when intranasally administered to ferrets [98]. In this study our main objective was not to compare rgRSV and rHRSV<sup>B05</sup>EGFP(5) directly, as the ATUs are in different positions of the genome. Rather rgRSV was included as reference since this virus, or the equivalent expressing a red fluorescent protein (rrRSV),

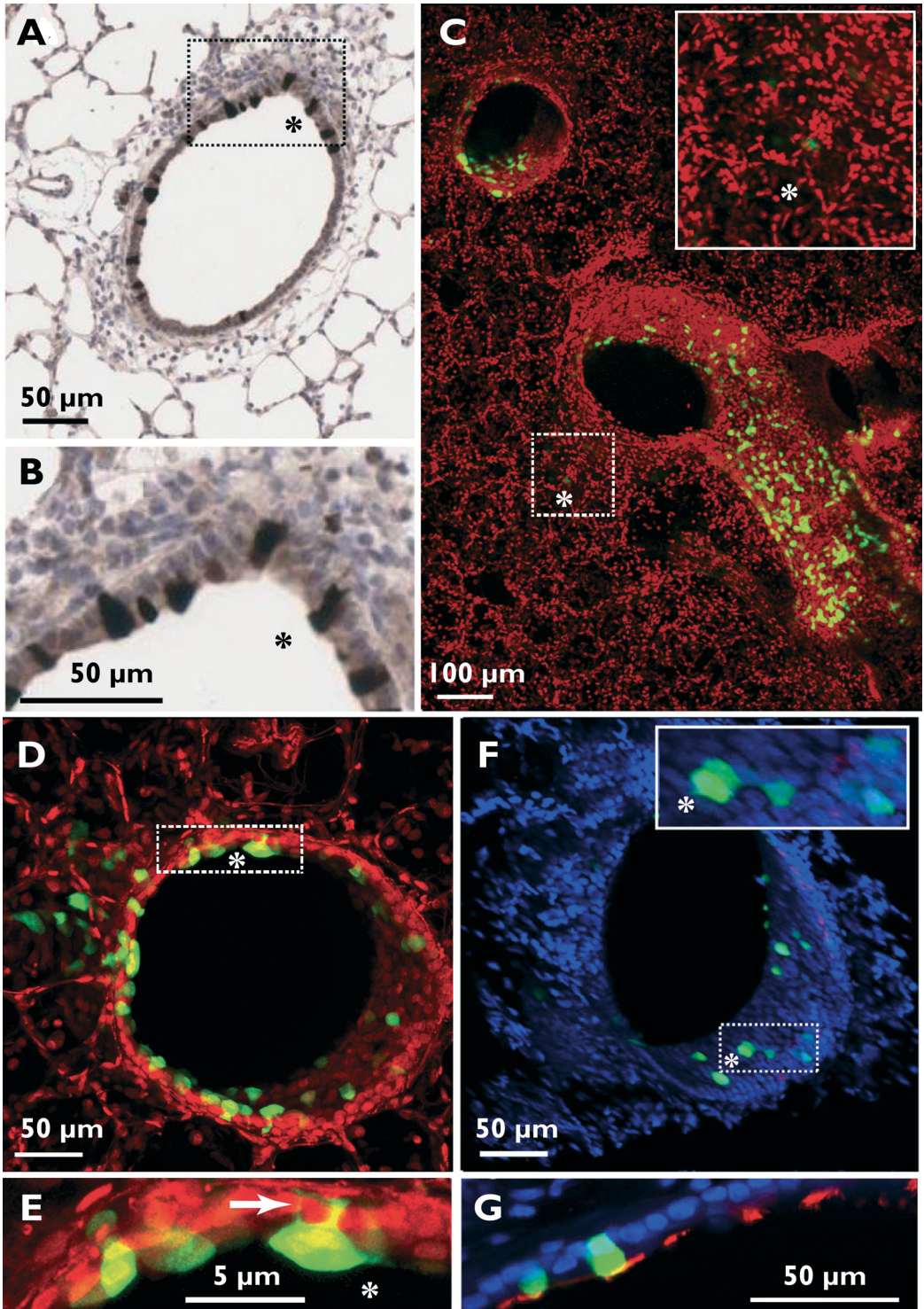


**Figure 4.** HRSV clinical isolate spreads very efficiently from cell-to-cell *in vivo*. A and B, asterisk) Standard IHC detection of rHRSV<sup>B05</sup>EGFP(5) in 7  $\mu$ m lung sections showing surface epithelial cells. It is not possible to identify infected cells in the parenchyma convincingly. C, D) Optical reconstruction of lung slices in 3D provides significantly more information on the spatial orientation and dramatic infection in the LRT and many more infected cells (green) are visible, nuclei are counterstained (red). E, arrow) Flooding the cytoplasm on infected cells with EGFP (green) illuminates fine cellular processes and intimately connected, but discrete epithelial cells serve to amplify the virus which spread from cell-to-cell (F, asterisk and S2 movie), nuclei are counterstained (blue). G) Triple, color high resolution CSLM proves infected cells (green) are  $\beta$ -tubulin positive (red) at the bronchiolar lumen, nuclei are counterstained (blue).

is the most widely used GFP-expressing rHRSV both *in vitro* [49,51,256] and *in vivo* [323-325].

Primary wd-NHBE cells were readily infected by rHRSV<sup>B05</sup>EGFP(5) without overt cytopathic changes. Strikingly, rHRSV<sup>B05</sup>EGFP(5) infected significantly higher numbers of wd-NHBE cells than rgRSV. However, a dramatic phenotypic paradox was evident when virus loads and genome equivalents were assessed in apical rinses from these cells. Even though rgRSV infected fewer cells, more virus was released apically suggesting that A2 strains have been selected for enhanced budding. The highly cell-associated nature of the clinical isolate was also apparent from the huge differences in genome equivalents present in the apical rinses from HRSV<sup>B05</sup>-infected cells compared to rgRSV-infected wd-NHBE cells. This could be due to apoptotic cells sloughing into the mucus, which appears to occur more frequently in HRSV<sup>B05</sup>-infected air-liquid interface cells. A potential confounder to this observation is that HEP-2 cells, to which rgRSV is optimally adapted, were used for virus isolations. However, growth curves show that both viruses replicate well in HEP-2 cells (Figure 11). In addition, when the two virus stocks were diluted to  $3 \times 10^6$  TCID<sub>50</sub> as measured in HEP-2 cells, they both contained  $3 \times 10^8$  HRSV genome equivalents as measured by qPCR. However, it cannot be excluded that there are fundamental differences in virion stability, F glycoprotein stability or re-adsorption efficiency between the viruses.

HRSV spread in differentiated human airway epithelial (HAE) cells has been described as a “comet like” spread, driven by the directionality of the beat of the cilia [51]. Equivalent “comets” were present in the nasal conchae of infected cotton rats, demonstrating this is relevant *in vivo* and not an *in vitro* artefact. Such localized cell-to-cell spread has significant implications for the development and delivery of HRSV antivirals. We tuned the model to mirror the 1-2% of human cases where virus triggers bronchiolitis or severe pneumonia by varying the inoculation volume to target mainly the URT or concurrently the URT and LRT. In agreement with the *in vitro* data, and in contrast to the numbers of cells infected in the upper or LRT, the amount of infectious cell-free rgRSV was higher than HRSV<sup>B05</sup>. This was most striking in the LRT where rgRSV-infected cells were virtually undetectable whereas HRSV<sup>B05</sup> infected many more cells throughout the branches of the bronchial tree. Infection levels with rHRSV<sup>B05</sup>EGFP(5) in the lungs were so high that the bronchial tree was illuminated, something which has never been recapitulated previously in an animal model of HRSV or, to the best of our knowledge any animal infected with any virus. This is important as it mirrors precisely the target cells in HRSV infected children [47]. Moreover, at 4 d.p.i. rHRSV<sup>B05</sup>EGFP(5) titers were similar to those obtained from patients or volunteers infected with HRSV [44,312,326].

This illustrates the strength of the cotton rat model and shows the power of targeted pathology, which is only feasible due to the possibility of identifying infected tissues for

blocking and processing immediately after necropsy. Such an approach has fundamentally changed our understanding of measles and canine distemper virus pathogenesis [92,94,98] and this is directly transferable to HRSV.

Reverse genetics of non-segmented negative strand RNA viruses has come a long way in the last twenty years following the recovery of rabies virus [327]. The challenges of generating recombinant viruses are far from trivial and much has been achieved with the original rHRSV systems [256,317]. Given the significant investment of time in establishing reverse genetics systems there tends to be a large activation energy required to develop second or third generation systems. This is particularly true for HRSV and, although tractable second generation systems have been developed [328], no one has successfully generated an rHRSV fully reflecting the sequence of a current, clinically relevant, wild-type strain. In addition, *in vitro* and *in vivo* models employing subgroup B HRSV strains have been scarce, and will be of crucial importance for preclinical testing of the effectiveness of new intervention strategies.

It is vital to extend ongoing studies and move in the direction of reverse genetics systems based on clinical isolates grown in disease-relevant cells. Only then will it be possible to understand HRSV pathogenesis fully and systematically test novel interventions. The recombinant B05 viruses will help in this endeavor and these should be augmented by the establishment of equivalent systems for subgroup A clinical isolates.

It has been shown that both in hospitalized children and in experimentally infected adults HRSV loads are directly associated with disease severity [44,312,326,329]. However, it is likely that this observation is a surrogate of the true mediators of disease, namely the

infected cells. Strains A2 and B05 demonstrate that cell-free virus loads may not always be directly related to the numbers of infected cells. The importance of this finding for the development of novel anti-HRSV therapeutics is evident as conclusions on drug efficacy based on decreased virus titers may be highly misleading. Rather we prove it is vital to target cell-to-cell spread *in vivo* making the virus and the models in this study invaluable.

### Materials & Methods

#### Determination of a complete HRSV subtype B genomic sequence directly from clinical material

Clinical material was kindly provided by Dr. Peter Coyle (Royal Victoria Hospital, Belfast). The sample was obtained from a tracheal rinse of an HRSV positive infant during the 2004/2005 HRSV season (HRSV<sup>B05</sup>). Total RNA was extracted from clinical material (500  $\mu$ l) using TRIzol LS reagent (Life Technologies). First-strand cDNA was generated using SuperScript III First-Strand Synthesis System (Life Technologies) and negative-sense genespecific primers based on conserved regions of the HRSV subtype B genome. PCR primers were designed to amplify the complete viral genome in six overlapping fragments. PCR was performed on the cDNA using Phusion High-Fidelity DNA Polymerase (New England Biolabs). PCR products were purified using QIAquick PCR purification kit (QIAGEN) and sequenced using primers spanning the viral genome. Sequences were assembled and a consensus determined using Lasergene 10 (DNASTAR). The complete genome sequence was submitted to GenBank (accession number KF640637). Primer sequences are available on request. rgRSV is a recombinant virus based on HRSV strain A2 which expresses EGFP from an ATU present the promoter proximal (position 1) of the genome [256].

### Construction of HRSV<sup>B05</sup> minigenomic and antigenomic plasmids

An HRSV minigenome plasmid, p(-)HRSV<sup>B05</sup> DI-EGFP, contained an EGFP open reading frame (ORF) flanked by the viral 3' and 5' termini and preceded upstream by a T7 promoter, guanine tri-nucleotide and ribozyme, and followed downstream by a hepatitis delta virus ribozyme and T7 terminator sequences. A negative-sense viral RNA was produced upon transcription by T7 RNA polymerase. The minigenome construct was synthesized by GeneArt Gene Synthesis (Life Technologies) and ligated into a modified pBluescript vector [330]. HRSV N, P, M2-1 and L expression plasmids were constructed in pCG(MPBS) [331]. A full-length, antigenomic HRSV plasmid, pHRSV<sup>B05</sup> was constructed following restriction enzyme digestion and sequential ligation into the modified pBluescript vector [330]. The viral genome sequence was orientated with respect to the T7 promoter to produce an antigenomic RNA upon transcription. The full-length HRSV plasmid was modified to contain an ATU encoding EGFP located between the P and M genes, pHRSV<sup>B05</sup>-EGFP(5).

### Development of a minigenome assay and recovery of rHRSV

Confluent HEp-2 cells (ATCC, CCL-23) were infected with MVA-T7 for 1 hr at 37°C. Inoculum was aspirated and Lipofectamine 2000 (Life Technologies) was used to transfect plasmid mixtures containing N, P, M2-1, L and full-length or minigenome constructs. After 18 hrs liposomes were removed and replaced with OptiMEM (2 ml) (Life Technologies) containing 2% (v/v) fetal bovine serum (FBS). Cells were incubated for up to 7 days at 37°C with 5% (v/v) CO<sub>2</sub>. Supernatants from cells transfected with full-length constructs were used to infect fresh HEp-2 monolayers and the presence of virus was confirmed by immunoplaque assay, fluorescence or CPE observed by phasecontrast microscopy. Cells, transfected

with the HRSV minigenome construct, were observed daily by fluorescence microscopy to detect EGFP expression. Virus stocks were prepared in HEp-2 cells. Virus titers were determined by endpoint titration in HEp-2 cells.

### *In vitro* infection assays and virus characterization

Growth kinetics was assessed by infection of HEp-2 cells at an MOI of 0.1. Triplicate samples were scraped, sonicated, centrifuged and snapfrozen. Virus present in the sample for each time-point was determined by endpoint titration in HEp-2 cells. Titers are expressed in 50% tissue culture infectious dose (TCID<sub>50</sub>) units calculated by the Reed and Muench method [332]. To determine GAG indices CHO cells expressing GAG or GAG deficient were infected and analyzed by flow cytometry [207]. wd-NHBE were cultured in 12 mm/0.4 µm pores inserts (Corning) on ALI [307]. The apical surface of cells (estimated to contain 10<sup>5</sup> cells exposed at the surface) were removed and the apical surfaces were washed three times with Dulbecco's phosphate-buffered saline (DPBS, 500 µl). At 2 d.p.i., DPBS (500 µl) was added to the apical compartment and the cells incubated at 37°C. After 10 minutes the DPBS and growth medium were harvested from the apical and basolateral compartments respectively for virus isolations and qPCR. Subsequently, automated whole well scans were made by CSLM with a LSM700 system fitted on an Axio Observer Z1 inverted microscope (Zeiss), followed by semi-automated enumeration of EGFP<sup>+</sup> cells (DotCount, MIT, Boston). Viruses were titrated in HEp-2 cells using ten- (growth kinetics) or three fold (apical rinse) dilutions in flat bottom 96-wells plates and cultured for 5-7 days at 37°C. The presence of HRSV genomes in samples was determined by TaqMan RT-PCR as previously described [333] with slight modifications. A quantified positive control for HRSV A or B (Vircell) was added

to compare genome copies of HRSV A and B. The cycle threshold (Ct) value was calculated automatically when the fluorophore signal (6-carboxyfluorescein (FAM) for HRSV A and tetramethylrhodamine (TAMRA) for HRSV B) was detected above the background level and was used to give a quantitative indication of viral copy numbers. All *in vitro* experiments were performed at least three times. Statistical analyses were performed with SPSS version 20.0.

### ***In vivo* infection experiment**

Six groups of six female, 3-4 week old cotton rats were infected intranasally with  $10^4$  TCID<sub>50</sub> of rHRSV in an inoculum volume of 10  $\mu$ l or 100  $\mu$ l to target the URT or LRT predominantly [219]. Animals (n=3/group) were euthanized by exsanguination at 4 or 6 d.p.i. The right lung was inflated with 2% (w/v) agarose (Sigma-Aldrich), sliced and submerged in media [306]. Post-mortem nasopharyngeal washings were collected, and the left lung was prepared for qPCR. Nasal concha, nasal septum and agarose-inflated right lung [306] were screened and scored for microscopic fluorescence (Zeiss, AxioVert-25). Mann-Whitney *U* tests were used to compare differences between groups and  $p \leq 0.05$  was considered statistically significant.

## **Supplementary Material & Methods**

### **HRSV immuno-plaque assay**

Serial 10-fold dilutions of HRSV were prepared in OptiMEM. Confluent HEp-2 cells cultured in 24-well plates (Greiner Bio-One) were infected with each dilution (200  $\mu$ l) for 1 hr at 37°C. Inoculum was aspirated and 0.8% carboxy-methylcellulose (2 ml; Sigma-Aldrich), in OptiMEM containing 2% (v/v) FBS, was added. Overlay medium was removed 4-5 d.p.i. and cells were fixed in cold 80% (v/v) methanol for 1 hr at 4°C. Plates were washed in distilled water and blocked with 5% (w/v) milk for 30 minutes. Goat anti-HRSV (Abcam

Ab20745-1) diluted 1:100 in blocking solution (200  $\mu$ l) was added. Following 1 hr incubation at room temperature with rocking, plates were washed in distilled water and rabbit anti-goat horseradish peroxidase (HRP) conjugate (Abcam Ab6741) diluted 1:100 in blocking solution (200  $\mu$ l) was added. Following 1 hr incubation at room temperature plates were rinsed and binding of the HRP-conjugated antibody was detected using 4-chloro-1-naphthol (200  $\mu$ l; Pierce).

### **Immunohistochemical analysis of formalin-fixed tissues**

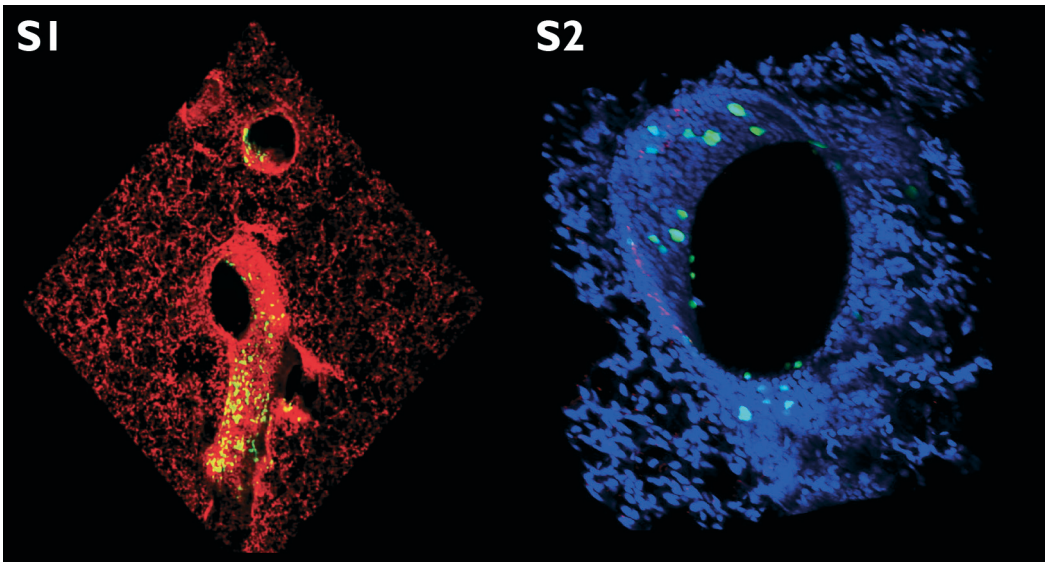
Paraffin embedded tissues were processed as previously described [92]. HRSV-infected cells were detected using a polyclonal rabbit antibody to EGFP (Invitrogen). All fluorescently stained slides were assessed and digital fluorescent images acquired with a Leica DF digital camera using Leica FW4000 software.

### **Live cell confocal laser scanning microscopy**

Nasal tissues and agarose inflated lung slices were fixed with PBS/ 4% (w/v) paraformaldehyde, permeabilized with PBS / 0.1% (v/v) Triton-X100 for 30 minutes, counterstained with the far red nuclear counterstain TO-PRO-3 (Invitrogen) or DAPI (Vectashield) and directly analyzed for EGFP fluorescence by the LSM700 system (Zeiss) or Leica SP5 microscope (Leica Microsystems). Three dimensional images and movies were generated using Zen (Zeiss) or LCS (Leica) software.

### **Acknowledgements**

The authors wish to thank Georgina Aron, Peter Coyle, Rory de Vries, Rachel Scheuer, Joyce Verburgh. We thank M.E. Peebles and P.L. Collins for providing rgRSV.



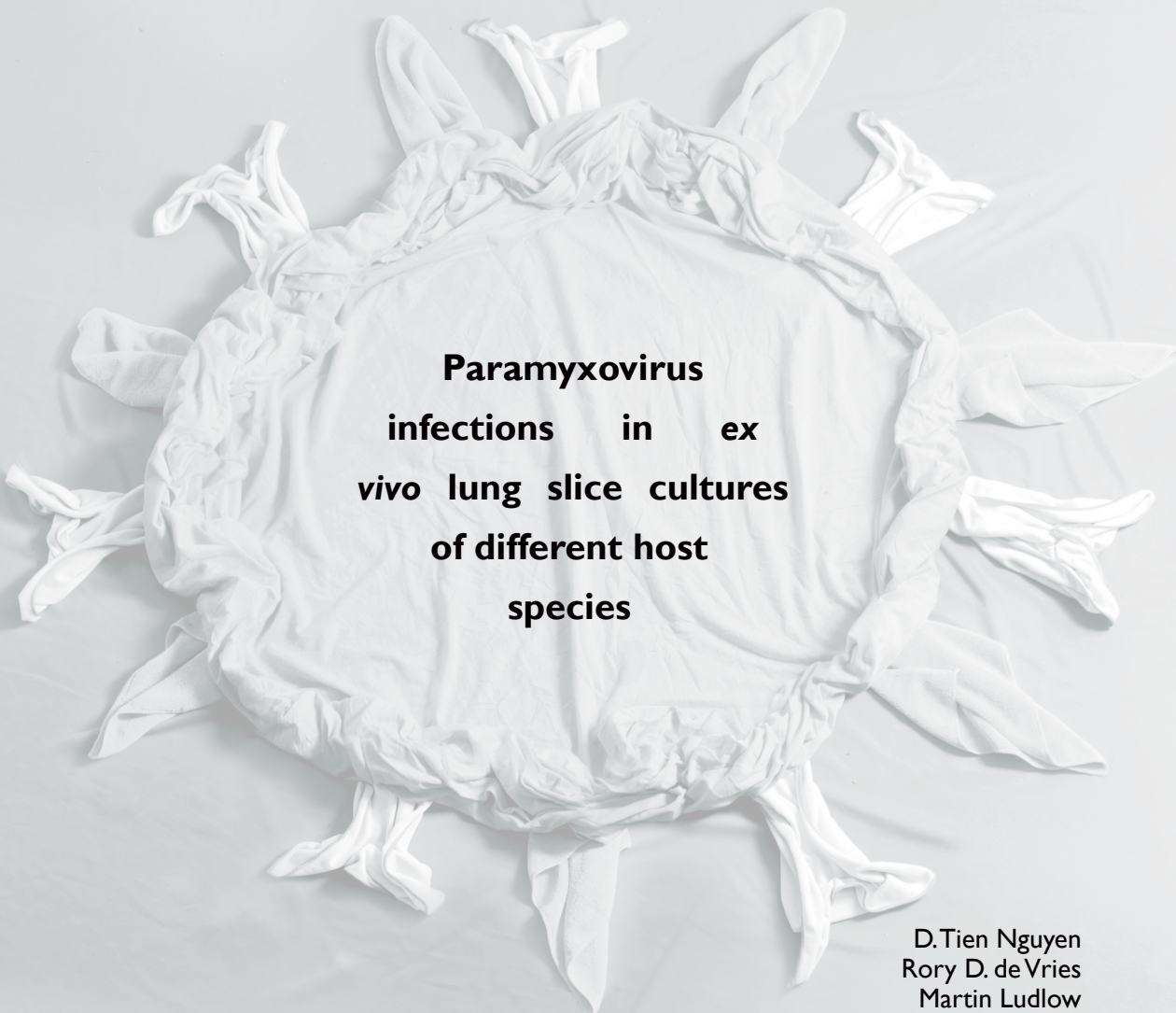
**Supplemental movie still 1.** Still of movie of an rHRSV<sup>B05</sup>EGFP(5)-infected lung reconstructed in 3D from optical sections obtained by CSLM. Lungs from infected cotton rats at 4 d.p.i. were agarose inflated and fixed with PBS/ 4% (w/v) paraformaldehyde, permeabilized with PBS / 0.1% (v/v) Triton-X100 for 30 minutes, counterstained with the far red nuclear counterstain TO-PRO-3 (red) and directly analyzed for EGFP fluorescence(green) using an Zeiss LSM700 CSLM. A three dimensional volume was generated permitting the spatial organization to be examined at high resolution. Movie generated using Zen (Zeiss) software. Extensive sheets of interconnected, rHRSV<sup>B05</sup>EGFP(5)-infected cells are present throughout the bronchioles and bronchiolar airways. Photomicrograph stills from this 3D dataset are shown in Figure 4C.

**Supplemental movie still 2.** Still movie of an rHRSV<sup>B05</sup>EGFP(5)-infected lung reconstructed in 3D from optical sections obtained by CSLM. Lungs from infected cotton rats at 4 d.p.i. were agarose inflated and fixed with PBS/ 4% (w/v) paraformaldehyde, permeabilized with PBS / 0.1% (v/v) Triton-X100 for 30 minutes. Nuclei were counterstained with DAPI (blue) and cilia were visualized by indirect immunofluorescence using a monoclonal antibody to  $\beta$ -tubulin detected using an anti-mouse/human Alexa 568 conjugated secondary antibody (red), nuclei were counterstained using DAPI in Vectashield mounting medium (blue). Virus infected cells were analyzed for EGFP fluorescence (green) using an Leica SP5 CSLM. A three dimensional volume was generated permitting the spatial organization to be examined at high resolution. Movie generated using Leica LCS software. Sheets of interconnected, rHRSV<sup>B05</sup>EGFP(5)-infected cells are present throughout the bronchioles and bronchiolar airways and  $\beta$ -tubulin-positive, virus infected cells were readily identified. Photomicrograph stills from this 3D dataset are shown in Figure 4F and G.





## **Chapter 6**



### **Paramyxovirus infections in ex vivo lung slice cultures of different host species**

**D.Tien Nguyen  
Rory D. deVries  
Martin Ludlow  
Bernadette G. van den Hoogen  
Ken Lemon  
Geert van Amerongen  
Albert D.M.E. Osterhaus  
Rik L. de Swart  
W. Paul Duprex**

*Journal of Virological Methods* 193(1): 159-165 (2013)

## Chapter 6

### Abstract

Paramyxoviruses, including measles virus (MV), human metapneumovirus (HMPV), human respiratory syncytial virus (HRSV) and canine distemper virus (CDV), are transmitted via the respiratory route. Despite their close phylogenetic relationship, the pathogenesis of these viruses is very different. To study viral tropism and replication *ex vivo*, a protocol for the inflation of lungs with low-melting-point agarose mixed with culture medium was established. Lung slices were prepared and remained viable in culture at 37°C for at least seven days. Lung slices obtained from different animal species were infected with recombinant paramyxoviruses expressing enhanced green fluorescent protein (EGFP).

Progression of infection was monitored in real time by detection of EGFP fluorescence. Flow cytometric analysis of cells emigrating into the culture medium proved to be a valuable tool for qualitative and quantitative assessment of infection over time. MV replicated optimally in lung slices of macaques, HMPV and HRSV in lung slices of cotton rats, and CDV in lung slices obtained from dogs and ferrets. In conclusion, these *ex vivo* lung slice cultures are discriminatory models for the study of respiratory virus infections and can be used to inform the design of future *in vivo* experiments, thereby reducing numbers of animals required.

## Introduction

Paramyxoviruses are enveloped viruses with a negative-sense, single strand RNA genome that belong to the order *Mononegavirales* [334]. They are transmitted via the respiratory route and cause significant disease in humans and animals. The family *Paramyxoviridae* is divided into two subfamilies, the *Paramyxovirinae* and *Pneumovirinae*. The subfamily *Paramyxovirinae* includes the genus *Morbillivirus*, of which measles virus (MV), the causative agent of measles in humans, and canine distemper virus (CDV), the causative agent of distemper in many carnivores, are well-known members [335]. The subfamily *Pneumovirinae* contains the genera *Pneumovirus* (including human respiratory syncytial virus [HRSV]) and *Metapneumovirus* (including human metapneumovirus [HMPV]), which are important causes of respiratory tract disease in children [58,232].

Traditionally, viral pathogenesis studies are performed *in vitro* in transformed cells or *in vivo* in animal models. Recently, more advanced and disease-relevant cell culture systems have been developed, such as well-differentiated primary normal human bronchial epithelial cells grown on air-liquid interface [208]. However, tissues like the respiratory tract are much more complex than these *in vitro* models as they also contain many other cell types such as interdigitating and motile immune cells.

*Ex vivo* models can provide a bridge between *in vitro* and *in vivo* models. Agarose-inflated lung slices have been used previously to study tissue physiology or infectious diseases [85,336,337]. In the present study, the development of a culture system in which these slices remain viable for at least one week is described, allowing accurate and reproducible assessment of respiratory virus infection and dissemination over time. It has been reported previously that recombinant viruses expressing fluorescent

proteins allow sensitive detection of virus-infected cells [51,92,100,280,338]. Use of these recombinant viruses allows for real time monitoring of infection processes, using multiple methods for measurement of fluorescence. In addition these slices are also suitable for immunohistochemistry, thereby visualizing virus cell tropism and precise localization of the virus within a tissue. The aim of this study was to investigate whether differences in tropism or replication kinetics of paramyxoviruses could be detected using *ex vivo* lung slice cultures from different host species.

## Materials & Methods

### Animals

Lungs or lung lobes were collected from cynomolgus macaques (*Macaca fascicularis*, n=3), dogs (mixed-breed, n=3), ferrets (*Mustela putorius furo*, n=3) and cotton rats (*Sigmodon hispidus*, n=3) during different unrelated experiments. Macaques were approximately 5-7 years old, seronegative for MV, CDV, HRSV and HMPV and weighed 4-7 kg. Dogs were euthanized in a study of cardiac arrhythmogenesis. Animals were approximately three years old and had a body weight of 22-36 kg. Ferrets had been infected previously with different influenza virus strains to prepare virus-specific polyclonal antisera. Animals were approximately 1 year old, weighed 0.8-1 kg and were euthanized after clearance of the virus when an efficient humoral immune response had developed at approximately two weeks post infection. Cotton rats were euthanized as control animals in a vaccination study. The animals were 4-8 weeks old and weighed 60-100 grams. A national animal experimentation ethics committee approved all animal protocols, and experiments were performed in compliance with Dutch and European

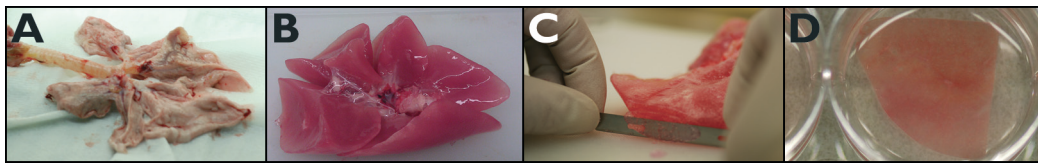


**Figure 1.** Stepwise procedure to obtain lung slices from animal lungs. A) Resected lungs including trachea were inflated with 2% (w/v) low-melting agarose in culture medium using a blunt-end needle, and placed on ice to solidify. B) Agarose-inflated lung lobes were separated from each other and fixed with needles to cut lung slices. C) Inflated lung lobes were cut manually in 1 mm slices with 80 mm microtome blades. D) Lung slices were transferred to a culture plate containing lung slice medium and incubated at 37°C in 5% CO<sub>2</sub> (v/v).

guidelines for animal experimentation.

### Viruses

Four recombinant paramyxoviruses encoding GFP or EGFP were used to study infection in lung slices. Recombinant (r) CDV strain Snyder Hill (rCDV<sup>SH</sup>EGFP), rMV strain KS (rMV<sup>KS</sup>EGFP), rHMPV strain NL/1/00 (rHMPV<sup>NL/1/00</sup>EGFP) and rRSV strain A2 (rRSV<sup>A2</sup>GFP or rRSV, a kind gift of Dr. M.E. Peeples and Dr. P.L. Collins) were used. Construction, rescue and propagation of these viruses have been described elsewhere [85,100,256,280]. Virus stocks which were grown on mycoplasma species-free cells. Virus titers for rCDV<sup>SH</sup>EGFP (measured in Vero-dogSLAM cells [286], gift from Dr. Y Yanagi), rMV<sup>KS</sup>EGFP (measured in Vero-humanSLAM cells [339], gift from Dr. Y. Yanagi), rHMPV<sup>NL/1/00</sup>EGFP (measured in Vero-118 cells [340]) and rRSV<sup>A2</sup>GFP (measured in HEp-2 cells, ATCC CCL-23) were 3.2x10<sup>6</sup>, 2.2x10<sup>6</sup>, 6.3x10<sup>6</sup> and 1.3x10<sup>7</sup> 50% tissue culture infectious dose (TCID<sub>50</sub>) per ml, respectively.

### Preparation of lung slices

Lungs including the distal part of the trachea were resected and transferred into phosphate buffered saline (PBS; Figure 1A). Lungs were inflated with 2% (w/v) low-melting 2-hydroxyethyl agarose (Sigma-Aldrich, A4018). To this end, a 4% agarose solution was prepared in PBS by heating (100°C) in a microwave and subsequently kept at 42°C until use the same day. Immediately prior to

inflation, this solution was mixed 1:1 with lung slice medium (DMEM / Ham's F-12 medium (50%/50% v/v) supplemented with L-glutamine (2 mM, Lonza), 10% (v/v) heat-inactivated fetal bovine serum (FBS, Sigma-Aldrich), penicillin (100 U/ml)/ streptomycin (100 mg/ml, Lonza) and amphotericin B (1 µg/ml, institutional pharmacist; Figure 1B)), pre-warmed at 42°C. Using a syringe the mix of agarose and medium was injected through the trachea into the lungs. The inflated lung was allowed to solidify on ice, and cut manually in 1 mm thick slices with 80 mm Edge-Rite<sup>®</sup> microtome blades (Thermo Scientific Richard-Allan, 4280L; Figure 1C). Subsequently, lung slices were gently transferred into 6- or 12-wells plates (Corning Costar; Figure 1D) that were pre-filled with lung slice culture medium and subsequently incubated at 37°C in 5% (v/v) CO<sub>2</sub>.

### Ex vivo virus infections of lung slices

One day after preparation, the lungs lung slices were gently transferred into empty 6- or 12-well plates using sterile disposable tweezers (Unomedical). This one-day delay was introduced to ensure standardization between experiments, because in some studies lungs only became available at the end of the day after completion of necropsies. Lung slices were infected with an inoculation volume of 150 µl of virus per slice. Medium served as a negative control. To reach comparable inoculation titers, HMPV and HRSV were diluted while the other virus stocks were

used undiluted, so the virus inoculum per slice was between 1 and  $5 \times 10^5$  TCID<sub>50</sub>/slice. After 1 hr incubation at 37°C, fresh lung slice medium was added. On 2, 4 and 6 or 7 days post infection (d.p.i.) lung slices were transferred into new plates and the medium of the old plate was harvested for flow cytometry. Six lung slices were used for infections with the four different viruses or for the medium control.

### Microscopic and macroscopic detection of fluorescence

Macroscopic imaging was performed as described previously [92]. Briefly, a lamp was custom-made containing six 5-volt LEDs (Luxeon Lumileds, lambertian, cyan, peak emission 490-495 nm) mounted with D480/40 bandpass filters (Chroma). Emitted fluorescence was visualized through the amber cover of a UV transilluminator (UVP) normally used for screening DNA gels. Photographs were made using a Nikon D80 digital SLR camera.

Microscopically, GFP<sup>+</sup> cells were identified by using an inverted fluorescence microscope (Zeiss Axiovert 25) or a confocal laser scanning microscope (Zeiss inverted AxioObserver Z1 equipped with LSM 700 scanning module). Complete lung slices were used for indirect immunofluorescence staining. Macaque lung slices were transferred to 4% (w/v) paraformaldehyde in PBS, permeabilized with 0.1% (v/v) Triton-X100 for 30 minutes and subsequently stained. Cilia were stained using a primary monoclonal antibody directed against class IV  $\beta$ -tubulin (clone MUI78-UC, Biogenex; clone ONS-1A6, Sigma) and a secondary Alexa Fluor<sup>®</sup> 594 goat anti-mouse IgG1. TO-PRO-3 (Invitrogen) was used to counterstain nuclei in red. All images were generated using Zen 2010 software (Zeiss).

### Flow cytometry

Supernatants from infected lung slice cultures were harvested at 2, 4 and 6/7 d.p.i. and

centrifuged for 10 minutes at 300  $\times$  g. Pellets of emigrated cells were transferred to a 96-wells V-bottom plate (Greiner Bio-One), washed once and resuspended in PBS / 2mM EDTA / 1% (w/v) bovine serum albumin. Percentages GFP<sup>+</sup> cells were determined by flow cytometry (FACS Canto II, Becton-Dickinson) by first gating viable cells based on forward and side scatter, followed by a second gate for GFP<sup>+</sup> cells. Mock-infected lung slices were used to set the gate for GFP<sup>+</sup> cells.

To identify which subsets of cells were infected by each virus, staining of specific cell types could be performed. Unfortunately, (cross-reactive) antibodies were not available for every animal species included in this study. Therefore, percentages GFP<sup>+</sup> cells were determined in lymphoid or non-lymphoid cells based on the forward and side scatter of these populations. Lymphoid cells typically have an intermediate forward scatter and small side-scatter, and can readily be identified as a separate cloud in a dot plot of FSC versus SSC. In that same dot plot, the non-lymphoid cell population forms a separate cloud of events, which are mainly characterized by a higher side scatter. Examples of gates that were used are shown in Figure 4.

## Results

### Agarose-inflated lung slices remain viable in culture for at least one week

Lungs were inflated with 2% (w/v) low melting point agarose (Figure 1A, B). To prevent punching holes in the trachea or bronchi, a 21 gauge blunt-end needle (Miltenyi Biotec) was used in certain cases. Due to their size, dog and macaque lungs were not inflated through the trachea, but through the left or right primary bronchus. Lung slices were cut manually (Figure 1C), had a thickness of approximately 1-2 mm, and were transferred to plates containing lung slice medium (Figure 1D). The next day slices were infected with one of the four paramyxoviruses and screened

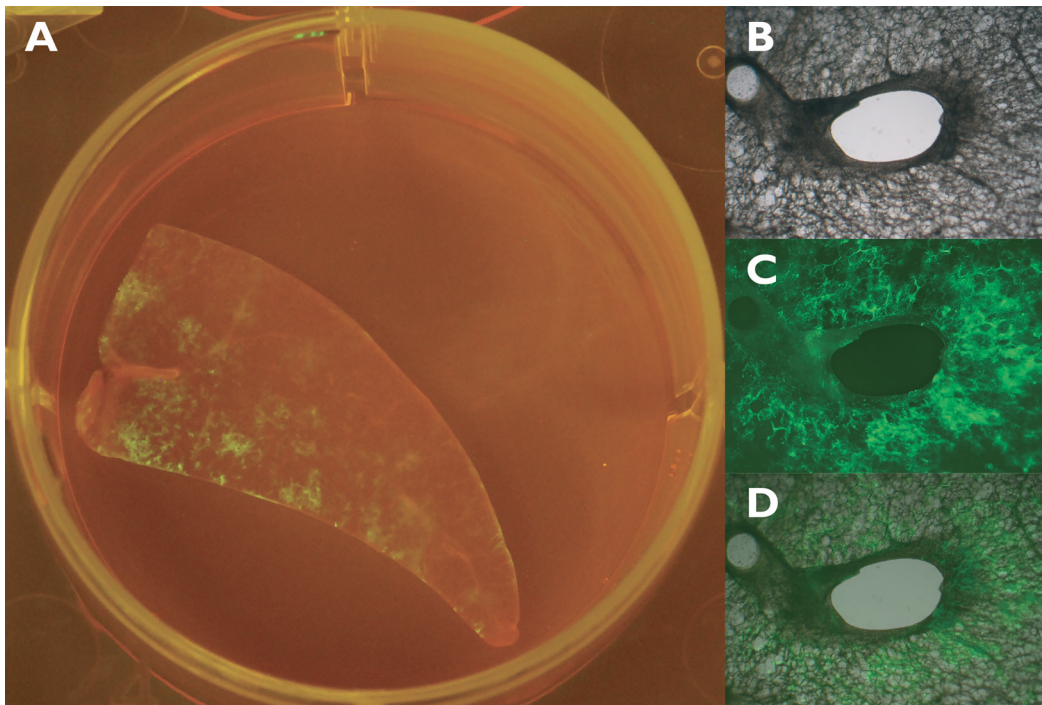


**Figure 2.** CDV-infected ferret lung slice. A) Macroscopic image of ferret lung slice infected with recombinant canine distemper virus (CDV) expressing EGFP, 9 d.p.i. EGFP<sup>+</sup> areas were mainly visible around the bronchial lumina B-D). Microscopic images of previous lung slice: brightfield (B), U.V. (C), and merged brightfield with U.V. (D; 100x).

for viability for the next 14 days. All lung slices remained viable as observed by beating cilia of bronchial epithelial cells until at least 7 d.p.i. (Movie 1). Between 7 and 14 d.p.i. viability was lost, therefore infections were not typically followed for longer than 7 to 9 d.p.i.

#### **Infection of lung slices with recombinant paramyxoviruses expressing GFP allows monitoring of virus spread in real time**

In addition to monitoring the viability of the slices, all lung slices were macroscopically and microscopically screened for the presence of GFP<sup>+</sup> cells. Numbers of GFP<sup>+</sup> cells after MV infection were highest in lung slices of macaques, whereas HMPV and HRSV replicated best in lung slices of cotton rats and CDV in canine and ferret lung slices. As an illustration, CDV infection in ferret lung slices resulted in diffuse cell-to-cell

spread throughout the lung slice (Figure 2A). Fluorescence microscopy revealed infection around the lumina of bronchioles, in which cilia movement was still present (Figure 2B-D).

#### **Flow cytometric assessment of paramyxovirus infection in cells emigrating from the lung slices**

Supernatants were collected, washed, and the percentage GFP<sup>+</sup> cells emigrating from the lung slices was assessed by flow cytometry at 2, 4, and 6/7 d.p.i. The percentages GFP<sup>+</sup> emigrant cells confirmed the macroscopic and microscopic observations of species-specific differences between the viruses. Up to 2.7% of the emigrant cells from MV-infected macaque lung slices were infected at 6/7 d.p.i., as compared to less than 0.2% in the other species (Figure 3A). Up to 1.15% of the

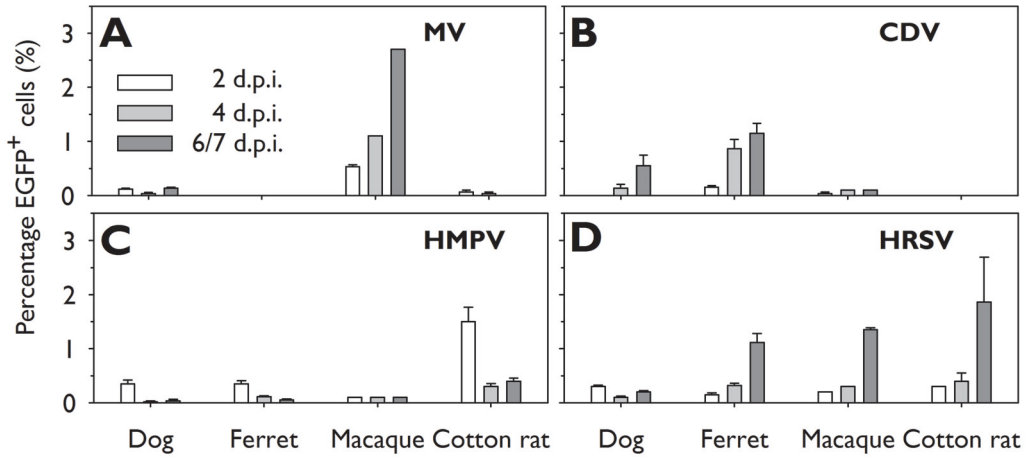


**Figure 3.** Infection percentages of four paramyxoviruses in emigrant cells collected from the supernatants of lung slice cultures of four host species at 2, 4, and 6/7 d.p.i. A) MV efficiently infected macaque lung slices. B) CDV only infected canine and ferret lung slices. C) HMPV primarily infected cotton rat lung slices. D) HRSV was able to infect and replicate in lung slices of all host species. Bars represent mean  $\pm$  SEM,  $n = 6$  lung slice cultures for dog, ferret, and cotton rat,  $n = 3$  for macaque lung slice cultures.

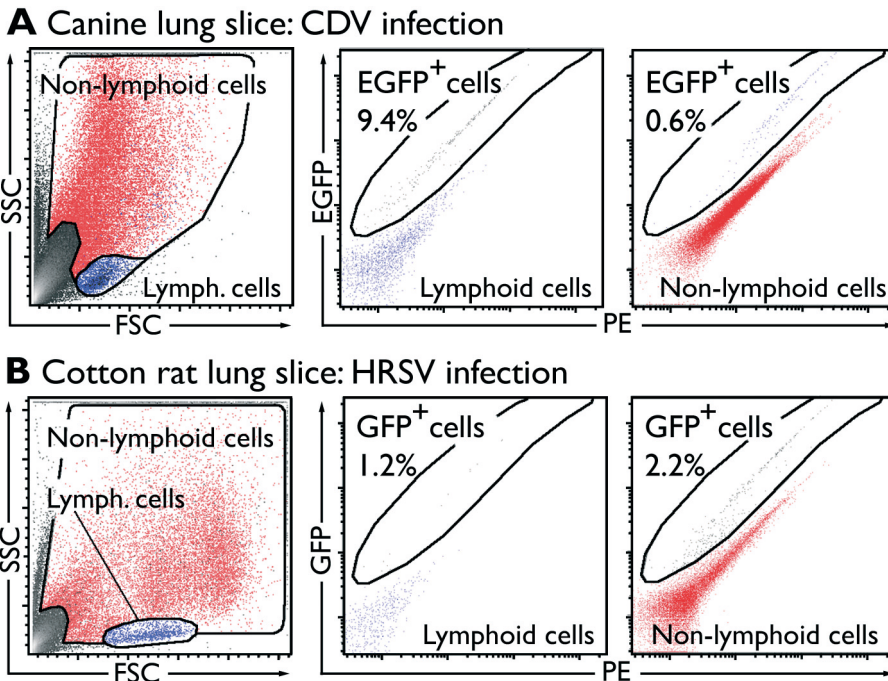


**Figure 4.** CDV and HRSV cell tropism. Based on gating on forward and side scatter emigrant lymphoid and non-lymphoid cells were selected. A) In a CDV-infected canine lung slice 9.4% of the lymphoid cells and 0.6% of the non-lymphoid cells were infected at 6 d.p.i. B) In a cotton rat lung slice 7 d.p.i. 1.2% of the lymphoid cells and 2.2% of the non-lymphoid cells were infected.

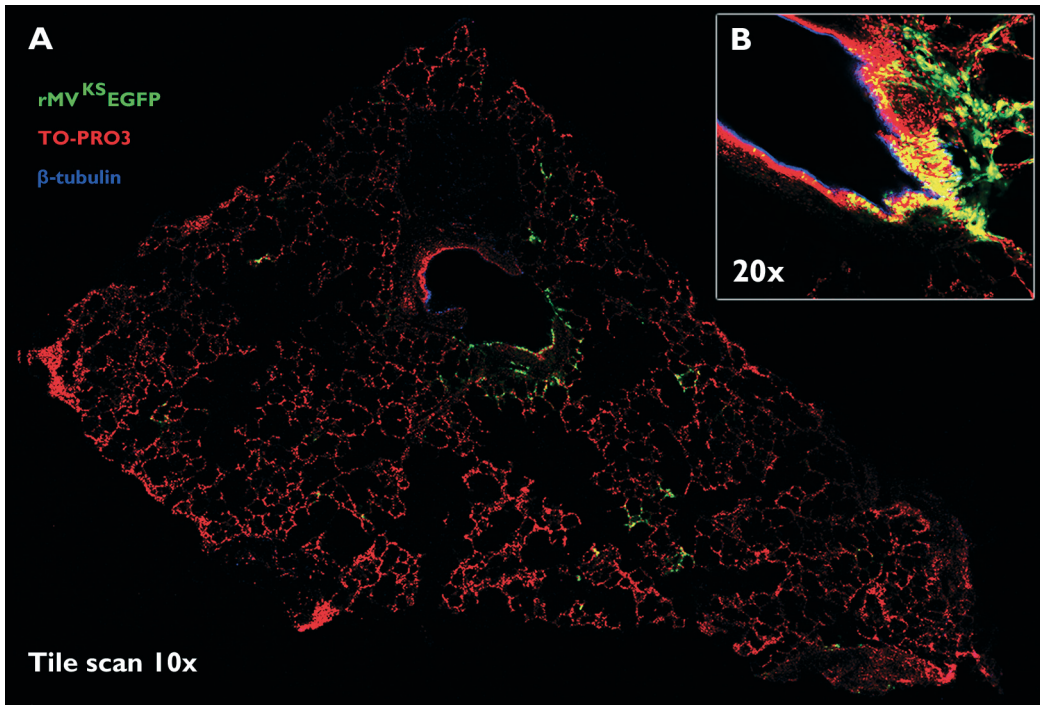


**Figure 5.** Confocal images of a MV-infected macaque lung slice. A) Confocal tile scan image of macaque lung slice infected with MV 6 d.p.i. shows mainly infected foci around the bronchial lumen (green), cilia (blue), and nuclei (red; 10x). B) Inset shows an infected spot next to a lumen of a bronchiole. The presence of a dense population of mononuclear cells suggests that this area is BALT (20x).

emigrant cells from CDV-infected canine and ferret lung slices were infected at 6/7 d.p.i., whereas no to minimal infection was detected in macaque and cotton rat lung slices (Figure 3B). HMPV was able to infect lung slices of all four species, although it only replicated efficiently in cotton rat lung slices (Figure 3C). Interestingly, HRSV infected and replicated in lung slices of all tested host species (up to 1.9% of emigrant cells), although in canine lung slices infection percentages were lower than in other hosts (Figure 3D).

In addition to the total viable emigrant cell population, infection percentages were also determined in lymphoid or non-lymphoid subpopulations. CDV and MV primarily infected lymphocytes, whereas HMPV and HRSV primarily infected non-lymphoid cells with a larger side scatter (Figure 4; data only

shown for CDV and HRSV). These results are consistent with previous observations [92,341].

#### **Analysis of infected cells using dual fluorescence staining**

Dual indirect immunofluorescence permitted the localization of MV infection within the lung slice. Nuclei (red) and cilia (blue) were visualized by TO-PRO-3 staining and  $\beta$ -tubulin class IV staining, respectively. MV-infected cells were detected by GFP fluorescence (green). A complete stained lung slice was imaged by confocal laser scanning microscopy (Figure 5A). MV was primarily detected in areas containing bronchus-associated lymphoid tissue (BALT), but also in the bronchial or bronchiolar epithelium and submucosa. A high power detailed image of a bronchiole



with substantial MV infection showed cilia and nuclei of bronchial epithelial and other cells (Figure 5B). In contrast, HMPV and HRSV infection were more diffuse and not limited to the areas around the lumina (data not shown).

### Discussion

In this study agarose-inflated lung slices of four different animal species were infected with four different paramyxoviruses. It was demonstrated that culturing lung slices of not only small animals [337], but also of large animals is possible for at least 7 days. The use of recombinant paramyxoviruses expressing GFP allowed sensitive detection of infection in real time. The viruses used showed different replication efficiency in lung slices of different host species. Indeed, the host species of which lung slices were most susceptible have all been used as animal models for these viruses: ferrets for CDV [100,342], macaques for MV [343], cotton rats for HMPV [344] and cotton rats, ferrets and macaques for HRSV [159,219,220,345]. Furthermore, cell tropism for each virus could be assessed by flow cytometry using cells emigrating out of the tissue. Hence, lung slices provide a useful and discriminatory *ex vivo* model to study the pathogenesis of respiratory viruses.

Although differences between viruses and *ex vivo* lung slices of different animal species were observed, certain procedures could be optimized. In this study microblades were used to manually cut slices of lungs after the inflated agarose solidified. This resulted in variable thickness of the lung slices compared to automated tissue slicers. However, the working space to cut animal lungs in an automated tissue slicer is limited and inflated lungs of large animals such as dogs and macaques used in this study would not fit in a commercially available standard tissue slicer. Finally, the availability of (uninfected) animals could be a limiting factor to perform these

experiments, especially for viruses, like MV, that have non-human primates as the best animal model.

A difficulty of the model is that quantification of the levels of virus infection remains difficult. Flow cytometric analysis of emigrant cells provides useful information, but it is difficult to assess whether or not different target cells can be detected with equal efficacy. It seems likely that naturally migrating cells such as lymphocytes or macrophages will be detected more efficiently than virus-infected epithelial cells, which need to be sloughed off the epithelium to become detectable in the culture supernatant. Furthermore, it remains difficult to discriminate virus infection and virus replication. In this respect, the observation that HMPV infection was more readily detectable in lung slices obtained from cotton rats than in those from macaques warrants more investigation. Indeed, *in vivo* infection models in macaques have required relatively high virus inocula to obtain reproducible infection [64,340], whereas cotton rats were previously identified as a permissive small animal model of HMPV [344].

The present study shows that lung slices can be used to investigate respiratory virus infections. Agarose-inflated lung slices can successfully be maintained in culture and can be productively infected with viruses, as shown macroscopically and microscopically with GFP-expressing cells. In addition, lung slices prepared according to this protocol can also be of use to screen lungs of animals after *in vivo* virus infection. This proved especially useful when screening for low-frequency events [85]. In addition, culturing lung slices prepared from animals infected *in vivo* provided a useful tool to study subsequent virus dissemination *ex vivo* [346]. The set of photographs of the same lung slice taken at different time points after culture also clearly shows that the lung slices not only become

infected, but that the viruses also replicate and spread within the slice [346]. Therefore, *ex vivo* lung slices provide a valuable model for studying the pathogenesis of respiratory viruses in various host species.

**Acknowledgements**

We thank Jet Beekman of the University Medical Center Utrecht, The Netherlands for her contribution to this study and Selma Yüksel, Joyce Verburgh, and Latoya Sarijoen for their technical assistance. This study received financial support from the VIRGO project, MRC (grant# G0801001), ZonMw (grant# 91208012) and FNIH (grant# DUPREX09GCGH0).





## Chapter 7

***Streptococcus*  
*pneumoniae* exposure  
is associated with  
human metapneumovirus  
seroconversion and increased  
susceptibility to *in vitro*  
HMPV infection**

Nelianne J. Verkaik  
D. Tien Nguyen  
Corné P. de Vogel  
Henriëtte A. Mol  
Henri A. Verbrugh  
Vincent W.V. Jaddoe  
Albert Hofman  
Willem J.B. van Wamel  
Bernadette G. van den Hoogen  
Ruvalic M.G.B. Buijs-Offerman  
Martin Ludlow  
Lot de Witte  
Albert D.M.E. Osterhaus  
Alex van Belkum  
Rik L. de Swart

## Chapter 7

### Abstract

It remains largely unknown which factors determine the clinical outcome of human metapneumovirus (HMPV) infections. The aim of the present study was to analyze whether exposure to bacterial pathogens can influence HMPV infections. From 57 children, serum samples and colonization data for *Haemophilus influenzae*, *Moraxella catarrhalis*, *Staphylococcus aureus* and *Streptococcus pneumoniae* were collected at 1.5, 6, 14 and 24 months of age. Seroconversion rates to HMPV were determined and related to bacterial carriage. Frequent nasopharyngeal carriage ( $\geq 2$  times in the first two years of life) of *S. pneumoniae*, but not of the other three pathogens, was associated with increased seroconversion

rates of infants to HMPV at the age of two (frequently vs. less exposed, 93% vs. 59%;  $p < 0.05$ ). Subsequently, the susceptibility of well-differentiated normal human bronchial epithelial cells (wd-NHBE) pre-incubated with bacterial pathogens to *in vitro* HMPV infection was evaluated. Pre-incubation of wd-NHBE with *S. pneumoniae* resulted in increased susceptibility to infection with HMPV-enhanced green fluorescent protein (EGFP), as determined by enumeration of EGFP<sup>+</sup> cells. This was not the case for cells pre-incubated with *H. influenzae*, *M. catarrhalis*, and *S. aureus*. We conclude that exposure to *S. pneumoniae* can modulate HMPV infection.

## Introduction

Acute respiratory tract infections (RTI) caused by bacterial or viral infections are responsible for considerable morbidity. Human metapneumovirus (HMPV), a member of the family *Paramyxoviridae*, is an important viral cause of RTI [59]. HMPV causes worldwide seasonal outbreaks of respiratory tract infections, in moderate climate zones predominantly during the winter season. The main risk groups for development of severe disease after HMPV infection are young infants, individuals with underlying disease and the elderly [63]. In patients with severe disease the main clinical diagnoses are bronchiolitis and pneumonia, occasionally leading to death [347].

In young infants, HMPV infection appears to be ubiquitous, as virtually all children are seropositive by the age of 5. Estimates of the percentage of acute pediatric lower RTI associated with HMPV range from 5% to 25% [63]. However, it remains largely unknown which factors determine the clinical outcome of HMPV infections. It has been speculated that disease severity could be enhanced by bacterial super-infections. Indeed, bacterial pathogens such as *Streptococcus pneumoniae* can often be detected in patients with HMPV-associated severe disease [81]. In addition, the incidence of invasive pneumococcal disease in children is associated with the seasonality of respiratory virus infections [244]. Furthermore, introduction of a multivalent pneumococcal conjugate vaccine resulted in reduction of pneumonias associated with respiratory virus infections [80]. In mice, HMPV infection was shown to influence subsequent super-infection with *S. pneumoniae* [348]. The aim of the present study was to analyze whether exposure to respiratory bacteria can influence HMPV infections.

## Materials & Methods

### Patients and samples

The study population consisted of 57 healthy children of the Generation R Focus Study [349]. Enrolled mothers were residents in the study area at their delivery date, which had to be between April 2002 and January 2006. Selection of eligible children for the present study was performed on basis of availability of adequate quantities of both nasal swab samples for bacterial culture and serial serum samples for assessment of HMPV seroconversion. Samples were collected after written informed consent from parents or guardians. The study was carried out in accordance with human experimentation guidelines in The Netherlands, and approved by the medical ethical committee of the Erasmus MC.

For all 57 children, 3 or 4 serial serum samples had been collected over a period of 2 years: 54 (95%) cord blood serum samples and 32 (56%), 46 (81%) and 45 (79%) serum samples collected at the ages of 6, 14 and 24 months of age, respectively. A nasopharyngeal swab was obtained for cultivation of *Haemophilus influenzae*, *Moraxella catarrhalis*, and *S. pneumoniae* and a nasal swab was obtained for cultivation of *Staphylococcus aureus*. Bacterial colonization data were collected at 1.5, 6, 14 and 24 months of age for 40 (70%), 49 (86%), 50 (88%) and 48 (84%) children, respectively. Children were classified as 'frequently exposed' if 2 or more swab cultures were positive for one of the bacterial species in the first 2 years of life. When a culture time-point was missing, this was considered negative. None of the patients had used antibiotics in the 48h before swab. Microbiological analyses were performed as described previously [350]. All children were fully vaccinated according to the Dutch National Immunization Program, including a vaccination with measles-mumps-rubella (MMR) around the age of 14 months. At the time of serum collection, vaccination

## Chapter 7

to *S. pneumoniae* was not part of the National Immunization Program.

### Serology

Serum IgG levels specific for HMPV and measles virus (MV) were quantified using ELISA as described previously [351]. Briefly, 96-wells plates were coated with inactivated MV or the recombinant fusion protein of HMPV. Serum samples were tested in duplicate in a 1:300 dilution; results are shown as mean OD-values after subtraction of background values. A greater than 2-fold increase in OD<sub>450</sub> resulting in a value above 0.5 was defined as seroconversion.

### Human bronchial epithelial cells

Normal human bronchial epithelial cells (NHBE) were obtained from Clonetics and used at passage 3-4. Undifferentiated NHBE cells were grown on 30 µg/ml type I collagen- and 10 µg/ml fibronectin-coated 75 cm<sup>2</sup>-flasks in serum-free bronchial epithelial cell basal medium supplemented with BEBMSingleQuots (Clonetics). At 60-80% confluency, cells were trypsinized and seeded at a cell density of  $1 \times 10^4$  viable cells onto type I collagen- and fibronectin-coated 6.5 mm transwell inserts with 0.4 µm pore size (Corning) in a 50:50 mixture of complete BEBM and Dulbecco's Modified Eagle Medium supplemented with 15 ng/ml retinoic acid. Medium was refreshed every other day until cells reached confluency, then an air-liquid interface (ALI) was created by removing medium from the apical side to promote mucociliary differentiation. Medium was refreshed basolaterally and the apical side was washed with Dulbecco's phosphate buffered saline (DPBS, Lonza) at 37°C every other day. Well-differentiated (wd-) NHBE cells were used for HMPV infection 21 days after ALI, at which stage beating cilia and mucus production were clearly detectable.

*H. influenzae* (ATCC 49247), *M. catarrhalis* (ATCC 25240), *S. aureus* (ATCC 25923), and *S. pneumoniae* (ATCC 49619) were grown twice to log phase in 2 consecutive days on blood agar plates (*H. influenzae* on chocolate plates). Prior to assays, bacteria were washed 2 times in antibiotics-free medium. Bacterial numbers were determined by optical density at 600 nm. Recombinant HMPV encoding enhanced green fluorescent protein (EGFP) isolate NL/1/00, further referred to as HMPV-EGFP, was grown as described previously [280] and had a titer of  $6.3 \times 10^6$  TCID<sub>50</sub>/ml. A recombinant HMPV strain encoding EGFP was used to enable assessment of numbers of infected cells in real-time (i.e. without fixation and immunofluorescent staining).

wd-NHBE cells were washed with DPBS preceding incubation with 50 µl of one of the four different species of bacteria ( $1.5 \times 10^6$  bacteria/ml) for 1 hr. After incubation with bacteria, HMPV-EGFP was added (multiplicity of infection [MOI] ~10, based on an estimated number of 25,000 wd-NHBE cells exposed to the apical surface). Finally, after 1 hr incubation with virus, cells were washed twice with DPBS. EGFP<sup>+</sup> cells were counted visually at 24 and 48 hrs post-infection (h.p.i.). This experiment was performed at least 3 times using quadruple measurements for each condition.

### Statistical analysis

Statistical analyses were performed with SPSS version 15.0. The Fisher's exact test was used for dichotomous outcomes. Mann-Whitney *U* tests were used to compare differences between mock-treated and *S. pneumoniae*-exposed wd-NHBE cells.  $p \leq 0.05$  was considered statistically significant.

## Results

### Dynamics of IgG antibody levels

Seroconversion to HMPV and MV was measured in healthy children during the first



## S. pneumoniae Exposure modulates HMPV Infection

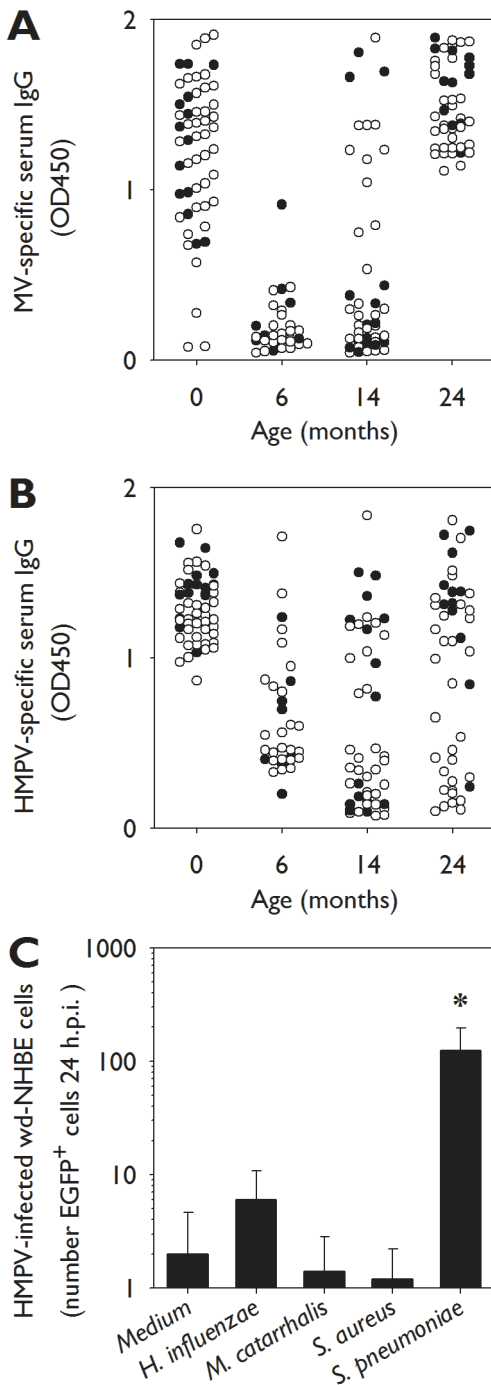


**Figure 1.** A, B) Measles virus (MV)- or human metapneumovirus (HMPV)-specific IgG levels in sera of healthy infants collected during the first 2 years of life. Black symbols represent *S. pneumoniae* frequently-exposed children (at least 2 positive nasal swabs during the 2 year study period), white symbols represent infants less exposed to *S. pneumoniae*. C) Well-differentiated normal human bronchial epithelial (NHBE) cells were incubated with *H. influenzae*, *M. catarrhalis*, *S. aureus*, or *S. pneumoniae* (or medium as a control) and subsequently infected with recombinant HMPV encoding enhanced GFP. Data are plotted as means  $\pm$  standard deviation of quadruplicate cultures. The experiment was repeated three times, in all cases resulting in significant enhancement of HMPV-EGFP infection of wd-NHBE cells pre-incubated with *S. pneumoniae* but not in those pre-incubated with any of the other bacterial species. h.p.i. = hrs post infection. \*  $p \leq 0.05$

2 years of life. In cord blood samples, high maternal antibody levels specific for both viruses could be detected, which gradually declined during the first 6 months of life as expected (Figure 1A, B). All children were vaccinated with a measles-containing vaccine around the age of 14 months, which resulted in seroconversion in all infants at 24 months of age (Figure 1A). This indicated that all children were immune-competent. At the age of 14 months 18/46 (39%) and at 24 months 29/45 (64%) of the infants had seroconverted to HMPV (Figure 1B).

### Relation between bacterial colonization and HMPV serology

HMPV seroconversion levels in children frequently exposed to one of the bacterial species (swab culture 2-4 times positive) were compared to those in less frequently exposed children (swab culture 0-1 time positive). Of the total number of children ( $n=57$ ), we only had combined seroconversion bacterial exposure data available for 52 children, and thus we limited our statistical analysis to this group. There was no significant association

**Table 1. Association between frequency of bacterial exposure and HMPV seroconversion during early life.**

Bacterial pathogen	Frequent exposure <sup>a</sup>	HMPV seroconversion	
		No: n = 16 (31%)	Yes: n = 36 (69%)
<i>H. influenzae</i>	No: n = 42 (81%)	14 (33%) <sup>b</sup>	28 (67%)
	Yes: n = 10 (19%)	2 (20%)	8 (80%)
<i>M. catarrhalis</i>	No: n = 41 (79%)	13 (32%)	28 (68%)
	Yes: n = 11 (21%)	3 (27%)	8 (73%)
<i>S. aureus</i>	No: n = 45 (87%)	14 (31%)	31 (69%)
	Yes: n = 7 (13%)	2 (29%)	5 (71%)
<i>S. pneumoniae</i>	No: n = 37 (71%)	15 (41%)	22 (59%)
	Yes: n = 15 (29%)	1 (7%)	14 (93%)*

<sup>a</sup> Frequent exposure is defined as at least 2 positive nasal or nasopharyngeal swabs during the 2 year study period.

<sup>b</sup> Data are shown as the number of children, followed by the percentage of either or not frequently exposed children between brackets. \*  $p < 0.05$  (Fisher's exact test).

between HMPV seroconversion and exposure to *H. influenzae*, *M. catarrhalis*, or *S. aureus* (Table 1,  $p > 0.05$ ). However, 14 out of 15 (93%) children frequently exposed to *S. pneumoniae* had seroconverted to HMPV at 24 months, versus 22 of 37 (59%) less exposed children (Table 1,  $p < 0.05$ ). In children who remained seronegative for HMPV during the first 2 years of life, only 1 of 16 (7%) was frequently exposed to *S. pneumoniae*. We conclude that children frequently exposed to *S. pneumoniae* mounted a stronger humoral immune response to the virus.

***S. pneumoniae* enhances HMPV infection of normal human bronchial epithelial cells**

The observations from the cohort study suggest that exposure to *S. pneumoniae* was associated with seroconversion to HMPV, which provided no evidence for a direct interaction between *S. pneumoniae* and HMPV infections. To test the hypothesis that bacterial exposure could enhance susceptibility to HMPV infection, we used NHBE cells differentiated at air-liquid interface. Epithelial

cells pre-incubated with *S. pneumoniae* were significantly more susceptible to infection with HMPV-EGFP than mock-treated cells, as evidenced by the enumeration of EGFP<sup>+</sup> epithelial cells 24 and 48 h.p.i. (Figure 1C,  $p < 0.05$ ; data shown for 24 h.p.i.). This was not the case for cells pre-incubated with *H. influenzae*, *M. catarrhalis* or *S. aureus* (Figure 1C,  $p > 0.05$ ; data shown for 24 h.p.i.).

**Discussion**

Interactions between viral and bacterial disease are usually interpreted as virus infections predisposing for severe bacterial infections [76,348]. Different mechanisms have been proposed, including virus-induced damage to respiratory cells predisposing to opportunistic bacterial infection, or upregulation of bacterial adhesion molecules by viral infection [242,245,246]. The aim of the present study was to analyze whether bacterial exposure can influence susceptibility to HMPV infection. First, we demonstrated for 57 healthy children that they were immune-competent; indeed all children had seroconverted to MV at the age

## ***S. pneumoniae* Exposure modulates HMPV Infection**

of 24 months, approximately half a year after MMR vaccination. Subsequently, we screened the colonization state of these 57 children for 4 common respiratory bacterial species (*H. influenzae*, *M. catarrhalis*, *S. aureus* and *S. pneumoniae*) in relation to seroconversion to HMPV during the first 2 years of life. Whereas no relationship was detected between exposure to *H. influenzae*, *M. catarrhalis* or *S. aureus* and HMPV seroconversion, *S. pneumoniae* exposure was significantly associated with increased seroconversion levels to HMPV. These increased HMPV seroconversion levels could be due to increased susceptibility to HMPV infection, increased viral replication or virus spread, or enhanced immune responses to infection.

Differences in bacterial exposure and HMPV seroconversion could also be related to a common external factor, e.g. attendance of a daycare center. However, in that case we would expect that the carrier state of *H. influenzae*, *M. catarrhalis*, *S. aureus*, and *S. pneumoniae* would also be affected. On the basis of the serology data we concluded that either HMPV infection leads to more frequent *S. pneumoniae* carriage or exposure to *S. pneumoniae* increases the susceptibility to HMPV infections.

To test our hypothesis that bacterial exposure could increase the susceptibility to HMPV infection, we used wd-NHBE cells cultured on air-liquid interface. The cells clearly showed beating cilia and mucus production, and may therefore be considered the best possible *in vitro* mimic of the target cells of HMPV infection *in vivo*. Surprisingly, apical infection of wd-NHBE cells with HMPV-EGFP at an estimated MOI of 10 resulted in a low frequency (<1%) of EGFP-expressing cells one to two days after infection. Apparently, apical HMPV infection of wd-NHBE cells is a relatively inefficient process. However, pre-incubation of the wd-NHBE cells with *S.*

*pneumoniae* resulted in increased susceptibility to HMPV infection as compared to mock controls, as evidenced by more than ten times higher numbers of infected cells (Figure 1C).

Several mechanisms could contribute to the observed increased seroconversion levels in children, or the increased numbers of *in vitro* infected wd-NHBE cells, after exposure to *S. pneumoniae*. Pneumococcal virulence and immune evasive factors, including capsule or pneumolysin, may facilitate HMPV infection in multiple ways. First, these factors may penetrate the mucus layer and inhibit ciliary beating of respiratory epithelial cells [352]. This could expose susceptible human epithelial cells resulting in enhancement of HMPV infection or spread. In addition, HMPV infection may be facilitated by influx or activation of immune cells (neutrophils, lymphocytes or dendritic cells) residing in or associated with the respiratory epithelium [352]. Moreover, bacterial factors stimulating TLR2 and TLR4 responses may provoke an enhanced immune response following HMPV infection. Furthermore, lipopeptides in the cell wall may lead to enhanced viral binding to target cells [284], facilitating HMPV infection and spread. In addition, pneumococcal immune evasive factors counteract host innate immune responses, which may also facilitate HMPV infection.

In conclusion, our combined *in vivo* and *in vitro* data suggest a specific interaction between *S. pneumoniae* and HMPV infection.

### **Acknowledgements**

The Generation R Study is conducted by the Erasmus MC, Rotterdam, in close collaboration with the School of Law and Faculty of Social Sciences of the Erasmus University Rotterdam, the Municipal Health Service Rotterdam area, the Rotterdam Homecare Foundation and the Stichting Trombosedienst & Artsenlaboratorium Rijnmond (STAR),

Rotterdam. We gratefully acknowledge the contribution of general practitioners, hospitals, midwives and pharmacies in Rotterdam. We thank Ad Luijendijk for technical supervision and Rogier Louwen for culturing bacteria at the Department of Medical Microbiology and Infectious Diseases, Erasmus MC, Rotterdam.





## Chapter 8

***Streptococcus  
pneumoniae serotype 19F  
enhances human respiratory  
syncytial virus infection  
in vitro and in vivo***

D.Tien Nguyen  
Rogier Louwen  
Karin Elberse  
Geert van Amerongen  
Selma Yüksel  
Ad Luijendijk  
Albert D.M.E. Osterhaus  
W. Paul Duprex  
Rik L. de Swart

*Submitted*

## Chapter 8

### Abstract

Human respiratory syncytial virus (HRSV) and *Streptococcus pneumoniae* are important causative agents of respiratory tract infections. Both pathogens are associated with seasonal disease outbreaks in the pediatric population, and can often be detected simultaneously in infants hospitalized with bronchiolitis or pneumonia. It has been described that respiratory virus infections may predispose for bacterial superinfections, resulting in severe disease. However, studies on the influence of bacterial colonization of the upper respiratory tract on the pathogenesis of subsequent respiratory virus infections are scarce. Here, we have investigated whether pneumococcal colonization enhances subsequent HRSV infection. We used a newly generated recombinant subgroup B HRSV strain that expresses enhanced green fluorescent protein and pneumococcal isolates obtained from healthy children in disease-relevant *in vitro* and *in vivo* model systems. Three pneumococcal serotypes specifically enhanced *in vitro* HRSV infection of primary well-differentiated normal human bronchial epithelial cells grown at air-liquid interphase, whereas two

other serotypes did not. Since previous studies reported that bacterial neuraminidase enhanced HRSV infection *in vitro*, we measured pneumococcal neuraminidase activity in these cultures but found no correlation with the observed infection enhancement in our model. Subsequently, a selection of pneumococcal serotypes was used to induce nasal colonization of cotton rats, the best available small animal model for HRSV. Intranasal HRSV infection three days later resulted in serotype-specific enhancement of HRSV replication *in vivo*. *S. pneumoniae* serotype 19F enhanced HRSV infection both *in vitro* and *in vivo*, and was also associated with enhanced syncytium formation *in vivo*. However, neither pneumococci nor HRSV were found to spread from the upper to the lower respiratory tract, and neither pathogen was transmitted to naive cagemates by direct contact. These results demonstrate for the first time that pneumococcal colonization can enhance subsequent HRSV infection, and provide tools for additional mechanistic and intervention studies.



### Introduction

Respiratory tract infections cause a significant global burden of morbidity and mortality in all age groups. In 2011 the World Health Organization estimated 1.3 million global deaths were due to acute respiratory infections, of which the majority occurred in developing countries in children under five years [353]. Of all respiratory pathogens *S. pneumoniae* or pneumococcus is the leading cause of death, accounting for more than 30% of the cases [353]. Many healthy children and adults carry pneumococci in their upper respiratory tract (URT) and *S. pneumoniae* colonizes the nasopharynx of up to 45% of children under three years and up to 20% of adults [73]. Colonization is a prerequisite for subsequent spread, which may result in respiratory tract infection (sinusitis, otitis media, pneumonia), meningitis or sepsis [354]. More than 90 *S. pneumoniae* serotypes have been identified, and pneumococcal vaccines have been developed containing antigens of up to 23 of the most important serotypes associated with human disease [74].

Human respiratory syncytial virus (HRSV) is a leading viral cause of respiratory tract infection in young infants [57]. HRSV is a member of the family *Paramyxoviridae*, a group of enveloped viruses with a single stranded RNA genome of negative polarity [17]. This family includes other important human pathogens such as human metapneumovirus (HMPV) and measles virus (MV). Despite the huge global burden of HRSV disease, no licensed vaccines are available [168]. Monoclonal antibody treatment (Palivizumab) is efficacious in high-risk infants [194], but the cost-effectiveness of this approach is under debate [184].

*S. pneumoniae* and HRSV occupy the same niche: pneumococcus colonizes the nasopharynx, where HRSV infects ciliated

epithelial cells. In addition, peak prevalence of disease burden for both occurs in winter [355,356], transmission occurs via direct contact and therefore crowding (e.g. in day care centers) contributes to spread of both pneumococci and HRSV [309,357,358]. Furthermore, risk factors for development of severe disease are highly similar for both pathogens, including premature birth, congenital heart disease, chronic lung disease and high age [309].

Several studies have described interactions between *S. pneumoniae* and HRSV [236,237,359]. Following the discovery of HRSV in 1956, it was described that pneumococci could be cultured from an HRSV-infected infant [11]. *In vitro* experiments showed that *S. pneumoniae* adheres better to HRSV-infected human epithelial cells [76] and conversely, HRSV binds directly to pneumococci [77,78]. In addition, HRSV infected mice showed significantly higher levels of pneumococcal bacteraemia than controls [78]. Collectively these data suggest that HRSV infection might predispose individuals to bacterial superinfection, potentially leading to dramatic increase of mortality.

It has also been suggested that bacterial colonization may enhance respiratory virus infections. A potential mechanism was shown previously by synthetic bacterial lipopeptide-mediated enhancement of HRSV infection [284]. Pre-incubation of well-differentiated normal human bronchial epithelial (wv-NHBE) cells with *S. pneumoniae* enhanced HMPV infection [307]. In addition, frequent nasopharyngeal carriage of pneumococci in children under two years was associated with increased seroconversion rates to HMPV [307]. Moreover, in a clinical trial pneumococcal vaccination reduced the incidence of hospitalization for pneumonia

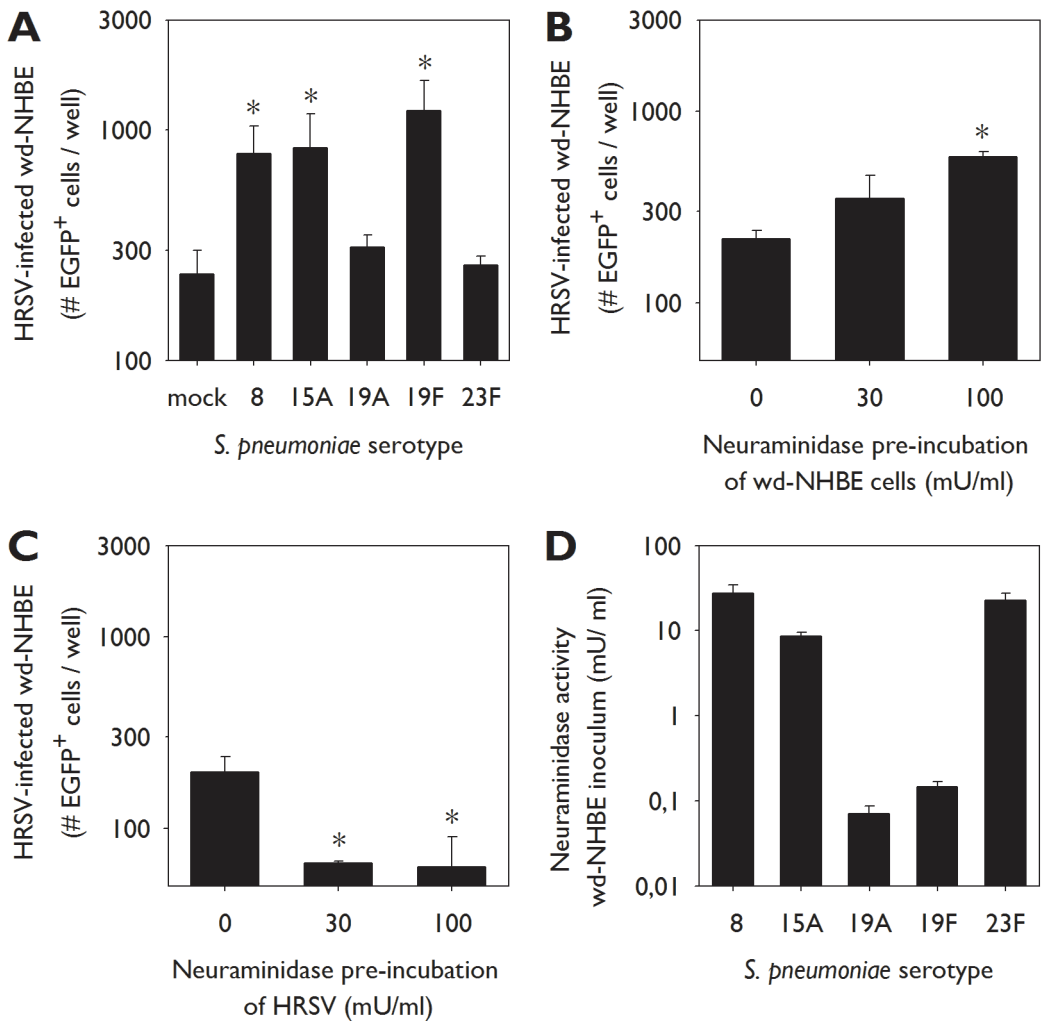


**Figure 1.** Enhancement of HRSV infection mediated by specific *S. pneumoniae* serotypes in wd-NHBE cells. A) wd-NHBE cells were inoculated with HRSV and one *S. pneumoniae* serotype with mock control. Serotype 8, 15A and 19F enhanced HRSV infection as evidenced by quantification of EGFP<sup>+</sup> cells 2 d.p.i. Data are represented as mean  $\pm$  SD. \*  $p \leq 0.05$ ; 2-tailed Mann-Whitney U test. B) wd-NHBE cells were treated with neuraminidase from *Vibrio cholerae*, followed by HRSV infection after washing. Two dpi the numbers of HRSV-infected cells were enumerated. Data are presented as means  $\pm$  SD. \*  $p \leq 0.05$ ; 2-tailed Mann-Whitney U test. C) HRSV was treated with neuraminidase from *Vibrio cholerae* before inoculation of wd-NHBE cells. Treated virus was incubated for 1 hr, followed by washing. HRSV-infected cells were enumerated 2 dpi. Data are presented as means  $\pm$  SD. \*  $p \leq 0.05$ ; 2-tailed Mann-Whitney U test. D) Apical inocula of the wd-NHBE experiment shown in Figure 1A were tested for neuraminidase activity using the NA-Star<sup>TM</sup> Influenza Neuraminidase Inhibitor Resistance Detection Kit (Applied Biosystems). Numbers correspond to *Vibrio cholerae*  $\mu$ U neuraminidase activity. Data are presented as means  $\pm$  SD.

associated with HRSV by 32% [80]. These observations indicate that pneumococcus and HRSV potentially have bidirectional interactions.

Therefore the aim of the current study was to assess the influence of pneumococcal colonization on subsequent HRSV infection using *in vitro* and *in vivo* models. We used wd-NHBE cells for *in vitro* studies and cotton rats (*Sigmodon Hispidus*) for *in vivo* studies, as the most susceptible and disease-relevant HRSV model systems currently available. *S. pneumoniae* isolates had previously been obtained from nasopharyngeal brushes of healthy infants. One additional *S. pneumoniae* strain was obtained from ATCC. For HRSV infections we used a recently generated recombinant (r) wild-type subgroup B HRSV strain expressing enhanced fluorescent protein (EGFP; rHRSV<sup>B05</sup>EGFP(5)) [360]. We demonstrate that *S. pneumoniae* serotype 19F significantly and reproducibly enhanced HRSV infection *in vitro* and *in vivo*.

### Results

#### **Specific *S. pneumoniae* serotypes enhance HRSV infection *in vitro***

We used wd-NHBE cells grown on air-liquid interphase expressing beating cilia and goblet cells as the best available *in vitro* model for HRSV infection. Also, we used rHRSV<sup>B05</sup>EGFP(5), which is the first HRSV strain displaying the full phenotype and genetic background of currently circulating wild-type viruses. Along these primary cells and recombinant virus low passage pneumococci were used to mimic the complex interplay between pneumococcus and HRSV. Initially the apical surface of wd-NHBE was incubated with *S. pneumoniae*, but epithelia cultured without antibiotics rapidly deteriorated and died. Therefore, we used an alternative approach, in which wd-NHBE cells were incubated with a mixture of streptococci and HRSV in the absence of antibiotics. Virus

and bacteria were removed after 2 hrs, and 4 hrs later the apical surface was washed with PBS supplemented with antibiotics and the basolateral medium was replaced by medium with antibiotics ensuring survival of the cultures. Co-administration of HRSV with three pneumococcus serotypes (8, 15A and 19F) resulted in significantly increased numbers of HRSV-infected cells ( $p < 0.05$ ), but two other serotypes (19A and 23F) did not modulate HRSV infection (Figure 1A).

#### **A potential role of bacterial neuraminidase?**

It was previously described that neuraminidase treatment of respiratory syncytial virus-infected cells enhanced cell-cell fusion and infection in an epithelial cell line [361]. Thus, neuraminidase could also influence fusion between the viral and host cell membranes. Treatment of wd-NHBE cells with commercially available bacterial neuraminidase of *Vibrio cholerae* resulted in a dose-dependent enhancement of HRSV infection (Figure 1B). However, in contrast to the observations published by Barretto et al., we only observed enhancement of infection when polarized cells were treated, and inhibition when the virus was pre-treated with neuraminidase (Figure 1C). To assess the potential role of bacterial neuraminidases in the observed enhancement of HRSV, we measured the neuraminidase activity of the virus / bacterium mixture after removal from the apical surface of the wd-NHBE cells shown in Figure 1A. However, neuraminidase activity did not correlate with the observed pattern of enhancement of HRSV infection (Figure 1D).

#### ***Streptococcus pneumoniae* colonization can enhance HRSV infection *in vivo***

In order to extrapolate our *in vitro* results a new *in vivo* pneumococcal colonization & HRSV infection model was developed. We established this model using four *S. pneumoniae* serotypes and the new recombinant HRSV (Figure 2A).

## Chapter 8

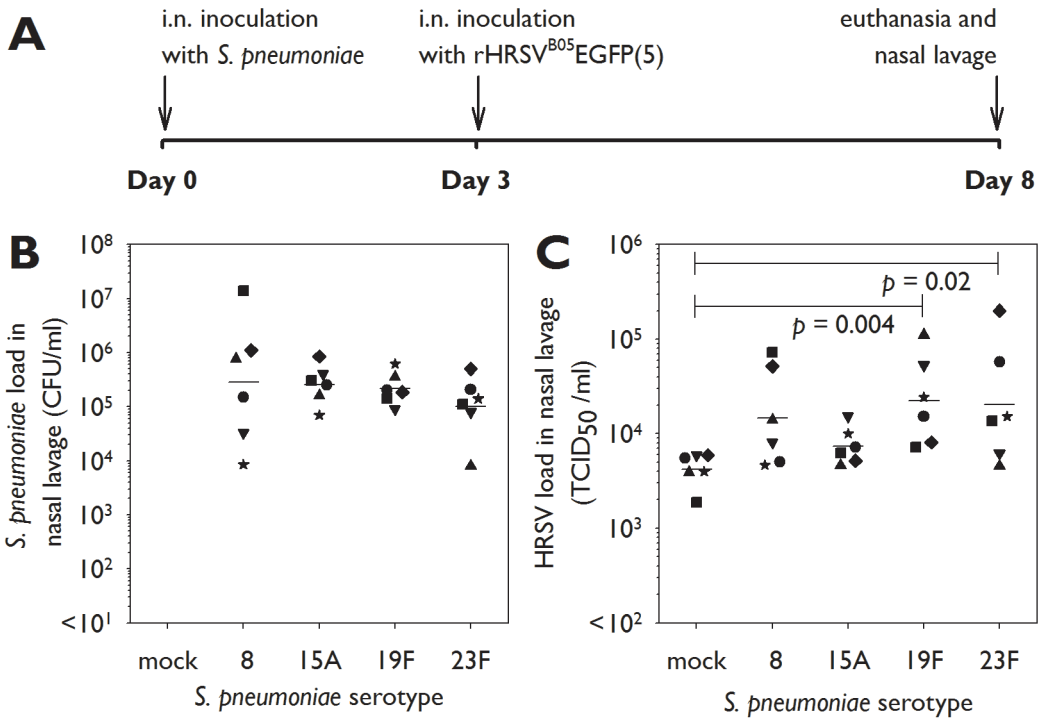


**Figure 2.** Bacterial and virus titers of HRSV infected *S. pneumoniae* colonized cotton rats. A) Experimental design. Pneumococcal carriage was induced by i.n. inoculation of cotton rats with  $5 \times 10^5$  CFU *S. pneumoniae* in  $10 \mu\text{l}$  at day 0. Three days later animals were infected with  $1 \times 10^4$  TCID<sub>50</sub> rHRSV<sup>B05</sup>EGFP(5) in PBS ( $10 \mu\text{l}$ ). At day 8 animals were euthanized. B) Bacterial titers eight days after induction of pneumococcal carriage. The geometric mean titer was about  $2 \times 10^5$  CFU/ml for the different serotypes. Data symbols represent individual animals, bars represent geometric mean titers (GMT) per group. \*  $p \leq 0.05$ ; 2-tailed Mann-Whitney U test. C) Virus titers five days after HRSV infection. Significantly higher virus load were detected in groups with nasal carriage of *S. pneumoniae* serotype 19F and 23F compared to mock-treated. \*  $p \leq 0.05$ ; 2-tailed Mann-Whitney U test.

Animals ( $n=6/\text{group}$ ) were intra-nasally (i.n.) inoculated with  $5 \times 10^5$  colony forming units (CFU) of pneumococci or with PBS as mock control. An inoculum volume of  $10 \mu\text{l}$  was used to prevent primary inoculation of the lower respiratory tract (LRT) [362]. Animals were infected 3 days post-colonization with  $1 \times 10^4$  50% tissue culture infectious doses (TCID<sub>50</sub>) of rHRSV<sup>B05</sup>EGFP(5) in PBS ( $10 \mu\text{l}$ ). No samples were collected until euthanasia at day 8 (i.e. day 5 after HRSV infection) to prevent any mechanical/physical interference with bacterial colonization or viral infection and spread. Nasopharyngeal lavages and lung

homogenates were collected post-mortem for isolation of pneumococci and HRSV. Nasal septum, conchae and agarose-inflated lungs were collected for immediate monitoring of EGFP<sup>+</sup> cells [92,306].

Bacteria were re-isolated from nasopharyngeal lavage from all animals i.n. inoculated with *S. pneumoniae* (Figure 2B). The geometric mean titers were about  $2 \times 10^5$  CFU/ml, with the highest variation for serotype 8. Bacteria could not be cultured from homogenized lungs of any of the animals showing the low volume

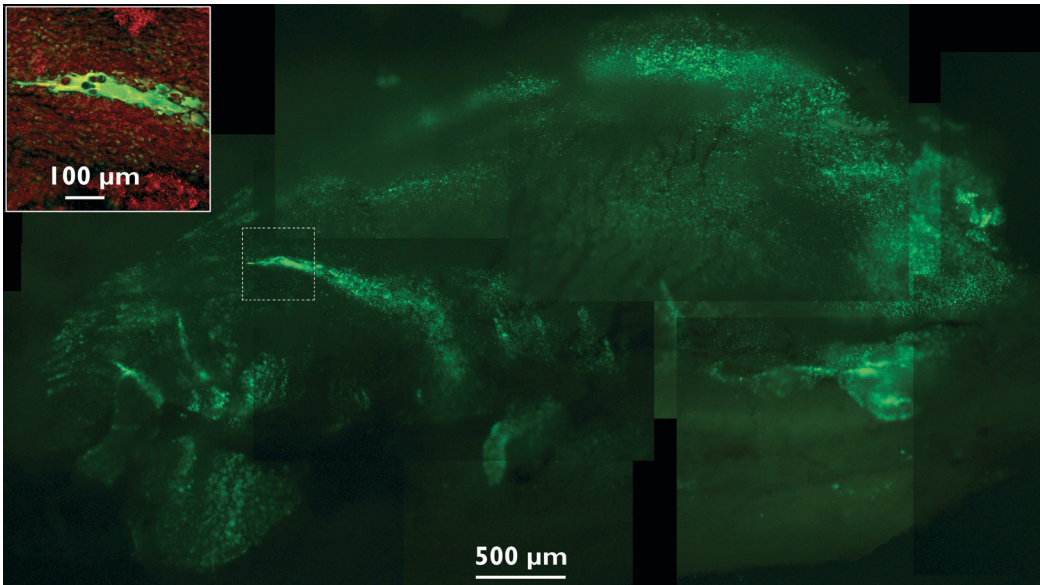


**Figure 3.** HRSV infection in nasal septum of a *S. pneumoniae* colonized cotton rat. Composite microscopic UV images of the complete nasal septum of a cotton rat 5 d.p.i. showing a representative syncytium in the middle (scale bar represents 500  $\mu\text{m}$ ). The inset is an magnification confocal tile scan image of nasal septum with nuclei stained with TO-PRO-3 (red; scale bar represents 100  $\mu\text{m}$ )

inoculum targeted the URT. At the same time point, rHRSV<sup>B05</sup>EGFP(5) was isolated from nasopharyngeal lavages of all animals (Figure 2C). The geometric mean titers were  $4.2 \times 10^3$ ,  $1.5 \times 10^4$ ,  $7.4 \times 10^3$ ,  $2.2 \times 10^4$  and  $2.0 \times 10^4$  TCID<sub>50</sub>/ml for the groups receiving mock or serotypes 8, 15A, 19F and 23F, respectively. Significantly higher virus loads were detected in groups inoculated with serotypes 19F and 23F ( $p < 0.05$ ) compared to the mock infection. For the other two serotypes there appeared to be a trend towards higher HRSV loads, but these did not reach statistical significance. Furthermore, the variation in virus loads within the colonized groups appeared to be higher.

Upon necropsy, EGFP<sup>+</sup> cells were detected in the nasal septum and conchae of all animals. No differences in numbers of EGFP<sup>+</sup> cells were observed between the different groups, although absolute enumeration of these cells was impossible. Syncytia were observed in the

nasal septum and conchae in 5 out of 6 animals of the group inoculated with *S. pneumoniae* serotype 19F as compared to 1 out of 6 animals of the mock group ( $p < 0.05$ , Figure 3). In the groups that had received *S. pneumoniae* serotypes 8, 15A or 23F these were seen in 1, 1 and 3 animals, respectively (not significantly different from the mock control). A small number of EGFP<sup>+</sup> cells was found in the lungs in two animals that had received *S. pneumoniae* 19F or 23F (data not shown).

### Cotton rat transmission study

*S. pneumoniae* serotype 19F had enhanced HRSV infection both *in vitro* and *in vivo*. We hypothesized that higher virus loads could facilitate transmission of virus or bacteria to contact animals. To test this hypothesis, and confirm the pneumococcal enhancement of HRSV infection *in vivo*, we designed a transmission experiment in cotton rats (Figure 4A). Two groups of index animals ( $n=6$ ) were mock-treated or i.n. inoculated

# Chapter 8

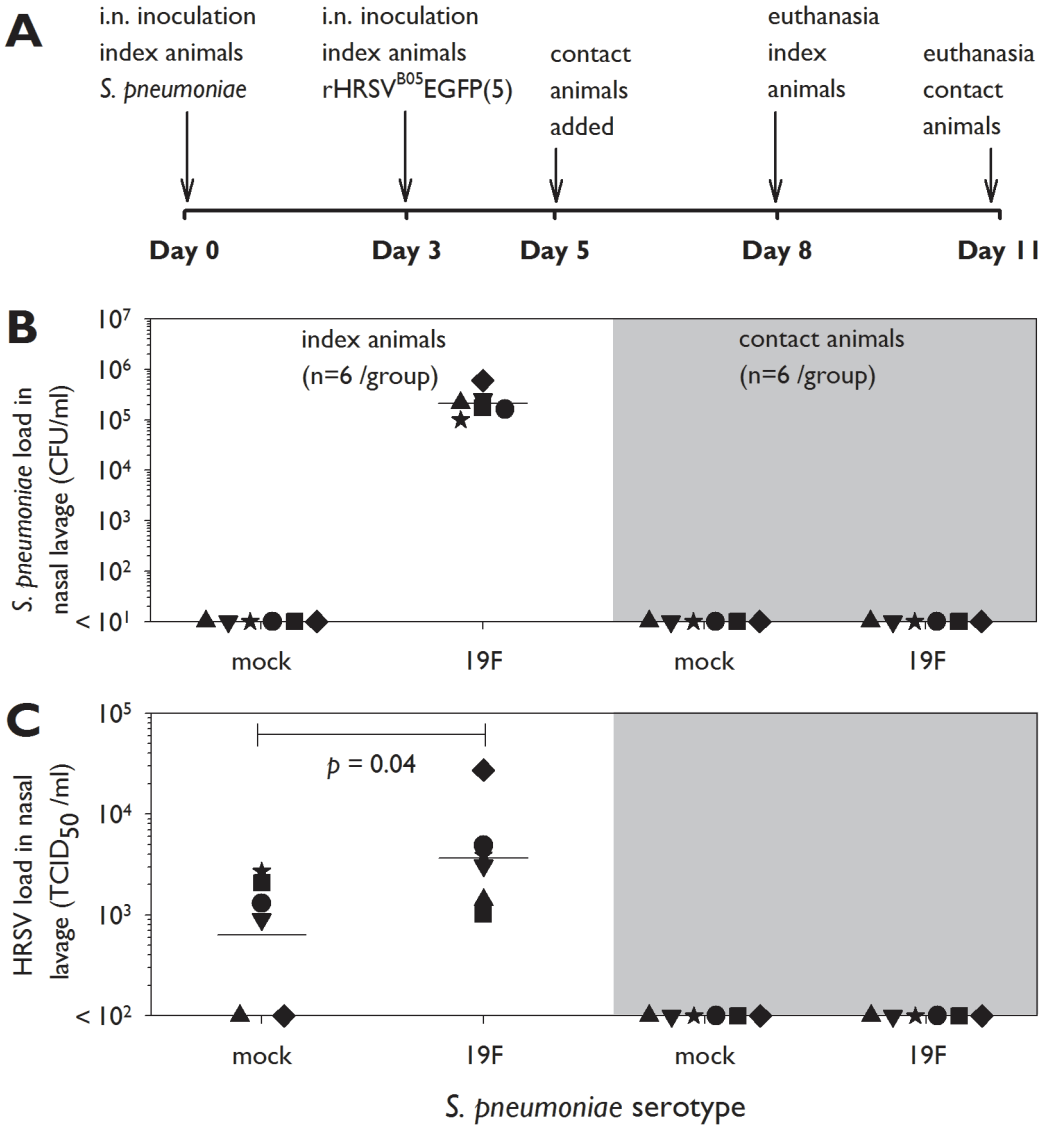


**Figure 4.** In vivo transmission study HRSV infection in *S. pneumoniae* colonized cotton rats. A) schematic representation of the time course of the experiment. Two days after HRSV infection pneumococcus colonized and HRSV naive contact animals were placed to the matching index animals. Index and contact animals were euthanized at day 8 or 11, respectively. B) Bacterial titer of index and contact animals. The geometric mean titer (GMT) was about  $2 \times 10^5$  CFU/ml for the index group, but no bacteria were isolated in the contact animals. Data symbol represents one animal, bars represent GMT. C) Virus titers of index and contact animals. Significant higher virus load were isolated in the index group with serotype 19F compared to mock-treated. In both contact groups no virus could be isolated out of the nose and lungs. \*  $p \leq 0.05$ ; 2-tailed Mann-Whitney U test.

## *S. pneumoniae* enhances HRSV Infection

with *S. pneumoniae* serotype 19F, with each animal being housed solitarily. Three days later all index animals were infected i.n. with rHRSV<sup>B05</sup>EGFP(5). At day 5 naive contact animals were added to each cage permitting direct physical contact between the index and contact animals for 72 hrs, including the anticipated peak of HRSV replication in the index animals. Index and contact animals were euthanized at days 8 and 11, respectively (Figure 4A). Bacterial and viral loads were determined in nasopharyngeal lavages and lung homogenates. In the colonized index group *S. pneumoniae* was cultured from the nasopharyngeal lavage of all animals, with a geometric mean titer of  $2.1 \times 10^5$  CFU/ml (Figure 4B). In addition, significantly higher virus loads were detected in the colonized index animals as compared to the mock control index animals (Figure 4C;  $p < 0.05$ ). On day 11 all contact animals were euthanized, and bacterial culture and HRSV re-isolation procedures were repeated. However, no *S. pneumoniae* or HRSV was detected in either the nose or the lungs of any of these animals (Figure 4C). We conclude that *in vivo* enhancement of HRSV infection by nasal colonization of cotton rats with *S. pneumoniae* serotype 19F proved to be reproducible, but that this did not result in transmission to naive cage mates via direct contact.

### Discussion

We have shown that specific *S. pneumoniae* serotypes enhance HRSV infections both *in vitro* and *in vivo*. In wd-NHBE cells simultaneously inoculated with HRSV and pneumococcus serotype 8, 15A or 19F, but not serotype 19A and 23F, significantly higher numbers of HRSV-infected epithelial cells. In cotton rats intra-nasally colonized with *S. pneumoniae* HRSV replicated to higher titers. However, in this case serotypes 19F and 23F resulted in enhancement of HRSV infection, whereas for serotypes 8 and 15A only a trend towards

higher virus loads was detected. Serotype 19F also promoted syncytium formation in the upper respiratory tract.

Co-infections with respiratory viruses and bacteria have been described, although their number is limited. Two prospective studies showed that 40% of children admitted to the pediatric intensive care unit with severe HRSV disease had a bacterial co-infection in the lower respiratory tract [196,237,363]. Similar observations have been described for influenza virus infections. During the influenza H1N1 pandemic in 1918-1919, an era in which no antibiotics were available, the majority of deaths was caused by *S. pneumoniae* [364,365]. In the most recent influenza virus pandemic starting in 2009 co-infection with *S. pneumoniae* was found to be associated with severe disease [366]. Diavatopoulos *et al.* found that influenza virus infection facilitated *S. pneumoniae* transmission and disease in suckling mice [367]. In addition to *S. pneumoniae*, *Haemophilus influenzae* and *Staphylococcus aureus* were also associated with influenza virus infection [368].

Studies on bacterial colonization modulating virus infections are scarce. Sajjan *et al.* reported that *H. influenzae* can potentiate airway epithelial cell responses to rhinovirus by increasing ICAM-1 and TLR3 expression *in vitro* [369]. However, these authors used an 8 hour apical incubation of wd-NHBE cells, which in our experience can result in a significant reduction in transepithelial electric resistance. Kuss *et al.* studied bacterial and viral interactions in the enteric tract and showed that the intestinal microbiota promoted poliovirus replication and systemic pathogenesis via binding to bacterial lipopolysaccharide [370]. Previously, we reported interactions between *S. pneumoniae* and HMPV infection *in vitro* and *in vivo* [307]. Madhi *et al.* showed in a large randomized clinical trial that pneumococcal conjugated

vaccination reduced HRSV pneumonia in human immunodeficiency virus (HIV)-1-uninfected children [80]. Interestingly, bacteria can also protect from pneumovirus infections. Nasally administered immunobiotics (immunoregulatory probiotic lactic acid bacteria) differentially modulate respiratory antiviral immune responses, thereby inducing protection against pneumonia virus of mice or the closely related HRSV [371,372].

Our *in vitro* co-cultures of *S. pneumoniae* and HRSV in wd-NHBE cells resulted in enhancement of HRSV infection for mediated by *S. pneumoniae* serotypes 8, 15A and 19F, but not 19A and 23F. We considered a potential role of pneumococcal neuraminidases to explain the differences between these serotypes. Barretto *et al.* demonstrated that neuraminidase can enhance HRSV infection [361]. They found that treatment of HRSV with neuraminidases of different bacteria led to enhancement of infection. Neuraminidases enzymatically remove sialic acids, which could result in improved interaction between an HRSV transmembrane glycoprotein and its cellular receptor. We repeated these studies with rHRSV<sup>B05</sup>EGFP(5) in HEp-2 cells, a larynx carcinoma cell line, and confirmed the previously reported findings (data not shown). However, neuraminidase treatment of rHRSV<sup>B05</sup>EGFP(5) resulted in a dose-dependent inhibition of HRSV infection in wd-NHBE cells. In contrast, neuraminidase treatment of wd-NHBE cells resulted in a dose-dependent enhancement of HRSV infection. We speculate that this difference is primarily related to the presence of mucus in wd-NHBE cells. Neuraminidase treatment of the epithelial surface may result in disruption of the mucus layer [373,374], while neuraminidase treatment of the virus may result in surface charge changes that promote HRSV interactions with mucus and inhibit HRSV binding to the target cells.

Pneumococcal carriage may have detrimental

consequences as the bacterium can spread to other parts of the human body. Pneumococcal vaccination has been proven effective in preventing colonization [375]. Current vaccines include up to 23 of the most prevalent and disease-relevant serotypes [375]. In our study we have used serotypes 19A, 19F and 23F which are included in current vaccine formulations, whereas serotypes 8 and 15A are not. As global prevalence of serotypes included in the vaccine diminishes, other serotypes may fill the niche. This phenomenon is also referred to as serotype replacement [376-378].

In order to study the effect of pneumococcal carriage on HRSV infection we set up a new pneumococcal colonization & HRSV infection cotton rat model. To our knowledge this is the first study describing induction of pneumococcal carriage in cotton rats. *S. pneumoniae* are autolytic at the end of the log-phase, which is caused by the major enzyme Lyt A [379,380]. Therefore, demonstration of high pneumococcal loads in nasopharyngeal lavages, but not in lung homogenates, 8 days after *i.n.* inoculation in 100% of the animals supports efficient pneumococcal colonization in the URT. Pneumococcal colonization appeared not to be detrimental to the animals, as no physical or behavioral signs of disease were observed. Body weights were minimally affected: all animals gained weight during the experiment but in the groups colonized with serotypes 8 and 15A there was a trend towards reduced gain in weights (data not shown). However, the differences were not significant and these two serotypes were not associated with significant enhancement of HRSV infection *in vivo*.

Interestingly, HRSV titers of mock-treated animals were quite homogeneous. In contrast, in some of the colonized animals with (enhancing) pneumococcal serotypes HRSV titers were almost 100-fold higher



than those in the mock controls. These animals could potentially be considered as “superspreaders” [381,381]. However, in this cotton rat model no transmission of either HRSV or *S. pneumoniae* could be detected, even when index and contact animals were housed together in the same cage. None of the animals displayed any clinical signs of HRSV upper respiratory tract infection such as rhinorrhea, sneezing, or coughing, reducing the chance of transmission to naive animals. We conclude that this model is not suitable for HRSV transmission studies.

In conclusion, using a new molecular clone of HRSV that mimics current wild-type strains in the genuine target cells (wd-NHBE cells) and a new pneumococcal colonization & HRSV infection animal model we have shown that *S. pneumoniae* modulates HRSV infections.

### Materials & Methods

#### Ethical statement

Animal experiments were conducted in strict accordance with European guidelines (EU directive on animal testing 86/609/EEC) and Dutch legislation (Experiments on Animals Act, 1997). The protocols were approved by the independent animal experimentation ethical review committee DCC in Driebergen, The Netherlands (approval number EMC2974). Animal welfare was monitored daily, and animal handling was performed under light anesthesia using isoflurane.

#### *S. pneumoniae*, HRSV and cell culture conditions

Four low passage clinical isolates of *S. pneumoniae* were obtained from nasopharyngeal swabs of children under two years. Strain 19F was purchased from ATCC (cat. Nr. 49619). Bacteria were serotyped via capsular sequence typing [383]. Live bacterial numbers for each serotype were determined by optical density at 600 nm and CFU counts

obtained from serial dilutions. One day prior to each experiment bacteria were cultured twice at 35°C (5% CO<sub>2</sub> [v/v]) to log phase on trypticase soy agar blood plates with 5% [v/v] sheep blood (TSA plates, BD). The following day, 12 hrs after growth on the second plate bacteria were harvested in 15 ml tubes and OD<sub>600</sub> values were determined. Bacterial suspensions were washed three times with PBS.

Low passage (6 and 7) rHRSV<sup>B05</sup>EGFP(5) had been generated previously [360]. Virus was grown in HEp-2 cells, and purified by a two-step sucrose gradient centrifugation. The final stock contained approximately 25% (w/v) sucrose, and had a titer of  $1.3 \times 10^7$  TCID<sub>50</sub>/ml.

Mycoplasma-free HEp-2 cells (ATCC CCL-23) were grown in DMEM (Lonza) with 10% (v/v) fetal bovine serum (Sigma-Aldrich). Well-differentiated human normal bronchial epithelial cells (wd-NHBE) were grown on air-liquid-interface in filters with 0.4 μm pore size (Corning) as described previously [307]. Importantly, cells were grown in antibiotics-free medium until after pneumococcus and/or virus inoculation. wd-NHBE cells were used 21 days after ALI, at which stage beating cilia and mucus production were clearly detectable.

#### Animals

Four- to five-week-old female cotton rats (*Sigmodon hispidus*) were obtained from a specific pathogen-free breeding colony (Harlan). Two or three animals were housed in individual ventilated cages (IVC) supplemented with a tin can as hiding place (height 107 mm, diameter 72 mm) and paper tissues as cage enrichment and received food and water *ad libitum*. Experiments started after an acclimatization period of 7-10 days.

#### wd-NHBE cells: Co-infection and (pneumococcal) neuraminidase assays

Bacterial suspensions were prepared as described above. Ratios of bacteria to cells and virus to cells were 30:1 and 0.4:1,

respectively, based on an estimated number of 25,000 cells on the apical surface. The mix (50  $\mu$ l) was left onto the apical surface for 2 hrs at 37°C (5% CO<sub>2</sub> [v/v]), followed by aspiration. After 4 hrs the apical surface was washed three times with Dulbecco's PBS at 37°C (100  $\mu$ l) and antibiotics (penicillin [100 U/ml] and streptomycin [100  $\mu$ g/ml]) were added to the basolateral compartment. Two d.p.i. automated whole well scans were made, followed by semi-automated enumeration of EGFP<sup>+</sup> cells (DotCount, MIT, Boston).

To study the effect of neuraminidase the apical surface of wd-NHBE cells were treated with neuraminidase from *Vibrio cholerae* (Sigma-Aldrich #N7885) at two different concentrations (30 or 100 mU/ml) for 1 hr in the incubator. Cells were infected with rHRSV<sup>B05</sup>EGFP(5) (ratio 0.4:1) after washing the apical surface twice with DPBS. After another 4 hrs wd-NHBE cells were washed three times and EGFP<sup>+</sup> cells were enumerated 2 d.p.i.

Apical inocula of the wd-NHBE co-infection experiments were used to quantify pneumococcal neuraminidase activity using the NA-Star™ Influenza Neuraminidase Inhibitor Resistance Detection Kit (Applied Biosystems) according to manufacturer's protocol. *Vibrio Cholerae* neuraminidase was used as positive control and reference. Briefly, inocula were diluted 1:5 with NA-Star Buffer and incubated for 20 min with NA-Star chemiluminescent substrate. Assay plates were placed in a luminometer equipped with an on-board injector (Tecan Infinite M200). Light signal intensities were measured after injection of accelerator solution.

### Infection of colonized animals and *in vivo* transmission study

Three animals were housed together in an IVC. After an acclimatization period of one week, pneumococcal carriage was induced by i.n. inoculation of 5x10<sup>5</sup> CFU in of PBS (10  $\mu$ l). Three days later animals were inoculated

i.n. with 1x10<sup>4</sup> TCID<sub>50</sub> (10  $\mu$ l) and at day eight animals were euthanized by exsanguation. All procedures were performed under 4% (v/v) isoflurane anesthesia. Post-mortem nasopharyngeal lavages and lungs were collected for isolation of pneumococci and HRSV. Post-mortem nasopharyngeal lavages were obtained by flushing with virus transport medium (1 ml) without antibiotics from the proximal trachea towards the nasal cavity. Right lungs were homogenized with a M-tube (GentleMACS, RNA program 0.10.2) in virus transport medium (2 ml) without antibiotics [92] and centrifuged at 400  $\times$  g for 10 min. For determination of bacterial titers *S. pneumoniae* selective blood agar plates were custom made (trypticase soy agar blood plates with 5% (v/v) sheep blood and 5  $\mu$ g/ml gentamycin) [384]. Plates were incubated at 35°C (5% [v/v] CO<sub>2</sub>) and CFU were counted manually the next day. Virus isolation from post-mortem nasopharyngeal lavages was performed as previously described [303,304]. The lower limit of detection of bacteria was 10 CFU/ml and for HRSV detections in nasopharyngeal lavages or lung homogenates were 30 or 10 TCID<sub>50</sub>/ml, respectively. Nasal septum, conchae, one agarose-inflated lung were collected in 2% (w/v) paraformaldehyde for real-time monitoring of EGFP<sup>+</sup> cells [92,306].

### Microscopic detection of fluorescence

Microscopically, EGFP<sup>+</sup> cells were identified by using an inverted fluorescence microscope (Zeiss Axiovert 25) or a confocal laser scanning microscope (Zeiss inverted AxioObserver Z1 equipped with LSM 700 scanning module). Nasal septum used for indirect immunofluorescence staining was transferred to PBS, permeabilized with 0.1% (v/v) Triton-X100 for 30 min and subsequently stained. TO-PRO-3 (Invitrogen) was used to counterstain nuclei (red). All images were generated using Zen 2010 software (Zeiss).

### **Statistical analysis**

All *in vitro* experiments were performed at least three times using triplicate or quadruple measurements. Statistical analyses were performed with SPSS version 20.0. Mann–Whitney *U*-tests were used to compare differences. A two-sided *p*-value  $\leq 0.05$  was considered statistically significant.

### **Acknowledgments**

We thank Liset Dullaart, Alwin de Jong, Anne van der Linden, Gerlinde Pluister, Carla Roodbol, Annemarie van Rossum, Rachel Scheuer, Joyce Verburgh and Rory de Vries for their contributions. This study received financial support from the VIRGO project, an innovative cluster approved by the Netherlands Genomics Initiative and partially funded by the Dutch Government (grant# BSIK03012), and ZonMw (grant# 91208012).



## **Chapter 9**

### **Summarizing Discussion**



## Chapter 9

### Summarizing Discussion

An estimated 6.7% of all global deaths are caused by lower respiratory tract infections (LRTI; <http://www.who.int/>). Most important causes of LRTI in children under five years are *Streptococcus pneumoniae*, *Haemophilus influenzae type b* (Hib), human respiratory syncytial virus (HRSV) and human metapneumovirus (HMPV) [4,58]. An estimated 1.5 million children under five years die annually due to infections with these pathogens. In this thesis I have described studies addressing interactions between bacterial and viral interactions. The effect of different TLR-ligands originating from bacteria on paramyxovirus infections was assessed in **Chapter 2** [284]. This study provided novel insights into interactions of widely used synthetic bacterial lipopeptides and HRSV infection. Results of this study formed the basis of two subsequent study objectives. In the first objective, synthetic infection-enhancing bacterial lipopeptides were evaluated as potential adjuvants in live-attenuated virus vaccines. **Chapters 3** and **4** [303,385] described the outcomes of this evaluation performed in two different vaccination / challenge models. **Chapter 5** (submitted) describes the generation and characterization of a new recombinant HRSV strain expressing EGFP, while **Chapter 6** [306] describes the development of an *ex vivo* model for studying respiratory virus infections in explant pulmonary cultures. Finally, the second major objective concerning the role of interactions between live *S. pneumoniae* and the pneumoviruses HRSV and HMPV in disease pathogenesis was addressed in **Chapters 7** [307] and **8** (submitted).

In **Chapter 2**, HRSV infection-modulating capacity of several (synthetic) bacterial TLR agonists, including Pam3CSK4 (TLR2/1), Pam2CSK4 (TLR2/6), FSL-1 (TLR2/6), lipopolysaccharide from *E. coli*. (TLR4) and

flagillin from *B. subtilis* (TLR5), were tested. Interestingly, Pam3CSK4 reproducibly and significantly enhanced HRSV infections in different cell types. It had been described previously that Pam3CSK4 enhanced infection or transmission of HIV-1 in different systems [253-255]. These data showed that Pam3CSK4-mediated enhancement of infection is not specific for HIV-1, but can also be shown for a number of other enveloped viruses including HRSV, HMPV and measles virus. Surprisingly, by blocking either binding to TLR1/2 or TLR1/2 signaling, enhancement of HRSV infection was demonstrated to be independent of TLR signaling. This was confirmed by the identification of two structurally-related lipopeptides (Pam-Cys-SK4 and PHCSK4) that could not stimulate TLR responses but were equally effective in enhancing infections with HRSV, HIV-1, HMPV and MV as Pam3CSK4. Moreover, other lipopeptides that could efficiently stimulate TLR2/1 responses such as Pam3CSP4 were unable to enhance virus infection. By using different virus binding assays enhancement of virus infection mediated by enhanced virus binding to the target cells was shown. By comparing the effects of a large set of synthetic lipopeptides it was concluded that the N-palmitoylated cysteine and the cationic lysines play a pivotal role in this enhanced virus binding. This finding formed the basis of two subsequent study objectives.

### TLR and non-TLR based immune adjuvants for (live-attenuated) virus vaccine

Vaccination is the most effective intervention strategy to reduce morbidity and mortality from infectious diseases. Over the last five decades, live-attenuated or inactivated virus vaccines have saved millions of lives. However, for some virus infections it has proven difficult to develop safe and effective vaccines.

HRSV vaccine development was initiated in the 1960s, when formalin-inactivated and alum-adjuvanted whole virus preparations (FI-RSV) were tested in clinical trials. These vaccines proved to predispose for enhanced disease during subsequent natural HRSV infections [157]. Similar vaccine-mediated immunopathological responses were later shown for formalin-inactivated HMPV vaccines tested in pre-clinical animal models [386-388]. The identification of vaccine-mediated enhanced HRSV and HMPV disease have significantly hampered vaccine development against these viruses.

The ideal vaccine against HRSV and/or HMPV has to deal with a number of important challenges. First of all, peak disease is observed in very young infants, and therefore a vaccine needs to be safe and effective in newborn infants, in the presence of maternal antibodies and a developing immune system. Furthermore, natural HRSV and HMPV infections usually induce poor immune responses, and thus the vaccine needs to perform better in this respect than the wild-type infection. Finally, and most importantly, the induction of both humoral and cellular immunity, probably with induction of a balanced CD4<sup>+</sup> and CD8<sup>+</sup> T-cell response without aberrant disease-enhancing Th2 or Th17 responses is required [168].

There are several approaches under development to achieve this. A possible method is to stimulate the innate immune system upon vaccination. As the innate immune response aids the subsequent development of adaptive immunity, this may accelerate and enhance the induction of desired vaccine-specific responses [389]. Triggering of the innate immune system via TLRs can lead to production of pro-inflammatory cytokines/chemokines and type I IFNs. Several studies report the use of TLR-ligands as adjuvants for viral or bacterial vaccines. For HRSV the use of TLR-stimulating adjuvants has been tested

in virosomes, which consist of HRSV viral envelopes containing the F and G membrane glycoproteins but not the RNA genome and thus are replication-deficient [295]. When the TLR2-ligand Pam3CSK4 were incorporated into the membrane of HRSV virosomes, HRSV VN antibodies and IFN- $\gamma$ -positive T-cells were induced *in vivo*. Upon challenge there were no signs of enhanced disease [295]. This approach also led to protection when the TLR2-ligand was replaced by the most potent TLR4-ligand, monophosphoryl lipid A. In mice and cotton rats HRSV virosomes adjuvanted with monophosphoryl lipid A provided protection against viral challenge without priming for enhanced disease in cotton rats [390,391]. In addition, HRSV virosomal vaccine formulated with TLR2-ligand or TLR9-ligand in combination with another member of the PRR family, NOD2 ligand, also induced mucosal and systemic immune responses [392,393].

The use of live-attenuated vaccines has proven a safe and effective approach for protection against several virus infections, as demonstrated by the widely used trivalent pediatric vaccines protecting against measles, mumps and rubella. However, development of live-attenuated HRSV vaccines has not yet been successful, due to difficulties in a balance between attenuation and immunogenicity [170]. A live-attenuated HRSV vaccine must be sufficiently attenuated to avoid inducing disease in the vaccinee but should also robustly elicit an immune response in order to induce protection. Live-attenuated HRSV vaccines have been developed by reverse genetics [169,304], and several have been evaluated in clinical trials [394,395]. Advantages for live-attenuated virus vaccines include the intranasal route of administration and induction of mucosal immune responses. However, a disadvantage is that the risk groups for developing (serious) adverse effects are also at risk to develop severe HRSV disease and stability of the virus, which was already pointed out in 1960 [11].

## Chapter 9

Based on the identification of the infection-enhancing lipopeptides as described in **Chapter 2**, and the previous use of Pam3CSK4 as adjuvant for non-replicating vaccines, it was hypothesized that these synthetic lipopeptides could potentially support vaccination with live-attenuated virus vaccines. Although classically such vaccines are administered without adjuvants, formulation of an attenuated virus vaccine in infection-enhancing lipopeptides could potentially support the first round of virus replication, thus stimulating the production of viral antigens and thereby the induction of virus-specific immune responses of a potentially slightly over-attenuated candidate vaccine virus. In **Chapters 3** and **4** the potential of synthetic bacterial lipopeptides as adjuvants for live-attenuated paramyxoviruses was assessed in two different animal models. In **Chapter 3** ferrets were vaccinated with a live-attenuated CDV strain in which the open reading frame encoding EGFP was cloned into the gene encoding the viral polymerase L. This virus had previously been reported to be over-attenuated in ferrets [101]. To avoid potential interfering T-cell responses directed against EGFP following challenge animals were challenged with a virus expressing the red fluorescent protein dTom [100]. Animals were vaccinated by intranasal vaccination in the presence or absence of infection-enhancing lipopeptides. In this experiment it was crucial that vaccination without lipopeptides led to suboptimal protection in the mock control vaccinated animals. Unfortunately, all animals vaccinated in the absence of lipopeptides developed protective immune responses. However, in animals inoculated with the vaccine virus formulated in infection-enhancing lipopeptides significantly higher vaccine virus loads were detected in nasopharyngeal lavages and peripheral blood mononuclear cells. Furthermore, these animals developed significantly higher CDV neutralizing antibody titers compared to animals vaccinated with

non-adjuvanted vaccine. In this study *ex vivo* agarose inflated lung slices were used to sensitively screen for CDV infected cells expressing dTom as described in **Chapter 6**.

In **Chapter 4** infection-enhancing lipopeptides were evaluated as potential adjuvants for a live-attenuated recombinant HRSV vaccine in the cotton rat model. This candidate vaccine lacking the G glycoprotein was previously shown to induce protective immunity in cotton rat [304]. In this study the use of a suboptimal vaccine virus dose was aimed in order to demonstrate the effect of the lipopeptide. Indeed, the administration of vaccine virus dose was suboptimal as not all animals inoculated with rHRSV $\Delta$ G in the absence of lipopeptide seroconverted to HRSV. Unfortunately, formulation of the vaccine with infection-enhancing lipopeptides did not increase vaccine virus replication or stimulate virus-specific immune responses. In contrast, there was a tendency of reduced seroconversion rates and reduced protection upon HRSV challenge infection. It can be concluded that despite the demonstration of *in vivo* infection enhancement in the ferret model our studies do not support further development of infection-enhancing lipopeptides as adjuvants for candidate live-attenuated HRSV vaccines.

As development of a pediatric HRSV vaccine has proven difficult, maternal vaccination is considered as a different strategy to protect newborns from severe HRSV disease. Maternal vaccination was previously shown to be effective for other infectious agents such as *Bordetella pertussis* and pandemic influenza virus H1N1 [396]. As the highest HRSV disease burden lies in infants younger than 6 months of age (see Figure 3 of the General Introduction), maternal immunization could potentially prevent a significant proportion of severe HRSV disease in early infancy. During pregnancy



IgG antibodies are being transferred to the fetus due to the fact that maternal blood is in direct contact with the chorionic trophoblast, also known as hemochorial placenta. Indeed, HRSV-specific virus neutralizing IgG antibodies are present in the sera of all full-term neonates as a result of transplacental transfer of maternal antibodies [174]. These transplacental maternal antibodies protect the newborn during the first period of life against all kinds of pathogens. This is confirmed by the observation that infants younger than 6 weeks are often spared from serious HRSV illness, an age when maternal antibodies are still significantly present [175]. HRSV-specific maternal antibodies detected at birth appeared to decline steadily over the first 3 months and were undetectable in the majority of infants at the age of 6 months, thereby the half-life was 26 days [176,177]. Surprisingly, the half-life was about 2.5 months in infants in a tropical country [397]. The goal of maternal immunization is to boost existing neutralizing antibody levels during pregnancy, resulting in an increased amount of serum neutralizing antibodies trans-placentally transferred from mother to infant [398]. Implementation of HRSV maternal immunization may reduce the incidence of HRSV hospitalization in infants significantly, however, first an effective (adjuvanted) HRSV vaccine must be developed and tested to boost HRSV VN antibodies in pregnant women to a level that would allow protection of their babies for the first half year.

### Interactions between live bacteria and respiratory viruses

Respiratory bacteria can asymptotically colonize the upper respiratory tract. Colonization in infants occurs frequently but is usually transient. Notorious bacterial colonizers are *Streptococcus pneumoniae* (pneumococcus), *Haemophilus influenzae*, *Moraxella catarrhalis*, or *Staphylococcus aureus* [72]. Thus, these bacteria may influence

subsequent infections with HRSV or HMPV that target the same niche. In **Chapter 7** the influence of respiratory bacteria exposure on HMPV infection was studied. Colonization by four respiratory bacteria was mimicked in the best available *in vitro* model for HMPV. In this system only *S. pneumoniae* enhanced HMPV infection. In an ongoing cohort of healthy children, nasopharyngeal swabs and serum samples from 57 children were collected at four time points in their first two years of life. Frequent nasopharyngeal carriage ( $\geq 2$  times out of 4) of *S. pneumoniae*, but not of the other three pathogens, was associated with increased seroconversion rates of infants to HMPV at the age of 2 years. Frequent nasopharyngeal carriage of *S. pneumoniae* was also associated with a tendency towards higher seroconversion levels against HRSV, but these differences did not reach statistical significance (unpublished data,  $p = 0.08$ ).

In **Chapter 8** the influence of *S. pneumoniae* colonization on HRSV infection was studied. In this study a new recombinant HRSV, rHRSV<sup>B05</sup>EGFP(5), used which is described in **Chapter 5**. This recombinant virus is closely related to a wild-type virus, with the addition that it can be tracked upon infection by studying EGFP fluorescence. Also, four pneumococcal serotypes of which three were clinical isolates were used *in vitro* and *in vivo*. Three serotypes were found to enhance HRSV-infection in wd-NHBE cells. Subsequently, cotton rats were intra-nasally colonized with these pneumococci. As *S. pneumoniae* is a human pathobiont, it was unknown what would happen in cotton rats. Eight days after inoculation of *S. pneumoniae* the bacterium could be re-isolated from all inoculated animals, providing the first evidence of successful colonization of cotton rats with *S. pneumoniae*. Two pneumococcal serotypes significantly enhanced HRSV replication *in vivo* and one serotype significantly promoted syncytium formation *in vivo* compared to

control. This study raises several questions. Is the interaction between virus and bacterium bidirectional (synergistic), or does only one pathogen have benefit? No prospective cohort studies have been performed to address these questions. However, Madhi *et al.* showed that the frequency of HRSV pneumonia was reduced after the introduction of pneumococcal conjugated vaccination, suggesting that HRSV can benefit from the bacterium [80]. Currently, the clinical impact of pneumococcal colonization and HRSV infection is unknown. A possible scenario is that HRSV can easier be spread to the LRT as significantly higher HRSV titers occur in presence of certain pneumococcal serotypes. In addition, subsequent spread of HRSV can facilitate spread of the bacterium to the LRT, resulting in a co-infection of the LRT. Additional studies are needed to address these questions, and could result in development of novel intervention strategies to address this deadly combination in the LRT.

In previous studies three different cationic synthetic lipopeptides were identified that can enhance HRSV and HMPV infections both *in vitro* and *in vivo*. Subsequently, it was also demonstrated that *S. pneumoniae* enhanced both HRSV and HMPV infections. However, addressing the mechanistic background of this enhancement proved to be difficult. Several mechanisms of infection enhancement have been described in literature. Several cationic compounds, including DEAE-dextran, polybrene, RANTES, and Semen-Derived Enhancer of Viral Infection (SEVI), have been shown to enhance viral infection [262,266,268]. Polybrene, a synthetic cationic polymer, neutralizing the charge repulsion between viral and target cell membranes leads to enhancement of infection of a variety of retroviruses, including HIV [269]. SEVI enhances HIV infection by cross-linking HIV particles to target cells, facilitating subsequent fusion [262,268]. RANTES, a cationic

chemokine, has been reported to enhance HIV-1 infection by binding to proteoglycans on the surface of target cells [270]. Essentially, the effect of these compounds is facilitating close contact between a virus and its target cell. Another mechanism to achieve this is spinoculation, i.e. centrifugation of a culture plate (15 minutes, 1400 × g) immediately after inoculation of a virus [399]. In many model systems, including paramyxovirus infections of adherent cells, this method can result in a more than ten-fold increase in virus infectivity. The method is routinely used by many diagnostic labs to increase the sensitivity of virus isolation procedures from clinical specimens.

Pam3CSK4 is a synthetic mimic of the N-terminal parts of lipopeptides present in the cell walls of gram-positive and gram-negative bacteria, which have been identified as TLR agonists [272]. Therefore, the biological property of these lipopeptides as potential enhancers of RSV binding could explain in part the observed interactions between HRSV and pneumococci. However, bacterial neuraminidases could represent another potential mechanism of infection enhancement. *S. pneumoniae* produces several neuraminidases, which “graze” sialic acids from epithelial cells resulting in a paved way for HRSV entry as these negatively charged sialic acids hinder HRSV entry [400]. Neuraminidase treatment of HRSV particles was previously shown to enhance virus infections *in vitro* [361].

In order to address potential overlaps between these mechanisms, competition experiments were performed. For these experiments input virus originated from the same vial. Endpoint virus titrations on B95a cells were performed using rMV<sup>IC323</sup>EGFP in presence or absence of lipopeptide (30 µl/ml), in addition plates were spinoculated or not spinoculated. When virus titration was

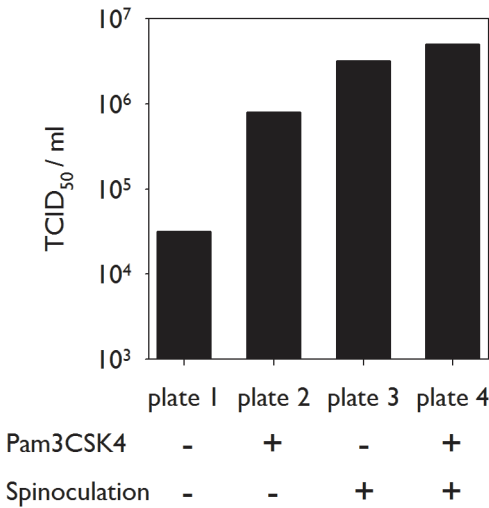


**Figure 1.** Enhancement of rMV<sup>C323</sup>EGFP infection in addition of lipopeptide and/or spinoculation. B95a cells were inoculated in presence or absence of lipopeptide (30 µg/ml). An additional treatment was spinoculation. All treatments resulted in significantly higher TCID<sub>50</sub>/ml, however, spinoculation and addition of lipopeptide did not increase infection significantly compared to spinoculation alone.

performed without lipopeptide and without spinoculation, a titer of approximately 3.2 × 10<sup>4</sup> TCID<sub>50</sub> per ml was measured (Figure 1, plate 1). Simultaneous addition of lipopeptide (plate 2) or use of spinoculation (plate 3) resulted in detection of significantly higher virus titers of 7.9 × 10<sup>5</sup> and 3.2 × 10<sup>6</sup> TCID<sub>50</sub>/ml, respectively. However, simultaneous use of Pam3CSK4 and spinoculation resulted in only a minor further increase in virus titer to 5.1 × 10<sup>6</sup> (plate 4). It can be concluded that apparently the infection enhancement of these two methods is not additive but largely competitive.

A similar approach was used to study the competition between lipopeptide-mediated and neuraminidase-mediated enhancement of infection. rHRSV<sup>B05</sup>EGFP(5) was treated with neuraminidase (0-30 mU/ml) only or lipopeptide (20 µg/ml) was simultaneously added for 1 hr. Subsequently, EBV-transformed

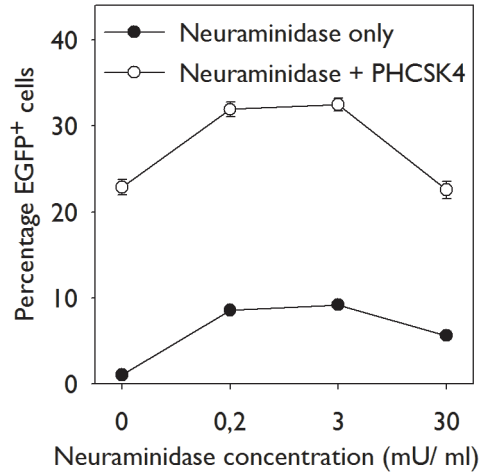


**Figure 2.** Enhancement of rHRSV<sup>B05</sup>EGFP(5) infection following neuraminidase and lipopeptide treatment. rHRSV<sup>B05</sup>EGFP(5) was treated with neuraminidase (0.2-30 mU/ml), then inoculated on B-LCL. HRSV infection was enhanced 1 d.p.i. (black circles). Enhancement was further increased by treating HRSV virus particles simultaneously with neuraminidase and lipopeptide (20 µg/ml; white circles). Data represent averages ± SD.

B-LCL were inoculated with the mix, incubated for 1 hr at 37°C (5% CO<sub>2</sub> [v/v]), washed after another hour, then cells were incubated at 37°C (5% CO<sub>2</sub> [v/v]). The next day infection percentages were measured using flow cytometry. Neuraminidase only treatment resulted in enhancement of HRSV infection (Figure 2; black circles). Similarly, addition of lipopeptide only resulted in significant enhancement of infection (white circles). However, the neuraminidase-mediated enhancement of infection was almost identical in cells with or without lipopeptide, strongly suggesting a different mode of action for these two infection enhancers.

### Concluding Remarks and Future Perspectives

An average adult inhales 12,000 liters of air every day. With every breath numerous potential pathogens are inhaled, which can lead to disease. The first encounter with many pathogens takes place in the respiratory tract. The upper respiratory tract (URT) harbors thousands of commensal bacterial species, but transiently potentially pathogenic bacteria can also be present. Inhaled viruses can interact with residing bacteria in the URT. I have shown that synthetic bacterial components enhance paramyxovirus infections, including human respiratory syncytial virus (HRSV) and human metapneumovirus (HMPV). Both viruses cause significant disease burdens and may even cause death. A revolutionary mode of action for these infection-enhancing lipopeptides was foreseen in live-attenuated virus vaccines, which are urgently needed for HRSV and HMPV. Unfortunately, two studies could not confirm that these lipopeptides could be exploited as adjuvants in live-attenuated vaccine virus formulations. Next, two studies showed that live bacteria (*S. pneumoniae*) are able to enhance HRSV and HMPV infection. This was unprecedented and radical according to the general dogma of bacterial super-infections following virus infection. However, these interactions are much more complex to explain directly and more studies are needed. For testing hypotheses in pathogenesis studies of infectious agents the best possible model system is usually the natural target organism (often animals or humans). However, because of ethical, logistical or financial restrictions this approach is not always possible. Therefore, *in silico*, *in vitro* or *ex vivo* studies supplemented with *in vivo* studies in animal models are the best surrogate methodologies available to answer pivotal questions in life sciences.

Therefore, unbiased, reproducible and generalizable data can only be obtained when in these methodologies genuine biological materials processed in a physiological way are used. In this thesis some of the best available models for HRSV and HMPV were used, such as disease-relevant cell lines to grow viruses, wd-NHBE and the cotton rat model. Notably, a new recombinant HRSV was generated and characterized. This virus can be considered as genuine as it resembles a wild-type virus with in addition a powerful tracking device as infection can be followed upon high sensitive fluorescence study. Next to the use of newly generated viruses (to be developed in the future: HRSV subtype A, HMPV subtypes A and B) with unmatched provenance *in vitro* and *in vivo* modeling can be optimized. HRSV and HMPV infections are most likely often initiated in the nasopharynx. However, at present there are no studies in disease-relevant *in vitro* systems (well-differentiated nasal epithelium cells, Langerhans cells) to address this. Ideally, a multilayered *in vitro* model consisting of well-differentiated nasal epithelium cells and Langerhans cells would provide novel insights into pneumovirus pathogenesis. Also, HRSV or HMPV infections in the current most used *in vivo* models do not fully resemble human infection and accompanying symptomatology. This was confirmed by the transmission cotton rat model for HRSV described in **Chapter 8**. Ferrets or other commonly used animals for pneumovirus studies could provide a highly useful alternative. Thus, future studies with relevant viruses, *in vitro* and *in/ex vivo* models are needed in order to improve our understanding of viral pathogenesis, and will ultimately contribute to development of novel intervention strategies.





## **Chapter 10**

### **Reference List**



- [1] Li Q, Zhou L, Zhou M, Chen Z, Li F, Wu H, Xiang N, Chen E, Tang F, Wang D, Meng L, Hong Z, Tu W, Cao Y, Li L, Ding F, Liu B, Wang M, Xie R, Gao R, Li X, Bai T, Zou S, He J, Hu J, Xu Y, Chai C, Wang S, Gao Y, Jin L, Zhang Y, Luo H, Yu H, Gao L, Pang X, Liu G, Shu Y, Yang W, Uyeki TM, Wang Y, Wu F, Feng Z. Preliminary Report: Epidemiology of the Avian Influenza A (H7N9) Outbreak in China. *N Engl J Med* 2013.
- [2] Zaki AM, van BS, Bestebroer TM, Osterhaus AD, Fouchier RA. Isolation of a novel coronavirus from a man with pneumonia in Saudi Arabia. *N Engl J Med* 2012;367:1814-20.  
Rudan I, El AS, Bhutta ZA, Black RE, Brooks A, Chan KY, Chopra M, Duke T, Marsh D, Pio A,
- [3] Simoes EA, Tamburini G, Theodoratou E, Weber MW, Whitney CG, Campbell H, Qazi SA. Setting research priorities to reduce global mortality from childhood pneumonia by 2015. *PLoS Med* 2011;8:e1001099.
- [4] Thompson WW, Shay DK, Weintraub E, Brammer L, Cox N, Anderson LJ, Fukuda K. Mortality associated with influenza and respiratory syncytial virus in the United States. *JAMA* 2003;289:179-86.
- [5] Rappuoli R, Mandl CW, Black S, De GE. Vaccines for the twenty-first century society. *Nat Rev Immunol* 2011;11:865-72.
- [6] Armstrong GL, Conn LA, Pinner RW. Trends in infectious disease mortality in the United States during the 20th century. *JAMA* 1999;281:61-6.
- [7] Blount RE, Jr., Morris JA, Savage RE. Recovery of cytopathogenic agent from chimpanzees with coryza. *Proc Soc Exp Biol Med* 1956;92(3):544-9.
- [8] Chanock RM, Parrott RH, Cook K, Andrews BE, BELL JA, Reichelderfer T, Kapikian AZ, Mastrota FM, Huebner RJ. Newly recognized myxoviruses from children with respiratory disease. *N Engl J Med* 1958;258:207-13.
- [9] Chanock RM, Roizman B, Myers R. Recovery from infants with respiratory illness of a virus related to chimpanzee coryza agent (CCA). I. Isolation, properties and characterization. *Am J Hyg* 1957;66:281-90.
- [10] Chanock RM, Finberg L. Recovery from infants with respiratory illness of a virus related to chimpanzee coryza agent (CCA). II. Epidemiologic aspects of infection in infants and young children. *Am J Hyg* 1957;66:291-300.
- [11] Beem M, Wright FH, Hamre D, Egerer R, Oehme M. Association of the chimpanzee coryza agent with acute respiratory disease in children. *N Engl J Med* 1960;263:523-30.
- [12] Chanock RM, Kim HW, Vargosko AJ, Deleva A, Johnson KM, Cumming C, Parrott RH. Respiratory syncytial virus. I. Virus recovery and other observations during 1960 outbreak of bronchiolitis, pneumonia, and minor respiratory diseases in children. *JAMA* 1961;176:647-53.
- [13] Parrott RH, Vargosko AJ, Kim HW, Cumming C, Turner H, Huebner RJ, Chanock RM. Respiratory syncytial virus. II. Serologic studies over a 34-month period of children with bronchiolitis, pneumonia, and minor respiratory diseases. *JAMA* 1961;176:653-7.
- [14] Kravetz HM, Knight V, Chanock RM, Morris JA, Johnson KM, Rifkind D, Utz JP. Respiratory syncytial virus. III. Production of illness and clinical observations in adult volunteers. *JAMA* 1961;176:657-63.
- [15] Johnson KM, Chanock RM, Rifkind D, Kravetz HM, Knight V. Respiratory syncytial virus. IV. Correlation of virus shedding, serologic response, and illness in adult volunteers. *JAMA* 1961;176:663-7.
- [16] Nair H, Nokes DJ, Gessner BD, Dherani M, Madhi SA, Singleton RJ, O'Brien KL, Roca A, Wright PF, Bruce N, Chandran A, Theodoratou E, Sutanto A, Sedyaningsih ER, Ngama M, Munywoki PK, Kartasmita C, Simoes EA, Rudan I, Weber MW, Campbell H. Global burden of acute lower



- respiratory infections due to respiratory syncytial virus in young children: a systematic review and meta-analysis. *Lancet* 2010;375:1545-55.
- [17] Collins PL, Karron RA. Respiratory syncytial virus and metapneumovirus. In: Knipe DM, Howley PM, editors. *Fields Virology*. 6 ed. Philadelphia: Wolters Kluwer | Lippincott Williams & Wilkins; 2013. p. 1086-123.
- [18] Collins PL, Mottet G. Post-translational processing and oligomerization of the fusion glycoprotein of human respiratory syncytial virus. *J Gen Virol* 1991;72:3095-101.
- [19] McLellan JS, Chen M, Leung S, Graepel KW, Du X, Yang Y, Zhou T, Baxa U, Yasuda E, Beaumont T, Kumar A, Modjarrad K, Zheng Z, Zhao M, Xia N, Kwong PD, Graham BS. Structure of RSV fusion glycoprotein trimer bound to a prefusion-specific neutralizing antibody. *Science* 2013;340:1113-7.
- [20] Kahn JS, Schnell MJ, Buonocore L, Rose JK. Recombinant vesicular stomatitis virus expressing respiratory syncytial virus (RSV) glycoproteins: RSV fusion protein can mediate infection and cell fusion. *Virology* 1999;254:81-91.
- [21] Levine S, Klaiber-Franco R, Paradiso PR. Demonstration that glycoprotein G is the attachment protein of respiratory syncytial virus. *J Gen Virol* 1987;68:2521-4.
- [22] Teng MN, Whitehead SS, Collins PL. Contribution of the respiratory syncytial virus G glycoprotein and its secreted and membrane-bound forms to virus replication *in vitro* and *in vivo*. *Virology* 2001;289:283-96.
- [23] Lambert DM. Role of oligosaccharides in the structure and function of respiratory syncytial virus glycoproteins. *Virology* 1988;164:458-66.
- [24] Wertz GW, Krieger M, Ball LA. Structure and cell surface maturation of the attachment glycoprotein of human respiratory syncytial virus in a cell line deficient in O glycosylation. *J Virol* 1989;63:4767-76.
- [25] Johnson PR, Spriggs MK, Olmsted RA, Collins PL. The G glycoprotein of human respiratory syncytial viruses of subgroups A and B: extensive sequence divergence between antigenically related proteins. *Proc Natl Acad Sci USA* 1987;84:5625-9.
- [26] Langedijk JPM, Schaaper WMM, Meloen RH, Van Oirschot JT. Proposed three-dimensional model for the attachment protein G of respiratory syncytial virus. *J Gen Virol* 1996;77:1249-57.
- [27] Olmsted RA, Collins PL. The IA protein of respiratory syncytial virus is an integral membrane protein present as multiple, structurally distinct species. *J Virol* 1989;63:2019-29.
- [28] Fuentes S, Tran KC, Luthra P, Teng MN, He B. Function of the respiratory syncytial virus small hydrophobic protein. *J Virol* 2007;81:8361-6.
- [29] Techaarpornkul S, Barretto N, Peeples ME. Functional analysis of recombinant respiratory syncytial virus deletion mutants lacking the small hydrophobic and/or attachment glycoprotein gene. *J Virol* 2001;75:6825-34.
- [30] Ling Z, Tran KC, Teng MN. Human respiratory syncytial virus nonstructural protein NS2 antagonizes the activation of beta interferon transcription by interacting with RIG-I. *J Virol* 2009;83:3734-42.
- [31] Boyapalle S, Wong T, Garay J, Teng M, San Juan-Vergara H, Mohapatra S, Mohapatra S. Respiratory syncytial virus NS1 protein colocalizes with mitochondrial antiviral signaling protein MAVS following infection. *PLoS ONE* 2012;7:e29386.
- [32] Bitko V, Shulyayeva O, Mazumder B, Musiyenko A, Ramaswamy M, Look DC, Barik S. Nonstructural proteins of respiratory syncytial virus suppress premature apoptosis by an NF-kappaB-dependent, interferon-independent mechanism and facilitate virus growth. *J Virol*

- 2007;81:1786-95.
- [33] Bermingham A, Collins PL. The M2-2 protein of human respiratory syncytial virus is a regulatory factor involved in the balance between RNA replication and transcription. *Proc Natl Acad Sci U S A* 1999;96:11259-64.
- [34] Fearn R, Collins PL. Role of the M2-1 transcription antitermination protein of respiratory syncytial virus in sequential transcription. *J Virol* 1999;73:5852-64.
- [35] Collins PL, Hill MG, Cristina J, Grosfeld H. Transcription elongation factor of respiratory syncytial virus, a nonsegmented negative-strand RNA virus. *Proc Natl Acad Sci U S A* 1996;93:81-5.
- [36] Hardy RW, Wertz GW. The product of the respiratory syncytial virus M2 gene ORF1 enhances readthrough of intergenic junctions during viral transcription. *J Virol* 1998;72:520-6.
- [37] Collins PL, Melero JA. Progress in understanding and controlling respiratory syncytial virus: still crazy after all these years. *Virus Res* 2011;162:80-99.
- [38] Hall CB, Douglas RG, Jr., Geiman JM. Possible transmission by fomites of respiratory syncytial virus. *J Infect Dis* 1980;141:98-102.
- [39] Falsey AR, Hennessey PA, Formica MA, Cox C, Walsh EE. Respiratory syncytial virus infection in elderly and high-risk adults. *N Engl J Med* 2005;352:1749-59.
- [40] Englund JA, Sullivan CJ, Jordan MC, Dehner LP, Vercellotti GM, Balfour HH, Jr. Respiratory syncytial virus infection in immunocompromised adults. *Ann Intern Med* 1988;109:203-8.
- [41] Hall CB, Powell KR, MacDonald NE, Gala CL, Menegus ME, Suffin SC, Cohen HJ. Respiratory syncytial viral infection in children with compromised immune function. *N Engl J Med* 1986;315:77-81.
- [42] Stensballe LG, Devasundaram JK, Simoes EA. Respiratory syncytial virus epidemics: the ups and downs of a seasonal virus. *Pediatr Infect Dis J* 2003;22:S21-S32.
- [43] McNamara PS, Smyth RL. The pathogenesis of respiratory syncytial virus disease in childhood. *Br Med Bull* 2002;61:13-28.
- [44] Devincenzo JP, Wilkinson T, Vaishnav A, Cehelsky J, Meyers R, Nochur S, Harrison L, Meeking P, Mann A, Moane E, Oxford J, Pareek R, Moore R, Walsh E, Studholme R, Dorsett P, Alvarez R, Lambkin-Williams R. Viral load drives disease in humans experimentally infected with respiratory syncytial virus. *Am J Respir Crit Care Med* 2010;182:1305-14.
- [45] Hall WJ, Hall CB, Speers DM. Respiratory syncytial virus infection in adults: clinical, virologic, and serial pulmonary function studies. *Ann Intern Med* 1978;88:203-5.
- [46] Tristram DA, Hicks W, Jr., Hard R. Respiratory syncytial virus and human bronchial epithelium. *Arch Otolaryngol Head Neck Surg* 1998;124:777-83.
- [47] Johnson JE, Gonzales RA, Olson SJ, Wright PF, Graham BS. The histopathology of fatal untreated human respiratory syncytial virus infection. *Mod Pathol* 2007;20(1):108-19.
- [48] Richardson LS, Belshe RB, Sly DL, London WT, Prevar DA, Camargo E, Chanock RM. Experimental respiratory syncytial virus pneumonia in cebus monkeys. *J Med Virol* 1978;2:45-59.
- [49] Villenave R, Thavagnanam S, Sarlang S, Parker J, Douglas I, Skibinski G, Heaney LG, McKaigue JP, Coyle PV, Shields MD, Power UF. *In vitro* modeling of respiratory syncytial virus infection of pediatric bronchial epithelium, the primary target of infection *in vivo*. *Proc Natl Acad Sci U S A* 2012;109:5040-5.
- [50] Wright PF, Ikizler MR, Gonzales RA, Carroll KN, Johnson JE, Werkhaven JA. Growth of respiratory syncytial virus in primary epithelial cells from the human respiratory tract. *J Virol* 2005;79:8651-4.

- [51] Zhang L, Peeples ME, Boucher RC, Collins PL, Pickles RJ. Respiratory syncytial virus infection of human airway epithelial cells is polarized, specific to ciliated cells, and without obvious cytopathology. *J Virol* 2002;76:5654-66.
- [52] Graham BS, Rutigliano JA, Johnson TR. Respiratory syncytial virus immunobiology and pathogenesis. *Virology* 2002;297:1-7.
- [53] Anderson JJ, Harrop JA, Peers H, Turnbull T, Toms GL, Scott R. Recognition of Respiratory Syncytial (RS) Virus Proteins by Human and BALB/C CD4<sup>+</sup> Lymphocytes. *J Med Virol* 1991;35:165-73.
- [54] Huang M, Bigos D, Levine M. Ventricular arrhythmia associated with respiratory syncytial viral infection. *Pediatr Cardiol* 1998;19:498-500.
- [55] Goulder PJR, Lechner F, Klenerman P, McIntosh K, Walker BD. Characterization of a novel respiratory syncytial virus-specific human cytotoxic T-lymphocyte epitope. *J Virol* 2000;74:7694-7.
- [56] Rock MT, Crowe Jr. JE. Identification of a novel human leucocyte antigen-A\*01-restricted cytotoxic T-lymphocyte epitope in the respiratory syncytial virus fusion protein. *Immunology* 2003;108:474-80.
- [57] Simoes EAF. Respiratory syncytial virus infection. *Lancet* 1999;354:847-52.
- [58] Schildgen V, van den Hoogen B, Fouchier R, Tripp RA, Alvarez R, Manoha C, Williams J, Schildgen O. Human Metapneumovirus: lessons learned over the first decade. *Clin Microbiol Rev* 2011;24:734-54.
- [59] van den Hoogen BG, de Jong JC, Groen J, Kuiken T, de Groot R, Fouchier RAM, Osterhaus ADME. A newly discovered human pneumovirus isolated from young children with respiratory tract disease. *Nat Med* 2001;7:719-24.
- [60] van den Hoogen BG, Bestebroer TM, Osterhaus ADME, Fouchier RAM. Analysis of the genomic sequence of a human metapneumovirus. *Virology* 2002;295:119-32.
- [61] Aberle JH, Aberle SW, Redlberger-Fritz M, Sandhofer MJ, Popow-Kraupp T. Human metapneumovirus subgroup changes and seasonality during epidemics. *Pediatr Infect Dis J* 2010;29:1016-8.
- [62] van den Hoogen BG, Herst S, Sprong L, Cane PA, Forleo-Neto E, De Swart RL, Osterhaus ADME, Fouchier RAM. Antigenic and genetic variability of human metapneumoviruses. *Emerg Infect Dis* 2004;10:658-66.
- [63] Williams JV, Wang CK, Yang CF, Tollefson SJ, House FS, Heck JM, Chu M, Brown JB, Lintao LD, Quinto JD, Chu D, Spaete RR, Edwards KM, Wright PF, Crowe Jr. JE. The role of human metapneumovirus in upper respiratory tract infections in children: a 20-year experience. *J Infect Dis* 2006;193:387-95.
- [64] van den Hoogen BG. Respiratory tract infection due to human metapneumovirus among elderly patients. *Clin Infect Dis* 2007;44:1159-60.
- [65] Crowe Jr. JE. Human metapneumovirus as a major cause of human respiratory tract disease. *Pediatr Infect Dis J* 2004;23:S215-S221.
- [66] Madhi SA, Ludewick H, Abed Y, Klugman KP, Boivin G. Human metapneumovirus-associated lower respiratory tract infections among hospitalized human immunodeficiency virus type 1 (HIV-1)-infected and HIV-1-uninfected African infants. *Clin Infect Dis* 2003;37:1705-10.
- [67] Honda H, Iwahashi J, Kashiwagi T, Imamura Y, Hamada N, Anraku T, Ueda S, Kanda T, Takahashi T, Morimoto S. Outbreak of human metapneumovirus infection in elderly inpatients in Japan. *J Am Geriatr Soc* 2006;54:177-80.
- [68] Louie JK, Schnurr DP, Pan CY, Kiang D, Carter C, Tougaw S, Ventura J, Norman A, Belmusto V,

- Rosenberg J, Trochet G. A summer outbreak of human metapneumovirus infection in a long-term-care facility. *J Infect Dis* 2007;196:705-8.
- [69] Osbourn M, McPhie KA, Ratnamohan VM, Dwyer DE, Durrheim DN. Outbreak of human metapneumovirus infection in a residential aged care facility. *Commun Dis Intell Q Rep* 2009;33:38-40.
- [70] Tu CC, Chen LK, Lee YS, Ko CF, Chen CM, Yang HH, Lee JJ. An outbreak of human metapneumovirus infection in hospitalized psychiatric adult patients in Taiwan. *Scand J Infect Dis* 2009;41:363-7.
- [71] Te Wierik MJ, Nguyen DT, Beersma MF, Thijsen SF, Heemstra KA. An outbreak of severe respiratory tract infection caused by human metapneumovirus in a residential care facility for elderly in Utrecht, the Netherlands, January to March 2010. *Euro Surveill* 2012;17(13):pii=20132.
- [72] Watson K, Carville K, Bowman J, Jacoby P, Riley TV, Leach AJ, Lehmann D. Upper respiratory tract bacterial carriage in Aboriginal and non-Aboriginal children in a semi-arid area of Western Australia. *Pediatr Infect Dis J* 2006;25:782-90.
- [73] Bogaert D, de Groot R, Hermans PW. *Streptococcus pneumoniae* colonisation: the key to pneumococcal disease. *Lancet Infect Dis* 2004;4(3):144-54.
- [74] Poolman JT, Peeters CC, van den Dobbelen GP. The history of pneumococcal conjugate vaccine development: dose selection. *Expert Rev Vaccines* 2013;12:1379-94.
- [75] Kim PE, Musher DM, Glezen WP, Rodriguez-Barradas MC, Nahm WK, Wright CE. Association of invasive pneumococcal disease with season, atmospheric conditions, air pollution, and the isolation of respiratory viruses. *Clin Infect Dis* 1996;22:100-6.
- [76] Hament JM, Aerts PC, Fleer A, van Dijk H, Harmsen T, Kimpen JL, Wolfs TF. Enhanced adherence of *Streptococcus pneumoniae* to human epithelial cells infected with respiratory syncytial virus. *Pediatr Res* 2004;55:972-8.
- [77] Avadhanula V, Wang Y, Portner A, Adderson E. Nontypeable *Haemophilus influenzae* and *Streptococcus pneumoniae* bind respiratory syncytial virus glycoprotein. *J Med Microbiol* 2007;56:1133-7.
- [78] Hament JM, Aerts PC, Fleer A, van Dijk H, Harmsen T, Kimpen JL, Wolfs TF. Direct binding of respiratory syncytial virus to pneumococci: a phenomenon that enhances both pneumococcal adherence to human epithelial cells and pneumococcal invasiveness in a murine model. *Pediatr Res* 2005;58:1198-203.
- [79] Simoes EA, Groothuis JR, Tristram DA, Alessi K, Lehr MV, Siber GR, Welliver RC. Respiratory syncytial virus-enriched globulin for the prevention of acute otitis media in high risk children. *J Pediatr* 1996;129:214-9.
- [80] Madhi SA, Klugman KP. A role for *Streptococcus pneumoniae* in virus-associated pneumonia. *Nat Med* 2004;10:811-3.
- [81] Madhi SA, Ludewick H, Kuwanda L, Niekerk N, Cutland C, Little T, Klugman KP. Pneumococcal co-infection with human metapneumovirus. *J Infect Dis* 2006;193:1236-43.
- [82] Griffin DE. Measles virus. In: Knipe DM, Howley PM, editors. *Fields Virology*. 6 ed. Philadelphia: Wolters Kluwer | Lippincott Williams & Wilkins; 2013. p. 1042-69.
- [83] WHO. Progress in global control and regional elimination of measles, 2000-2011. *Wkly Epidemiol Rec* 2013;88:29-36.
- [84] Ludlow M, De Vries RD, Lemon K, McQuaid S, Millar E, Van Amerongen G, Yüksel S, Verburgh RJ, Osterhaus ADME, De Swart RL, Duprex WP. Infection of lymphoid tissues in the macaque upper respiratory tract contributes to the emergence of transmissible measles virus. *J Gen Virol* 2013;94:1933-44.

- [85] Lemon K, De Vries RD, Mesman AW, McQuaid S, Van Amerongen G, Yüksel S, Ludlow M, Rennick LJ, Kuiken T, Rima BK, Geijtenbeek TBH, Osterhaus ADME, Duprex WP, De Swart RL. Early target cells of measles virus after aerosol infection of non-human primates. *PLoS Pathog* 2011;7:e1001263.
- [86] De Vries RD, McQuaid S, Van Amerongen G, Yüksel S, Verburgh RJ, Osterhaus ADME, Duprex WP, De Swart RL. Measles immune suppression: lessons from the macaque model. *PLoS Pathog* 2012;8:e1002885.
- [87] Noyce RS, Bondre DG, Ha MN, Lin LT, Sisson G, Tsao MS, Richardson CD. Tumor cell marker PVRL4 (nectin 4) is an epithelial cell receptor for measles virus. *PLoS Pathog* 2011;7:e1002240.
- [88] Mühlebach MD, Mateo M, Sinn PL, Prufer S, Uhlig KM, Leonard VH, Navaratnarajah CK, Frenzke M, Wong XX, Sawatsky B, Ramachandran S, McCray Jr. PB, Cichutek K, von Messling V, Lopez M, Cattaneo R. Adherens junction protein nectin-4 is the epithelial receptor for measles virus. *Nature* 2011;480:530-3.
- [89] De Vries RD, Mesman AW, Geijtenbeek TBH, Duprex WP, De Swart RL. The pathogenesis of measles. *Curr Opin Virol* 2012;2:248-55.
- [90] Ludlow M, Lemon K, De Vries RD, McQuaid S, Millar E, Van Amerongen G, Yüksel S, Verburgh RJ, Osterhaus ADME, De Swart RL, Duprex WP. Measles virus infection of epithelial cells in the macaque upper respiratory tract is mediated by sub-epithelial immune cells. *J Virol* 2013;87:4033-42.
- [91] Duprex WP, McQuaid S, Roscic-Mrkic B, Cattaneo R, McCallister C, Rima B. *In vitro* and *in vivo* infection of neural cells by a recombinant measles virus expressing enhanced green fluorescent protein. *J Virol* 2000;74:7972-9.
- [92] De Swart RL, Ludlow M, De Witte L, Yanagi Y, Van Amerongen G, McQuaid S, Yüksel S, Geijtenbeek TBH, Duprex WP, Osterhaus ADME. Predominant infection of CD150+ lymphocytes and dendritic cells during measles virus infection of macaques. *PLoS Pathog* 2007;3:e1178.
- [93] Ludlow M, Duprex WP, Cosby SL, Allen IV, McQuaid S. Advantages of using recombinant measles viruses expressing a fluorescent reporter gene with vibratome slice technology in experimental measles neuropathogenesis. *Neuropathol Appl Neurobiol* 2008;34:424-34.
- [94] Ludlow M, Rennick LJ, Nambulli S, De Swart RL, Duprex WP. Using the ferret model to study morbillivirus entry, spread, transmission and cross-protection. *Curr Opin Virol* 2014;4:15-23.
- [95] Yoshikawa Y, Ochikubo F, Matsubara Y, Tsuruoka H, Ishii M, Shirota K, Nomura Y, Sugiyama M, Yamanouchi K. Natural infection with canine distemper virus in a Japanese monkey (*Macaca fuscata*). *Vet Microbiol* 1989;20:193-205.
- [96] Qiu W, Zheng Y, Zhang S, Fan Q, Liu H, Zhang F, Wang W, Liao G, Hu R. Canine distemper outbreak in rhesus monkeys, China. *Emerg Infect Dis* 2011;17:1541-3.
- [97] Sakai K, Nagata N, Ami Y, Seki F, Suzaki Y, Iwata-Yoshikawa N, Suzuki T, Fukushi S, Mizutani T, Yoshikawa T, Otsuki N, Kurane I, Komase K, Yamaguchi R, Hasegawa H, Saijo M, Takeda M, Morikawa S. Lethal canine distemper virus outbreak in cynomolgus monkeys in Japan in 2008. *J Virol* 2013;87:1105-14.
- [98] von Messling V, Milosevic D, Cattaneo R. Tropism illuminated: lymphocyte-based pathways blazed by lethal morbillivirus through the host immune system. *Proc Natl Acad Sci USA* 2004;101:14216-421.
- [99] Beineke A, Puff C, Seehusen F, Baumgartner W. Pathogenesis and immunopathology of systemic and nervous canine distemper. *Vet Immunol Immunopathol* 2009;127:1-18.
- [100] Ludlow M, Nguyen DT, Silin D, Lyubomska O, De Vries RD, von Messling V, McQuaid S, De

- Swart RL, Duprex WP. Recombinant canine distemper virus strain Snyder Hill expressing green or red fluorescent proteins causes meningoencephalitis in the ferret. *J Virol* 2012;86:7508-19.
- [101] Silin D, Lyubomska O, Ludlow M, Duprex WP, Rima BK. Development of a challenge-protective vaccine concept by modifying the viral RNA-dependent RNA polymerase of canine distemper virus. *J Virol* 2007;81:13649-58.
- [102] Deliolanis NC, Kasmieh R, Wurdinger T, Tannous BA, Shah K, Ntziachristos V. Performance of the red-shifted fluorescent proteins in deep-tissue molecular imaging applications. *J Biomed Opt* 2008;13:044008.
- [103] Shaner NC, Campbell RE, Steinbach PA, Giepmans BN, Palmer AE, Tsien RY. Improved monomeric red, orange and yellow fluorescent proteins derived from *Discosoma* sp. red fluorescent protein. *Nat Biotechnol* 2004;22:1567-72.
- [104] Lieleg O, Vladescu I, Ribbeck K. Characterization of particle translocation through mucin hydrogels. *Biophys J* 2010;98:1782-9.
- [105] Rastogi D, Ratner AJ, Prince A. Host-bacterial interactions in the initiation of inflammation. *Paediatr Respir Rev* 2001;2:245-52.
- [106] Boyton RJ, Openshaw PJM. Pulmonary defences to acute respiratory infection. *Br Med Bull* 2002;61:1-12.
- [107] Seth RB, Sun L, Chen ZJ. Antiviral innate immunity pathways. *Cell Res* 2006;16:141-7.
- [108] Loo YM, Fornek J, Crochet N, Bajwa G, Perwitasari O, Martinez-Sobrido L, Akira S, Gill MA, Garcia-Sastre A, Katze MG, Gale M, Jr. Distinct RIG-I and MDA5 signaling by RNA viruses in innate immunity. *J Virol* 2008;82:335-45.
- [109] Kumar H, Kawai T, Akira S. Toll-like receptors and innate immunity. *Biochem Biophys Res Comm* 2009;388:621-5.
- [110] Sabbah A, Chang TH, Harnack R, Frohlich V, Tominaga K, Dube PH, Xiang Y, Bose S. Activation of innate immune antiviral responses by Nod2. *Nat Immunol* 2009;10:1073-80.
- [111] Yoneyama M, Kikuchi M, Natsukawa T, Shinobu N, Imaizumi T, Miyagishi M, Taira K, Akira S, Fujita T. The RNA helicase RIG-I has an essential function in double-stranded RNA-induced innate antiviral responses. *Nat Immunol* 2004;5:730-7.
- [112] Schroder M, Bowie AG. TLR3 in antiviral immunity: key player or bystander? *Trends Immunol* 2005;26:462-8.
- [113] Okabayashi T, Kojima T, Masaki T, Yokota SI, Imaizumi T, Tsutsumi H, Himi T, Fujii N, Sawada N. Type-III interferon, not type-I, is the predominant interferon induced by respiratory viruses in nasal epithelial cells. *Virus Res* 2011;160:360-6.
- [114] Rosenberg HF, Domachowske JB. Inflammatory responses to respiratory syncytial virus (RSV) infection and the development of immunomodulatory pharmacotherapeutics. *Curr Med Chem* 2012;19:1424-31.
- [115] Habibi MS, Openshaw PJ. Benefit and harm from immunity to respiratory syncytial virus: implications for treatment. *Curr Opin Infect Dis* 2012;25:687-94.
- [116] Garg R, Shrivastava P, van Drunen Littel-van den Hurk S. The role of dendritic cells in innate and adaptive immunity to respiratory syncytial virus, and implications for vaccine development. *Expert Rev Vaccines* 2012;11:1441-57.
- [117] Banchereau J, Briere F, Caux C, Davoust J, Lebecque S, Liu YJ, Pulendran B, Palucka K. Immunobiology of dendritic cells. *Annu Rev Immunol* 2000;18:767-811. 767-811.
- [118] Johnson TR, Johnson CN, Corbett KS, Edwards GC, Graham BS. Primary human mDC1, mDC2, and pDC dendritic cells are differentially infected and activated by respiratory syncytial virus. *PLoS ONE* 2011;6:e16458.

- [119] Le Nouen C, Hillyer P, Winter CC, McCarty T, Rabin RL, Collins PL, Buchholz UJ. Low CCR7-mediated migration of human monocyte derived dendritic cells in response to human respiratory syncytial virus and human metapneumovirus. *PLoS Pathog* 2011;7:e1002105.
- [120] Garofalo R, Welliver RC, Ogra PL. Clinical aspects of bronchial reactivity and cell-virus interaction. In: Ogra PL, Lamm ME, Bienenstock J, Mestecky J, Strober W, Mcghee JR, editors. *Mucosal Immunology*. 2 ed. San Diego:Academic Press; 1999. p. 1223-37.
- [121] Jafri HS. Role of chemokines in respiratory syncytial virus disease. *Pediatr Infect Dis J* 2002;21:454-6.
- [122] Johnson JE, Gonzales RA, Olson SJ, Wright PF, Graham BS. The histopathology of fatal untreated human respiratory syncytial virus infection. *Mod Pathol* 2007;20(1):108-19.
- [123] Everard ML, Swarbrick A, Wright M, McIntyre J, Dunkley C, James PD, Sewell HF, Milner AD. Analysis of cells obtained by bronchial lavage of infants with respiratory syncytial virus infection. *Arch Dis Child* 1994;71:428-32.
- [124] Holtzman MJ, Tyner JW, Kim EY, Lo MS, Patel AC, Shornick LP, Agapov E, Zhang Y. Acute and chronic airway responses to viral infection: implications for asthma and chronic obstructive pulmonary disease. *Proc Am Thorac Soc* 2005;2:132-40.
- [125] Lo MS, Brazas RM, Holtzman MJ. Respiratory syncytial virus nonstructural proteins NS1 and NS2 mediate inhibition of Stat2 expression and alpha/beta interferon responsiveness. *J Virol* 2005;79:9315-9.
- [126] Munir S, Le NC, Luongo C, Buchholz UJ, Collins PL, Bukreyev A. Nonstructural proteins 1 and 2 of respiratory syncytial virus suppress maturation of human dendritic cells. *J Virol* 2008;82:8780-96.
- [127] Gagro A, Tominac M, Krsulovic-Hresic V, Bace A, Matic M, Drazenovic V, Mlinaric-Galinovic G, Kosor E, Gotovac K, Bolanca I, Batinica S, Rabatic S. Increased Toll-like receptor 4 expression in infants with respiratory syncytial virus bronchiolitis. *Clin Exp Immunol* 2004;135:267-72.
- [128] Boukhvalova MS, Prince GA, Soroush L, Harrigan DC, Vogel SN, Blanco JC. The TLR4 agonist, monophosphoryl lipid A, attenuates the cytokine storm associated with respiratory syncytial virus vaccine-enhanced disease. *Vaccine* 2006;24:5027-35.
- [129] Kunzelmann K, Sun J, Meanger J, King NJ, Cook DI. Inhibition of airway Na<sup>+</sup> transport by respiratory syncytial virus. *J Virol* 2007;81:3714-20.
- [130] Miyairi I, Devincenzo JP. Human genetic factors and respiratory syncytial virus disease severity. *Clin Microbiol Rev* 2008;21:686-703.
- [131] Cyr SL, Angers I, Guillot L, Stoica-Popescu I, Lussier M, Qureshi S, Burt DS, Ward BJ. TLR4 and MyD88 control protection and pulmonary granulocytic recruitment in a murine intranasal RSV immunization and challenge model. *Vaccine* 2009;27:421-30.
- [132] Numata M, Chu HW, Dakhama A, Voelker DR. Pulmonary surfactant phosphatidylglycerol inhibits respiratory syncytial virus-induced inflammation and infection. *Proc Natl Acad Sci U S A* 2010;107:320-5.
- [133] Tal G, Mandelberg A, Dalal I, Cesar K, Somekh E, Tal A, Oron A, Itskovich S, Ballin A, Houry S, Beigelman A, Lider O, Rechavi G, Amariglio N. Association between common Toll-like receptor 4 mutations and severe respiratory syncytial virus disease. *J Infect Dis* 2004;189:2057-63.
- [134] Mandelberg A, Tal G, Naugolny L, Cesar K, Oron A, Houry S, Gilad E, Somekh E. Lipopolysaccharide hyporesponsiveness as a risk factor for intensive care unit hospitalization in infants with respiratory syncytial virus bronchiolitis. *Clin Exp Immunol* 2006;144:48-52.
- [135] Awomoyi AA, Rallabhandi P, Pollin TI, Lorenz E, Szein MB, Boukhvalova MS, Hemming VG, Blanco JC, Vogel SN. Association of TLR4 polymorphisms with symptomatic respiratory

- syncytial virus infection in high-risk infants and young children. *J Immunol* 2007;179:3171-7.
- [136] Paulus SC, Hirschfeld AF, Victor RE, Brunstein J, Thomas E, Turvey SE. Common human Toll-like receptor 4 polymorphisms--role in susceptibility to respiratory syncytial virus infection and functional immunological relevance. *Clin Immunol* 2007;123:252-7.
- [137] Douville RN, Lissitsyn Y, Hirschfeld AF, Becker AB, Kozyrskyj AL, Liem J, Bastien N, Li Y, Victor RE, Sekhon M, Turvey SE, HayGlass KT. TLR4 Asp299Gly and Thr399Ile polymorphisms: no impact on human immune responsiveness to LPS or respiratory syncytial virus. *PLoS One* 2010;5:e12087.
- [138] Lofgren J, Marttila R, Renko M, Ramet M, Hallman M. Toll-like receptor 4 Asp299Gly polymorphism in respiratory syncytial virus epidemics. *Pediatr Pulmonol* 2010;45:687-92.
- [139] Taylor G, Stott EJ, Hughes M, Collins AP. Respiratory syncytial virus infection in mice. *Infect Immun* 1984;43:649-55.
- [140] Devincenzo JP, Aitken J, Harrison L. Respiratory syncytial virus (RSV) loads in premature infants with and without prophylactic RSV fusion protein monoclonal antibody. *J Pediatr* 2003;143:123-6.
- [141] Piedra PA, Jewell AM, Cron SG, Atmar RL, Glezen WP. Correlates of immunity to respiratory syncytial virus (RSV) associated-hospitalization: establishment of minimum protective threshold levels of serum neutralizing antibodies. *Vaccine* 2003;21:3479-82.
- [142] Prince GA, Horswood RL, Chanock RM. Quantitative aspects of passive immunity to respiratory syncytial virus infection in infant cotton rats. *J Virol* 1985;55:517-20.
- [143] Tregoning JS, Schwarze J. Respiratory viral infections in infants: causes, clinical symptoms, virology, and immunology. *Clin Microbiol Rev* 2010;23:74-98.
- [144] Chandwani S, Borkowsky W, Krasinski K, Lawrence R, Welliver R. Respiratory syncytial virus infection in human immunodeficiency virus-infected children. *J Pediatr* 1990;117:251-4.
- [145] Alwan WH, Record FM, Openshaw PJM. CD4<sup>+</sup> T cells clear virus but augment disease in mice infected with respiratory syncytial virus. Comparison with the effects of CD8<sup>+</sup> T cells. *Clin Exp Immunol* 1992;88:527-36.
- [146] Cannon MJ, Stott EJ, Taylor G, Askonas BA. Clearance of persistent respiratory syncytial virus infections in immunodeficient mice following transfer of primed T cells. *Immunology* 1987;62:133-8.
- [147] Jans J, Vissers M, Heldens JG, de Jonge MI, Levy O, Ferwerda G. Fc gamma receptors in respiratory syncytial virus infections: implications for innate immunity. *Rev Med Virol* 2013;in press.
- [148] Kruijssen D, Bakkers MJ, van Uden NO, Viveen MC, van der Sluis TC, Kimpen JL, Leusen JH, Coenjaerts FE, Van Bleek GM. Serum antibodies critically affect virus-specific CD4<sup>+</sup>/CD8<sup>+</sup> T cell balance during respiratory syncytial virus infections. *J Immunol* 2010;185:6489-98.
- [149] Schijf MA, Lukens MV, Kruijssen D, van Uden NO, Garssen J, Coenjaerts FE, Van't LB, Van Bleek GM. Respiratory Syncytial Virus Induced Type I IFN Production by pDC Is Regulated by RSV-Infected Airway Epithelial Cells, RSV-Exposed Monocytes and Virus Specific Antibodies. *PLoS One* 2013;8:e81695.
- [150] Varga SM, Braciale TJ. The adaptive immune response to respiratory syncytial virus. *Curr Top Microbiol Immunol* 2013;372:155-71. doi: 10.1007/978-3-642-38919-1\_8.:155-71.
- [151] Guerrero-Plata A. Dendritic cells in human Pneumovirus and Metapneumovirus infections. *Viruses* 2013;5:1553-70.
- [152] Kilani RA. Respiratory syncytial virus (RSV) outbreak in the NICU: description of eight cases. *J Trop Pediatr* 2002;48:118-22.



- [153] Abadeso C, Almeida HI, Virella D, Carreiro MH, Machado MC. Use of palivizumab to control an outbreak of syncytial respiratory virus in a neonatal intensive care unit. *J Hosp Infect* 2004;58:38-41.
- [154] Groothuis J, Bauman J, Malinoski F, Eggleston M. Strategies for prevention of RSV nosocomial infection. *J Perinatol* 2008;28:319-23.
- [155] Kurz H, Herbich K, Janata O, Sterniste W, Bauer K. Experience with the use of palivizumab together with infection control measures to prevent respiratory syncytial virus outbreaks in neonatal intensive care units. *J Hosp Infect* 2008;70:246-52.
- [156] Fulginiti VA, Eller JJ, Sieber OF, Joyner JW, Minamitani M, Meiklejohn G. Respiratory virus immunization. I. A field trial of two inactivated respiratory virus vaccines; an aqueous trivalent parainfluenza virus vaccine and an alum-precipitated respiratory syncytial virus vaccine. *Am J Epidemiol* 1969;89:435-48.
- [157] Kapikian AZ, Mitchell RH, Chanock RM, Shvedoff RA, Stewart CE. An epidemiologic study of altered clinical reactivity to respiratory syncytial (RS) virus infection in children previously vaccinated with an inactivated RS virus vaccine. *Am J Epidemiol* 1969;89:405-21.
- [158] Kim HW, Canchola JG, Brandt CD, Pyles G, Chanock RM, Jensen K, Parrott RH. Respiratory syncytial virus disease in infants despite prior administration of antigenic inactivated vaccine. *Am J Epidemiol* 1969;89:422-34.
- [159] De Swart RL, Kuiken T, Timmerman HH, Van Amerongen G, van den Hoogen BG, Vos HW, Neijens HJ, Andeweg AC, Osterhaus ADME. Immunization of macaques with formalin-inactivated respiratory syncytial virus (RSV) induces interleukin-13-associated hypersensitivity to subsequent RSV infection. *J Virol* 2002;76:11561-9.
- [160] Graham BS. Pathogenesis of respiratory syncytial virus vaccine-augmented pathology. *Am J Respir Crit Care Med* 1995;152:S63-S66.
- [161] Connors M, Kulkarni AB, Firestone C-Y, Holmes KL, Morse III HC, Sotnikov AV, Murphy BR. Pulmonary histopathology induced by respiratory syncytial virus (RSV) challenge of formalin-inactivated RSV-immunized BALB/c mice is abrogated by depletion of CD4<sup>+</sup> T cells. *J Virol* 1992;66:7444-51.
- [162] Graham BS, Henderson GS, Tang Y-W, Lu X, Neuzil KM, Colley DG. Priming immunization determines T helper cytokine mRNA expression patterns in lungs of mice challenged with respiratory syncytial virus. *J Immunol* 1993;151:2032-40.
- [163] Connors M, Giese NA, Kulkarni AB, Firestone C-Y, Morse III HC, Murphy BR. Enhanced pulmonary histopathology induced by respiratory syncytial virus (RSV) challenge of formalin-inactivated RSV-immunized BALB/c mice is abrogated by depletion of interleukin-4 (IL-4) and IL-10. *J Virol* 1994;68:5321-5.
- [164] Hussell T, Baldwin CJ, O'Garra A, Openshaw PJM. CD8<sup>+</sup> T cells control Th2-driven pathology during pulmonary respiratory syncytial virus infection. *Eur J Immunol* 1997;27:3341-9.
- [165] Olson MR, Varga SM. CD8<sup>+</sup> T-Cells Inhibit Respiratory Syncytial Virus (RSV) Vaccine-Enhanced Disease. *J Immunol* 2007;179:5415-24.
- [166] Polack FP, Teng MN, Collins PL, Prince GA, Exner M, Regele H, Lirman DD, Rabold R, Hoffman SJ, Karp CL, Kleeberger SR, Wills-Karp M, Karron RA. A role for immune complexes in enhanced respiratory syncytial virus disease. *J Exp Med* 2002;196:859-65.
- [167] Delgado MF, Coviello S, Monsalvo AC, Melendi GA, Hernandez JZ, Batalle JP, Diaz L, Trento A, Chang HY, Mitzner W, Ravetch J, Melero JA, Irusta PM, Polack FP. Lack of antibody affinity maturation due to poor Toll-like receptor stimulation leads to enhanced respiratory syncytial virus disease. *Nat Med* 2009;15:34-41.

## Chapter 10

- [168] Graham BS. Biological challenges and technological opportunities for respiratory syncytial virus vaccine development. *Immunol Rev* 2011;239:149-66.
- [169] Collins PL, Murphy BR. New generation live vaccines against human respiratory syncytial virus designed by reverse genetics. *Proc Am Thorac Soc* 2005;2:166-73.
- [170] Power UF. Respiratory syncytial virus (RSV) vaccines--two steps back for one leap forward. *J Clin Virol* 2008;41:38-44.
- [171] Hurwitz JL. Respiratory syncytial virus vaccine development. *Expert Rev Vaccines* 2011;10:1415-33.
- [172] Rudraraju R, Jones BG, Sealy R, Surman SL, Hurwitz JL. Respiratory syncytial virus: current progress in vaccine development. *Viruses* 2013;5:577-94.
- [173] Lindsey B, Kampmann B, Jones C. Maternal immunization as a strategy to decrease susceptibility to infection in newborn infants. *Curr Opin Infect Dis* 2013;26:248-53.
- [174] Parrott RH, Kim HW, Arrobio JO, Hodes DS, Murphy BR, Brandt CD, Camargo E, Chanock RM. Epidemiology of respiratory syncytial virus infection in Washington, D.C. II. Infection and disease with respect to age, immunologic status, race and sex. *Am J Epidemiol* 1973;98:289-300.
- [175] Domachowske JB, Rosenberg HF. Respiratory syncytial virus infection: immune response, immunopathogenesis, and treatment. *Clin Microbiol Rev* 1999;12:298-309.
- [176] Brandenburg AH, Groen J, Van Steensel-Moll HA, Claas EJC, Rothbarth PH, Neijens HJ, Osterhaus ADME. Respiratory syncytial virus specific serum antibodies in infants under six months of age: limited serological response upon infection. *J Med Virol* 1997;52:97-104.
- [177] Groothuis JR, Hoopes JM, Hemming VG. Prevention of serious respiratory syncytial virus-related illness. II: Immunoprophylaxis. *Adv Ther* 2011;28:110-25.
- [178] Mejias A, Ramilo O. Review of palivizumab in the prophylaxis of respiratory syncytial virus (RSV) in high-risk infants. *Biologics* 2008;2:433-9.
- [179] Wu H, Pfarr DS, Losonsky GA, Kiener PA. Immunoprophylaxis of RSV infection: advancing from RSV-IGIV to palivizumab and motavizumab. *Curr Top Microbiol Immunol* 2008;317:103-23.:103-23.
- [180] Groothuis JR, Simoes EAF, Levin MJ, Hall CB, Long CE, Rodriguez WJ, Arrobio J, Meissner HC, Fulton DR, Welliver RC, Tristram DA, Siber GR, Prince GA, Van Raden M, Hemming VG, The Respiratory Syncytial Virus Immune Globulin Study Group. Prophylactic administration of respiratory syncytial virus immune globulin to high-risk infants and young children. *N Engl J Med* 1993;329:1524-30.
- [181] Wu H, Pfarr DS, Johnson S, Brewah YA, Woods RM, Patel NK, White WI, Young JF, Kiener PA. Development of motavizumab, an ultra-potent antibody for the prevention of respiratory syncytial virus infection in the upper and lower respiratory tract. *J Mol Biol* 2007;368:652-65.
- [182] Beeler JA, van Wyke CK. Neutralization epitopes of the F glycoprotein of respiratory syncytial virus: effect of mutation upon fusion function. *J Virol* 1989;63:2941-50.
- [183] Johnson S, Oliver C, Prince GA, Hemming VG, Pfarr DS, Wang SC, Dormitzer M, O'Grady J, Koenig S, Tamura JK, Woods R, Bansal G, Couchenour D, Tsao E, Hall WC, Young JF. Development of a humanized monoclonal antibody (MEDI-493) with potent *in vitro* and *in vivo* activity against respiratory syncytial virus. *J Infect Dis* 1997;176:1215-24.
- [184] Rietveld E, Steyerberg EW, Polder JJ, Veeze HJ, Vergouwe Y, Huysman MW, de Groot R, Moll HA. Passive immunisation against respiratory syncytial virus: a cost-effectiveness analysis. *Arch Dis Child* 2010;95:493-8.
- [185] Brand PL. Respiratory syncytial virus and recurrent wheeze. *N Engl J Med* 2013;369:782.

- [186] Zhu Q, McAuliffe JM, Patel NK, Palmer-Hill FJ, Yang CF, Liang B, Su L, Zhu W, Wachter L, Wilson S, MacGill RS, Krishnan S, McCarthy MP, Losonsky GA, Suzich JA. Analysis of respiratory syncytial virus preclinical and clinical variants resistant to neutralization by monoclonal antibodies palivizumab and/or motavizumab. *J Infect Dis* 2011;203:674-82.
- [187] Gill MA, Welliver RC. Motavizumab for the prevention of respiratory syncytial virus infection in infants. *Expert Opin Biol Ther* 2009;9(10):1335-45.
- [188] Carbonell-Estrany X, Simoes EA, Dagan R, Hall CB, Harris B, Hultquist M, Connor EM, Losonsky GA. Motavizumab for prophylaxis of respiratory syncytial virus in high-risk children: a noninferiority trial. *Pediatrics* 2010;125:e35-e51.
- [189] Wu SJ, Schmidt A, Beil EJ, Day ND, Branigan PJ, Liu C, Gutshall LL, Palomo C, Furze J, Taylor G, Melero JA, Tsui P, Del Vecchio AM, Kruszynski M. Characterization of the epitope for anti-human respiratory syncytial virus F protein monoclonal antibody 101F using synthetic peptides and genetic approaches. *J Gen Virol* 2007;88:2719-23.
- [190] McLellan JS, Yang Y, Graham BS, Kwong PD. Structure of respiratory syncytial virus fusion glycoprotein in the postfusion conformation reveals preservation of neutralizing epitopes. *J Virol* 2011;85:7788-96.
- [191] Corti D, Bianchi S, Vanzetta F, Minola A, Perez L, Agatic G, Guarino B, Silacci C, Marcandalli J, Marsland BJ, Piralla A, Percivalle E, Sallusto F, Baldanti F, Lanzavecchia A. Cross-neutralization of four paramyxoviruses by a human monoclonal antibody. *Nature* 2013;501:439-43.
- [192] Wright M, Piedimonte G. Respiratory syncytial virus prevention and therapy: past, present, and future. *Pediatr Pulmonol* 2011;46:324-47.
- [193] Broughton S, Greenough A. Drugs for the management of respiratory syncytial virus infection. *Curr Opin Investig Drugs* 2004;5:862-5.
- [194] Chu HY, Englund JA. Respiratory syncytial virus disease: prevention and treatment. *Curr Top Microbiol Immunol* 2013;372:235-58.
- [195] Kneyber MC, Blusse vO-A, van VM, Uiterwaal CS, Kimpen JL, van Vught AJ. Concurrent bacterial infection and prolonged mechanical ventilation in infants with respiratory syncytial virus lower respiratory tract disease. *Intensive Care Med* 2005;31:680-5.
- [196] Thorburn K, Harigopal S, Reddy V, Taylor N, van Saene HK. High incidence of pulmonary bacterial co-infection in children with severe respiratory syncytial virus (RSV) bronchiolitis. *Thorax* 2006;61:611-5.
- [197] Sims DG, Downham MA, Gardner PS, Webb JK, Weightman D. Study of 8-year-old children with a history of respiratory syncytial virus bronchiolitis in infancy. *Br Med J* 1978;1:11-4.
- [198] McConnochie KM, Roghmann KJ. Bronchiolitis as a possible cause of wheezing in childhood: new evidence. *Pediatrics* 1984;74:1-10.
- [199] Mok JY, Simpson H. Outcome for acute bronchitis, bronchiolitis, and pneumonia in infancy. *Arch Dis Child* 1984;59:306-9.
- [200] Murray M, Webb MS, O'Callaghan C, Swarbrick AS, Milner AD. Respiratory status and allergy after bronchiolitis. *Arch Dis Child* 1992;67:482-7.
- [201] Osundwa VM, Dawod ST, Ehlayel M. Recurrent wheezing in children with respiratory syncytial virus (RSV) bronchiolitis in Qatar. *Eur J pediatr* 1993;152:1001-3.
- [202] Noble V, Murray M, Webb MS, Alexander J, Swarbrick AS, Milner AD. Respiratory status and allergy nine to 10 years after acute bronchiolitis. *Arch Dis Child* 1997;76:315-9.
- [203] Stein RT, Sherrill D, Morgan WJ, Holberg CJ, Halonen M, Taussig LM, Wright AL, Martinez FD. Respiratory syncytial virus in early life and risk of wheeze and allergy by age 13 years. *Lancet* 1999;354:541-5.

## Chapter 10

- [204] Sigurs N, Bjarnason R, Sigurbergsson F, Kjellman B. Respiratory syncytial virus bronchiolitis in infancy is an important risk factor for asthma and allergy at age 7. *Am J Respir Crit Care Med* 2000;161:1501-7.
- [205] Krishnamoorthy N, Khare A, Oriss TB, Raundhal M, Morse C, Yarlagadda M, Wenzel SE, Moore ML, Peebles RS, Jr., Ray A, Ray P. Early infection with respiratory syncytial virus impairs regulatory T cell function and increases susceptibility to allergic asthma. *Nat Med* 2012;18:1525-30.
- [206] Blanken MO, Rovers MM, Molenaar JM, Winkler-Seinstra PL, Meijer A, Kimpen JL, Bont L. Respiratory syncytial virus and recurrent wheeze in healthy preterm infants. *N Engl J Med* 2013;368:1791-9.
- [207] Hallak LK, Kwilas SA, Peeples ME. Interaction between respiratory syncytial virus and glycosaminoglycans, including heparan sulfate. *Methods Mol Biol* 2007;379:15-34.
- [208] Gray TE, Guzman K, Davis CW, Abdullah LH, Nettekheim P. Mucociliary differentiation of serially passaged normal human tracheobronchial epithelial cells. *Am J Respir Cell Mol Biol* 1996;14:104-12.
- [209] Belshe RB, Richardson LS, London WT, Sly DL, Lorfeld JH, Camargo E, Prevar DA, Chanock RM. Experimental respiratory syncytial infection of four species of primates. *J Med Virol* 1977;1:157-62.
- [210] Murphy BR, Hall SL, Kulkarni AB, Crowe Jr. JE, Collins PL, Connors M, Karron RA, Chanock RM. An update on approaches to the development of respiratory syncytial virus (RSV) and parainfluenza virus type 3 (PIV3) vaccines. *Virus Res* 1994;32:13-36.
- [211] Hancock GE, Smith JD, Heers KM. Serum neutralizing antibody titers of seropositive chimpanzees immunized with vaccines coformulated with natural fusion and attachment proteins of respiratory syncytial virus. *J Infect Dis* 2000;181:1768-71.
- [212] Teng MN, Whitehead SS, Bermingham A, St CM, Elkins WR, Murphy BR, Collins PL. Recombinant respiratory syncytial virus that does not express the NS1 or M2-2 protein is highly attenuated and immunogenic in chimpanzees. *J Virol* 2000;74:9317-21.
- [213] Prince GA, Suffin SC, Prevar DA, Camargo E, Sly DL, London WT, Chanock RM. Respiratory syncytial virus infection in owl monkeys: viral shedding, immunological response, and associated illness caused by wild-type virus and two temperature-sensitive mutants. *Infect Immun* 1979;26:1009-13.
- [214] Graham BS, Perkins MD, Wright PF, Karzon DT. Primary respiratory syncytial virus infection in mice. *J Med Virol* 1988;26:153-62.
- [215] Openshaw PJM. Immunity and immunopathology to respiratory syncytial virus. The mouse model. *Am J Respir Crit Care Med* 1995;152:S59-S62.
- [216] Stark JM, McDowell SA, Koenigsknecht V, Prows DR, Leikauf JE, Le Vine AM, Leikauf GD. Genetic susceptibility to respiratory syncytial virus infection in inbred mice. *J Med Virol* 2002;67:92-100.
- [217] Jafri HS, Chavez-Bueno S, Mejias A, Gomez AM, Rios AM, Nassi SS, Yusuf M, Kapur P, Hardy RD, Hatfield J, Rogers BB, Krisher K, Ramilo O. Respiratory syncytial virus induces pneumonia, cytokine response, airway obstruction, and chronic inflammatory infiltrates associated with long-term airway hyperresponsiveness in mice. *J Infect Dis* 2004;189:1856-65.
- [218] Stokes KL, Chi MH, Sakamoto K, Newcomb DC, Currier MG, Huckabee MM, Lee S, Goleniewska K, Pretto C, Williams JV, Hotard A, Sherrill TP, Peebles RS, Jr., Moore ML. Differential pathogenesis of respiratory syncytial virus clinical isolates in BALB/c mice. *J Virol* 2011;85:5782-93.
- [219] Prince GA, Jensen AB, Horswood RL, Camargo E, Chanock RM. The pathogenesis of

- respiratory syncytial virus infection in cotton rats. *Am J Pathol* 1978;93:771-91.
- [220] Boukhvalova MS, Prince GA, Blanco JCG. The cotton rat model of respiratory viral infections. *Biologicals* 2009;37:152-9.
- [221] Green MG, Huey D, Niewiesk S. The cotton rat (*Sigmondon hispidus*) as an animal model for respiratory tract infections with human pathogens. *Lab Anim (NY)* 2013;42:170-6.
- [222] Dreizin RS, Vyshnevetskaia LO, Bagdamian EE, Iankevich OD, Tarasova LB. [Experimental RSV infection of cotton rats. A viral and immunofluorescent study]. *Vopr Virusol* 1971;16:670-6.
- [223] Zhao X, Chen FP, Sullender WM. Respiratory syncytial virus escape mutant derived *in vitro* resists palivizumab prophylaxis in cotton rats. *Virology* 2004;318:608-12.
- [224] Zhao X, Chen FP, Megaw AG, Sullender WM. Variable resistance to palivizumab in cotton rats by respiratory syncytial virus mutants. *J Infect Dis* 2004;190:1941-6.
- [225] Zeitlin L, Bohorov O, Bohorova N, Hiatt A, Kim dH, Pauly MH, Velasco J, Whaley KJ, Barnard DL, Bates JT, Crowe JE, Jr., Piedra PA, Gilbert BE. Prophylactic and therapeutic testing of Nicotiana-derived RSV-neutralizing human monoclonal antibodies in the cotton rat model. *MAbs* 2013;5:263-9.
- [226] Bem RA, Domachowske JB, Rosenberg HF. Animal models of human respiratory syncytial virus disease. *Am J Physiol Lung Cell Mol Physiol* 2011;301:L148-L156.
- [227] Taylor G, Thomas LH, Wyld SG, Furze J, Sopp P, Howard CJ. Role of T-lymphocyte subsets in recovery from respiratory syncytial virus infection in calves. *J Virol* 1995;69:6658-64.
- [228] Antonis AFG, Schrijver RS, Daus FJ, Steverink PJGM, Stockhofe N, Hensen EJ, Langedijk JPM, Van der Most RG. Vaccine-induced immunopathology during bovine respiratory syncytial virus infection: exploring the parameters of pathogenesis. *J Virol* 2003;77:12067-73.
- [229] Antonis AFG, Claassen EAW, Hensen EJ, Groot RJ, Groot-Mijnes JDF, Schrijver RS, Van der Most RG. Kinetics of antiviral CD8<sup>+</sup> T-cell responses during primary and post-vaccination secondary bovine respiratory syncytial virus infection. *Vaccine* 2006;24:1551-61.
- [230] Derscheid RJ, Ackermann MR. Perinatal lamb model of respiratory syncytial virus (RSV) infection. *Viruses* 2012;4:2359-78.
- [231] Derscheid RJ, Gallup JM, Knudson CJ, Varga SM, Grosz DD, van GA, Hostetter SJ, Ackermann MR. Effects of Formalin-Inactivated Respiratory Syncytial Virus (FI-RSV) in the Perinatal Lamb Model of RSV. *PLoS One* 2013;8:e81472.
- [232] Collins PL, Crowe Jr. JE. Respiratory syncytial virus and metapneumovirus. In: Knipe DM, Howley PM, editors. *Fields Virology*. 5 ed. Philadelphia: Lippincott Williams & Wilkins; 2007. p. 1601-46.
- [233] Neilson KA, Yunis EJ. Demonstration of respiratory syncytial virus in an autopsy series. *Pediatr Pathol* 1990;10:491-502.
- [234] Lazar I. Human metapneumovirus and severity of respiratory syncytial virus disease. *Emerg Infect Dis* 2004;10:1318-20.
- [235] Semple MG, Cowell A, Dove W, Greensill J, McNamara PS, Halfhide C, Shears P, Smyth RL, Hart CA. Dual infection of infants by human metapneumovirus and human respiratory syncytial virus is strongly associated with severe bronchiolitis. *J Infect Dis* 2005;191(3):382-6.
- [236] Timmons OD, Yamauchi T, Collins SR, Newbern DG, Sweatt JA, Jacobs RF. Association of respiratory syncytial virus and *Streptococcus pneumoniae* infection in young infants. *Pediatr Infect Dis J* 1987;6:1134-5.
- [237] Duttweiler L, Nadal D, Frey B. Pulmonary and systemic bacterial co-infections in severe RSV bronchiolitis. *Arch Dis Child* 2004;89:1155-7.

- [238] Jansen AGSC, Sanders EAM, van der Ende ME, van Loon AM, Hoes AW, Hak E. Invasive pneumococcal and meningococcal disease: association with influenza virus and respiratory syncytial virus activity? *Epidemiol Infect* 2008;136:1448-54.
- [239] Murdoch DR, Jennings LC. Association of respiratory virus activity and environmental factors with the incidence of invasive pneumococcal disease. *J Infect* 2009;58:37-46.
- [240] McGillivray G, Mason KM, Jurcisek JA, Peebles ME, Bakaletz LO. Respiratory syncytial virus-induced dysregulation of expression of a mucosal beta-defensin augments colonization of the upper airway by non-typeable *Haemophilus influenzae*. *Cell Microbiol* 2009;11:1399-408.
- [241] Heikkinen T. The role of respiratory viruses in otitis media. *Vaccine* 2000;19 Suppl 1:S51-S55.
- [242] Hament JM, Kimpen JL, Fleer A, Wolfs TF. Respiratory viral infection predisposing for bacterial disease: a concise review. *FEMS Immunol Med Microbiol* 1999;26:189-95.
- [243] O'Brien KL, Walters MI, Sellman J, Quinlisk P, Regnery H, Schwartz B, Dowell SF. Severe pneumococcal pneumonia in previously healthy children: the role of preceding influenza infection. *Clin Infect Dis* 2000;30:784-9.
- [244] Ampofo K, Bender J, Sheng X, Korgenski K, Daly J, Pavia AT, Byington CL. Seasonal invasive pneumococcal disease in children: role of preceding respiratory viral infection. *Pediatrics* 2008;122:229-37.
- [245] Avadhanula V, Rodriguez CA, Devincenzo JP, Wang Y, Webby RJ, Ulett GC, Adderson EE. Respiratory viruses augment the adhesion of bacterial pathogens to respiratory epithelium in a viral species- and cell type-dependent manner. *J Virol* 2006;80:1629-36.
- [246] Hussell T, Williams A. Menage a trois of bacterial and viral pulmonary pathogens delivers coup de grace to the lung. *Clin Exp Immunol* 2004;137:8-11.
- [247] Boehme KW, Compton T. Innate sensing of viruses by toll-like receptors. *J Virol* 2004;78:7867-73.
- [248] Droemann D, Goldmann T, Branscheid D, Clark R, Dalhoff K, Zabel P, Vollmer E. Toll-like receptor 2 is expressed by alveolar epithelial cells type II and macrophages in the human lung. *Histochem Cell Biol* 2003;119:103-8.
- [249] Phipps S, Lam CE, Foster PS, Matthaei KI. The contribution of toll-like receptors to the pathogenesis of asthma. *Immunol Cell Biol* 2007;85:463-70.
- [250] Regueiro V, Moranta D, Campos MA, Margareto J, Garmendia J, Bengoechea JA. *Klebsiella pneumoniae* increases the levels of Toll-like receptors 2 and 4 in human airway epithelial cells. *Infect Immun* 2009;77:714-24.
- [251] Zhang J, Li G, Bafica A, Pantelic M, Zhang P, Broxmeyer H, Liu Y, Wetzler L, He JJ, Chen T. *Neisseria gonorrhoeae* enhances infection of dendritic cells by HIV type 1. *J Immunol* 2005;174:7995-8002.
- [252] Thibault S, Tardif MR, Barat C, Tremblay Mj. TLR2 signaling renders quiescent naive and memory CD4<sup>+</sup> T cells more susceptible to productive infection with X4 and R5 HIV-type 1. *J Immunol* 2007;179:4357-66.
- [253] De Jong MAWP, De Witte L, Oudhoff MJ, Gringhuis SI, Gallay P, Geijtenbeek TBH. TNF-alpha and TLR agonists increase susceptibility to HIV-1 transmission by human Langerhans cells *ex vivo*. *J Clin Invest* 2008;118:3440-52.
- [254] Ogawa Y, Kawamura T, Kimura T, Ito M, Blauvelt A, Shimada S. Gram-positive bacteria enhance HIV-1 susceptibility in Langerhans cells, but not in dendritic cells, via Toll-like receptor activation. *Blood* 2009;113:5157-66.
- [255] Thibault S, Fromentin R, Tardif MR, Tremblay Mj. TLR2 and TLR4 triggering exerts contrasting effects with regard to HIV-1 infection of human dendritic cells and subsequent virus transfer

- to CD4<sup>+</sup> T cells. *Retrovirology* 2009;6:42.
- [256] Hallak LK, Collins PL, Knudson W, Peeples ME. Iduronic acid-containing glycosaminoglycans on target cells are required for efficient respiratory syncytial virus infection. *Virology* 2000;271:264-75.
- [257] Meng G, Rutz M, Schiemann M, Metzger J, Grabiec A, Schwandner R, Luppa PB, Ebel F, Busch DH, Bauer S, Wagner H, Kirschning CJ. Antagonistic antibody prevents toll-like receptor 2-driven lethal shock-like syndromes. *J Clin Invest* 2004;113:1473-81.
- [258] Parcina M, Wendt C, Goetz F, Zawatzky R, Zahringer U, Heeg K, Bekeredjian-Ding I. *Staphylococcus aureus*-induced plasmacytoid dendritic cell activation is based on an IgG-mediated memory response. *J Immunol* 2008;181:3823-33.
- [259] Buwitt-Beckmann U, Heine H, Wiesmuller KH, Jung G, Brock R, Akira S, Ulmer AJ. Toll-like receptor 6-independent signaling by diacylated lipopeptides. *Eur J Immunol* 2005;35:282-9.
- [260] Ebbesen P. DEAE-dextran and polybrene cation enhancement and dextran sulfate anion inhibition of immune cytolysis. *J Immunol* 1972;109:1296-9.
- [261] Konopka K, Stamatatos L, Larsen CE, Davis BR, Duzgunes N. Enhancement of human immunodeficiency virus type 1 infection by cationic liposomes: the role of CD4, serum and liposome-cell interactions. *J Gen Virol* 1991;72:2685-96.
- [262] Roan NR, Munch J, Arhel N, Mothes W, Neidleman J, Kobayashi A, Smith-McCune K, Kirchhoff F, Greene WC. The cationic properties of SEVI underlie its ability to enhance human immunodeficiency virus infection. *J Virol* 2009;83:73-80.
- [263] Lamb RA, Jardetzky TS. Structural basis of viral invasion: lessons from paramyxovirus F. *Curr Opin Struct Biol* 2007;17:427-36.
- [264] Jin MS, Kim SE, Heo JY, Lee ME, Kim HM, Paik SG, Lee H, Lee JO. Crystal structure of the TLR1-TLR2 heterodimer induced by binding of a tri-acylated lipopeptide. *Cell* 2007;130:1071-82.
- [265] Wolf B, Uhl B, Hauschildt S, Metzger J, Jung G, Bessler WG. Interaction of the lymphoid cell line BCL1 with lipopeptide analogues of bacterial lipoprotein: electron energy loss spectroscopy (EELS) as a novel method to detect the distribution of the activator within the cells. *Immunobiol* 1989;180:93-100.
- [266] Rossi CR, Kiesel GK. Bovine respiratory syncytial virus infection of bovine embryonic lung cultures: enhancement of infectivity with diethylaminoethyl-dextran and virus-infected cells. *Arch Virol* 1978;56:227-36.
- [267] Hallak LK, Spillmann D, Collins PL, Peeples ME. Glycosaminoglycan sulfation requirements for respiratory syncytial virus infection. *J Virol* 2000;74:10508-13.
- [268] Münch J, Rucker E, Ständker L, Adermann K, Goffinet C, Schindler M, Wildum S, Chinnadurai R, Rajan D, Specht A, Gimenez-Gallego G, Sanchez PC, Fowler DM, Koulov A, Kelly JW, Mothes W, Grivel JC, Margolis L, Keppler OT, Forssmann WG, Kirchhoff F. Semen-derived amyloid fibrils drastically enhance HIV infection. *Cell* 2007;131:1059-71.
- [269] Davis HE, Rosinski M, Morgan JR, Yarmush ML. Charged polymers modulate retrovirus transduction via membrane charge neutralization and virus aggregation. *Biophys J* 2004;86:1234-42.
- [270] Trkola A, Gordon C, Matthews J, Maxwell E, Ketas T, Czaplowski L, Proudfoot AE, Moore JP. The CC-chemokine RANTES increases the attachment of human immunodeficiency virus type 1 to target cells via glycosaminoglycans and also activates a signal transduction pathway that enhances viral infectivity. *J Virol* 1999;73:6370-9.
- [271] Elliott MB, Tebbey PW, Pryharski KS, Scheuer CA, Laughlin TS, Hancock GE. Inhibition of respiratory syncytial virus infection with the CC chemokine RANTES (CCL5). *J Med Virol*

- 2004;73:300-8.
- [272] Akira S. Mammalian Toll-like receptors. *Curr Opin Immunol* 2003;15:5-11.
- [273] Khan S, Bijker MS, Weterings JJ, Tanke HJ, Adema GJ, van Hall T, Drijfhout JW, Melief CJM, Overkleef HS, van der Marel GA, Filippov DV, van der Burg SH, Ossendorp F. Distinct uptake mechanisms but similar intracellular processing of two different toll-like receptor ligand-peptide conjugates in dendritic cells. *J Biol Chem* 2007;282:21145-59.
- [274] Lombardi V, Van Overtvelt L, Horiot S, Moussu H, Chabre H, Louise A, Balazuc AM, Mascarell L, Moingeon P. Toll-like receptor 2 agonist Pam3CSK4 enhances the induction of antigen-specific tolerance via the sublingual route. *Clin Exp Allergy* 2008;38:1819-29.
- [275] Khan S, Weterings JJ, Britten CM, de Jong AR, Graafland D, Melief CJ, van der Burg SH, van der Marel G, Overkleef HS, Filippov DV, Ossendorp F. Chirality of TLR-2 ligand Pam(3)CysSK(4) in fully synthetic peptide conjugates critically influences the induction of specific CD8<sup>+</sup> T-cells. *Mol Immunol* 2009;46:1084-91.
- [276] Collins PL, Murphy BR. Respiratory syncytial virus: reverse genetics and vaccine strategies. *Virology* 2002;296:204-11.
- [277] Ten Berge B, Muskens F, Kleinjan A, Hammad H, Hoogsteden HC, Lambrecht BN, Van den Blink B. A novel method for isolating dendritic cells from human bronchoalveolar lavage fluid. *J Immunol Methods* 2009;351:13-23.
- [278] Van Binnendijk RS, Poelen MCM, Kuijpers KC, Osterhaus ADME, UytdeHaag FGCM. The predominance of CD8<sup>+</sup> T cells after infection with measles virus suggests a role for CD8<sup>+</sup> class I MHC-restricted cytotoxic T lymphocytes (CTL) in recovery from measles. *J Immunol* 1990;144:2394-9.
- [279] Allard SD, Pletinckx K, Breckpot K, Heirman C, Bonehill A, Michiels A, Van Baalen CA, Gruters RA, Osterhaus ADME, Lacor P, Thielemans K, Aerts JL. Functional T-cell responses generated by dendritic cells expressing the early HIV-1 proteins Tat, Rev and Nef. *Vaccine* 2008;26:3735-41.
- [280] de Graaf M, Herfst S, Schrauwen EJ, van den Hoogen BG, Osterhaus ADME, Fouchier RAM. An improved plaque reduction virus neutralization assay for human metapneumovirus. *J Virol Methods* 2007;143:169-74.
- [281] Hashimoto K, Ono N, Tatsuo H, Minagawa H, Takeda M, Takeuchi K, Yanagi Y. SLAM (CD150)-independent measles virus entry as revealed by recombinant virus expressing green fluorescent protein. *J Virol* 2002;76:6743-9.
- [282] De Vries RD, Lemon K, Ludlow M, McQuaid S, Yüksel S, Van Amerongen G, Rennick LJ, Rima BK, Osterhaus ADME, De Swart RL, Duprex WP. *In vivo* tropism of attenuated and pathogenic measles virus expressing green fluorescent protein in macaques. *J Virol* 2010;84:4714-24.
- [283] Harder TC, Osterhaus ADME. Canine distemper virus - a morbillivirus in search of new hosts? *Trends Microbiol* 1997;5:120-4.
- [284] Nguyen DT, De Witte L, Ludlow M, Yüksel S, Wiesmuller K-H, Geijtenbeek TBH, Osterhaus ADME, De Swart RL. The synthetic bacterial lipopeptide Pam3CSK4 modulates respiratory syncytial virus infection independent of TLR activation. *PLoS Pathog* 2010;6:e1001049.
- [285] Takeuchi O, Sato S, Horiuchi T, Hoshino K, Takeda K, Dong Z, Modlin RL, Akira S. Cutting edge: role of Toll-like receptor 1 in mediating immune response to microbial lipoproteins. *J Immunol* 2002;169:10-4.
- [286] Seki F, Ono N, Yamaguchi R, Yanagi Y. Efficient isolation of wild strains of canine distemper virus in Vero cells expressing canine SLAM (CD150) and their adaptability to marmoset B95a cells. *J Virol* 2003;77:9943-50.



- [287] Scagliarini A, Dal Pozzo F, Gallina L, Vaccari F, Morganti L. TaqMan based real time PCR for the quantification of canine distemper virus. *Vet Res Commun* 2007;31 (Suppl. 1):261-3.
- [288] Van Kaer L. Alpha-Galactosylceramide therapy for autoimmune diseases: prospects and obstacles. *Nat Rev Immunol* 2005;5:31-42.
- [289] Ko SY, Ko HJ, Chang WS, Park SH, Kweon MN, Kang CY. alpha-Galactosylceramide can act as a nasal vaccine adjuvant inducing protective immune responses against viral infection and tumor. *J Immunol* 2005;175:3309-17.
- [290] Kopecky-Bromberg SA, Fraser KA, Pica N, Carnero E, Moran TM, Franck RW, Tsuji M, Palese P. Alpha-C-galactosylceramide as an adjuvant for a live attenuated influenza virus vaccine. *Vaccine* 2009;27:3766-74.
- [291] BenMohamed L, Wechsler SL, Nesburn AB. Lipopeptide vaccines--yesterday, today, and tomorrow. *Lancet Infect Dis* 2002;2:425-31.
- [292] Deres K, Schild H, Wiesmuller KH, Jung G, Rammensee HG. *In vivo* priming of virus-specific cytotoxic T lymphocytes with synthetic lipopeptide vaccine. *Nature* 1989;342:561-4.
- [293] BenMohamed L, Gras-Masse H, Tartar A, Daubersies P, Brahimi K, Bossus M, Thomas A, Druilhe P. Lipopeptide immunization without adjuvant induces potent and long-lasting B, T helper, and cytotoxic T lymphocyte responses against a malaria liver stage antigen in mice and chimpanzees. *Eur J Immunol* 1997;27(5):1242-53.
- [294] Jayakumar A, Castilho TM, Park E, Goldsmith-Pestana K, Blackwell JM, Mahon-Pratt D. TLR1/2 activation during heterologous prime-boost vaccination (DNA-MVA) enhances CD8<sup>+</sup> T Cell responses providing protection against Leishmania (Viannia). *PLoS Negl Trop Dis* 2011;5:e1204.
- [295] Stegmann T, Kamphuis T, Meijerhof T, Goud E, De Haan A, Wilschut J. Lipopeptide-adjuvanted respiratory syncytial virus virosomes: A safe and immunogenic non-replicating vaccine formulation. *Vaccine* 2010;28:5543-50.
- [296] Schultz RD, Thiel B, Mukhtar E, Sharp P, Larson LJ. Age and long-term protective immunity in dogs and cats. *J Comp Pathol* 2010;142:S102-S108.
- [297] Stephensen CB, Welter J, Thaker SR, Taylor J, Tartaglia J, Paoletti E. Canine distemper virus infection of ferrets as a model for testing morbillivirus vaccine strategies: NYVAC-and ALVAC-based CDV recombinants protect against symptomatic infection. *J Virol* 1997;71:1506-13.
- [298] Falsey AR, Walsh EE, Looney RJ, Kolassa JE, Formica MA, Criddle MC, Hall WJ. Comparison of respiratory syncytial virus humoral immunity and response to infection in young and elderly adults. *J Med Virol* 1999;59(2):221-6.
- [299] Falsey AR, Singh HK, Walsh EE. Serum antibody decay in adults following natural respiratory syncytial virus infection. *J Med Virol* 2006;78(11):1493-7.
- [300] Collins PL. Human respiratory syncytial virus. In: Samal SK, editor. *The biology of paramyxoviruses*. 1 ed. Norfolk, UK: Caister Academic Press; 2011. p. 341-410.
- [301] Anderson LJ, Dormitzer PR, Nokes DJ, Rappuoli R, Roca A, Graham BS. Strategic priorities for respiratory syncytial virus (RSV) vaccine development. *Vaccine* 2013;31 Suppl 2:B209-B215.
- [302] Borchers AT, Chang C, Gershwin ME, Gershwin LJ. Respiratory syncytial virus - a comprehensive review. *Clin Rev Allergy Immunol* 2013; in press.
- [303] Nguyen DT, Ludlow M, Van Amerongen G, De Vries RD, Yüksel S, Verburgh RJ, Osterhaus ADME, Duprex WP, De Swart RL. Evaluation of synthetic infection-enhancing lipopeptides as adjuvants for a live-attenuated canine distemper virus vaccine administered intra-nasally to ferrets. *Vaccine* 2012;30:5073-80.
- [304] Widjoatmodjo MN, Boes J, Van Bers M, Van Remmerden Y, Roholl PJM, Luytjes W. A highly attenuated recombinant human respiratory syncytial virus lacking the G protein induces long-

- lasting protection in cotton rats. *Virology* 2010;7:114.
- [305] Van Remmerden Y, Xu F, Van Eldik M, Heldens JGM, Huisman W, Widjoatmodjo MN. An improved respiratory syncytial virus neutralization assay based on the detection of green fluorescent protein expression and automated plaque counting. *Virology* 2012;9:253.
- [306] Nguyen DT, De Vries RD, Ludlow M, van den Hoogen BG, Lemon K, Van Amerongen G, Osterhaus ADME, De Swart RL, Duprex WP. Paramyxovirus infections in *ex vivo* lung slice cultures of different host species. *J Virol Methods* 2013;193:159-65.
- [307] Verkaik NJ, Nguyen DT, de Vogel CP, Moll HA, Verbrugh HA, Jaddoe VVV, Hofman A, Van Wamel WJB, van den Hoogen BG, Buijs-Offerman RMGB, Ludlow M, De Witte L, Osterhaus ADME, van Belkum A, De Swart RL. *Streptococcus pneumoniae* exposure is associated with human metapneumovirus seroconversion and increased susceptibility to *in vitro* HMPV infection. *Clin Microbiol Infect* 2011;17:1840-4.
- [308] Welliver R. The relationship of meteorological conditions to the epidemic activity of respiratory syncytial virus. *Paediatr Respir Rev* 2009;10 Suppl 1:6-8.
- [309] Hall CB, Simoes EAF, Anderson LJ. Clinical and epidemiological features of respiratory syncytial virus. *Curr Top Microbiol Immunol* 2013;372:39-57.
- [310] Krzyzaniak MA, Zumstein MT, Gerez JA, Picotti P, Helenius A. Host cell entry of respiratory syncytial virus involves macropinocytosis followed by proteolytic activation of the F protein. *PLoS Pathog* 2013;9:e1003309.
- [311] Tan L, Coenjaerts FE, Houspie L, Viveen MC, Van Bleek GM, Wiertz EJ, Martin DP, Lemey P. The comparative genomics of human respiratory syncytial virus subgroups A and B: genetic variability and molecular evolutionary dynamics. *J Virol* 2013;87(14):8213-26.
- [312] Bagga B, Woods CV, Veldman TH, Gilbert A, Mann A, Balaratnam G, Lambkin-Williams R, Oxford JS, McClain MT, Wilkinson T, Nicholson BP, Ginsburg GS, Devincenzo JP. Comparing influenza and RSV viral and disease dynamics in experimentally infected adults predicts clinical effectiveness of RSV antivirals. *Antivir Ther* 2013;18:785-91.
- [313] Falzarano D, Groseth A, Hoenen T. Development and application of reporter-expressing mononegaviruses: current challenges and perspectives. *Antiviral Res* 2014;103:78-87.
- [314] Trento A, Galiano M, Videla C, Carballal G, Garcia-Barreno B, Melero JA, Palomo C. Major changes in the G protein of human respiratory syncytial virus isolates introduced by a duplication of 60 nucleotides. *J Gen Virol* 2003;84(Pt 11):3115-20.
- [315] Trento A, Casas I, Calderon A, Garcia-Garcia ML, Calvo C, Perez-Brena P, Melero JA. Ten years of global evolution of the human respiratory syncytial virus BA genotype with a 60-nucleotide duplication in the G protein gene. *J Virol* 2010;84:7500-12.
- [316] van Niekerk S, Venter M. Replacement of previously circulating respiratory syncytial virus subtype B strains with the BA genotype in South Africa. *J Virol* 2011;85:8789-97.
- [317] Collins PL, Hill MG, Camargo E, Grosfeld H, Chanock RM, Murphy BR. Production of infectious human respiratory syncytial virus from cloned cDNA confirms an essential role for the transcription elongation factor from the 5' proximal open reading frame of the M2 mRNA in gene expression and provides a capability for vaccine development. *Proc Natl Acad Sci U S A* 1995;92:11563-7.
- [318] Grosfeld H, Hill MG, Collins PL. RNA replication by respiratory syncytial virus (RSV) is directed by the N, P, and L proteins; transcription also occurs under these conditions but requires RSV superinfection for efficient synthesis of full-length mRNA. *J Virol* 1995;69:5677-86.
- [319] Jin H, Clarke D, Zhou HZ, Cheng X, Coelingh K, Bryant M, Li S. Recombinant human

- respiratory syncytial virus (RSV) from cDNA and construction of subgroup A and B chimeric RSV. *Virology* 1998;251:206-14.
- [320] Collins PL, Mink MA, Hill MG, III, Camargo E, Grosfeld H, Stec DS. Rescue of a 7502-nucleotide (49.3% of full-length) synthetic analog of respiratory syncytial virus genomic RNA. *Virology* 1993;195:252-6.
- [321] Luytjens W, Krystal M, Enami M, Parvin JD, Palese P. Amplification, expression, and packaging of foreign gene by influenza virus. *Cell* 1989;59:1107-13.
- [322] Radecke F, Spielhofer P, Schneider H, Kaelin K, Huber M, Dotsch C, Christiansen G, Billeter MA. Rescue of measles viruses from cloned DNA. *EMBO J* 1995;14:5773-84.
- [323] Grieves JL, Jurcisek JA, Quist B, Durbin RK, Peeples ME, Durbin JE, Bakaletz LO. Mapping the anatomy of respiratory syncytial virus infection of the upper airways in chinchillas (*Chinchilla lanigera*). *Comp Med* 2010;60:225-32.
- [324] Ruckwardt TJ, Malloy AM, Morabito KM, Graham BS. Quantitative and qualitative deficits in neonatal lung-migratory dendritic cells impact the generation of the CD8<sup>+</sup> T cell response. *PLoS Pathog* 2014;10:e1003934.
- [325] Zhang W, Yang H, Kong X, Mohapatra S, Juan-Vergara HS, Hellermann G, Behera S, Singam R, Lockey RF, Mohapatra SS. Inhibition of respiratory syncytial virus infection with intranasal siRNA nanoparticles targeting the viral NS1 gene. *Nat Med* 2005;11:56-62.
- [326] El Saleeby CM, Bush AJ, Harrison LM, Aitken JA, Devincenzo JP. Respiratory syncytial virus load, viral dynamics, and disease severity in previously healthy naturally infected children. *J Infect Dis* 2011;204:996-1002.
- [327] Schnell MJ, Mebatsion T, Conzelmann KK. Infectious rabies viruses from cloned cDNA. *EMBO J* 1994;13:4195-203.
- [328] Hotard AL, Shaikh FY, Lee S, Yan D, Teng MN, Plemper RK, Crowe JE, Jr., Moore ML. A stabilized respiratory syncytial virus reverse genetics system amenable to recombination-mediated mutagenesis. *Virology* 2012;434:129-36.
- [329] Houben ML, Coenjaerts FE, Rossen JW, Belderbos ME, Hofland RV, Kimpen JL, Bont L. Disease severity and viral load are correlated in infants with primary respiratory syncytial virus infection in the community. *J Med Virol* 2010;82:1266-71.
- [330] Chambers P, Rima BK, Duprex WP. Molecular differences between two Jeryl Lynn mumps virus vaccine component strains, JL5 and JL2. *J Gen Virol* 2009;90:2973-81.
- [331] Lemon K, Rima BK, McQuaid S, Allen IV, Duprex WP. The F gene of rodent brain-adapted mumps virus is a major determinant of neurovirulence. *J Virol* 2007;81(15):8293-302.
- [332] Reed LJ, Muench H. A simple method of estimating fifty percent endpoints. *Am J Hygiene* 1938;27:493-7.
- [333] Dewhurst-Maridor G, Simonet V, Bornand JE, Nicod LP, Pache JC. Development of a quantitative TaqMan RT-PCR for respiratory syncytial virus. *J Virol Methods* 2004;120:41-9.
- [334] The biology of paramyxoviruses. College Park, MD, USA: Caister Academic Press; 2011.
- [335] Griffin DE. Measles virus. In: Knipe DM, Howley PM, editors. *Fields Virology*. 5 ed. Philadelphia: Lippincott Williams & Wilkins; 2007. p. 1551-85.
- [336] Dandurand RJ, Wang CG, Phillips NC, Eidelman DH. Responsiveness of individual airways to methacholine in adult rat lung explants. *J Appl Physiol* 1993;75:364-72.
- [337] Bergner A, Sanderson MJ. Acetylcholine-induced calcium signaling and contraction of airway smooth muscle cells in lung slices. *J Gen Physiol* 2002;119(2):187-98.
- [338] Duprex WP, McQuaid S, Hangartner L, Billeter MA, Rima BK. Observation of measles virus cell-to-cell spread in astrocytoma cells by using a green fluorescent protein-expressing

## Chapter 10

- recombinant virus. *J Virol* 1999;73:9568-75.
- [339] Ono N, Tatsuo H, Hidaka Y, Aoki T, Minagawa H, Yanagi Y. Measles viruses on throat swabs from measles patients use signaling lymphocytic activation molecule (CDw150) but not CD46 as a cellular receptor. *J Virol* 2001;75:4399-401.
- [340] Kuiken T, van den Hoogen BG, van Riel DA, Laman JD, Van Amerongen G, Sprong L, Fouchier RAM, Osterhaus ADME. Experimental human metapneumovirus infection of cynomolgus macaques (*Macaca fascicularis*) results in virus replication in ciliated epithelial cells and pneumocytes with associated lesions throughout the respiratory tract. *Am J Pathol* 2004;164:1893-900.
- [341] Collins PL, Graham BS. Viral and host factors in human respiratory syncytial virus pathogenesis. *J Virol* 2008;82:2040-55.
- [342] Pillet S, Svitek N, von Messling V. Ferrets as a model for morbillivirus pathogenesis, complications, and vaccines. *Curr Top Microbiol Immunol* 2009;330:73-87.
- [343] De Swart RL. Measles studies in the macaque model. *Curr Top Microbiol Immunol* 2009;330:55-72.
- [344] Williams JV, Tollefson SJ, Johnson JE, Crowe Jr. JE. The cotton rat (*Sigmodon hispidus*) is a permissive small animal model of human metapneumovirus infection, pathogenesis, and protective immunity. *J Virol* 2005;79:10944-51.
- [345] Prince GA, Porter DD. The pathogenesis of respiratory syncytial virus infection in infant ferrets. *Am J Pathol* 1976;82:339-52.
- [346] Mesman AW, De Vries RD, McQuaid S, Duprex WP, De Swart RL, Geijtenbeek TBH. A prominent role for DC-SIGN+ dendritic cells in initiation and dissemination of measles virus infection in non-human primates. *PLoS One* 2012;7:e49573.
- [347] van den Hoogen BG, van Doornum GJ, Fockens JC, Cornelissen JJ, Beyer WE, de Groot R, Osterhaus ADME, Fouchier RAM. Prevalence and clinical symptoms of human metapneumovirus infection in hospitalized patients. *J Infect Dis* 2003;188:1571-7.
- [348] Kukavica-Ibrulj I, Hamelin ME, Prince GA, Gagnon C, Bergeron Y, Bergeron MG, Boivin G. Infection with human metapneumovirus predisposes mice to severe pneumococcal pneumonia. *J Virol* 2009;83:1341-9.
- [349] Jaddoe VW, van Duijn CM, van der Heijden AJ, Mackenbach JP, Moll HA, Steegers EA, Tiemeier H, Uitterlinden AG, Verhulst FC, Hofman A. The Generation R Study: design and cohort update until the age of 4 years. *Eur J Epidemiol* 2008;23:801-11.
- [350] Lebon A, About JA, Verbrugh HA, Jaddoe VW, Hofman A, van Wamel W, Moll HA, van Belkum A. Dynamics and determinants of *Staphylococcus aureus* carriage in infancy: the Generation R Study. *J Clin Microbiol* 2008;46:3517-21.
- [351] Herfst S, de Graaf M, Schrauwen EJ, Ulbrandt ND, Barnes AS, Senthil K, Osterhaus ADME, Fouchier RAM, van den Hoogen BG. Immunization of Syrian golden hamsters with F subunit vaccine of human metapneumovirus induces protection against challenge with homologous or heterologous strains. *J Gen Virol* 2007;88:2702-9.
- [352] Kadioglu A, Weiser JN, Paton JC, Andrew PW. The role of *Streptococcus pneumoniae* virulence factors in host respiratory colonization and disease. *Nat Rev Microbiol* 2008;6:288-301.
- [353] Fischer Walker CL, Rudan I, Liu L, Nair H, Theodoratou E, Bhutta ZA, O'Brien KL, Campbell H, Black RE. Global burden of childhood pneumonia and diarrhoea. *Lancet* 2013;381:1405-16.
- [354] Simell B, Auranen K, Kayhty H, Goldblatt D, Dagan R, O'Brien KL. The fundamental link between pneumococcal carriage and disease. *Expert Rev Vaccines* 2012;11:841-55.
- [355] Talbot TR, Poehling KA, Hartert TV, Arbogast PG, Halasa NB, Edwards KM, Schaffner W,

- Craig AS, Griffin MR. Seasonality of invasive pneumococcal disease: temporal relation to documented influenza and respiratory syncytial viral circulation. *Am J Med* 2005;118:285-91.
- [356] Weinberger DM, Grant LR, Steiner CA, Weatherholtz R, Santosham M, Viboud C, O'Brien KL. Seasonal drivers of pneumococcal disease incidence: impact of bacterial carriage and viral activity. *Clin Infect Dis* 2014;58:188-94.
- [357] Hoti F, Erasto P, Leino T, Auranen K. Outbreaks of *Streptococcus pneumoniae* carriage in day care cohorts in Finland - implications for elimination of transmission. *BMC Infect Dis* 2009;9:102.
- [358] Pessoa D, Hoti F, Syrjanen R, Sa-Leao R, Kajjalainen T, Gomes MG, Auranen K. Comparative analysis of *Streptococcus pneumoniae* transmission in Portuguese and Finnish day-care centres. *BMC Infect Dis* 2013;13:180.
- [359] Bosch AA, Biesbroek G, Trzcinski K, Sanders EA, Bogaert D. Viral and bacterial interactions in the upper respiratory tract. *PLoS Pathog* 2013;9:e1003057.
- [360] Lemon K, Nguyen DT, Ludlow M, Rennick LJ, Yuksel S, Van Amerongen G, McQuaid S, Rima BK, De Swart RL, Duprex P. Recombinant subgroup B human respiratory syncytial virus expressing EGFP highlights a role for cell-to-cell spread in HRSV pathogenesis. submitted 2014.
- [361] Barretto N, Hallak LK, Peeples ME. Neuraminidase treatment of respiratory syncytial virus-infected cells or virions, but not target cells, enhances cell-cell fusion and infection. *Virology* 2003;313:33-43.
- [362] Miller MA, Stabenow JM, Parvathareddy J, Wodowski AJ, Fabrizio TP, Bina XR, Zalduondo L, Bina JE. Visualization of murine intranasal dosing efficiency using luminescent *Francisella tularensis*: effect of instillation volume and form of anesthesia. *PLoS ONE* 2012;7:e31359.
- [363] Thorburn K, van Saene HK. Pulmonary bacterial co-infection in children ventilated for severe respiratory syncytial virus bronchiolitis is common. *Intensive Care Med* 2007;33:565.
- [364] Brundage JF, Shanks GD. Deaths from bacterial pneumonia during 1918-19 influenza pandemic. *Emerg Infect Dis* 2008;14:1193-9.
- [365] McCullers JA. Insights into the interaction between influenza virus and pneumococcus. *Clin Microbiol Rev* 2006;19:571-82.
- [366] Palacios G, Hornig M, Cisterna D, Savji N, Bussetti AV, Kapoor V, Hui J, Tokarz R, Briese T, Baumeister E, Lipkin WI. *Streptococcus pneumoniae* co-infection is correlated with the severity of H1N1 pandemic influenza. *PLoS One* 2009;4:e8540.
- [367] Diavatopoulos DA, Short KR, Price JT, Wilksch JJ, Brown LE, Briles DE, Strugnell RA, Wijburg OL. Influenza A virus facilitates *Streptococcus pneumoniae* transmission and disease. *Faseb J* 2010;24:1789-98.
- [368] Wang XY, Kilgore PE, Lim KA, Wang SM, Lee J, Deng W, Mo MQ, Nyambat B, Ma JC, Favorov MO, Clemens JD. Influenza and bacterial pathogen co-infections in the 20th century. *Interdiscip Perspect Infect Dis* 2011;2011:146376.
- [369] Sajjan US, Jia Y, Newcomb DC, Bentley JK, Lukacs NW, LiPuma JJ, Hershenson MB. *H. influenzae* potentiates airway epithelial cell responses to rhinovirus by increasing ICAM-1 and TLR3 expression. *Faseb J* 2006;20:2121-3.
- [370] Kuss SK, Best GT, Etheredge CA, Pruijssers AJ, Frierson JM, Hooper LV, Dermody TS, Pfeiffer JK. Intestinal microbiota promote enteric virus replication and systemic pathogenesis. *Science* 2011;334:249-52.
- [371] Tomosada Y, Chiba E, Zelaya H, Takahashi T, Tsukida K, Kitazawa H, Alvarez S, Villena J. Nasally administered *Lactobacillus rhamnosus* strains differentially modulate respiratory antiviral immune responses and induce protection against respiratory syncytial virus infection. *BMC Immunol* 2013;14:40.

- [372] Gabryszewski SJ, Bachar O, Dyer KD, Percopo CM, Killoran KE, Domachowske JB, Rosenberg HF. Lactobacillus-mediated priming of the respiratory mucosa protects against lethal pneumovirus infection. *J Immunol* 2011;186:1151-61.
- [373] Scanlon KL, Diven WF, Glew RH. Purification and properties of *Streptococcus pneumoniae* neuraminidase. *Enzyme* 1989;41:143-50.
- [374] Cohen M, Zhang XQ, Senaati HP, Chen HW, Varki NM, Schooley RT, Gagneux P. Influenza A penetrates host mucus by cleaving sialic acids with neuraminidase. *Virology* 2013;10:321.
- [375] Pittet LF, Posfay-Barbe KM. Pneumococcal vaccines for children: a global public health priority. *Clin Microbiol Infect* 2012;18 Suppl 5:25-36. doi: 10.1111/j.1469-0691.2012.03938.x. Epub; 2012 Aug 6.;25-36.
- [376] Feikin DR, Kagucia EW, Loo JD, Link-Gelles R, Puhan MA, Cherian T, Levine OS, Whitney CG, O'Brien KL, Moore MR. Serotype-specific changes in invasive pneumococcal disease after pneumococcal conjugate vaccine introduction: a pooled analysis of multiple surveillance sites. *PLoS Med* 2013;10:e1001517.
- [377] Elberse KE, van der Heide HG, Witteveen S, van de Pol I, Schot CS, van der Ende A, Berbers GA, Schouls LM. Changes in the composition of the pneumococcal population and in IPD incidence in The Netherlands after the implementation of the 7-valent pneumococcal conjugate vaccine. *Vaccine* 2012;30:7644-51.
- [378] Weinberger DM, Malley R, Lipsitch M. Serotype replacement in disease after pneumococcal vaccination. *Lancet* 2011;378:1962-73.
- [379] Kadioglu A, Weiser JN, Paton JC, Andrew PW. The role of *Streptococcus pneumoniae* virulence factors in host respiratory colonization and disease. *Nat Rev Microbiol* 2008;6:288-301.
- [380] Martner A, Skovbjerg S, Paton JC, Wold AE. *Streptococcus pneumoniae* autolysis prevents phagocytosis and production of phagocyte-activating cytokines. *Infect Immun* 2009;77:3826-37.
- [381] Lloyd-Smith JO, Schreiber SJ, Kopp PE, Getz WM. Superspreading and the effect of individual variation on disease emergence. *Nature* 2005;438:355-9.
- [382] Paunio M, Peltola H, Valle M, Davidkin I, Virtanen M, Heinonen OP. Explosive school-based measles outbreak: intense exposure may have resulted in high risk, even among revaccinees. *Am J Epidemiol* 1998;148:1103-10.
- [383] Bentley SD, Aanensen DM, Mavroidi A, Saunders D, Rabinowitsch E, Collins M, Donohoe K, Harris D, Murphy L, Quail MA, Samuel G, Skovsted IC, Kalltoft MS, Barrell B, Reeves PR, Parkhill J, Spratt BG. Genetic analysis of the capsular biosynthetic locus from all 90 pneumococcal serotypes. *PLoS Genet* 2006;2:e31.
- [384] Converse GM, III, Dillon HC, Jr. Epidemiological studies of *Streptococcus pneumoniae* in infants: methods of isolating pneumococci. *J Clin Microbiol* 1977;5:293-6.
- [385] Nguyen DT, Boes J, Van Amerongen G, Van Remmerden Y, Yüksel S, Guichelaar T, Osterhaus ADME, De Swart RL. Infection-enhancing lipopeptides do not improve intranasal immunization of cotton rats with a delta-G candidate live-attenuated human respiratory syncytial virus vaccine. *Hum Vaccin Immunother* 2013;9:2578-83.
- [386] De Swart RL, van den Hoogen BG, Kuiken T, Herfst S, Van Amerongen G, Yüksel S, Sprong L, Osterhaus ADME. Immunization of macaques with formalin-inactivated human metapneumovirus induces hypersensitivity to hMPV infection. *Vaccine* 2007;25:8518-28.
- [387] Hamelin ME, Couture C, Sackett MK, Boivin G. Enhanced lung disease and Th2 response following human metapneumovirus infection in mice immunized with the inactivated virus. *J Gen Virol* 2007;88:3391-400.

- [388] Yim KC, Cragin RP, Boukhvalova MS, Blanco JCG, Hamelin ME, Boivin G, Porter DD, Prince GA. Human metapneumovirus: enhanced pulmonary disease in cotton rats immunized with formalin-inactivated virus vaccine and challenged. *Vaccine* 2007;25:5034-40.
- [389] Pasare C, Medzhitov R. Toll-like receptors and acquired immunity. *Semin Immunol* 2004;16:23-6.
- [390] Kamphuis T, Meijerhof T, Stegmann T, Lederhofer J, Wilschut J, de HA. Immunogenicity and protective capacity of a virosomal respiratory syncytial virus vaccine adjuvanted with monophosphoryl lipid A in mice. *PLoS One* 2012;7:e36812.
- [391] Kamphuis T, Stegmann T, Meijerhof T, Wilschut J, de HA. A virosomal respiratory syncytial virus vaccine adjuvanted with monophosphoryl lipid A provides protection against viral challenge without priming for enhanced disease in cotton rats. *Influenza Other Respir Viruses* 2013;7:1227-36.
- [392] Shafique M, Wilschut J, De Haan A. Induction of mucosal and systemic immunity against respiratory syncytial virus by inactivated virus supplemented with TLR9 and NOD2 ligands. *Vaccine* 2012;30:597-606.
- [393] Shafique M, Meijerhof T, Wilschut J, De Haan A. Evaluation of an intranasal virosomal vaccine against respiratory syncytial virus in mice: effect of TLR2 and NOD2 ligands on induction of systemic and mucosal immune responses. *PLoS One* 2013;8:e61287.
- [394] Wright PF, Karron RA, Belshe RB, Thompson J, Crowe Jr. JE, Boyce TG, Halburnt LL, Reed GW, Whitehead SS, Anderson EL, Wittek AE, Casey R, Eichelberger M, Thumar B, Randolph VB, Udem SA, Chanock RM, Murphy BR. Evaluation of a live, cold-passaged, temperature-sensitive, respiratory syncytial virus vaccine candidate in infancy. *J Infect Dis* 2000;182:1331-42.
- [395] Karron RA, Wright PF, Belshe RB, Thumar B, Casey R, Newman F, Polack FP, Randolph VB, Deatly A, Hackell J, Gruber W, Murphy BR, Collins PL. Identification of a recombinant live attenuated respiratory syncytial virus vaccine candidate that is highly attenuated in infants. *J Infect Dis* 2005;191:1093-104.
- [396] Rohner GB, Meier S, Bel M, Combescure C, Othenin-Girard V, Swali RA, de Tejada BM, Siegrist CA. Influenza Vaccination Given at Least 2 Weeks before Delivery to Pregnant Women Facilitates Transmission of Seroprotective Influenza-Specific Antibodies to the Newborn. *Pediatr Infect Dis J* 2013;52:20.
- [397] Ochola R, Sande C, Fegan G, Scott PD, Medley GF, Cane PA, Nokes DJ. The level and duration of RSV-specific maternal IgG in infants in Kilifi Kenya. *PLoS ONE* 2009;4:e8088.
- [398] Esposito S, Bosis S, Morlacchi L, Baggi E, Sabatini C, Principi N. Can infants be protected by means of maternal vaccination? *Clin Microbiol Infect* 2012;18 Suppl 5:85-92. doi: 10.1111/j.1469-0691.2012.03936.x. Epub; 2012 Aug 6.:85-92.
- [399] O'Doherty U, Swiggard WJ, Malim MH. Human immunodeficiency virus type 1 spinoculation enhances infection through virus binding. *J Virol* 2000;74:10074-80.
- [400] Gualdi L, Hayre JK, Gerlini A, Bidossi A, Colomba L, Trappetti C, Pozzi G, Docquier JD, Andrew P, Ricci S, Oggioni MR. Regulation of neuraminidase expression in *Streptococcus pneumoniae*. *BMC Microbiol* 2012;12:200.





## **Chapter II**

### **Nederlandse Samenvatting**



## Chapter 11

Wereldwijd veroorzaken luchtweg-infectieziekten door bacteriën en virussen een belangrijke ziektelast. Luchtwegbacteriën kunnen zich nestelen in de neus en/ of in het bovenste gedeelte van de keel (nasofarynx) en kunnen hier voor korte of langere tijd verblijven zonder ziekte te veroorzaken. Dit wordt bacterieel dragerschap genoemd en komt voornamelijk voor bij kinderen onder de vijf jaar. Vier luchtwegbacteriën spelen hierin een belangrijke rol: *Streptococcus pneumoniae* (pneumokok), *Haemophilus influenzae*, *Moraxella catarrhalis* en *Staphylococcus aureus*. Het domein waar deze bacteriën zich bevinden kan gedeeld worden met luchtwegvirussen zoals humaan respiratoir syncytieel virus (HRSV) en humaan metapneumovirus (HMPV). Het is dus mogelijk dat deze bacteriën en virussen interacties met elkaar hebben, waarbij de ziekte in de mens mogelijk verergerd kan worden.

Het onderzoek beschreven in dit proefschrift is gericht op interacties tussen luchtwegbacteriën en – virussen in gekweekte cellen en proefdiermodellen. Hierbij lag de nadruk op studies naar interacties tussen *S. pneumoniae* en HRSV of HMPV.

*Streptococcus pneumoniae* veroorzaakt wereldwijd de grootste ziektelast en sterfte bij kinderen onder de vijf jaar. De pneumokok heeft een scala aan componenten beschikbaar om zich in de nasofarynx te nestelen zonder ziekte te veroorzaken. Tot 60% van kinderen onder de vijf jaar draagt tijdelijk één van de 92 pneumokok varianten bij zich. Dragerschap van pneumokokken is een vereiste voor eventuele verdere verspreiding door het lichaam. Afhankelijk naar welk deel van het lichaam de pneumokok zich verspreidt, kan het levensbedreigende ziekten veroorzaken zoals een longontsteking, een hersenvliesontsteking en een bloedvergiftiging. Voor een aantal pneumokok varianten bestaat een beschermend vaccin.

HRSV kan wereldwijd ernstige luchtweginfecties veroorzaken, voornamelijk bij jonge kinderen. Ieder tweejarig kind heeft minstens éénmalig een HRSV infectie doorgemaakt. In het overgrote deel betreft dit een milde en zelflimiterende infectie van de bovenste luchtwegen, waarbij het geïnfecteerde individu verkouden is, niest en/ of hoest. Echter, bij een minderheid kan het virus zich verspreiden naar de lagere luchtwegen, resulterend in longontsteking of zelfs de dood. Dit ziektebeeld wordt het meest gezien in kinderen onder de zes maanden, maar ook in ouderen en mensen met een verminderd afweer.

HMPV is nauw verwant aan HRSV en veroorzaakt in dezelfde groepen nagenoeg dezelfde klachten, echter deze zijn milder en de ziektelast is kleiner. De ziektelast voor beide virussen is het grootst tijdens de winter in het noordelijk en zuidelijk halfrond en tijdens het regenseizoen in de tropen. Helaas bestaat er op dit moment voor beide virussen geen vaccin. Een vaccin is niet alleen nodig om de sterfte onder kinderen te verminderen, maar ook om de druk op ziekenhuisopnames en werkverzuim voor de ouders te reduceren.

**Hoofdstuk 2** beschrijft het effect van een aantal bacteriële componenten op HRSV infecties in celkweken. Dergelijke bacteriële componenten kunnen het menselijke immuunsysteem activeren. Het bleek dat één van de geteste bacteriële componenten (Pam3CSK4) HRSV infecties significant kan versterken. Verrassend genoeg was deze versterking onafhankelijk van activatie van het menselijke immuunsysteem. Daarnaast kon deze bacteriële component ook infecties met HMPV, mazelen virus en het humaan immunodeficiëntievirus (HIV) versterken. Deze bevinding leidde tot vervolgonderzoek, gericht op (1) de mogelijke bijdrage van Pam3CSK4 aan de ontwikkeling van een HRSV vaccin en (2) meer inzicht in de bijdrage van bacteriën aan de pathogenese van

luchtwegvirus infecties.

Voor HRSV en HMPV wordt vanuit verschillende invalshoeken gewerkt aan ontwikkeling van een effectief vaccin. Een veelbelovende invalshoek is het gebruik van een levend-verzwakt virus vaccin. In dergelijke vaccins, zoals in het huidige bof, mazelen en rode hond (BMR) vaccin, zijn virussen dusdanig verzwakt dat ze geen substantiële ziekte meer kunnen veroorzaken, maar wel een immuunrespons induceren die beschermt tegen toekomstige infecties. Voor HRSV en HMPV vaccins is deze balans tussen verzwakking en inductie van beschermende immuniteit lastiger te vinden. Een nog iets meer verzwakt virus kan geen ziekte veroorzaken, maar leidt tegelijkertijd ook niet tot een beschermende immuunrespons. Een infectie-versterkende bacteriële component kan een oplossing bieden voor dit probleem. Het gelijktijdig gebruik van zo'n virus met een infectie-versterkende bacteriële component zou wel tot een beschermende immuunrespons kunnen leiden. Het grote voordeel van deze nieuw te ontwikkelen vaccins is dat ze via de neus kunnen worden toegediend zonder dat er een naald vereist is.

De toepasbaarheid van het synthetisch bacteriële component (Pam3CSK4) als hulpstof bij levende vaccins is in twee proefdiermodellen getest. In **Hoofdstuk 3** werd gebruik gemaakt van een levend-verzwakt hondenziektevirus (canine distemper virus of CDV), dat nauw verwant is aan het mazelen virus. Deze virussen behoren tot dezelfde familie als HRSV en HMPV. De proefdieren werden via de neus gevaccineerd met levend-verzwakt CDV in aan- of afwezigheid van Pam3CSK4. In dit proefdiermodel werd de infectie-versterkende eigenschap van Pam3CSK4 bevestigd: de aanwezigheid van deze bacteriële component leidde tot meer virusreproductie in de neus van de gevaccineerde dieren. Ook leidde vaccinatie in aanwezigheid

van de bacteriële component tot meer beschermende antistoffen. In **Hoofdstuk 4** werd een zelfde soort studie uitgevoerd met een levend-verzwakt kandidaat vaccin virus voor HRSV. In dit tweede proefdiermodel kon helaas geen positief effect van het toevoegen van Pam3CSK4 aangetoond worden. Verder onderzoek is nodig om het eventuele nut van deze bacteriële component bij levende vaccins te verkennen.

Om robuuste resultaten in laboratoriumstudies te behalen die naar de mens vertaald kunnen worden is het noodzakelijk om modellen te gebruiken die de realiteit zo goed mogelijk nabootsen. In het vervolg van dit proefschrift werd gebruik gemaakt van een celkweek systeem, zgn. primaire normale humane bronchiale epitheel (NHBE) cellen. Van tot nu toe bestaande systemen bootsen deze NHBE cellen als beste de luchtwegcellen in een lichaam na. Luchtwegcellen in de neus en longen vormen de belangrijkste doelwitcellen van zowel HRSV als HMPV. In **Hoofdstuk 5** is beschreven hoe een nieuw genetisch gemodificeerd HRSV is gemaakt en gekarakteriseerd. Dit virus kan beschouwd worden als een bestaand circulerend virus, echter bij infectie maakt dit virus ook een fluorescent eiwit aan, wat uitermate snel en precies te detecteren is. Dit nieuwe virus werd vergeleken met een veelgebruikte HRSV stam die ook een fluorescent eiwit aanmaakt. Echter, dit virus is zo lang gekweekt in het laboratorium dat het niet meer beschouwd kan worden als een ziekteverwekkende HRSV stam. In de twee voor HRSV beste modelsystemen (NHBE cellen en katoenratten) veroorzaakte het nieuwe virus significant meer infectie vergeleken met het oude virus. In **Hoofdstuk 6** is een nieuw *ex vivo* modelsysteem beschreven voor luchtwegvirus infecties met het doel om biologisch relevante studies te kunnen doen met minder proefdieren. Met behulp van virus infecties in levend gehouden longplakjes zou

bij voorbaat een proefdiermodel geselecteerd kunnen worden. Tevens bleek dit model goed bruikbaar om infectie van cellen in longplakjes te vervolgen voor een bepaalde periode.

Het is bekend dat na virale luchtweginfecties bacteriële infecties kunnen opkomen, zogeheten secundaire bacteriële infecties of bacteriële superinfecties. Gezien het behaalde resultaat in **Hoofdstuk 2**, waarbij er aangetoond was dat bacteriële componenten virus infecties kunnen versterken, zou er ook sprake kunnen zijn van virale superinfecties gedurende bacterieel dragerschap.

**Hoofdstuk 7** beschrijft de interactie tussen de vier belangrijkste luchtwegbacteriën en HMPV. Dragerschap werd geïmiteerd door eerst de bacteriën aan de NHBE cellen toe te voegen en vervolgens het virus. Van de ze vier meest veelvoorkomende en gebruikte bacteriën versterkte alleen de pneumokok HMPV infectie in NHBE cellen. In gezonde kinderen is er ook een associatie tussen pneumokokken dragerschap en HMPV infectie aangetoond. Met deze twee resultaten kan er geconcludeerd worden, dat een interactie tussen pneumokok dragerschap en HMPV infectie bestaat.

In **Hoofdstuk 8** is een potentiële interactie tussen dragerschap van verschillende types pneumokokken en HRSV bestudeerd. Hierbij is gebruik gemaakt van het nieuwe genetisch gemodificeerd virus dat beschreven is in **Hoofdstuk 5**. Het effect van vijf verschillende types pneumokokken en HRSV werd als eerste in NHBE cellen geëvalueerd. Drie hiervan konden HRSV infecties significant versterken. In een proefdiermodel voor HRSV werd getest of pneumokokken HRSV infecties kunnen versterken en werd gekeken naar de hoeveelheid bacteriën en virussen in de neus en in de longen. Om dragerschap te simuleren werd een kleine hoeveelheid bacteriën in de neus van katoenratten toegediend. Drie

dagen later werden de dieren met een kleine hoeveelheid HRSV geïnfecteerd. Met deze procedure was het mogelijk om dragerschap van pneumokokken in deze dieren te simuleren zonder dat ze ziekte vertoonden. In dit model versterkten twee pneumokok varianten HRSV infectie significant. In deze dieren werd er meer virus geproduceerd en werden meer cellen geïnfecteerd. Ook waren er in deze dieren significant meer meerkernige reuzencellen (syncytia) te zien, waar HRSV zijn naam aan dankt. In deze twee modellen is aangetoond dat sommige pneumokok varianten HRSV infectie significant versterken. Echter, de ernst van ziekte en verspreiding van het virus of de bacterie kon in dit model niet bestudeerd worden vanwege het gebrek aan klinische verschijnselen in dit model. Deze bevinding kan leiden tot gerichtere pneumokokken vaccinatie waarbij ook de kans op een ernstige HRSV infectie verminderd kan worden.

Samenvattend heeft het onderzoek beschreven in dit proefschrift geleid tot nieuwe inzichten in interacties tussen luchtwegbacteriën en virussen en tot betere inzichten in de pathogenese van HRSV. Met name het nieuw ontwikkelde virus waarmee HRSV infecties nauwgezet gevolgd kunnen worden, zal verder gebruikt worden in andere lijnen van HRSV onderzoek. Hiermee kunnen we ons begrip van het virus enorm vergroten. Dit zal een grote bijdrage leveren aan het ontwikkelen van een HRSV vaccin en nieuwe effectieve behandelmethoden.





## Chapter 12

**Tóm tắt tiếng Việt**

A white, ruffled, circular object, possibly a piece of fabric or a decorative item, centered on a light gray background. The object has a gathered, elasticated edge and several pointed, ruffled protrusions around its perimeter, resembling a large, flat, white flower or a decorative cushion. The background is a plain, light gray surface with a subtle crease running vertically through the center.

Hiện nay, các bệnh truyền nhiễm do vi khuẩn và virus gây ra ở đường hô hấp đang trở thành gánh nặng y tế cho toàn thế giới. Vi khuẩn đường hô hấp có thể tồn tại ở mũi hoặc hầu họng trong thời gian ngắn hoặc lâu hơn mà không gây bệnh (được gọi là người lành mang mầm bệnh) và chủ yếu là ở trẻ em dưới năm tuổi. Bốn loại vi khuẩn đường hô hấp đóng vai trò quan trọng: *Streptococcus pneumoniae* (Phế cầu khuẩn), *Haemophilus influenzae*, *Moraxella catarrhalis* và *Staphylococcus aureus*. Ở nơi lưu trú của các vi khuẩn trên đồng thời cũng có sự hiện diện của một số virus hô hấp khác gây bệnh ở người như là virus hô hấp hợp bào (HRSV) và human metapneumovirus (HMPV). Do vậy, các vi khuẩn và virus này rất có thể tương tác với nhau dẫn đến bệnh trạng nghiêm trọng hơn.

Nghiên cứu mô tả trong luận án này tìm hiểu sự tương tác giữa các vi khuẩn và virus đường hô hấp trong mô hình nuôi cấy tế bào và mô hình động vật đặc biệt là sự tương tác giữa phế cầu khuẩn với HRSV hoặc HMPV.

Bệnh do phế cầu khuẩn gây ra có tỷ lệ tử vong cao nhất thế giới ở trẻ em dưới năm tuổi và là gánh nặng bệnh tật toàn cầu. Phế cầu khuẩn có một phổ rộng các loại huyết thanh có thể lưu trú trong hầu họng mà không gây bệnh. Khoảng 60% trẻ dưới năm tuổi đang mang tạm thời một trong 92 loại huyết thanh phế cầu khuẩn. Người lành mang phế cầu là yếu tố tiềm năng cho việc phát tán vi khuẩn trong cơ thể. Phế cầu khuẩn có thể gây ra các bệnh đe dọa đến tính mạng như viêm phổi, viêm tai giữa, viêm màng não hoặc nhiễm trùng huyết do vi khuẩn, tùy vào nơi phát tán vi khuẩn trong cơ thể. Vắc xin đang được phép lưu hành có thể bảo vệ cơ thể chống lại một số loại huyết thanh phế cầu khuẩn.

HRSV có thể gây nhiễm trùng đường hô hấp nặng, đặc biệt ở trẻ nhỏ. Trẻ dưới hai tuổi từng bị nhiễm HRSV ít nhất một lần. Phần lớn nhiễm trùng đường hô hấp trên thường là nhẹ và tự khỏi với các triệu chứng như cảm lạnh, hắt hơi và/hoặc ho. Tuy nhiên, một số ít virus có thể lây sang đường hô hấp dưới, gây viêm phổi thậm chí tử vong. Điều này xảy ra chủ yếu ở trẻ dưới sáu tháng tuổi, người già và những người suy giảm miễn dịch. HMPV cũng gây ra các triệu chứng lâm sàng tương tự như HRSV, tuy nhiên, nhiễm trùng HMPV nhẹ hơn và ít lo ngại hơn. Bệnh nhiễm trùng do 2 loại virus này gây ra phát triển thuận lợi nhất là vào mùa đông ở Bắc và Nam bán cầu và mùa mưa của vùng nhiệt đới. Do đó nó mang lại gánh nặng rất lớn không những cho ngành y tế mà còn ảnh hưởng đến kinh tế xã hội trong suốt thời gian này. Điều đáng tiếc là hiện nay vẫn chưa có vắc xin cho cả hai loại virus. Vắc xin không chỉ có thể giảm được tỷ lệ tử vong ở trẻ, mà còn có thể giảm số ca nhập viện và số ngày nghỉ của cha mẹ.

**Chương 2** mô tả tác động của một số thành phần vi khuẩn khi nhiễm HRSV trong nuôi cấy tế bào. Các thành phần vi khuẩn có thể kích hoạt hệ miễn dịch của con người. Chúng tôi quan sát thấy rằng một trong những thành phần vi khuẩn (Pam3CSK4) được thử nghiệm có thể làm gia tăng đáng kể việc xâm nhiễm HRSV vào tế bào. Điều ngạc nhiên hơn là sự gia tăng này hoàn toàn độc lập với sự kích hoạt của hệ miễn dịch. Bên cạnh đó, Pam3CSK4 còn có thể tăng cường khả năng nhiễm HMPV, virus sởi và virus gây suy giảm miễn dịch ở người (HIV). Kết quả này đưa đến nghiên cứu sâu hơn về (1) vai trò của Pam3CSK4 cho việc phát triển một loại vắc xin HRSV và (2) có cái nhìn sâu sắc hơn về sự đóng góp của vi khuẩn trong cơ chế sinh bệnh học của bệnh nhiễm virus đường hô hấp.



Một trong những cách tiếp cận đầy hứa hẹn để phát triển vắc xin cho HRSV và HMPV là việc sử dụng vắc xin virus sống giảm độc lực. Vắc xin đang được phép lưu hành cho bệnh quai bị, sởi và “rubella” (MMR) là vắc xin được phát triển dựa theo phương pháp này, trong đó virus đã được làm giảm độc tính và không thể gây bệnh nhưng vẫn đủ để tạo đáp ứng miễn dịch bảo vệ cơ thể chống lại việc nhiễm các virus này trong tương lai. Đối với HRSV và HMPV vắc xin thì khó có thể đạt được sự cân bằng giữa giảm độc lực và tạo đáp ứng miễn dịch. Nếu virus quá yếu thì chẳng những không gây bệnh mà cũng không đủ khả năng kích thích hệ miễn dịch tạo kháng thể bảo vệ. Do đó, một thành phần vi khuẩn dùng để tăng cường việc nhiễm virus rất có thể là một giải pháp cho vấn đề nan giải này. Sử dụng đồng thời các virus này với thành phần tăng cường nhiễm trùng của vi khuẩn có thể sẽ tạo đáp ứng miễn dịch bảo vệ cơ thể. Lợi thế rất lớn của các loại vắc xin mới được phát triển này là có thể được sử dụng qua đường mũi mà không cần phải tiêm chích.

Việc sử dụng thành phần vi khuẩn sinh tổng hợp (Pam3CSK4) như chất bổ trợ cho vắc xin virus sống giảm độc lực đã được thử nghiệm trên hai mô hình động vật. Trong **Chương 3** chúng tôi sử dụng một loại virus sống giảm độc lực gây bệnh ở chó (CDV). Virus này cùng họ với virus gây bệnh sởi, HRSV và HMPV. Động vật được tiêm vắc xin CDV qua mũi có hoặc không có Pam3CSK4. Ở thí nghiệm này, một lần nữa khả năng gia tăng nhiễm trùng của Pam3CSK4 lại được khẳng định: Sự hiện diện của thành phần vi khuẩn này giúp cho virus nhân bản nhiều hơn trong mũi của nhóm động vật được chủng ngừa. Ngoài ra, tiêm chủng với Pam3CSK4 cũng tạo đáp ứng miễn dịch bảo vệ cao hơn. Ở **Chương 4** thí nghiệm

tương tự được tiến hành với một vắc xin HRSV sống giảm độc lực. Tuy nhiên, trong mô hình động vật thứ hai này việc bổ sung Pam3CSK4 lại không cho kết quả như mong đợi. Do vậy cần tiến hành các nghiên cứu sâu hơn để đánh giá được hiệu quả của thành phần vi khuẩn này với vắc xin virus sống giảm độc lực.

Việc sử dụng các mô hình mô phỏng này càng thực tế càng tốt. Qua đó đạt được kết quả chính xác trong các thí nghiệm, và rồi có thể được áp dụng cho con người, là điều hết sức cần thiết. Trong phần còn lại của luận án này, chúng tôi sử dụng tế bào nuôi cấy là nguyên bào biểu mô phế quản ở người bình thường (primary normal human bronchial epithelial cell-NHBE). NHBE là sự tương trưng tốt nhất cho các tế bào ở đường hô hấp của người với tất cả các hệ thống có sẵn. Tế bào hô hấp trong mũi và phổi là các tế bào mục tiêu quan trọng nhất của cả hai loại virus HRSV và HMPV. **Chương 5** mô tả đặc điểm của một virus mới đã được biến đổi gen HRSV. Virus này có thể được xem như là một virus đang lưu hành, tuy nhiên khi xâm nhiễm virus này có thể tạo ra một loại protein phát huỳnh quang, giúp chúng ta tìm thấy virus một cách nhanh chóng và có độ nhạy cao. Virus mới này cũng tương đương như chủng HRSV phát huỳnh quang đã và đang được sử dụng nhiều. Tuy vậy, virus này đã được nuôi cấy một thời gian dài trong phòng thí nghiệm do đó nó không được coi là một virus gây bệnh. Thử nghiệm trên hai mô hình tốt nhất cho HRSV (tế bào NHBE và ‘chuột bông’), chúng tôi quan sát thấy rằng: virus mới gây nhiễm trùng nhiều hơn hẳn so với virus cũ. Trong **Chương 6** một mô hình mới thực hiện ngoài cơ thể sống (*ex vivo*) được sử dụng với mục tiêu tiến hành các nghiên cứu sinh học với ít động vật hơn. Mô hình động vật có thể được lựa chọn bằng cách cho nhiễm virus

vào các lát phổi nuôi cấy. Chúng ta cũng có thể theo dõi các tế bào nhiễm virus của lát phổi trong vài ngày.

Chúng ta biết rằng, sau khi nhiễm virus hô hấp có thể sẽ bị bội nhiễm thậm chí bội nhiễm nặng với vi khuẩn. Như đã trình bày trong **Chương 2**, thành phần vi khuẩn có thể làm gia tăng nhiễm virus, và rất có thể xảy ra trường hợp bội nhiễm virus nặng trong trường hợp người lành mang mầm vi khuẩn.

**Chương 7** mô tả sự tương tác giữa bốn loại vi khuẩn đường hô hấp khác nhau và HMPV. Để mô phỏng cho người lành mang vi khuẩn, đầu tiên chúng tôi cho vi khuẩn vào tế bào NHBE sau đó mới thêm virus. Trong số bốn loại vi khuẩn phổ biến nhất được sử dụng để nghiên cứu, chỉ phế cầu khuẩn mới có khả năng tăng cường nhiễm HMPV vào các tế bào NHBE. Có thể quan sát thấy mối tương quan giữa người lành mang cầu khuẩn và nhiễm virus HMPV ở trẻ em khỏe mạnh. Từ những kết quả này chúng tôi có thể kết luận rằng sự tương tác giữa người lành mang cầu khuẩn và HMPV là hoàn toàn có thật.

Trong **Chương 8** sự tương tác tiềm năng giữa người lành mang các biến thể phế cầu khuẩn khác nhau và HRSV được nghiên cứu. Trong thí nghiệm này, chúng tôi sử dụng virus mới biến đổi gen như đã đề cập ở **Chương 5**. Ảnh hưởng của năm kiểu phế cầu khuẩn đối với HRSV trước tiên được đánh giá trên tế bào NHBE. Trong số đó, ba kiểu phế cầu khuẩn gia tăng đáng kể nhiễm trùng HRSV. Trong mô hình động vật HRSV, sự tác động của phế cầu khuẩn lên việc tăng cường nhiễm HRSV cũng được nghiên cứu. Số lượng vi khuẩn và virus trong mũi và phổi được đo. Để mô phỏng động vật lành mang phế cầu khuẩn, một lượng nhỏ vi

khẩn được tiêm vào trong mũi của 'chuột bông'. Ba ngày sau, nhóm 'chuột bông' này được gây nhiễm thêm một lượng nhỏ virus HRSV. Cách này có thể mô phỏng động vật lành mang phế cầu khuẩn mà không biểu hiện bất kỳ dấu hiệu nào của bệnh như ở người. Trong mô hình này hai biến thể phế cầu khuẩn gia tăng đáng kể nhiễm HRSV. Ở nhóm động vật này, virus được sản sinh nhiều hơn và các tế bào bị nhiễm nhiều hơn. Cũng ở động vật có mang phế cầu khuẩn, chúng tôi quan sát thấy có nhiều tế bào khổng lồ đa nhân (hợp bào), đây là đặc điểm như đúng tên gọi của virus HRSV (virus hợp bào gây bệnh ở người). Hai mô hình này cho thấy rằng một số biến thể phế cầu khuẩn gia tăng đáng kể nhiễm HRSV. Tuy nhiên, mức độ nghiêm trọng của bệnh cũng như lây truyền virus hoặc phế cầu khuẩn chưa được nghiên cứu do thiếu các biểu hiện lâm sàng trong mô hình này. Phát hiện này có thể dẫn đến việc chủng ngừa phế cầu khuẩn cụ thể trong đó có thể giảm được nhiễm trùng nặng với HRSV.

Phần kết luận của nghiên cứu mô tả trong luận án này cung cấp những hiểu biết mới về sự tương tác giữa các vi khuẩn và virus đường hô hấp và có cái nhìn sâu sắc hơn trong cơ chế sinh bệnh học của HRSV. Đặc biệt, sự phát triển virus mới tạo điều kiện giám sát bệnh nhiễm trùng HRSV với độ chính xác cao sẽ tiếp tục được sử dụng trong các lĩnh vực khác của nghiên cứu về HRSV. Từ đó giúp chúng ta có thêm hiểu biết về virus. Điều này sẽ có lợi thế rất lớn cho sự phát triển vắc xin HRSV và các chiến lược phòng bệnh hiệu quả.





## **Addenda**

**Addendum I: About the Author**

**Addendum II: PhD Portfolio**

**Addendum III: List of Publications**

**Addendum IV: Dankwoord**

## **Addendum I**

### **Curriculum Vitae**

Duy Tien Nguyen was born on May 7th, 1981 in Enschede, the Netherlands. He graduated from high school at Jacobus college in Enschede in 1999. The same year he began to study Applied Mathematics at University Twente. In 2000, he started to study Econometrics & Operational Research at the Erasmus University Rotterdam. Finally, in 2002 he commenced his medical school at the same university. In 2004, he was selected to start the Research Master of Science program Clinical Epidemiology at the Netherlands Institute for Health Sciences (Nihes) in parallel with the medical curriculum. He obtained his bachelor degree in Econometrics & Operational Research and his Master of Science degree in medicine in 2005 and 2006, respectively. After graduating he worked in the then Health Care Logistics Group at the Erasmus Medical Center. He received his Master of Science degree in Clinical Epidemiology in 2007 and his medical degree in 2009. In April 2009, he started as a PhD student at the department of Viroscience of the Erasmus Medical Center in Rotterdam under supervision of prof.dr. A.D.M.E. Osterhaus and dr. R.L. de Swart. During his PhD project he had the great opportunity to complete the Research Master of Science programme 'Infection & Immunity' at the Postgraduate School Molecular Medicine. In July 2014, he will start his residency in medical microbiology under supervision of prof.dr. H.A. Verbrugh and dr. R.W. Vreede.

## Addendum II

### PhD Portfolio

Name: Duy Tien Nguyen  
Research group: Erasmus MC, department of Viroscience  
Research school: Post-graduate Molecular Medicine  
PhD period: 2009 - 2013  
Promotor: Prof.dr. Albert D.M.E. Osterhaus  
Copromotor: Dr. Rik L. de Swart

### In-dept courses

Article 9 course (course on animal experiments)  
Course in Adobe Indesign  
Course in Adobe Photoshop and Illustrator  
Course in R  
Course in Research Integrity  
Course in Virology  
Practical Introduction to Laser Scanning Microscopy  
Summer course 1 and 2 (part of Research Master programme 'Infection & Immunity')  
Winter course 1 and 2 (part of Research Master programme 'Infection & Immunity')

### Presentations

Scientific Spring Meeting KNVM & NVMM, Papendal, the Netherlands (oral)	2014
NVMM Fall Meeting 2013, Utrecht, the Netherlands (oral)	2013
5th European Congress of Virology, Lyon, France (oral)	2013
Scientific Spring Meeting KNVM & NVMM, Papendal, the Netherlands (poster)	2013
15th International Symposium on Respiratory Viral infections, Rotterdam, the Netherlands (poster)	2013
Comparative Pathology meeting, Rotterdam, the Netherlands (oral)	2013
17th Molecular Medicine day, Rotterdam, the Netherlands (poster)	2013
16th Molecular Medicine day, Rotterdam, the Netherlands (poster)	2012
8th Respiratory Syncytial Virus symposium, Santa Fe, USA (oral)	2012
15th Molecular Medicine day, Rotterdam, the Netherlands (poster)	2011
Vaccine Symposium, Utrecht, the Netherlands (oral)	2011
7th Respiratory Syncytial Virus symposium, Rotterdam, the Netherlands (oral)	2010
14th International Conference on Negative Strand Viruses, Brugge, Belgium (poster)	2010
14th Molecular Medicine day, Rotterdam, the Netherlands (poster)	2010
Virology meeting, Dakar, Senegal (oral)	2009

**Attended conferences and symposia**

Oration Symposium prof. dr. Eric van Gorp	2013
Dutch Annual Virology Symposium, Amsterdam, the Netherlands	2013
Masterclass Prof. dr. R. Rappuoli, Amsterdam, the Netherlands	2010
Mucosal Immunology symposium and Masterclass, Rotterdam, the Netherlands	2011
Scientific Spring Meeting KNVM & NVMM, Papendal, the Netherlands	2011
Advanced Immunology symposium, Amsterdam, the Netherlands	2010
13th Molecular Medicine day, Rotterdam, the Netherlands	2009

**Awards**

Bursary Awardee 5th European Congress of Virology, Lyon, France  
Travel Awardee 8th Respiratory Syncytial Virus symposium, Santa Fe, USA

**Teaching activities**

Lab rotation MSc students "Infection and Immunity"  
Co-supervision of BSc student (LS)



## Addendum III

### List of Publications

*Streptococcus pneumoniae* modulates human respiratory syncytial virus infection *in vitro* and *in vivo*.  
**Nguyen DT**, Louwen R, Elberse K, van Amerongen G, Yüksel S, Luijendijk A, Osterhaus AD, Duprex WP, de Swart RL  
2014, submitted

Recombinant subgroup B human respiratory syncytial virus expressing EGFP highlights a role of cell-to-cell spread in HRSV pathogenesis.  
Lemon K\*, **Nguyen DT** \*, Ludlow M, Rennick LJ, Yüksel S, van Amerongen G, McQuaid S, Rima BK, de Swart RL, Duprex WP  
2014, submitted  
\*Both authors contributed equally

Measles Vaccination of Non-Human Primates Provides Partial Protection against Infection with Canine Distemper Virus.  
de Vries RD, Ludlow M, Verburgh RJ, van Amerongen G, Yüksel S, **Nguyen DT**, McQuaid S, Osterhaus AD, Duprex WP, de Swart RL  
*J Virol.* 2014 Apr;88(8):4423-33.

Infection-enhancing lipopeptides do not improve intranasal immunization of cotton rats with a delta-G candidate live- attenuated human respiratory syncytial virus vaccine  
**Nguyen DT**, Boes J, van Amerongen G, van Remmerden Y, Yüksel S, Guichelaar T, Osterhaus AD, de Swart RL  
*Hum Vaccin Immunother.* 2013 Dec;9(12):2578-83

Paramyxovirus infections in *ex vivo* lung slice cultures of different host species  
**Nguyen DT**, de Vries RD, Ludlow M, van den Hoogena BG, Lemon K, van Amerongen G, Osterhaus AD, de Swart RL, Duprex WP  
*J Virol Methods.* 2013 Oct;193(1):159-65

Evaluation of synthetic infection-enhancing lipopeptides as adjuvants for a live-attenuated canine distemper virus vaccine administered intra-nasally to ferrets.  
**Nguyen DT**, Ludlow M, van Amerongen G, de Vries RD, Yüksel S, Verburgh RJ, Osterhaus AD, Duprex WP, de Swart RL  
*Vaccine.* 2012 Jul 20;30(34):5073-80

Recombinant canine distemper virus strain Snyder Hill expressing green or red fluorescent proteins causes meningoencephalitis in the ferret.  
Ludlow M, **Nguyen DT**, Silin D, Lyubomska O, de Vries RD, von Messling V, McQuaid S, De Swart RL, Duprex WP  
*J Virol.* 2012 Jul;86(14):7508-19.

An outbreak of severe respiratory tract infection caused by human metapneumovirus in a residential care facility for elderly in Utrecht, the Netherlands, January to March 2010.

Te Wierik MJ, **Nguyen DT**, Beersma MF, Thijsen SF, Heemstra KA

*Euro Surveill.* 2012 Mar 29;17(13).

*Streptococcus pneumoniae* exposure is associated with human metapneumovirus seroconversion and increased susceptibility to *in vitro* HMPV infection

Verkaik NJ, **Nguyen DT**, de Vogel CP, Moll HA, Verbrugh HA, Jaddoe VW, Hofman A, van Wamel WJ, van den Hoogen BG, Buijs-Offerman RM, Ludlow M, de Witte L, Osterhaus AD, van Belkum A, de Swart R

*Clin Microbiol Infect.* 2011 Dec;17(12):1840-4.

The synthetic bacterial lipopeptide Pam3CSK4 modulates respiratory syncytial virus infection independent of TLR activation

**Nguyen DT**, de Witte L, Ludlow M, Yüksel S, Wiesmüller KH, Geijtenbeek TB, Osterhaus AD, de Swart RL

*PLoS Pathog.* 2010 Aug 19;6(8)

Predicting the unpredictable: a new prediction model for operating room times using individual characteristics and the surgeon's estimate

Eijkemans MJ, van Houdenhoven M, **Nguyen DT**, Boersma E, Steyerberg EW, Kazemier G

*Anesthesiology.* 2010 Jan;112(1):41-9

Optimizing intensive care capacity using individual length- of-stay prediction models

Van Houdenhoven M, **Nguyen DT**, Eijkemans MJ, Steyerberg EW, Tilanus HW, Gommers D, Wullink G, Bakker J, Kazemier G

*Crit Care.* 2007;11(2):R42.

## Addendum IV

### Dankwoord

Dit proefschrift vloeit voort uit een reeks van (on)bewuste ontwikkelingen. Ik ben een groot aantal mensen heel dankbaar voor hun wetenschappelijke, laboratorium technische en zeker ook sociale steun. Een aantal personen wil ik graag in het bijzonder noemen.

Allereerst gaat mijn dank uit naar Ab, mijn promotor. Beste Ab, bedankt dat je me de kans hebt gegeven om mijn promotie-onderzoek op de afdeling Viroscience uit te voeren. Het proefschrift omvat verschillende onderwerpen, zelfs bacteriologische! Wereldwijd ben je welbekend om je geniale geest, minder bekend is dat je ook een humoristisch, rechtvaardig en solidair mens onder de mensen bent! Tevens wil ik je bedanken dat je me de mogelijkheid hebt gegeven de research master I&I af te ronden tijdens mijn tijd op de 17e verdieping, waarop creatie en recreatie onlosmakelijk met elkaar verbonden zijn.

Rik, na bijna vijf jaar vele dingen van je geleerd te hebben, is hier het boekje. Bedankt voor je ideeën, suggesties, hulp en tijd. Ik waardeer het zeer dat ik ieder moment kon binnen lopen om dingen te bespreken, maar ook dat je zelfs buiten werktijd (inclusief het weekend) mij telefonisch te woord kon staan. Met jou als supervisor heb ik veel ervaring opgedaan over het bedenken van een experiment en het kritisch schrijven van manuscripten. Ook heb ik geleerd van je relativiseringsvermogen na een mislukt experiment of in minder leuke situaties. Ik wil ook jou bedanken voor de kans om de research master I&I te voltooien.

Prof.dr.dr. Van Belkum, beste Alex, het waren aangename besprekingen over het leuke, maar complexe onderzoek over één virus en meerdere bacteriën! Uiteraard was er één plek voor jou gereserveerd in deze kleine commissie. Dank voor het plaatsnemen hierin.

Prof.dr. Koopmans, dank voor het plaatsnemen als secretaris in de kleine commissie. Ik heb er alle vertrouwen in dat in de toekomst de afdeling Viroscience exponentieel zal groeien.

Prof.dr. De Groot, prof.dr. Van Gorp, prof.dr. Endtz, en dr. Van Rossum wil ik hierbij bedanken voor hun bereidheid zitting te nemen in de promotiecommissie.

Georgina, inmiddels is het alweer 5,5 jaar geleden, dat ik onder jouw toezicht oog opnieuw een pipet vasthield “op de besmette kweek”, nadat je terug kwam van vakantie. Alhoewel, ik na mijn stage ‘naar boven’ ging, zal ik als het goed is binnen een aantal jaar weer stage lopen bij jou. Dit keer niet op de 3e, maar op de 10e. Dankjewel voor alles en ook dat je naast me wilt staan als paranimf.

Selma, je hebt me vanaf het begin alle pipetteerkunsten met grote precisie bijgebracht, waarna ik zelfstandig verder kon. Echter, je pipetteersnelheid zal ik nooit krijgen. Ik waardeerde/ waardeer ten eerste dat je zelfs in het weekend mij kwam helpen, als het nodig was. Bedankt voor de gezelligheid en betrokkenheid op het lab en in de kamer. Ik koester je vriendschap. Je bent een fantastisch mens!

Jeroen, de terugvlucht van Dakar, dat was het begin van ons vriendschap. Inmiddels zijn we vijf jaar verder en naast het pipetteren tot laat in de avond hebben we ons goed vermaakt. Niet alleen op de afdeling (lunches, borrels, legendarische SinterKerst-feesten, inclusief band en eten dat Michelin ster waardig is) hebben we genoten, maar ook daarbuiten (Curaçao, PP/ 't Vat, barbecues, etentjes en feestdagen). Dankjewel voor alles en ook dat je mijn paranimf wilt zijn.

## Addendum IV

Lotte, jij hebt het begin gecreëerd, en ik ben ermee verder gegaan. Je briljante geest heeft dit werk enorm geholpen. Inmiddels ben jij bijna psychiater, onderzoeker en ook nog eens moeder. Grappig, dat jij uiteindelijk psychiatrie gekozen hebt en ik het andere. Veel succes met het afronden van je opleiding, je vervolgonderzoek en veel plezier met de kleine en Matthieu!

Geert, je bent niet alleen een expert in je werk, maar ook daarbuiten. Bedankt voor al je hulp, je adviezen en het delen van je heldere visies. We gaan nog een keer Viëtnames eten. Ik hoop, dat het dan net zo lekker is, als je toen in Viëtnam gegeten hebt.

Martin, thank you for your presence and cooperation at the beginning of my PhD, and after that when you came back to the department multiple times as a 'visitor'. Dankeschön for your ideas, the discussions about work or any other thing. I wish you all the best wherever you (two) are! We are honoured that you are here in June.

Paul, thank you for your extensive collaboration, your important contributions to different manuscripts and enthusiasm. In my mind you already are an Ironman. Your visits to Rotterdam have always been great and productive.

Linda, Ken, Stephen and Emma, thank you for the cooperation and pleasant time when you visited us.

Uiteraard ook dank aan alle (ex-) collegae van de afdeling Viroscience:

Prof.dr. Van Doornum, bedankt voor uw begeleiding. Ik heb er veel van geleerd.

Mouring, Bé, Guido, en Mikel, bedankt voor jullie hulp en gezelligheid. Koos<sup>†</sup>, we denken vaak aan je.

Jolanda, veel plezier thuis met de kleine en natuurlijk Pascal in jullie warme huis. Tot snel!

Hans, bedankt voor de bestellingen en voor de data!

Jolanda, bedankt voor het PCR'en en sequenzen van de Coxsackievirussen.

Thijs, bedankt voor de samenwerking. Het is een mooi artikel geworden.

Anne, bedankt voor je hulp met de assays!

Carola, Sourani, Truus, Coby, Darina, Helène en Truus, jullie ook bedankt voor alles.

Oanh, het was gezellig tijdens lunches, etentjes en feestjes! Jammer van VN 2014! Zie je snel weer!

Lisette, dushi, je bruiloft op Curaçao was super mooi! Ik ga ervan uit, dat alles voor jou en Dwight naar wens gaat in de Caraïben. Voor SinterKerst 2010 heb je je eigen haute couture collectie ontworpen. Tot ziens!

Stephanie, veel succes met het afronden van je promotie. Bedankt voor de gezellige tijd op de afdeling, maar ook daarbuiten.

Bri, adik, dankjewel voor je gezelligheid, je positieve energieke instelling, al je souvenirs en eten. Ik wens je ook veel succes met het behalen van je master en veel plezier met je toekomstige promotie-onderzoek.

Rachel, bedankt voor je hulp. Het was gezellig met jou in ons lab en daarbuiten!

Marco en Lennert, succes met het afronden van jullie promotie en opleiding. Ik ga jullie zeker nog in de toekomst zien of zelfs met jullie samenwerken. De trip naar Lyon was super gaaf.

Fasa, enjoy spending time with you wife this year. Don't work too much! Good luck with your PhD. Please, take care of adik Bri.

Do, wish you all the best. Please, sleep well!

Minoushka, Latoya, Fenny, Eury, Javier, Sander, Varsha, Jurre, Byron en Penelope, veel plezier in de toekomst. All the best!

Fatiha, bedankt voor de introductie en rondleiding tijdens MolMed 2009 en de A549 cellen.

Rory, carpaccio master, bedankt voor de samenwerking.

Werner, ook met jou was het een voortreffelijke tijd. Jij ook bedankt voor je ideeën en discussies. Papendal 2014 zal je nu nooit meer vergeten. Veel plezier met 'middle' Sander.

Gijs, als je iets niet weet, vraag het aan Gijs! Lopend encyclopedie met een goed gevoel voor humor. Dank voor je tips! Succes met het afronden van je promotie.

Monique, pienter, optimistisch en vol energie. Deze energie kwam goed van pas met jaren 90 liedjes tijdens de karaoke borrel.

Alwin, bedankt voor al je hulp. Je bent geen stagiair, maar een volwaardig laborant. Heel veel succes met het afronden van je opleiding en je toekomstige carrière.

Stella, je aanwezigheid wordt gemist. Succes met je carrière, en alweer je grote meid.

Sarah, goed bezig op en voor de afdeling!

Anita, geniet van het zonlicht!

Marleen, dank voor je hulp met de AutoMACS en het lenen van de digitale pipetten.

Arno, jammer genoeg geen genomics kunnen doen. Hopelijk waren Rik (,Paul), en ik niet te luid tijdens het skypen.

Simone, Loubna, Maria en Anouk (en Sabine), buurvrouwen, bedankt voor de administratieve ondersteuning en gezelligheid.

Marina, dank voor de samenwerking. Ik wens jou en Martin heel veel geluk samen.

Stefan, Jonneke, Bernadette, bedankt voor jullie hulp rondom reagentia voor zowel HRSV als HMPV.

Maria, je kunt goed acteren! En oh ja, je krijgt nog 5 euro van mij. Bedankt voor alle positieve energie op het lab! Je hart is van goud!

Lauren, kort, maar krachtig. Dankjewel voor de gezelligheid. Jij bent binnenkort aan de beurt!

Fleur, succes met het afronden van je promotie en je opleiding.

Tiny, dankjewel voor de gesprekken, als ik je op de gang zag of bij de FACS. Je gaat de afdeling ook al bijna verlaten. Geniet ervan!

Marine, Maarten, Henk-Jan, Stella, dank jullie wel voor de koekjes!

Brooke, je PhD en kind in één jaar?

Dineke, 7 mei is het feest!

David, dankjewel voor je statistische suggesties!

Peter, bedankt voor de coupes. Ze zijn nog steeds mooi!

Robert, bedankt voor alles (van bidest tot King Foeng). De goodie-goodie box doet wonderen na een lange dag werken.

## Addendum IV

Wim,Ajla, Sumyra, Avinash, Fernanda, bedankt voor de organisatie rondom financiën, urenstaten, etc.

Bjorn, een flu-project zat er niet in. Bedankt voor de gezelligheid.

Vincent en Dennis, Dennis en Vincent, ik denk dat jullie inmiddels ook tot de afdeling Viroscience behoren. Het was lachen, maar zeker ook schrikken en 'oh' roepen. Bedankt voor alle zorg en tijd, zelfs in het weekend!

Daarnaast wil ik Bernike, Carolien, Debby, Freek, Johanna, Joost, Joyce, Judith, Kirsty, Leslie, Monique, Pascal, Patrick, Rogier, Sander, Sander, Stalin, Theo Sander bij naam noemen om hen te bedanken.

Mijn dank gaat ook uit naar dr. Bart, dr. Byron, prof.dr. Charles, dr. Georges, prof.dr. Guus, dr. Martin, dr. Pieter, dr. Rob, prof.dr. Ron, en prof. dr. Thijs, wier ik veel geleerd heb tijdens de werkbesprekingen.

En natuurlijk de sponsors en organisatoren van alle borrels en SinterKerst-feesten!

Aslam, Climmy, Cox, Eefje, Iqbal, Joan, Josanne, Linda, Tarique, and Yelvi, we did it. I wish you all the best! Joan en Josanne, veel succes met het afronden van jullie promotie.

Jan, Frank en Joris, bedankt voor alle organisatie binnen en buiten de research Master I&I!

Khoa, zie je op de 9e binnenkort. Heel veel plezier met de uitbreiding van je gezin!

Matthew, inmiddels ken je ons alle drie.

Rogier, inmiddels kom ik een aantal jaar langs jou. Het was altijd gezellig en constructief. Bedankt voor de zeer aangename samenwerking! Tot snel (fietsend, op de 9e en/of NVMM)!

Luna, dankjewel voor je hulp bij het opzetten van hét HRSV *in vitro* model. Het heeft tot verschillende publicaties geleid.

Nelianne, bedankt voor de prettige samenwerking in het verleden, wellicht ook in de toekomst?

Jolande, het ging toch anders dan we hoopten.. Het was gezellig in Bilthoven.

Carla en Liset, bedankt voor jullie hulp ook!

Karin, HRSV 15,2 kB... hahaha. Dank voor de samenwerking.

René, bedankt voor de begeleiding van mijn bachelor-onderzoek en de samenwerking die eruit voort vloeide. Ik heb veel van je geleerd. Inmiddels ben ik ook overgestapt op R.

Ewout, dank voor je heldere uitleg tijdens je colleges en de samenwerking.

Ineke, bedankt voor je warme hart en al je adviezen!

Ylian, jouw verhaal over Bolivia, Spitsbergen , etc. vind ik nog steeds mooi! Heel veel succes als nefrologe en veel geluk met Jonas!

Nano, Rudi, en Robin, bedankt voor het oplossen van alle ICT-problemen.

Ook wil ik mijn ex-collegae van de voormalige Health Care Logistics Group bedanken in het bijzonder:

Mark, bedankt voor de mogelijkheid, die je me toen geboden had. Je enthousiasme werkt aanstekelijk. Wellicht tot ziens in het ErasmusMC?

Prof.dr. Geert, dank voor je samenwerking en hopelijk zijn er nog vele artikelen uit de verzamelde databases gekomen.

Ellen, dank voor alle zorg tijdens het werk op 12 Zuid. Fijn, dat je ook op deze dag erbij bent.

Cees en Inge, bedankt voor alles! Yvette, goed bezig! De NIAZ accreditaties blijven binnen komen. Marloes, zie ik je weer in Rotterdam op de fiets? Erik bij Dijkers?

Herbert, het was gezellig op 12 Zuid, maar ook op de 17e.

En natuurlijk: Francine, leuk je weer kort gesproken te hebben. Ik heb onze gesprekken gemist. Jij ook bedankt voor je adviezen! Ik vond het super leuk, dat je samen met andere collegae langs kwam om te eten tijdens mijn co-schappen in Tilburg. Leuk, dat je erbij bent!

Prof.dr. Tilanus, het belang van de patiënt staat bij u altijd op de eerste plaats. Bedankt voor uw visie en samenwerking.

Lenny, Sylvia, en Conny, bedankt voor alle databases!

Elly, bedankt voor de leuke gesprekken in het hoekje van Sylvia.

Graag wil ik alle collegae van Viroclinics B.V. bedanken in het bijzonder noemen:

Harriët, dankjewel voor de uitstekende samenwerking! Ik heb het als zeer prettig ervaren. Ik heb er alle vertrouwen in, dat je een goede manager zal worden.

Andres, Aida, Bianca, Lotte, thank you all for the pleasant collaboration! I believe we all did a great job on - in my view - the most difficult subject called: communication. Andres and Aida, I wish you a bright future here in Holland with new sponsors for the Helpdesk or back in Spain! Bianca, spannende tijden! Je zorgvuldigheid heeft de Helpdesk goed gedaan. Lotte, bedankt voor de gezelligheid!

Bas, veel succes met je opleiding straks in Amsterdam.

Paul, bedankt voor de introductie en ondersteuning, als deze nodig was.

Liesbeth, ik wil jou ook bedanken voor de ondersteuning.

Koert, bedankt dat ik met jou kon werken. Ik heb er veel van geleerd. Hopelijk gaat het nieuwe model het helemaal worden om nieuwe interventies te ontwikkelen.

Leon, graag wil ik jou ook bedanken voor de tijd op de 17e en in de RST. Het was gezellig in Santa Fé: ja, ik ben echt ouder dan 21 jaar.

Edwin, bedankt voor je belangstelling en adviezen rondom de studie met maternale antistoffen en voor de prettige samenwerking in de RST.

Ikrame, Patricia, Ronald, Saskia, Saskia, Willem, jullie ook bedankt voor de prettige samenwerking. Petje af voor de snelle, maar zeer adequate uitvoering van meerdere experimenten tegelijk.

Esther en Cindy, mijn buurvrouwen voor een korte periode. Veel plezier bij Viroclinics!

Maartje, Jeanette, Carla, Jacqueline, Melle, Lesley, Leo, Tamara, Sylvia en André, jullie ook bedankt!

En natuurlijk, Bob, Hans, Olaf, en Elina, dank jullie wel voor de mogelijkheid, dat ik bij Viroclinics B.V. terecht kon. Graag zie ik jullie weer in de toekomst! Ik heb er zeer veel van geleerd en Bob: ik ben beter geworden, dan toen ik begon!

## Addendum IV

Thao, Huu, Jasmijn, Thomas, nog vele en vele jaren gezelligheid in Amsterdam of Rotterdam.

Nhu, echt knap wat jij allemaal gepresteerd hebt afgelopen jaren. Uiteraard ga ik je in het nederlands bedanken en niet in het vietnamees. Bedankt voor het nakijken van de vietnamese tekst dat in dit proefschrift staat! Ik wens je al het beste met Oscar en Marvin.

Ngân, cảm ơn Ngân về tất cả những điều tốt đẹp. Chúng ta đã có sự vui chơi trong phòng thí nghiệm. Evelyn và Tiến rất vinh dự khi Ngân có mặt ở đây, hôm nay, hai ngày đặc biệt đối với chúng tôi.

Theun, ik vind het knap hoe jij alles in balans houdt. Respect! Ik wens je het allerbeste met Jona en straks twee kleine dames. Tot snel!

Ronald, leuke psychologie en mooie bloemen! Veel plezier en succes met de opleiding! Zie je snel weer aan de overkant van het water.

Millad, het was leuk in Boston! Succes met het afronden van je opleiding.

Wing Chi, het was leuk op de 22e, maar de lunch was nog leuker. Succes met het afronden van je opleiding.

Lan en Poy-Mea, gezellig en lekker eten. Zie jullie snel weer in het oosten/ westen/ zuiden of Rome?

Ivouné en Nitz, wish you all the best in San Diego! Thank you for your very special wedding!

Marije en Karla, bedankt voor de langdurige vriendschap. Tot ziens in Mexico!

Queenayda, altijd gezellig met jou. We komen snel weer langs.

Marjan en Dave, dank jullie wel voor de gezellige en heerlijke etentjes.

Osama, Kitty, Mohammed, Asrar, Lwai en Mahdi, de tijd dat ik bij jullie geweest ben, is me heel dierbaar. Jullie zijn nog steeds een voorbeeld voor mij.

Suze, het was mijn genoegen om dinsdags naar Berkel te gaan!

### Tenslotte wil ik mijn familie bedanken:

Ba và má yêu thương, ba má đã để lại quê hương của ba má vì tương lai của anh em chúng con. Lòng biết ơn đó, con không thể diễn tả. Nhưng nó là một cái gì đó giống như tất cả những giọt mưa rơi không ngừng trên mảnh đất này, mảnh đất được gọi là Hà Lan. Một người không thể mong muốn được một cha mẹ tốt hơn thế. Xin cảm ơn tình yêu vô điều kiện của ba má.

Anh hai, chi Lien en Alyssa, anh ba, Trang en Thai, het waren en zijn drukke tijden. Het lijkt alleen nog maar drukker te worden. Toch maken we met grote regelmaat tijd voor elkaar en dat betekent voor mij heel veel. Dank jullie wel voor al jullie steun (één telefoontje en jullie kwamen letterlijk vanuit alle windstreken) en geduld!

Oma†, wij missen u! Alda, namens mijn hele familie bedankt voor alles wat je voor mijn familie en vele andere families gedaan hebt! Alhoewel ik me de tijd dat jullie in Enschede woonden niet herinner, waren oma en jij samen een tweede moeder voor mij. Dit boekje is ook een deel van jou.

Henk en Janine, jullie ook bedankt voor alle hulp en gezelligheid!



Ông† bà† nội, ông† bà† ngoại, dì dưỡng† bốn, dì dưỡng năm, cậu mợ bảy, cậu mợ mười, chú thím Thừa, xin cảm ơn vì tất cả những lo lắng và chăm sóc trong quá khứ.

Anh Khải và chị Diễm, cảm ơn anh chị và toàn thể gia đình vì lòng tốt của anh chị. Chúng tôi rất biết ơn. Andy, Demi en Lily, de kermis was leuk!

Chi Hien, anh Sinh, Tuan en Lisa, tot snel!

Chi Hang, bedankt voor de gezelligheid. Al het beste met Marco! Het is al weer een tijd geleden sushi in Amsterdam, dat gaan we snel weer doen, maar eerst twee grote feesten.

Glenn, 's zomers voetballen en honkballen, dat waren nog eens tijden. Suong, we zien jullie snel in Enschede en wensen jullie succes met de drie bedrijven!

Hung, Tuyet, Romy, Lya en Kyan, ik hoop jullie nog vaker te kunnen zien als jullie eenmaal verhuisd zijn. Hung, dankjewel voor al je hulp. Zonder je inzet zou dit boekje niet compleet zijn. Nogmaals bedankt! Lya en Kyan, nu al jullie eigen boekje!

Vuong, samen zijn we naar Rotterdam gegaan. Ik mis deze fantastische tijd! Bedankt voor alles! We zien je graag samen met Cam en Nathan in Londen!

Toan en Tuyen, ik vind het jammer dat jullie in Almere woonden, gelukkig hadden we elkaar nog vaak gezien! Zie jullie snel weer.

Thuy, Tuyet, Thu, nu al jongedames. De tijd vliegt! Zie jullie weer in Enschede.

Phuc, Thong, Minh, het was altijd gezellig bij ootmarsumbrink! Phuc, SSF puzzle en Adana? Nu is het Vuong en Mason. Thong, van Amsterdam naar Kopenhagen en weer naar Amsterdam? Heel veel plezier in september met Dion in Vietnam en in jullie verder toekomst! Minh, Mailey, Jayden en Vinh, heel veel plezier met de gezinnetjes en tot snel!

Phi, Phuc, en Phu, aan de zomers heb ik fijne herinneringen.

Beste (toekomstige) schoonouders en tante Lan, dank jullie wel voor de gezellige bezoeken met lekker indonesisch eten!

Erika en Filip, altijd gezellig met jullie. Over een aantal maanden deel drie van ons traditie.

Everest, manusje-van-alles, bedankt voor je hulp!

Uncle Rudi, aunt Yun, aunt Ina and aunt Lily, thank you for your presence. We hope to visit you in Australia and Indonesia in the future.

Last but not least: Evelyn! Bedankt voor al je steun, al je begrip en al je geduld, maar zeer zeker ook al je hulp! Dit boekje is ook van jou! Aku, 10, cinta kamu, 2!

